Brighton & Sussex Medical School

MULTIMODAL ANALYSIS OF THE NEURAL CORRELATES OF DECISION MAKING IN THE CONTEXT OF FINANCIAL RISK

LUDOVICO MINATI

A thesis submitted in partial fulfilment of the requirements of the University of Brighton and the University of Sussex for the degree of Doctor of Philosophy

Aug 2012

In collaboration with the
Fondazione IRCCS Istituto Neurologico “Carlo Besta”

Declaration

I declare that the research contained in this thesis, unless otherwise formally indicated within the text, is the original work of the author. The thesis has not been previously submitted to these or any other university for a degree, and does not incorporate any material already submitted for a degree

Signed

Date

Abstract

Everyday life is pervaded by prospects presenting risks and potential rewards, and the ability to decide effectively is critical for survival. Existing literature implicates integrated action of multiple neocortical and subcortical areas, yet the mechanisms underlying risky decision-making remain debated. Here, the processing of elementary prospects, bearing variable potential losses, gains and associated outcome probabilities was investigated through multiple modalities. Autonomic monitoring indicated very limited involvement of peripheral arousal in economic parameter representation, qualifying the somatic marker hypothesis. Electroencephalography demonstrated marked dissociation between long-latency cortical potentials, tracking potential gains and value, and alpha-band arousal response to potential losses and amount magnitude. Univariate functional MRI revealed a differential cortical representation of potential losses and gains, action of the mesial prefrontal cortex as decisional comparator and involvement of the insula in encoding outcome uncertainty. Subsequent graph-based network analysis demonstrated that the medial and anterior lateral prefrontal cortices harbour key value-integrating hubs, characterized by large numbers of effective connections and high topological centrality. Predicated on the apparent lack of striatal involvement indicated by functional MRI, a behavioural experiment was conducted on patients with basal ganglia degeneration, confirming normal decisional performance. Exploring the role of the lateral prefrontal cortex in regulating risk propensity and representation of gains and losses, a direct-current neuromodulation experiment was performed: though no changes in decisional pattern were observed, enhancing right hemisphere activity boosted confidence, echoing the biases observed in pathological gamblers. These results highlight that value determination proceeds through a distributed neocortical representation of specific economic parameters, particularly losses, feeding into densely-interconnected integrative hubs in the mesial and anterior lateral prefrontal cortex. Future work will need to confirm the effect of real vs. virtual financial endowment, explore the generalization to prospects presenting different combinations of options and investigate relevant patient populations.

Index

Associated publications

The results of all experiments reported in the present thesis, and all associated data, have also formed the basis for the following peer-reviewed articles:

Minati L, Campanhã C, Critchley HD, Boggio PS (2011) Effects of transcranial direct–current stimulation (tDCS) of the dorsolateral prefrontal cortex (DLPFC) during a mixed–gambling risky decision-making task. Cognitive Neuroscience, Epub 3 Oct 2011; DOI: 10.1080/17588928.2011.628382

As detailed in Chapter 8, CC alongside other students assisted with delivering the task instructions in Portuguese, obtaining informed consent and applying the stimulation device, in compliance with local regulations.PB provided advice and guidance on the use of tDCS to study decision making and on experiment design, and supervised the experiments. The author of the present thesis formulated the study hypotheses, designed the decisional paradigm, analyzed and interpreted the data, and prepared the manuscript with significant editorial contributions and advice from all authors.

Minati L, Grisoli M, Franceschetti S, Epifani F, Granvillano A, Medford N, Harrison NA, Piacentini S, Critchley HD (2012) Neural signatures of economic parameters during decision-making: a functional MRI (FMRI), electroencephalography (EEG) and autonomic monitoring study. Brain Topogr 25:73-96; DOI: 10.1007/s10548-011-0210-1

As detailed in Chapters 4 and 5, FE and AG provided technical assistance during the acquisition of EEG and fMRI data, to comply with local regulations. MG provided advice

and guidance on the use of fMRI to study decision making and experiment design, and supervised the fMRI experiments. SF did the same for the EEG experiments. SP supervised the administration of the paradigm and the acquisition and analysis of the behavioural data, and provided advice on the interpretation of the behavioural results. NAH provided general advice on the interpretation of the fMRI findings and senior advice during preparation of the publication. The author of the present thesis designed the task, designed the fMRI and EEG experiments and formulated the associated hypotheses, developed the data acquisition and data analysis software, administered the decisional paradigm and recorded the data with the support of FE and AG, analyzed and interpreted the data, and prepared the manuscript with significant editorial contributions and advice from all authors.

Minati L, Grisoli M, Seth AK, Critchley HD (2012) Decision-making under risk: A graph-based network analysis using functional MRI. Neuroimage 60:2191-205; DOI: 10.1016/j.neuroimage.2012.02.048

AKS provided general advice on the analysis and interpretation of the effective connectivity findings and senior advice during preparation of the publication. The author of the present thesis formulated the study hypotheses, developed and implemented the graph-oriented analysis PPI technique at the basis of the investigation, analysed and interpreted the data, and prepared the manuscript with significant editorial contributions and advice from all authors.

Minati L, Piacentini S, Ferrè F, Nanetti L, Romito L, Mariotti C, Grisoli M, Medford N, Critchley HD, Albanese A (2011) Choice-option evaluation is preserved in early Huntington and Parkinson's disease. Neuroreport 22:753-7; DOI: 10.1097/WNR.0b013e32834acb6e

As detailed in Chapter 7, SP and FF materially administered the behavioural tests to the patients, as required by local rules preventing the author from testing patients directly. LN, LR, CM and AA identified, recruited and characterized neurologically and genetically the patients. The author of the present thesis formulated the study hypotheses, designed the task, co-ordinated the experiments and the administration of the decisional paradigm, analyzed and interpreted the data, and prepared the manuscript with significant editorial contributions and advice from all authors.

For all publications listed above, HDC, NM and MG (in their roles of supervisors of the present doctoral research) provided senior research supervision, mentoring and advice.

Further detail is provided in the "Acknowledgements" section below.

Acknowledgements

This research would have been entirely inconceivable without the support and guidance received from many. First, I would like to thank my supervisors, Prof. Hugo Critchley, Dr. Nick Medford and Dott.ssa Marina Grisoli, for inspiration, senior supervision throughout all experiments, and invaluable advice on study design, data interpretation and earlier versions of the present thesis and the associated manuscripts. I would like to thank my colleagues and friends Dott.ssa Sylvie Piacentini, for inspiring discussions and useful advice in early phases of the project, and Dr Dennis Chan, for insightful comments on earlier drafts. Due to regulatory as well as logistic reasons, data acquisition for many of the experiments would not have been at all possible without the support received from many healthcare professionals, who kindly and humbly accepted to support me in enacting my research plans. I would like to thank Dott.ssa Marina Grisoli, senior neuroradiologist, and TSRM Francesca Epifani, radiographer, for assistance during the acquisition of functional MRI data; additional support received from Dott.ssa Maria Grazia Bruzzone, senior neuroradiologist and Dott.ssa Stefania Ferraro, neuropsychologist, during initial scans is also gratefully acknowledged. I would like to thank Dott.ssa Silvana Franceschetti, senior neurophysiologist, TNFP Alice Granvillano and TNFP Elena Schiaffi, neurophysiology technicians, for assistance during the acquisition of EEG data; additional technical support received from Ing. Ferruccio Panzica is also gratefully acknowledged. I would like to thank Dott.ssa Sylvie Piacentini and Dott.ssa Francesca Ferrè for testing behaviourally patients with Parkinson's disease and Huntington's disease on my behalf, as local rules prevented me from doing so directly; I would like to thank them also for insightful advice on the design of the behavioural experiment and related data interpretation. I would like to thank Dott. Luigi Romito, Dott.ssa Caterina Mariotti,

Dott. Lorenzo Nanetti for identifying and recruiting suitable neurological patients, and for characterizing them clinically and genetically. I am also sincerely grateful to Prof. Alberto Albanese for many insightful discussions and senior advice on the study of neurological patients. I would like to thank Dr. Anil Seth for sparking my interest in the study of brain connectivity through many exciting informal discussions, and later for insightful comments and advice on the interpretation of effective connectivity data. I would like to warmly thank Camila Campanhã for introducing me to the world of neuromodulation, and for inviting me to conduct an experiment at the MacKenzie University in São Paulo. I would like to thank Prof. Paulo Boggio for hosting me and making this experiment possible, and for endless, highly stimulating discussions on the matter; my gratitude also goes to research students and assistants Karina Di Siervi, Ana Alem and Nathalia Baptista who helped me overcome language barriers and made it possible to test Portuguese-speaking participants as a part of my research. No less importantly, I would like to thank thesis panel members Dr. Dennis Chan and Prof. Jenny Rusted, for their encouraging feedback and many highly relevant comments offered during progress review meetings. The feedback received from several anonymous peer reviewers has also been invaluably useful to improve the robustness and impact of the manuscripts, and the quality of the associated thesis chapters has undoubtedly benefited as well. I would like to thank all decision-makers at the Brighton & Sussex Medical School and Fondazione IRCCS Istituto Neurologico Carlo Besta, particularly Prof. Kevin Davies and Prof. Ferdinando Cornelio, for believing in my ability to bring this challenging international collaborative project to successful completion. I would also like to thank the Fondazione IRCCS Istituto Neurologico Carlo Besta as a whole for funding me as an employee through my doctoral studies. Last, but not less importantly, I would like to thank all study participants, and collectively all colleagues and friends at the Brighton & Sussex Medical School and Fondazione IRCCS Istituto Neurologico Carlo Besta for friendly advice and support.

List of Figures

List of Tables

Abbreviations

ACC: Anterior Cingulate Cortex

ALL: Automated Anatomical Labelling

ALPFC: Anterior Lateral Pre-Frontal Cortex

aMCC: Anterior Mid-Cingulate Cortex

AMYG: Amygdala

ANG: Angular gyrus

ANOVA: Analysis Of Variance

ANS: Autonomic Nervous System

BAI: Beck's Anxiety Inventory

BDI: Beck's Depression Inventory

BIS: Barratt's Impulsiveness Scale

BOLD: Blood-Oxygen Level-Dependent

BP: Blood Pressure

BPRS: Brief Psychiatric Rating Scale

CAG: Cytosine-Adenine-Guanine

CAUD: Caudate Nucleus

CRP: Correct-Related Positivity

CRT: Cathode Ray Tube

CTRL: Control

DCM: Dynamic Causal Modelling

DLPFC: Dorsal Lateral PreFrontal Cortex

DMN: Default Mode Network

DMPFC: Dorsal Medial PreFrontal Cortex

dPCC: Dorsal Posterior Cingulate Cortex

DTI: Diffusion Tensor Imaging

EEG: ElectroEncephaloGraphy

ERN: Error-Related Negativity

ERP: Event-Related Potential

EV: Expected Value

fMRI: Functional Magnetic Resonance Imaging

FWE: Family-Wise Error

H&Y: Hoehn & Yahr

HD: Huntington's Disease

HPP: Hippocampus

IBI: Inter Beat Interval

IGT: Iowa Gambling Task

LCD: Liquid Screen Display

LEDD: Levodopa Equivalent Daily Dose

LENT: Lenticular Nucleus

MAP: Mean Arterial Pressure

MCC: Medial Cingulate Cortex

MFN: Medial Frontal Negativity

MI: Primary Motor area

MoCA: Montreal Cognitive Assessment battery

MRI: Magnetic Resonance Imaging

OCC: Occipital

OFC: Orbital Frontal Cortex

pACC: Posterior Anterior Cingulate Cortex

PCC: Posterior Cingulate Cortex

PD: Parkinson's Disease

pMCC: Posterior Mid-Cingulate Cortex

PPI: Psycho-Physiological Interaction

PREC: Precuneus

RA: Respiratory Amplitude

RI: Respiratory Interval

ROI: Region Of Interest

rPTT: R-Wave to Pulse Transit Time

rs-fMRI: Resting-State fMRI

RT: Reaction Time

rTMS: Repetitive Transcranial Magnetic Stimulation

SCL: Skin Conductance Level

SI: Primary Somatosensory area

SII: Secondary Somatosensory area

sLORETA: Standardized Low-Resolution Electromagetic Brain Tomography

SMA: Supplementary Motor Area

SPM: Statistical Parametric Map

SWP: Slow-Wave Potential

tDCS: Transcranial Direct Current Stimulation

TFC: Total Functional Capacity

THAL: Thalamus

UHDRS: Unified Huntingon's Disease Rating Scale

UPDRS: Unified Parkinson's Disease Rating Scale

VLPFC: Ventral Lateral PreFrontal Cortex

VMPFC: Ventral Medial PreFrontal Cortex

VS: Ventral Striatum

Economic parameters

The following economic parameters are defined for each gamble, and reported here for convenience. See Chapter 2 for full definitions. Those marked with "(*)" are explicitly displayed.

k_{WIN} (*)	Potential gain
k_{LOSE} (*)	Potential loss
p_{WIN} (*)	Probability of winning
$k_{WIN} \times p_{WIN}$	Potential gain weighted by the probability of winning
$k_{LOSE} \times (1-p_{WIN})$	Potential loss weighted by the probability of losing
EV	Expected value
$\langle k_{WIN}, k_{LOSE} \rangle$	Average between potential gain and potential loss
$EV/\langle k_{WIN}, k_{LOSE} \rangle$	Normalized risk-advantageousness, i.e. -1 completely disadvantageous, 0 indifferent, +1 completely advantageous
Var	Variance among all possible gamble outcomes
$\lvert p_{WIN}-0.5 \rvert$	Deviation of outcome probability from 50/50 point
$\lvert EV/\langle k_{WIN}, k_{LOSE} \rangle \rvert$	Deviation of normalized risk-advantageousness from indifference point

1. Introduction

1.1 General framework

Should a lizard spring out of hiding to capture a large insect, at the risk of exposing itself to a predator? Should a child run to cross a street away from traffic lights to catch the passing school bus, at the risk of being struck by a car? Should an entrepreneur put the survival of her company at risk for the opportunity of embracing a revolutionary product line? The life of non-human animals and humans alike is pervaded by situations where the ability to take effective decisions is fundamental to survival. We take decisions many hundreds of times per day, sometimes without even being aware of it, and the quality of our decisions profoundly impacts all aspects of existence, from physical survival to financial and affective accomplishment (Kalenscher and van Wingerden, 2011).

Irrespective of the exact nature of the situation, many decisions involve accepting or rejecting a risk for the prospect of potentially harvesting a reward, be it capturing food, catching a bus or earning money. In some conditions all information is explicitly available, i.e. the entity of the potential losses, gains and the associated probabilities are known, or at least estimable from the available information. In others, there are inherent elements of ambiguity which imply that multiple rounds of interaction and feedback are required to gather information on the subjective value of choosing a given option rather than another (e.g., Wilkinson, 2008).

The first known formal account of decisional theory dates back to 1738, when Daniel Bernoulli, prominent Swiss mathematician, introduced the concept of expected utility, that is of weighting potential outcomes, having positive or negative value, by their respective probabilities. According to the classical formulation of expected utility theory, a

rational agent faced with a risky decision always chooses the option associated with the highest expected value, i.e. with the most advantageous combination of potential beneficial and detrimental outcomes weighted by their respective probabilities (Von Neumann and Morgenstern, 1944; Bernoulli, 1954). Expected utility theory can be extended to include non-linear utility functions, which represent the fact that in most circumstances living beings preferentially reject "fair" gambles (or equivalent naturalistic prospects) where, considering all possible outcomes, the total expected value of a given choice option evaluates to zero (McFarland, 1997; Kalenscher and van Wingerden, 2011).

Indeed, human decision-making under risk does not represent a simple approximation of a hypothetical "rational" agent that weights losses and equivalent gains equally. On the contrary, there are pervasive biases, partly related to emotions and visceral feeling states, which are observed throughout the most disparate decisional situations and which represent adaptive changes, plausibly evolved to protect an individual's long-term survival. For example, when evaluating a risky choice-option potential losses are typically weighted considerably more than equivalent gains: a likely motivation for this bias is that losses can be fatal, even when received in response to choosing an action that was, overall, expected to be advantageous. As a consequence, one tends to avoid taking risks unless the associated expected utility is very clearly positive and a prospect is framed in a situation where no subjectively preferable options are available. Another pervasive bias is that one tends to overestimate the probability of improbable events, and underestimate that of near-certain occurrences. Empirical evidences of these biases were given a solid conceptual framework in 1979 with Kahneman and Tversky's "Prospect theory: An Analysis of Decision Under Risk", a highly influential paper which interpreted such economic observations in light of cognitive psychology concepts, and which arguably give birth to a new field, dubbed behavioural economics (Kahneman and Tversky, 1979).

1.2 From behavioural economics to clinical neurology

Though economics and ethology have proceeded separately for a long time, already by the 1970s it had became clear that animal decision-making and human financial decision-making share very substantial theoretical similarities, whereby the focus is on optimality of behaviour to sustain an external pressure and maximise reproductive fitness or capital profit. Dealing effectively with risk is a fundamental prerequisite for survival, a more abstract but by no means less important capacity than the physical fitness to capture food, avoid predators and reproduce. An animal that is physically powerful but acts in a fashion that ignores potential rewards and dangers has no hope for long-term survival. Similarly, a human being who is physically fit and has normal perceptual, motor, cognitive and emotional skills but no ability to weight potential risks and rewards effectively is likely to succumb in society (McFarland, 1997; Kalenscher and van Wingerden, 2011).

The bases of decision-making behaviour have been of interest to psychologists for over a century, e.g. since the times of Thorndike's law of effect (1911), which postulated that "responses producing a rewarding effect in a given situation are more likely to be re-enacted again in that situation in the future". In the century which separates such statement from today, the neural bases of an overwhelming range of psychological phenomena have been discovered and characterized, adding a biological dimension and causative models to accounts that were, initially, purely behavioural. Yet, the study of decision-making has remained alien land for neuroscience and clinical neurology until very recently, specifically until Schultz and co-workers's (1993) discovery of the role of the mesolimbic dopamine system in encoding reward and reward prediction error. In the years following their discovery, the rapid development of powerful non-invasive tools to study brain function with good anatomical detail has fuelled the growth of a new field, dubbed neuroeconomics, concerned with the characterization of the neural substrates of decision-

making behaviour (e.g., Trepel et al., 2005; Platt and Huettel, 2008; Kable and Glimcher, 2009).

The ability to make effective decisions in the face of risk and ambiguity has remained and still for the most part remains outside the radar of clinical neurology and psychiatry: patients are routinely assessed, for example, for sensorimotor, language, memory, general cognitive deficits and emotional dysregulation, yet formal standardized tools are very seldom applied to assess the way in which neurological and psychiatric pathologies can affect decision-making processes, such as one's capability to mentally represent risks and potential rewards and the associated probabilities, even in critical situations such as deciding one's fitness to drive a vehicle. This is a striking fact, considering that the capacity to decide effectively when faced with risks and potential rewards is crucially important for independent life, less evidently but not less fundamentally than, for example, the ability to memorize or communicate verbally. At present, clinical neurology and psychiatry de-facto take, in the vast majority of circumstances, a binary approach to a patient's ability to make decisions: either they have it, or they are deemed to be mentally incapacitated (though incapacity may be transient, e.g. in delirium secondary to sepsis), according to legal criteria that vary from state to state and are generally rather restrictive. While highly refined and sensitive scales are used to recognize even mild deficits in language, memory and many other cognitive functions in the diagnostic, prognostic and treatment follow-up process, one's ability to take effective decisions is often ignored until the point of obvious and catastrophic failure, i.e. full-blown mental incapacity (e.g., Dunn et al., 2006; Appelbaum, 2007).

One may argue that the importance of assessing general decision-making functions in clinical neurological populations first became clear with the emergence of dopamine dysregulation syndrome. Due to the increasing availability of more potent and specific dopaminergic medication, in the early 2000s the number of patients with Parkinson's

disease who developed pathological gambling and liquidated their finances soared, leading to recognition of the importance that including decision-making abilities in the spectrum of cognitive and emotional functions to monitor would have (e.g., Seedat et al., 2000; Evans and Lees, 2004; Pezzella et al., 2005). Throughout the last decade, a substantial number of exploratory studies have demonstrated the presence of abnormalities in the decisional behaviour of patients with mild cognitive impairment and Alzheimer's disease (Delazer et al., 2007; Sinz et al., 2008; Caselli et al., 2011; Zamarian et al., 2011), other forms of dementia (Manes et al., 2010; Manes et al., 2011; Gleichgerrcht et al., 2012), Parkinsonism (Mimura et al., 2006; Pagonabarraga et al., 2007; Kobayakawa et al., 2008; Delazer et al., 2009; Gescheidt et al., 2011), other movement disorders (Watkins et al., 2000; Stout et al., 2001), macroscopic brain lesions following tumour resection or ischemic insult (Clark et al., 2003; Weller et al., 2009; De Martino et al., 2010), systemic cardiovascular disease (Gaviria et al., 2011) and healthy ageing (Brown and Ridderinkhof, 2009; Hommet et al., 2010). Converging evidence indicates that the reward element of decision making is heavily influenced by the status of multiple hormonal and neurotransmitter systems, mainly dopamine, central opiates, serotonin and acetylcholine (Martin-Soelch et al., 2003; Goudriaan et al., 2004; Caldú and Dreher, 2007; Petrovic et al., 2008; Duka and Crews, 2009). The strength of the link between decision-making abilities and biochemical factors is further remarked by observations that individual decision-making style, particularly the sensitivity to losses and gains, is strongly determined by genetic polymorphisms in proteins related dopamine receptor D4 and catechol-O-methyltransferase (Roiser et al., 2009; Marco-Pallarés et al., 2009; Camara et al., 2010).

Systematically investigating the neural bases of decision making is therefore strongly motivated not only to serve the purpose of deepening our understanding of cognition and behaviour in general, but also to provide a solid theoretical basis enabling

neurologists and psychiatrists to detect, understand and manage the decisional dysfunctions observed in a wide range of conditions.

1.3 The current state of neuroeconomics and the role of "fruit fly"

The development of neuroeconomics as a leading field of neuroscientific research has shed light on the neural systems broadly involved in a wide range of decisional processes. In part, research has followed the tracks of experimental psychology, for example studying the correlates of conditioning paradigms, and in part it has built more directly behavioural economics, exploring the neural correlates of phenomena such as loss aversion, non-linear probability weighting and delayed discounting. Functional MRI studies have extensively mapped the brain regions involved not only in elementary gambling tasks (e.g., Trepel et al., 2005; Platt and Huettel, 2008; Rushworth and Behrens, 2008; Kable and Glimcher, 2009) but also in highly abstract economic paradigms probing, for example, strategic thinking during competitive games (e.g., Daw et al., 2006; Coricelli and Nagel, 2009), social decision-making and associated biases (e.g., Sanfey et al., 2003; Bault et al., 2011; Corradi-Dell'acqua et al., 2012).

In general, functional MRI and lesion modelling studies indicate that decision-making abilities are subserved by an interplay between associative neocortical regions, primarily within the inferior, inferior-lateral and mesial prefrontal neocortex and parietal lobe, and evolutionarily-older structures such as the striatum, amygdala and insula (Trepel et al., 2005; Platt and Huettel, 2008; Rushworth and Behrens, 2008; Wang, 2008; Andersen and Cui, 2009; Kable and Glimcher, 2009; Levine, 2009; Clark, 2010; Rangel and Hare, 2010; Wallis and Kennerley, 2010; Alexander and Brown, 2011). The striatum and the mesolimbic dopamine system are key to processing feedback information, and support the updating of subjective beliefs and strategic learning through their projections to the frontal

neocortex. Invasive neurophysiological recordings have demonstrated that the activity of this system directly represents the expectation of a reward prior to the corresponding action being enacted, and the error between the expected and the received reward once the consequence of the decision is revealed (e.g., Schultz et al., 1993; Fiorillo et al., 2003; Ramnani et al., 2004; Knutson and Cooper, 2005; Pessiglione et al., 2006). In spite of the enormous amount of experimental evidence, the exact functional correlates of the other brain regions and systems during decision-making remain debated.

In part, this is likely due to the fact that their engagement is highly situation-dependent, i.e. separate regions can display markedly different responses to economic parameters as a function of the specific task employed, for example depending on the presence or not of elements of ambiguity (e.g., Krain et al., 2006) and on the exact characteristics of the "editing" phase, such as choosing between a non-zero value option and a zero-value one or choosing between multiple non-zero value options (e.g., Kahnt et al., 2010). The problem is exacerbated by the fact that behavioural phenomena such as risk-aversion plausibly do not reflect unitary neural processes, but are to a large extent influenced by situation-dependent heuristics, as implied by economic experiments indicating that different risk-propensity levels are observed in given individuals as a function of decisional context (e.g., Weber et al., 2002; Botella et al., 2008). Another substantial problem is that the majority of current neuroeconomics research remains anchored to localizationist notions of direct brain structure-function relationships, i.e. attempts to establish one-to-one associations between the magnitude of the neural responses in isolated regions and individual economic parameters. Correlative studies, even when based on explicit computational models linking neural responses to generative models (e.g., O'Doherty et al., 2007; Guitart-Masip et al., 2012), do not account for the fact that the abstract representation and computation of economic variables, and the related internally-competitive neural dynamics which support choice, are unlikely to be localized

to isolated regions but rather, in connectionistic views, emerge from large-scale interactions across dynamic networks. This is not to imply that univariate analysis of regional brain activity has no value, but it is likely that the current difficulty in identifying consistent neural substrates for decisional behaviours is largely related to the fact that the role each region plays is not fixed, but at least partially bound to network-level dynamics that are intrinsically invisible to univariate approaches (Rumelhart et al., 1986; Mesulam, 1998; Sporns and Tononi, 2001; Stephan, 2004; Bassett and Bullmore, 2006; Meyer and Damasio, 2009; Sporns, 2009).

One of the most elementary decisional scenarios is choosing whether or not to take the risk of incurring a loss for an opportunity to harvest a potential reward. In economic terms, this corresponds to comparing a zero-value situation of no risk and no potential gain, with a situation whose expected value is given by the summation of the potential losses and gains, weighted by their respective outcome probabilities. Inevitably this is a rather simplified scenario – in real life most decisions imply complex multifactorial trade-offs, and often involve dealing with elements of ambiguity that can only be resolved through interacting with the environment (or an opponent) and suitably processing the feedback thus obtained. Yet, as Kahneman (writing on behalf of the late Tversky) put it, this simple gambling scenario has been and remains the "fruit fly" of behavioural economics: the number of variables is small enough to permit rigorous modelling and validation, yet all key deviations from locally-rational behaviour, such as non-linear weighting of value and outcome probabilities, can be reliably elicited and studied with this paradigm (Kahneman and Tversky, 2000).

When one is faced with such a decision, the lateral prefrontal cortex and the parietal cortex are heavily involved in the mental representation of the available economic parameters and in their integration into more abstract variables that support the decisional process, for example weighing the value of each possible outcome by the respective

probability (e.g., Clark et al., 2003; Trepel et al,. 2005; Krain et al., 2006; Tom et al., 2007; Kable and Glimcher, 2009; Kahnt et al., 2010). On the other hand, the representation of abstract value as such is hypothesized to be centred around a cortical-subcortical circuit involving the mesial prefrontal and orbitofrontal cortices, and possibly the striatum, acting as integrators or comparators among possible choice options (Tom et al., 2007; Chib et al., 2009; Kable and Glimcher, 2009; Gläscher et al., 2009; Smith et al., 2010; Venkatraman et al., 2009; Wunderlich et al., 2009). The insula, cingulate cortex and amygdala are also deemed to be involved, particularly in supporting the generation of risk, uncertainty and conflict signals, and in their visceral embodiment into peripherally-expressed feeling states (e.g., Kahn et al., 2002; Critchley, 2005; Trepel et al,. 2005; Preuschoff et al., 2008; Weller et al., 2009; De Martino et al., 2010; Medford and Critchley, 2010).

A definite, falsifiable functional model of how value computation is performed by the brain in the face of a risky prospect remains largely lacking, and attaining a detailed level of understanding of the underlying neural processes would be particularly important, as the ability to assign a judgement of value or advantageousness to choice options is fundamental in virtually all decisional scenarios. The present doctoral project was therefore motivated to expand the understanding of how economic parameters related to an elementary mixed-gamble are represented in the brain. A uniform gambling task was used throughout and was investigated thoroughly in a series of related experiments probing autonomic physiology, neuroelectrical activity, regional haemodynamic responses, network-level dynamics, behaviour in neurological patients and healthy participants undergoing neuromodulation. The spirit of the present investigation was to contribute to existing neuroeconomics literature, where several advanced decisional tasks have been broadly explored, with a comprehensive multimodal investigation of an elementary decisional situation. It was also aimed at identifying and characterizing a range of imaging and electrophysiological markers of value processing potentially applicable in future

studies to elucidate the bases of altered decision making in neurological and psychiatric patient populations. Given the abstract nature of the processes of interest, which involve interplay among multiple cognitive, emotional and visceral representations, a multimodal investigational approach appears of particular value here. Though the level of spatial detail is comparatively limited with respect to functional MRI, electroencephalography has a complementary sensitivity pattern, emphasizing rapid temporally-synchronized activity and potentially revealing dissociations between long-latency integrative processing and broader changes in spontaneous rhythms reflecting central arousal (Pfurtscheller, 2001; Oakes et al., 2004; Minati et al., 2008). On the other hand, explicit recording of systemic physiological parameters can enable one to answer questions regarding the extent to which given situational parameters, such as risk or conflict, are represented in bodily sensations (Critchley, 2005). Notwithstanding the limited temporal resolution of fMRI, multivariate modelling of the statistical properties of the haemodynamic time-courses can reveal the information-integration processes taking places in putative "hub" regions, which may not necessarily display an intensity of activity directly correlating with task parameters and which therefore may be invisible to traditional univariate analysis (Friston et al., 1997; Sporns and Tononi, 2001; Stephan, 2004; Bassett and Bullmore, 2006; Sporns, 2009). Since it is difficult to draw definite inferences on functional involvement purely on the basis of neuroimaging or neurophysiological correlations, the study of neurological patients as "system lesion" models and the use of neuromodulation techniques may further aid in confirming or refuting hypotheses related to the involvement of specific regions in economic parameter representation (Clark et al., 2003; Knoch et al., 2006; Fecteau et al., 2007; Delazer et al., 2009; Beste et al., 2010; De Martino et al., 2010).

In summary, the present doctoral project had the following aims:

- Develop and characterize behaviourally an elementary risky decision-making task based on mixed-gambles;

- Determine whether the economic parmeters characterizing each prospect are represented in significant modulations of peripheral autonomic responses, particularly electrodermal and cardiovascular activity;
- Determine how the economic parameters characterizing each prospect influence neuroelectrical activity following gamble presentation, and in particular search for specific associations with mid- and long-latency potentials (taken as empirical markers of abstract processing) and with power density of spontaneous oscillations in the main frequency bands (taken as empirical marker of general brain state);
- Determine how the economic parameters characterizing each prospect are represented in regional haemodynamic activity, particularly to identify the structures representing value, the overlap or separation between the areas involved in encoding potential losses and gain, and the substrates of the representation of risk and uncertainty signals;
- Explore, using a novel network-oriented approach based on explicit topological modelling, the architecture of effective connectivity underlying the computation and reprensetation of value, particularly aiming to identify and localize putative "integrative hubs";
- Determine, through behavioural testing of patients with early-stage Parkinson's disease and Huntington's disease (taken as "system lesion" models) whether the striatum has an essential, causative role in value computation in the face of risky prospects;
- Determine, through behavioural testing of healthy participants undergoing prefrontal neuromodulation, whether straightforward, direct associations exist between hemispheric balance and excitability, and level of risk propensity and differential weighting of potential losses and gains.

2. Behavioural paradigm

2.1 Task design and economic parameters

The experiments presented in the following chapters are based on a unified paradigm, consisting of presenting risky gambles in the absence of any element of ambiguity or on-line outcome feedback. Each gamble was determined by three displayed values: a potential loss thereafter referred to as k_{LOSE}, a potential win k_{WIN} and a probability of winning p_{WIN}, represented in percent units (Figure 1).

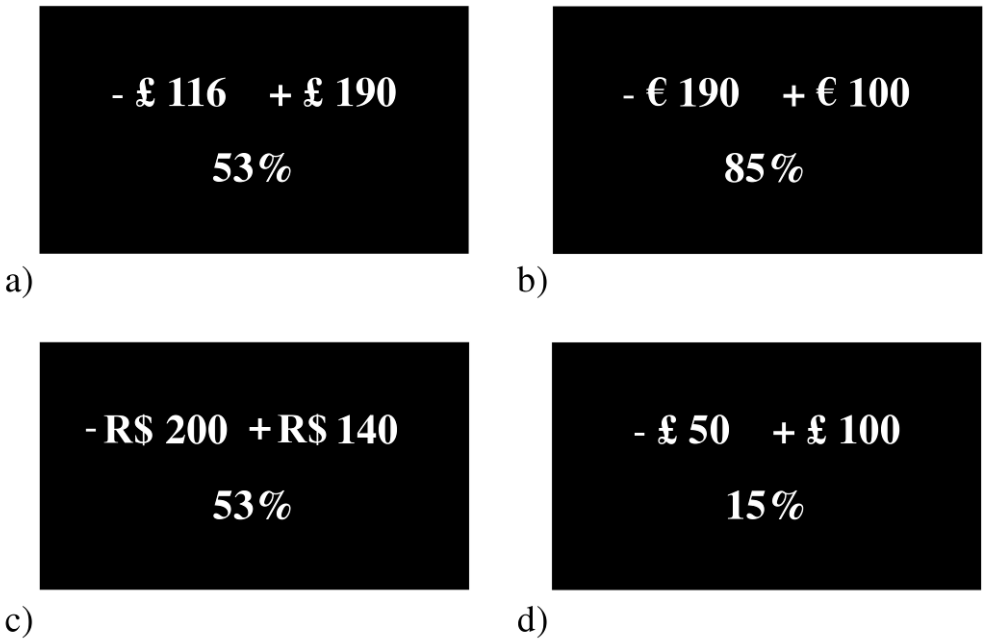

Figure 1. Examples of gamble presentation format, shown for a) a risk-advantageous gamble with $k_{WIN}>k_{LOSE}$, b) a risk-advantageous gamble with $k_{WIN}<k_{LOSE}$, c) a risk-disadvantageous gamble with $k_{WIN}<k_{LOSE}$, and d) a risk-disadvantageous gamble with $k_{WIN}>k_{LOSE}$.

Participants were requested to evaluate each gamble in isolation, deciding whether to take the associated risk for an opportunity to gain a reward (which would not be revealed, given the absence of ongoing feedback) or leave it. In other words, a situation of risky decision-making was created by forcing choice between a zero-expected value (EV=0), risk-free option and a risky one having $EV=k_{WIN}\times p_{WIN}-k_{LOSE}\times(1-p_{WIN})$.

Participants responded to each gamble using a graded scale, comprising four levels defined as "confident reject", "unsure reject", "unsure accept" and "confident accept". As suggested in Tom et al. (2007), the use of this graded scale was not predicated on economic hypotheses, but simply a way to force participants to encode and process each gamble deeply, rather than potentially applying to a simple decisional rule to support yes/no responses. The time-line of the task is represented in Figure 2.

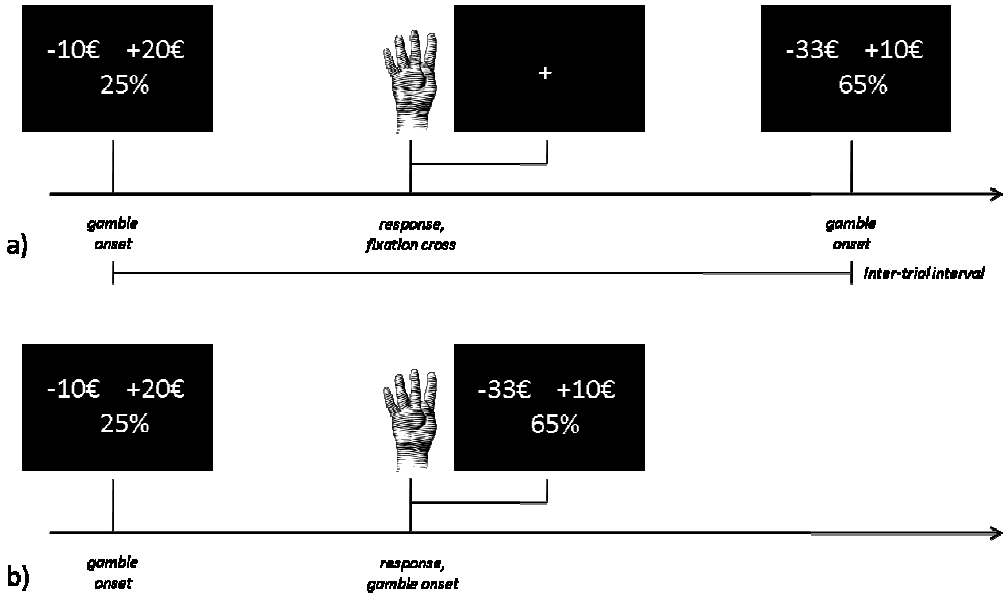

Figure 2. Time-line of the task. Each gamble was evaluated in isolation. a) In the autonomic, EEG and functional MRI experiments, after a response was made a fixation cross appeared and remained on the screen until a pre-defined inter-trial interval. b) In the neurological patients and neuromodulation experiments, a new gamble immediately appeared after each response.

Owing to the variable outcome probability p_{WIN}, the task, despite its elementary nature and straightforwardness, enables probing the representation of a comprehensive set of economic parameters in addition to those directly displayed. First, the separate positive and negative terms of the value equation, i.e. $k_{WIN} \times p_{WIN}$ and $k_{LOSE} \times (1-p_{WIN})$; these are not equivalent to potential win and potential loss, because they are weighted by the corresponding probabilities, therefore representing "expected potential win" and "expected potential loss", whose summation leads to expected value. Second, average amount magnitude between potential gain and loss, referred to as $\langle k_{WIN}, k_{LOSE} \rangle$, representing "how much is at stake" in a given prospect. Third, *EV* normalized by amount magnitude, i.e. $EV/\langle k_{WIN}, k_{LOSE} \rangle$, representing dimensionless "risk advantageousness", i.e. how convenient a given gamble is irrespectively of the amount of money at stake. Fourth, the deviation from risk indifference thus defined, i.e. $|EV/\langle k_{WIN}, k_{LOSE} \rangle|$, presenting a measure of how clearly advantageous or disadvantageous each gamble is. Fifth, the outcome uncertainty, defined simply as $|p_{WIN}-0.5|$, independently of risk advantageousness. Lastly, the variance among the possible outcomes, representing a more abstract index of uncertainty and defined as $Var = p_{WIN} \times (k_{WIN}-EV)^2 + (1-p_{WIN}) \times (-k_{LOSE}-EV)^2$. With respect to the existing imaging and neurophysiology studies on decision-making where fewer parameters were varied (e.g., Tom et al., 2007), this paradigm enables probing the neural representation of a risky decisional situation along a more comprehensive set of non-collinear axes.

Prior to performing the task, participants read an instruction sheet, whose key points were later reinforced verbally by the experimenter. They were requested to equally weight all three parameters before taking a decision, conjointly considering them rather than focusing on one or two; examples were given to represent how concentrating on one or two parameters only would lead to poor performance. Participants were requested to refrain from performing any mathematical computation, relying instead on their "gut

feeling" of convenience and trying to be as fast as they could. They were asked to consider each gamble in isolation, without making any reference to the previous ones and their associated responses. They were told that no feedback on the outcome of each gamble would be shown, but the experimenter stressed that the outcomes were not pre-specified, but would be determined by the computer, according to the probability shown, at the time of pressing the "accept" button. They were asked to play with the aim of earning as much money as possible throughout the whole task, trying to behave as they would if they had been playing with their own personal money.

In practice, it was not possible to offer any real financial endowment due to regulatory limitations, i.e. ethical restrictions and gambling laws in Italy, and participants were therefore told that they would receive no material reward. Yet, they were informed that the computer would keep track of all wins and losses, in the form of a virtual bank account recording a positive or negative transaction each time a gamble was accepted. To further increase motivation, they were told that the usefulness of their participation would depend on their ability to earn a large sum of money, and that the amount earned or lost overall would be displayed at the end of the whole session. The task instructions provided examples of advantageous, disadvantageous and near-indifferent gambles, including non-trivial advantageous gambles having $k_{WIN}<k_{LOSE}$ and disadvantageous gambles having $k_{WIN}>k_{LOSE}$. (Figure 1). The task instructions were initially written in Italian. For the autonomic response monitoring experiment, they were translated into English by the author and verified by a native speaker (Prof. Hugo Critchley). For the neuromodulation experiment, as the author was unable to do this directly, they were translated into Brazilian Portuguese by a local researcher (Ms. Camila Campanhã) and verified by the head of the laboratory (Prof. Paulo Boggio). Prior to data collection, participants always practiced with ten sample gambles.

2.2 Gamble pool generation and stimulus delivery

The gambles utilized in all experiments were drawn from a common pool of 10,000 items, which was generated using a script developed by the author under the Matlab 7 language (MathWorks Inc., Natick MA, USA) according to the following procedure. First, a uniform distribution for p_{WIN} was generated between 0.1 and 0.9. Second, a symmetric U-shape distribution for intermediate parameter k was generated in the range [-0.5, 0.5], having approximately 1% of counts in the range [0, 0.1], 4% in [0.1, 0.2], 8.5% in [0.2, 0.3], 14.2% in [0.3, 0.4] and 22% in [0.4, 0.5], and a uniform distribution for intermediate parameter m was generated between 10 and 200. Subsequently, the gamble amounts were calculated with

$$\begin{aligned} k_{LOSE} &= m \cdot (2p_{WIN} - k) \\ k_{WIN} &= 2m - k_{LOSE} \end{aligned},$$

and only gambles having $0<k_{LOSE}<300$ and $0<k_{WIN}<300$ were retained and corresponding values were rounded.

The statistical properties of the overall gamble pool thus obtained are represented in Figure 3. As indicated above, the range for k_{WIN} and k_{LOSE} was between 0 and 300 , while p_{WIN} was between 0.1 and 0.9. In order to avoid introducing bias, it is necessary that the distributions of the positive and negative value term parameters are balanced. Non-parametric Mann-Whitney tests were performed to confirm the absence of differences between the distributions of k_{WIN} and k_{LOSE} (p=0.6), and between the distributions of $k_{WIN}\times p_{WIN}$ and $k_{LOSE}\times(1-p_{WIN})$ (p=0.7). It is also essential that the distribution of EV is centred around zero. To test this hypothesis, a one-sample t-test was performed, confirming that the average EV, which was 0.5±43.4, was not significantly different from zero (p=0.8). This was further confirmed by calculating the skewness of the EV distribution, which was zero. As revealed by a Kolmogorov-Smirnov test, the distribution was not perfectly normal

(Z=2.4, p=0.02), i.e. it was slightly leptokurtic, having excess kurtosis 0.8; this is, however, irrelevant for the purposes of the present investigations. In Figure 4, scatter plots for the correlation between EV and the displayed parameters k_{WIN}, k_{LOSE} and p_{WIN} are shown. The linear correlation coefficients were comparable, i.e. r=0.32 for k_{WIN}, r=0.34 for k_{LOSE} and r=0.36 for p_{WIN}. Such balancing is relevant to ensure that if a participant decides purely on the basis of EV, as a locally rational observer should, then no preferential weighting of the positive and negative terms of the value equation will emerge.

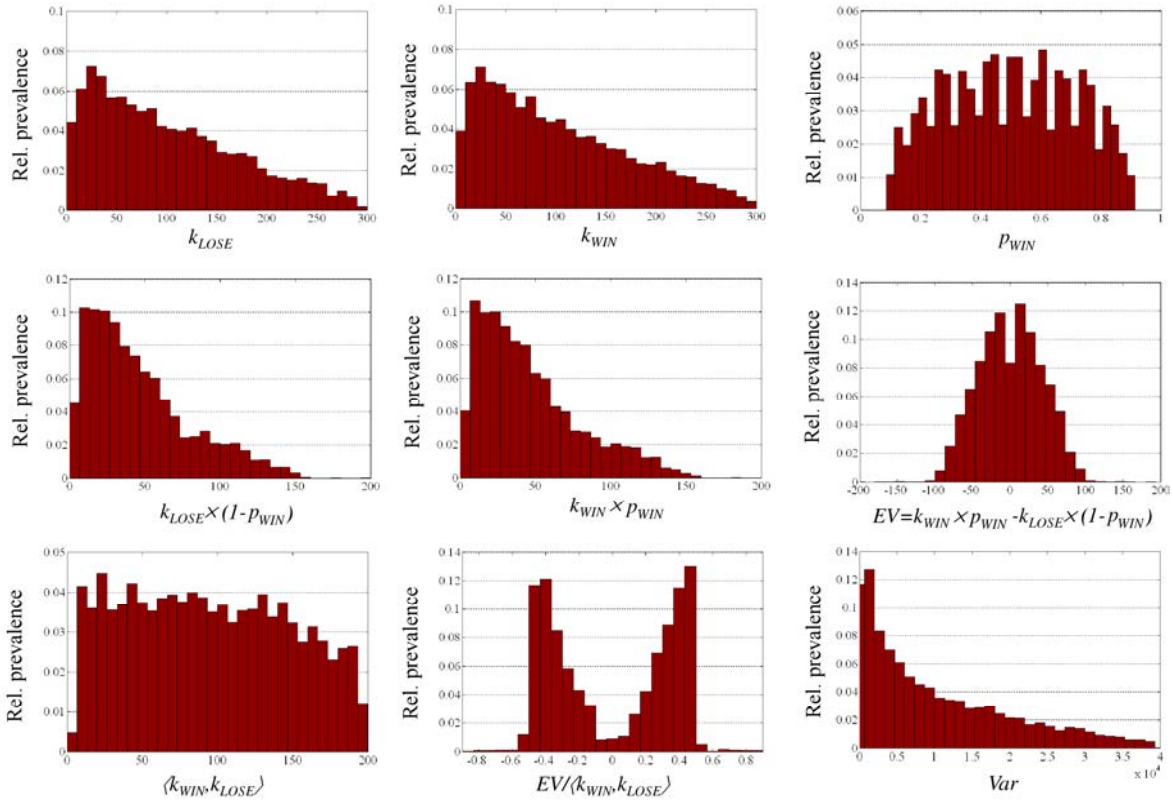

Figure 3. Histograms depicting the distribution of the values of the key economic parameters in the pool of stimuli. The y-axes represent the relative prevalence of each parameter value across the gambles in the pool.

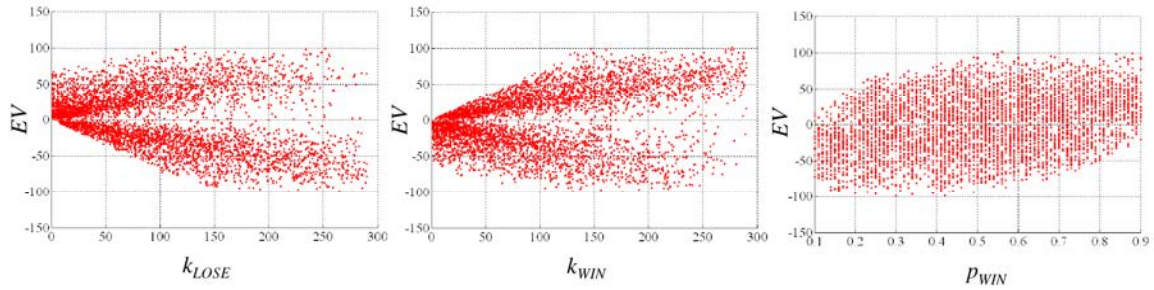

Figure 4. Scatter plots representing the relationships between EV and k_{WIN}, k_{LOSE} and p_{WIN}.

In the autonomic response monitoring experiment, conducted in Great Britain, the amounts were expressed in British Pounds (£). In the electroencephalography, functional MRI and patient experiments, conducted in Italy, the amounts were expressed in Euros (€). In the neuromodulation experiment, conducted in Brazil, the amounts were expressed in Reais (R$). To avoid altering the stimulus material, the display unit was simply swapped without introducing conversion factors; this was deemed acceptable considering that 1 £, 1 € and 1 R$ have, in spite of rather different foreign exchange rates, locally roughly similar purchasing power for everyday goods.

As shown in Figure 2, the gambles were presented in Arial font (size 36 points) in white colour over a black screen background. Potential loss always appeared on the top left, potential win on the top right, and winning probability at the bottom centre. The stimulus delivery and response collection paradigm was developed by the author under Matlab, using functions from the Cogent 2000 toolkit (Wellcome Laboratory of Neurobiology, UCL, London, UK); the script was adapted to meet hardware synchronization needs in each experiment.

2.3 Behavioural data analysis

For the purpose of characterizing the behavioural responses to the task, data from all healthy participants studied during the autonomic response monitoring, electroencephalography and functional MRI experiments were pooled together, yielding an aggregate group of 60 subjects (32 female, average age 34 years). Full demographic information and description of the data acquisition settings are provided in the relevant chapters. For organizational reasons only data from the first three experiments were considered for the present overall behavioural evaluation, as the patient behavioural experiment and the neuromodulation experiment were performed at significantly later dates.

First, within each individual session the reaction times (RTs) were z-transformed and trials for which they were outside 3 standard deviations from the average or exceeded 6 s were rejected (approximately 0.5%). Then, the EV sign discrimination, i.e. the ratio of accepted positive-EV gambles and rejected negative-EV gambles with respect to the total number of gambles, was calculated, alongside the overall ratio of gambles accepted (referred to as "acceptance rate") and the equivalent amount earned per-gamble, defined as the sum of the EVs of the accepted gambles divided by the total number of gambles (this normalization was necessary because the total number of gambles was different in the three experiments owing to different inter-trial interval and experiment duration).

Subsequently, in order to determine the predictive power of each individual economic parameter with respect to gamble acceptance or rejection, nine logistic regressions were performed, separately for k_{WIN}, k_{LOSE}, p_{WIN}, $k_{WIN} \times p_{WIN}$, $k_{LOSE} \times (1-p_{WIN})$, EV, $\langle k_{WIN}, k_{LOSE} \rangle$, $EV/\langle k_{WIN}, k_{LOSE} \rangle$ and Var. Such regressions were performed individually for each participant and, in order to adjust for inter-individual differences in overall task

performance, the corresponding Wald scores were normalized with respect to that for *EV*. Furthermore, the ratio of the logistic regression coefficients for the effect of potential gain and potential loss was also calculated, i.e. $\lambda=-\beta_{LOSE}/\beta_{WIN}$, as this provides a specific account of loss aversion.

To model the effect of the economic parameters on the RTs, individual linear regressions were also performed, having RT as dependent variable and each economic parameter as independent variable; here, $|p_{WIN}-0.5|$ and $|EV/\langle k_{WIN}, k_{LOSE}\rangle|$ were also considered, whereas they were excluded from logistic regression analyses, above, as they most likely have a non-monotonic relation to acceptance rate. The acceptance probability *w* as a function of *EV* was also calculated for each participant through bi-linear interpolation.

Statistical analysis was then conducted as follows. First, in order to confirm whether participants successfully distinguished risk-advantageous and disadvantageous gambles beyond random level, the individual *EV* sign discrimination scores were compared to 0.5 using a two-tailed one-sample t-test. Overall earnings per gamble were similarly compared against 0 £/€. Then, in order to check whether participants were deciding in a significantly risk-averse way, a one-sample t-test was performed to compare gamble acceptance rate values with respect to 0.5, and another one-sample t-test was performed to compare the regression ratio λ against 1. Subsequently, one-way between-subjects ANOVAs were performed, followed by Scheffé post-hoc comparisons, to test the hypothesis that these behavioural parameters (i.e. *EV* sign discrimination, overall acceptance rate, overall earnings and logistic regression ratio λ) were different across the three experiments (which could be due, for example, to the fact that the participants were recruited from different populations and other contextual factors).

As the aim was to characterize neural function related to the elementary representation of the economic parameters, one needs to ensure that the decisional prospects are being evaluated one-by-one and not in relation to the previous trials. To test this hypothesis, for each participant the acceptance rate was re-calculated separately for all trials preceded by an accepted or a rejected gamble; the procedure was repeated considering trials preceded by two consecutive accepted or rejected gambles. The resulting acceptance rates were compared using paired two-sample t-tests.

From the expected curvature of the value function one expects that the slope of the acceptance probability function with respect to EV may be different in the positive and negative domains (e.g., Kahneman and Tversky, 1979; Kahneman and Tversky, 1984; Kahneman, 2003; Wilkinson, 2008). To test this hypothesis, the acceptance probability curves were partitioned in three regions (EV<-20 £/€, -20 £/€<EV<20 £/€ or EV>20 £/€, see results), corresponding slopes were calculated by linear regressions, and compared using a one-way repeated-measures ANOVA, followed by Bonferroni-corrected post-hoc t-tests (over the 3 regions).

Also, a one-way within-subjects ANOVA was performed on the logistic regression Wald scores to test the hypothesis that the economic parameters under consideration (k_{WIN}, k_{LOSE}, p_{WIN}, $k_{WIN}\times p_{WIN}$, $k_{LOSE}\times(1-p_{WIN})$, EV, $\langle k_{WIN}, k_{LOSE}\rangle$, $EV/\langle k_{WIN}, k_{LOSE}\rangle$ and Var) have different power to predict gamble acceptance; here, Bonferroni-corrected post-hoc t-tests were applied with correction over the 9 parameters of interest. A similar analysis was performed to model confident/unsure responses, independently of the decision to accept or reject. Lastly, one-sample two-tailed t-tests with respect to 0 were performed to test the hypothesis that the linear regression coefficients modelling the effect of the economic parameters on the RTs are significantly different from zero; here, Bonferroni's correction was applied accounting for 11 comparisons over the parameters of interest (those listed above plus $|p_{WIN}-0.5|$ and $|EV/\langle k_{WIN}, k_{LOSE}\rangle|$).

2.4 Results

The full behavioural parameters for the three experiments, separately and together, are provided in Table 1. As expected, participants robustly differentiated between gambles having positive and negative *EV* above chance level (*EV* sign discrimination 0.82±0.08 vs. 0.5; one-sample t-test $t(59)=31$, $p<0.001$), and thereby earned a positive amount of currency throughout the task (average earn per gamble 12.4±3.0 £ vs. 0 £; one-sample t-test $t(59)=32$, $p<0.001$). Across the three experiments, there was a significant difference in *EV* sign discrimination ($F(2,59)=5$, $p=0.01$), i.e. participants differentiated positive and negative *EV* better in the autonomic response monitoring experiment than in the fMRI experiment (0.86±0.08 vs.0.79±0.08; p(Scheffé)=0.01), but the difference was relatively limited and did not impact the overall amount earned, which overlapped between the three groups.

Participants rejected the majority of gambles (acceptance rate 0.44±0.08 vs. 0.5; one-sample t-test $t(59)=5.5$, $p<0.001$), assigning more weight to potential losses than equivalent gains (logistic regression ratio $\lambda=1.3\pm0.7$, median 1.2, range 0.5-4.5; one-sample t-test $t(59)=3.5$, $p<0.001$). Also here, there was a significant difference between experiments ($F(2,59)=4.1$, $p=0.02$), in that participants in the EEG experiment were slightly more risk adverse than those in the fMRI experiment (0.42±0.09 vs. 0.48±0.06; p(Scheffé)=0.04), yet the regression ratio λ was comparable across experiments.

The propensity to accept was insensitive to the choice made on the previous trial (0.46±0.08 vs. 0.44±0.09; paired t-test p=0.1) and previous two trials (0.44±0.11 vs. 0.44±0.10; p=0.9). As shown in Figure 5a, the acceptance rate vs. *EV* curves for the participants in the three experiments were largely overlappable, and exhibited a monotonic increase: for the $EV<<0$ £/€ region, a plateau was observed, followed by a sharp increase in

the $EV \approx 0$ £/€ region and a shallower increase for $EV >> 0$ £/€; accordingly, the slopes were significantly different across these regions ($m = 0.5 \pm 1.6 \times 10^{-3}$ for $EV < 20$ £/€, $m = 1.6 \pm 0.4 \times 10^{-2}$ for -20 £/€ $< EV < 20$ £/€ and $m = 1.9 \pm 2.4 \times 10^{-3}$ for $EV > 20$ £/€; $F(2,118) = 420$, $p < 0.001$ and post-hoc $p(Bonf) < 0.001$).

As shown in Figure 5b, the Wald scores for predicting accept/reject response differed across the parameters under consideration ($F(8,472) = 106.7$, $p < 0.001$). There was no difference between k_{WIN} and k_{LOSE}, and the scores for these parameters were larger than for p_{WIN} (0.44±0.41 vs. 0.28±0.61; paired t-test $p(Bonf) = 0.01$). Accordingly, the Wald scores for $k_{WIN} \times p_{WIN}$ and $k_{LOSE} \times (1-p_{WIN})$ were comparable and larger than the average score for k_{WIN}, k_{LOSE} and p_{WIN} together (0.56±0.17 vs. 0.44±0.41; $p(Bonf) = 0.04$). Further, the relative score for EV was larger than those for $k_{WIN} \times p_{WIN}$ and $k_{LOSE} \times (1-p_{WIN})$ (1±0 vs. 0.56±0.17; $p(Bonf) < 0.001$), but was exceeded by that for dimensionless risk-advantageousness $EV/\langle k_{WIN}, k_{LOSE} \rangle$ than EV (1.19±0.22 vs. 1±0; $p(Bonf) < 0.001$). On the other hand, the relative Wald scores for $\langle k_{WIN}, k_{LOSE} \rangle$ and Var (0.04±0.06 and 0.04±0.07 respectively) were much smaller and did not differ significantly from zero.

The average RT was 3.0±0.8 s, and was significantly different across the three experiments ($F(2,59) = 13.2$, $p < 0.001$), i.e. RTs were shorter in the fMRI session than in the other experiments (2.4±0.6 vs. 3.4±0.7; $p(Scheffé) < 0.001$). As represented in Figure 5c, the RTs correlated positively with k_{WIN} ($r = 0.06 \pm 0.13$, $t(59) = 3.5$, $p(Bonf) = 0.009$), $k_{WIN} \times p_{WIN}$ ($r = 0.06 \pm 0.15$, $t(59) = 3.1$, $p(Bonf) = 0.03$), $\langle k_{WIN}, k_{LOSE} \rangle$ ($r = 0.04 \pm 0.11$, $t(59) = 3.0$, $p(Bonf) = 0.04$) and $|p-0.5|$ ($r = 0.06 \pm 0.11$, $t(59) = 4.2$, $p(Bonf) < 0.001$), and strongly negatively with $|EV/\langle k_{WIN}, k_{LOSE} \rangle|$ ($r = -0.20 \pm 0.13$, $t(59) = 9.8$, $p(Bonf) < 0.001$).

As anticipated, there was a strongly significant ($F(3,174) = 426.2$, $p < 0.001$) grading of EV across the four response levels (confident reject -32±33 £/€, unsure reject -12±14 £/€, unsure accept 27±27 £/€, confident accept 30±31£/€). There was a significant

interaction between choice and confidence, indicating a greater difference in *EV* between confident and unsure responses for rejected than accepted gambles ($F(1,58)=61.0$, $p<0.001$). Across all participants, confident responses were associated with lower acceptance rate (0.38±0.37 vs. 0.52±0.52, $t(59)=3.3$, $p=0.002$) and better *EV* sign discrimination (0.86±0.90 vs. 0.78±0.78, $t(59)=5.7$, $p<0.001$). They also attracted shorter RTs (2.9±0.7 s vs. 3.4±1.1 s, $t(59)=6.5$, $p<0.001$). T-tests demonstrated that confident responses were predicted by large k_{LOSE} (106.5±14.5 vs. 86.6±18.0 £/€, $t(59)=6.3$, $p(Bonf)<0.001$), small k_{WIN} (102.4±14.4 vs. 90.5±12.5 £/€, $t(59)=4.4$, $p(Bonf)<0.001$), negative *EV* (7.5±10.1 vs. -8.2±11.3 £/€, $t(59)=6.6$, $p(Bonf)<0.001$), negative $EV/\langle k_{WIN}, k_{LOSE}\rangle$ (0.10±0.12 vs. -0.08±0.12, $t(59)=7.1$, $p(Bonf)<0.001$), large $k_{LOSE}\times(1-p_{WIN})$ (38.0±7.4 vs. 46.9±7.0 £/€, $t(59)=6.5$, $p<0.001$), small $k_{WIN}\times p_{WIN}$ (38.7±6.2 vs. 45.4±8.8 £/€, $t(59)=4.3$, $p(Bonf)<0.001$) and large $|EV/\langle k_{WIN}, k_{LOSE}\rangle|$ (0.39±0.03 vs. 0.37±0.07, $t(59)=2.9$, $p(Bonf)=0.04$); no significant effects were found for p_{WIN}, $|p_{\mathrm{WIN}}-0.5|$, $\langle k_{WIN}, k_{LOSE}\rangle$ and *Var*. Accordingly, the Wald scores for predicting confident/unsure responses (independently of accept/reject decision) differed across the parameters under consideration ($F(10,590)=20.6$, $p<0.001$). The score for $EV/\langle k_{WIN}, k_{LOSE}\rangle$ was significantly larger than all others (14.8±8.3, $p<0.001$); whereas the scores for $|p_{WIN}-0.5|$ and $|EV/\langle k_{WIN}, k_{LOSE}\rangle|$ were smaller by comparison, i.e. 3.2±0.8 and 5.2±2.2, respectively.

Table 1 (following page). Full behavioural parameters for the three groups, given as mean±standard deviation. See text for parameter description. ANS: autonomic monitoring experiment. EEG: electroencephalography experiment: fMRI: functional MRI experiment.

Parameter	*EEG group*	*fMRI group*	*ANS group*	*Overall*
EV sign discrimination	0.81±0.07	0.79±0.08	0.86±0.08	0.82±0.08
Equiv. earned-per-gamble €/£	12.2±2.5 €	11.5±3.4 €	13.7±2.9 £	12.4±3.0 €/£
Acceptance rate $\langle w \rangle$	0.42±0.09	0.48±0.06	0.43±0.07	0.44±0.08
Acceptance $\langle w \rangle$ (previous 1 accepted)	0.45±0.09	0.48±0.07	0.43±0.08	0.46±0.08
Acceptance $\langle w \rangle$ (previous 1 rejected)	0.40±0.09	0.48±0.08	0.43±0.07	0.44±0.09
Acceptance $\langle w \rangle$ (previous 2 accepted)	0.45±0.11	0.47±0.07	0.40±0.13	0.44±0.11
Acceptance $\langle w \rangle$ (previous 2 rejected)	0.39±0.09	0.49±0.11	0.43±0.07	0.44±0.10
Regression ratio $\lambda=-\beta_{LOSE}/\beta_{WIN}$	1.53±0.90	1.21±0.48	1.24±0.63	1.32±0.68
Wald(k_{WIN}) / Wald(EV)	0.28±0.21	0.58±0.62	0.40±0.29	0.43±0.44
Wald(k_{LOSE}) / Wald(EV)	0.33±0.21	0.68±0.63	0.32±0.21	0.45±0.45
Wald(p_{WIN}) / Wald(EV)	0.19±0.15	0.37±0.97	0.27±0.28	0.28±0.61
Wald($k_{WIN} \times p_{WIN}$) / Wald(EV)	0.52±0.22	0.45±0.15	0.72±0.36	0.56±0.27
Wald($k_{LOSE} \times (1-p_{WIN})$) / Wald($EV$)	0.53±0.16	0.56±0.16	0.59±0.27	0.56±0.20
Wald($\langle k_{WIN}, k_{LOSE} \rangle$) / Wald($EV$)	0.03±0.05	0.03±0.04	0.06±0.09	0.04±0.06
Wald($EV/\langle k_{WIN}, k_{LOSE} \rangle$) / Wald($EV$)	1.21±0.20	1.30±0.18	1.07±0.24	1.19±0.22
Wald(Var) / Wald(EV)	0.03±0.05	0.04±0.05	0.05±0.10	0.04±0.07
Average RT	3.35±0.70 s	2.40±0.59 s	3.36±0.79 s	3.00±0.83 s
RT r-val for k_{WIN}	0.02±0.14	0.12±0.14	0.01±0.07	0.06±0.13
RT r-val for k_{LOSE}	-0.02±0.10	0.08±0.12	-0.03±0.09	0.02±0.12
RT r-val for p_{WIN}	0.02±0.13	-0.03±0.14	0.008±0.08	-0.002±0.12
RT r-val for $k_{WIN} \times p_{WIN}$	0.02±0.19	0.13±0.14	0.03±0.10	0.06±0.15
RT r-val for $k_{LOSE} \times (1-p_{WIN})$	-0.06±0.12	0.07±0.14	0.002±0.09	0.008±0.13
RT r-val for EV	0.09±0.21	-0.03±0.15	0.04±0.10	0.04±0.16
RT r-val for $\langle k_{WIN}, k_{LOSE} \rangle$	-0.02±0.11	0.17±0.11	-0.01±0.07	0.04±0.11
RT r-val for $EV/\langle k_{WIN}, k_{LOSE} \rangle$	0.09±0.21	-0.03±0.15	0.04±0.10	0.03±0.16
RT r-val for $\lvert EV/\langle k_{WIN}, k_{LOSE} \rangle \rvert$	-0.16±0.14	-0.33±0.13	-0.08±0.07	-0.20±0.13
RT r-val for $\lvert p_{WIN}-0.5 \rvert$	0.11±0.11	0.04±0.07	0.02±0.12	0.06±0.11
RT r-val for Var	-0.02±0.11	0.09±0.11	-0.005±0.08	0.03±0.12

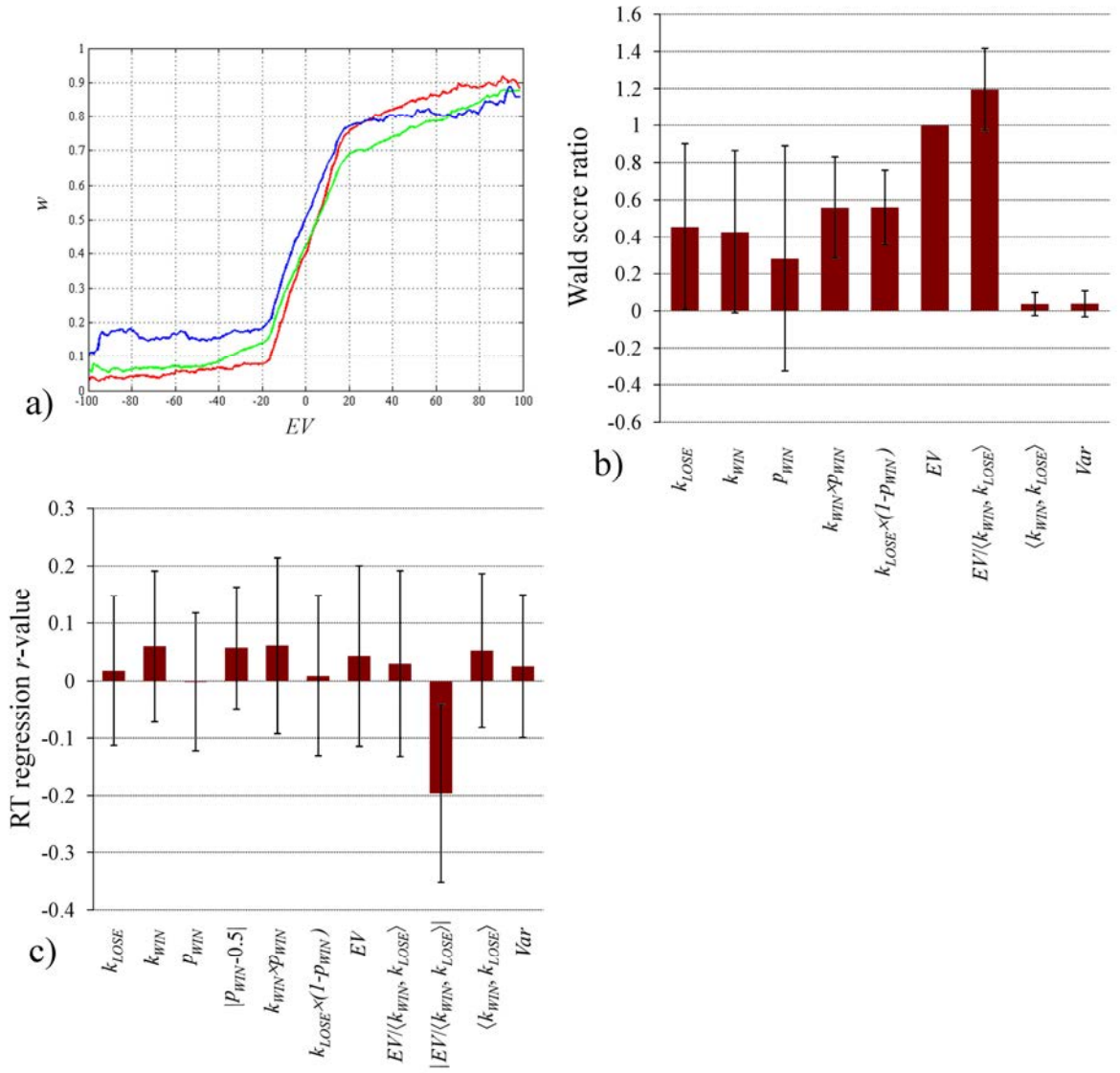

Figure 5. Behavioural responses to the risky decision-making task. a) Gamble acceptance rate (*w*) as a function of expected value (*EV*); the three curves correspond to averages in the autonomic monitoring (red), electroencephalography (green) and functional MRI (blue) experiments. b) Wald score ratios, representing the "relative weight" of each economic parameter in determining accept/reject response, relative to that of *EV*. c) Reaction-time (RT) regression coefficients (r-values), representing the positive or negative correspondence between the economic parameters and RTs. In b) and c), data from all three experiments were pooled together and error bars represent 1 standard deviation.

2.5 Discussion

2.5.1 Statistical properties of the gambles

In this investigation, particular care was taken to make sure that the gamble pool had statistical properties carefully controlled in order to avoid biasing the behavioural findings, e.g. artefactually enhancing the impact of a decisional parameter due to unbalanced correlation with *EV*. Of note, while it is customary in behavioural economics experiments to pay careful attention to these design aspects (e.g., Wilkinson, 2008), neuroeconomics studies tend to report limited information on the statistical properties of the stimulus material.

2.5.2 Decisional behaviour

As expected, participants robustly distinguished between positive- and negative-*EV* gambles, and performed the task in a significantly risk-averse manner, rejecting the majority of gambles in spite of the fact that the value distribution was symmetric with respect to zero. As represented by the ratio of the logistic regression coefficients, participants weighted potential losses more than corresponding gains. These findings provide some reassurance that, in spite of the absence of feedback and real economic endowment, participants did not simply perform a "cold" computation, but attached subjective valence to the potential losses and gains.

These results are in agreement with previous studies of inter-individual differences in risk and loss aversion, where participants were financially rewarded with a fraction of their earnings (Engelmann and Tamir, 2009). Due to the absence of real financial endowment, the level of loss aversion observed here was weaker with respect to real-world

economic behaviour, where potential losses are normally weighted around twice as much as equivalent gains (Tversky and Kahneman, 1992; Abdellaoui et al., 2007; Tom et al., 2007). Yet, the observation that "virtual endowment", i.e. task instructions in the absence of a real financial reward, was sufficient to obtain good performance and elicit clearly risk-averse behaviour is reassuring for the validity of the present experiment. Notably, behavioural studies indicate that small incentives such those commonly offered in experimental settings do not necessarily increase task performance, but may even have paradoxical effects, i.e. can reduce commitment by eliminating an "intrinsic motivation" element, and may also introduce socioeconomic status confounds (Gneezy and Rustichini, 2000; Wilkinson, 2008).

One expects that the function mapping expected value to the subjective attractiveness of a risky prospect should be concave for gains, and convex and considerably steeper for losses (Kahneman and Tversky, 1979; Kahneman and Tversky, 1984; Kahneman, 2003; Wilkinson, 2008). Yet, here it was observed that for $EV<<0$ the probability of gamble acceptance was essentially insensitive to EV, whereas in the $EV>>0$ regime a positive slope was apparent. This apparent inconsistency can be accounted for by considering that for $EV<<0$ the acceptance probability was so low that it introduced a "floor" effect, masking any potential continuous effect of EV on acceptance probability in this regime.

2.5.3 Independence of the responses to each prospect

As the interest here was on value computation and choice-option selection, no outcome feedback was provided, to eliminate reward-delivery and prediction error processing, attenuate or eliminate reward expectations, and thus avoid potential reinforcement through feedback and related changes in gambling strategy. Yet, it is

possible that participants, even though they did not know their ongoing "virtual balance", could still have attempted to mentally keep track of it based on the expected outcome of each accepted gamble, and that the reference against which each gamble is evaluated could therefore have fluctuated as a consequence, rather than representing a "pure" individual comparison between a riskless $EV=0$ prospect and a risky $EV\neq0$ one. This possibility can be excluded given that the propensity to accept was unaffected by the decision history up to two previous gambles, confirming that potential losses and gains were being evaluated only with respect to the available options within each individual gamble.

2.5.4 Differences across experimental sessions

There were minor behavioural differences between the experiments, manifesting in the RTs, *EV* sign discrimination and acceptance rate. These were, likely, attributable to contextual factors such as the specific population participants had been recruited from (including potential inter-cultural as well as professional background differences, e.g. academics vs. clinicians) and especially to the effect of the specific experimental settings (i.e. noisy, aversive MRI environment contrasted to quiet and dim lab). Such differences were, however, comparatively small and did not impact overall performance, intended as the overall ability to earn during the task.

2.5.5 Effect of the economic parameters on reaction times

In line with existing literature on response conflict, participants responded faster to gambles that were obviously advantageous or disadvantageous, and were considerably slower in deliberating on those that were nearly risk-indifferent, i.e. had $|EV/\langle k_{WIN}, k_{LOSE}\rangle|\cong0$ (e.g., see Carp et al., 2010). Further, participants responded faster to gambles

having $p_{WIN} \rightarrow 0.5$; rather than having to do with abstract economic processing, this effect most probably just reflected the fact that for $p_{WIN} \cong 0.5$ the task can be approximated as simple, direct comparison between potential gain and loss whereas for outcome probabilities distant from 50/50 level more demanding multi-parametric integration is necessary.

Additionally, it was observed that the gambles characterized by large average amount $\langle k_{WIN}, k_{LOSE} \rangle$, large potential gain k_{WIN} and large expected gain $k_{WIN} \times p_{\mathrm{WIN}}$ attracted slower responses. Such finding is in line with some (Tobler et al., 2007; Tom et al., 2007) but not all (Ernst et al., 2004; Matthews et al., 2004) previous studies, and is interpreted here as a specific form of behavioural risk aversion, by virtue of which one is more hesitant to deliberate on prospects presenting a large amount at stake, and prospects that appear to be particularly favourable upon a first evaluation (i.e., in terms of positive domain rather than full *EV* determination).

2.5.6 Effect of the economic parameters on confidence

Intuitively, one would expect response confidence to be mainly determined by whether a gamble has unitless risk-advantageousness $|EV/\langle k_{WIN}, k_{LOSE} \rangle|$ far or close to zero, i.e. to observe more confident responses to prospects that are obviously advantageous or disadvantageous. Surprisingly, this was not the case here: the effect of $|EV/\langle k_{WIN}, k_{LOSE} \rangle|$ was weaker in comparison to that of potential loss, gain and *EV*.

It was observed that confident responses were characterized by better *EV*-sign discrimination ability and reduced propensity to accept. Therefore, to the extent to which one considers *EV*-sign discrimination as a measure of task performance, response confidence was in part driven by metacognitive evaluation of the quality of one's value

representation and subsequent decision (Akama and Yamauchi, 2004; Brevers et al., 2012), but this was largely decoupled from "how obvious" each gamble was (indexed by $|EV/\langle k_{WIN}, k_{LOSE}\rangle|$).

Yet, self-awareness of decisional performance cannot explain the difference in acceptance rate, and the fact that confident responses were associated with large potential losses, small potential gain and negative expected value. These two findings can be interpreted as a form of behavioural risk aversion, whereby one is more subjectively confident in rejecting a given disadvantageous gamble than accepting a specular advantageous one. Further, the fact that confidence was more sensitive to *EV* for rejected than accepted gambles may be interpreted as indicating enhanced representation of negative with respect to positive value, potentially related to the different regimes of the value function (Kahneman, 2003).

3. Autonomic response monitoring

3.1 Background and motivation

It is well-established that in real-life circumstances decisions are based not only on "cold" cognitive evaluation of weighted outcome values but are also powerfully guided by emotional state and motivational responses (e.g., Critchley, 2005; Coricelli et al., 2007). The influence of such factors plausibly underlies, at least partially, the deviations from locally-rational behaviour like risk aversion which consistently characterize human and animal behaviour, and which support long-term survival by biasing decisions away from local optima when choosing them would not maximise long-term fitness, for example by prompting the avoidance of significant dangers (e.g. Damasio, 1996; Rolls, 1999; Coricelli et al., 2007; Platt and Huettel, 2008; Kalenscher and van Wingerden, 2011). A trivial metaphor could be a situation whereby one, faced with being in the desert with a single water tank, is likely to be driven away in fear from the prospect of filling up three more tanks if this entails even a minute risk of losing the only tank available and thereby inevitably dying. Additionally, convergent evidence suggests that emotional responses may not only "bias" decisional behaviour towards risk avoidance, but may act more generally also as "affective heuristics" that supplement and perhaps even supplant slower cognitive evaluation under situations where very little time is available and rapid "gut decisions" are needed (e.g., Jones et al., 2011).

In Jamesian views, the expression of emotions into peripheral autonomic arousal is not merely incidental, but drives feedback mechanisms which subserve the generation and maintenance of central representations of feeling states (e.g., Critchley, 2005). A natural extension of this concept is that autonomic feedback could be directly functional to

supporting and guiding decision-making. Such hypothesis, termed the "somatic marker hypothesis", was formulated by Damasio and co-workers (1996) on the basis of results showing that during the Iowa gambling task (which involves picking cards from different and unknown decks and learning which decks are "good", i.e. yield more cards leading to significant earnings, and which ones are "bad") healthy volunteers develop significant electrodermal responses to picking cards from "bad" decks even before they become consciously aware of which decks are "good" and which ones are "bad". In other words, bodily responses appear to develop and predict risky choices even before a participant becomes explicitly aware of the expected value associated with the choice they are about to make. In Damasio's views, such responses are functional to the establishment of effective central representations of the consequences of specific decisions, that are initially rooted in conditioned responses while high-level cognitive associations are established (Bechara et al., 1997).

While the somatic marker hypothesis was specifically formulated in the context of a complex task involving ongoing outcome feedback and substantial elements of uncertainty, the question arises whether associations between specific decisional parameters or situations and autonomic responses may exist generally. This initial experiment was therefore aimed at testing whether the economic parameters that characterize a risky prospect are significantly embodied in autonomic arousal, using a multimodal monitoring approach investigating a comprehensive set of sympathetic and parasympathetic axes.

Specifically, based on the reported association between choosing "bad" card decks and sympathetic arousal (Damasio, 1996; Bechara, 2004; Dunn et al., 2006), the prediction was formulated that gambles associated with negative expected value, large potential losses, highly unpredictable outcome and large variance would be associated with

enhanced autonomic arousal, particularly manifesting in the amplitude of electrodermal responses, and in fluctuations of cardiac frequency and blood pressure.

3.2 Participants, methods and data analysis

The experiment was performed on 19 healthy volunteers (11 females, 32±5 years, education 20±2 years), recruited among postgraduate students and academic staff at the University of Sussex Falmer campus. All participants had been educated in Great Britain, and were naive to the task and study design. None had received specific academic or business economics training, or had active experience in banking, financial investments or gambling beyond the level expected for the general population. No participant held a degree in Economics or similar subject, but approximately 20% were affiliated with the Department of Psychology and were thus broadly acquainted with decision-making research. Preliminary comparisons confirmed that the behavioural parameters, namely *EV* sign discrimination, gamble acceptance rate, RTs and logistic regression coefficients for this subgroup where within 2 standard deviations of the overall average and substantially overlapped those of the other participants. The experiment was formally approved by the research governance and ethics committee of the Brighton & Sussex Medical School (BSMS; PhD project no. 10/056/MIN) and conducted in the psychophysiology laboratory of the Psychiatry unit. As with the other experiments, participants did not receive any financial or material compensation. As detailed in the previous chapter, for this experiment the gambles were presented in British Pounds (£). No participant was taking any medication active on the nervous system, and no participant had a self-reported history of or current neurological or psychiatric problems, including significant depression and anxiety. All participants were clearly right-handed as determined with the Edinburgh

handedness inventory (Oldfield, 1971). All data acquisition and analysis steps were performed by the author personally.

Upon arrival, the purpose of the experiment was explained as detailed in the previous chapter, informed consent was obtained and participants sat on a comfortable chair situated approximately 1 m away from a 17" CRT computer screen in a dimly lit room. The electrocardiogram was recorded using Ag–AgCl cup electrodes positioned on the left and right arm, and left leg for reference (Einthoven's lead I configuration). The electrodes for recording electrodermal activity were positioned on the index and middle finger and filled with isotonic gel. In order to record real-time beat-to-beat blood pressure, a volume-clamp device (Finometer, Finapres BV, Arnhem, NL) was utilized; the cuff was positioned on the thumb and the hydrostatic height reference was secured at heart level behind the chair. In order to effectively record thoracical and abdominal respiration, a custom remote pressure sensor respiratory plethysmography device, previously engineered and tested by the author, was utilized with the pressure-sensitive belts positioned at nipple and umbilicus level (see Caldiroli and Minati, 2007).

Participants responded using the 1-4 keys of a standard computer keyboard, corresponding to confident reject, unsure reject, unsure accept and confident accept. The experimental paradigm was divided in four parts, each lasting approximately 7 min, separated by brief pauses. In order to reduce electrodermal habituation and limit discomfort due to finger volume clamping, half way through the session the electrodermal recording electrodes and the volume clamping cuff were moved to the contralateral hand. The left/right order was counterbalanced across participants, and the free hand was used to deliver all responses using the keyboard.

The electrocardiographic signal was amplified with an isolated instrumentation preamplifier (mod. 1902, CED Ltd., Cambridge, UK), and the electrodermal signal was converted using a transconductance amplifier (mod. 2502, CED). All signals were digitized

through a 'power1401' converter (CED) operating at a sample rate of 200 Hz. As detailed in the previous chapter, gamble presentation and equipment synchronization were controlled by a script written by the author in Matlab and Cogent. In order to maintain measurement accuracy, the Finometer device requires frequent calibration, which blanks the signal. To overcome this problem, the author reverse-engineered the device communication protocol and implemented synchronization with the stimulation paradigm through an RS232 link, making sure that calibration would occur before each gamble, blanking the signal at a moment when this results in no loss of information. For this experiment, 160 gambles were shown. A slow, randomly-jittered design was utilized, in order to permit analysis without making assumptions on the summation of individual responses and limiting physiological habituation. The inter-trial interval was 11.0±1.2 s. The first 4 gambles following each pause were always considered "warm-up" and not considered for further analysis.

All physiological data were analyzed with custom Matlab scripts developed by the author. Firstly, all signals were band-pass filtered with second-order Butterworth filters, applied on the direct and temporally inverted time-series to compensate temporal shifts. For the electrocardiogram, the filter range was set to 1-30 Hz. For the blood pressure signal, the range was 0.01-10 Hz. For the electrodermal signal, the range was 0.01-5 Hz. For respiration, it was 0.001-0.5 Hz. Subsequently, the electrocardiogram was processed with a peak-picking algorithm yielding the beat-to-beat inter-beat interval. The respiration signal was similarly processed to obtain the respiratory interval and the peak-to-peak amplitude, correlating linearly with tidal volume (Caldiroli and Minati, 2007). The blood pressure signal was processed extracting the systoles and diastoles to derive the corresponding mean arterial pressure. To obtain a proxy of vascular tone, the transit time between R-wave and pressure wave was also calculated. The time-courses of the resulting physiological variables were firstly interpolated to 10 Hz to permit subsequent windowing,

then detrended with fourth-degree polynomials to remove variance related to spontaneous drifts, and finally transformed into percent change values, to remove the effect on inter-individual differences in average levels. The resulting signals were epoched between [-2, 12] s with respect to stimulus onset and the pre-stimulus period was subtracted as baseline reference.

The resulting grand-average traces are shown in Figure 6. Predicated on these traces, the following averaging windows of interest were defined: [2.4, 3.4] s, [3.8, 4.8] s and [6, 8] s for ΔIBI (inter-beat interval), [2.5, 3.5] s, [5.8, 7.1] s and [9, 10] s for ΔMAP (mean arterial pressure), [2.5, 3.5] s, [3.8, 4.8] s and [5.7,7.7] s for ΔrPTT (R-wave to pulse transit time), [1.6, 3.8] s, [4.8, 6.8] s and [8,10] s for ΔSCL (skin conductance level), and [4, 6] s for ΔRI (respiratory interval) and ΔRA (respiratory amplitude).

After computation of the averages, outlier rejection was performed using the criterion of 3 standard deviations from the average. Approximately 5% of measurements overall were rejected, mainly due to movement artefacts. Firstly, one-sample two-tailed t-tests with respect to 0% change were performed, to test the hypothesis that gamble presentation overall (i.e., irrespective of the parameters) elicited significant autonomic arousal. Subsequently, linear regressions were performed, separately for each individual, having as independent variable each decisional parameter and as dependent variable each physiological measure. The RTs were always included as nuisance covariate. The resulting correlation coefficients were taken as summary statistics and entered in one-sample two-tailed t-tests with respect to zero to test the hypothesis of significant correlation at group level. Similarly, F-values for the orthogonalized effects of accept/reject and confident/unsure responses were entered in second-level analyses to test for autonomic correlates of response. Bonferroni's correction was applied multiplying the uncorrected p-values by the number of economic parameters, i.e. 11.

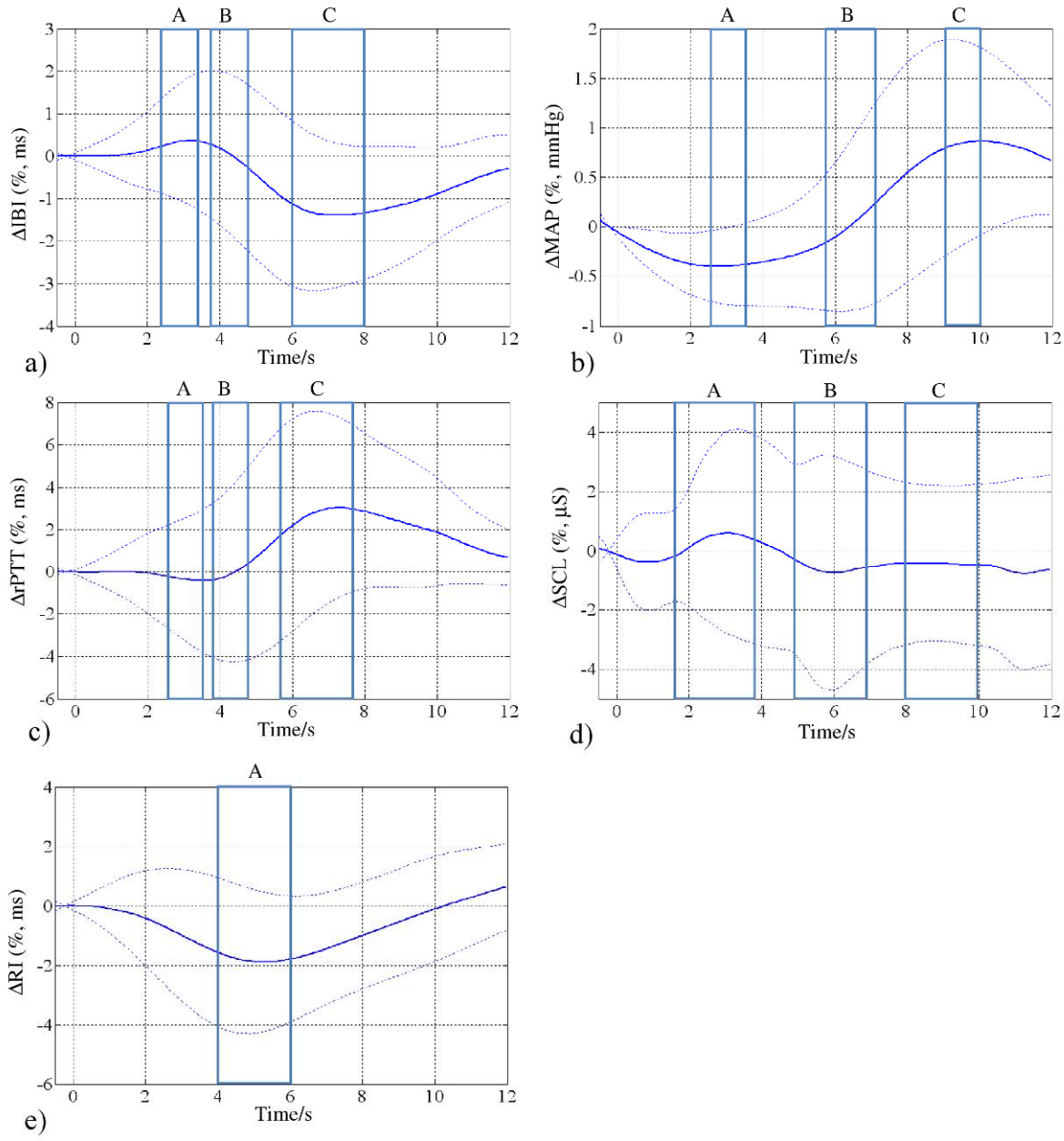

Figure 6. Grand-average traces representing the autonomic responses to gamble presentation, independently of the economic parameters. The dotted lines represent 1 standard deviation, and the boxes correspond to the averaging windows utilized for statistical analysis.

3.3 Results

The grand-average autonomic responses are charted in Figure 6. As shown, gamble processing elicited a initial slowing of the heart rate, represented as a longer inter-beat interval (IBI), which was, however, not significant (0.3±1.4%, [2.4, 3.4] s window).This was followed by a significant acceleration occurring around 3 s later (-1.3±1.7%, [6, 8] s; t(18)=3.5, p=0.003). After stimulus onset, the mean arterial pressure (MAP) initially dropped significantly (-0.4±0.3%, [2.5, 3.5] s; t(18)=5, p<0.001), and subsequently raised after a delay of around 7 s (0.8±1.0%, [9, 10] s; t(18)=3.7, p=0.002). The pulse transit time (rPTT) initially became slightly shorter (-0.4±3.1%, [2.5, 3.5] s) then increased significantly after around 3 s (2.8±4.5%, [5.7,7.7] s; t(18)=2.8, p=0.01). Throughout the experimental session, the skin conductance level (SCL) fluctuated randomly, without clearly identifiable responses to the gambles. On average, there was an initial elevation (0.4±2.9%, [1.6, 3.8] s) followed by a drop (-0.6±3.5%, [4.8, 6.8] s; -0.4±2.6%, [8,10] s), but neither effect was statistically significant. Lastly, after appearance of each gamble the respiratory interval (RI), interpolated across breaths, briefly dropped (-1.8±2.4%, [4, 6] s; t(18)=3.4, p=0.003); no significant effect on respiratory amplitude (RA) was observed.

The initial elevation of ΔIBI ([2.4, 3.4] s) correlated positively with $|p_{WIN}-0.5|$ (r-value 0.07±0.08, t(18)=3.4, p(Bonf)=0.03, see Figure 7a), and a non-significant trend, not surviving correction for multiple comparisons, was also observed in the intermediate, zero-crossing window ([3.8, 4.8] s, r-value 0.06±0.09, t(18)=3.0, p(Bonf)=0.09, see Figure 7b). Further, the ΔMAP in the intermediate window ([5.8, 7.1] s) exhibited a trend towards positive correlation with $k_{WIN} \times p_{WIN}$ (r-value 0.04±0.05, t(18)=3.2, p(Bonf)=0.06, see Figure 7c), which however did not survive correction for multiple comparisons. No other modulatory effects were observed; particularly, correlations with SCL were clearly absent,

and EV , k_{LOSE} and $k_{LOSE}\times(1-p_{WIN})$ did not correlate with any autonomic variable, even at un-corrected thresholds. No effect of accept vs. reject or confident vs. unsure responses were found.

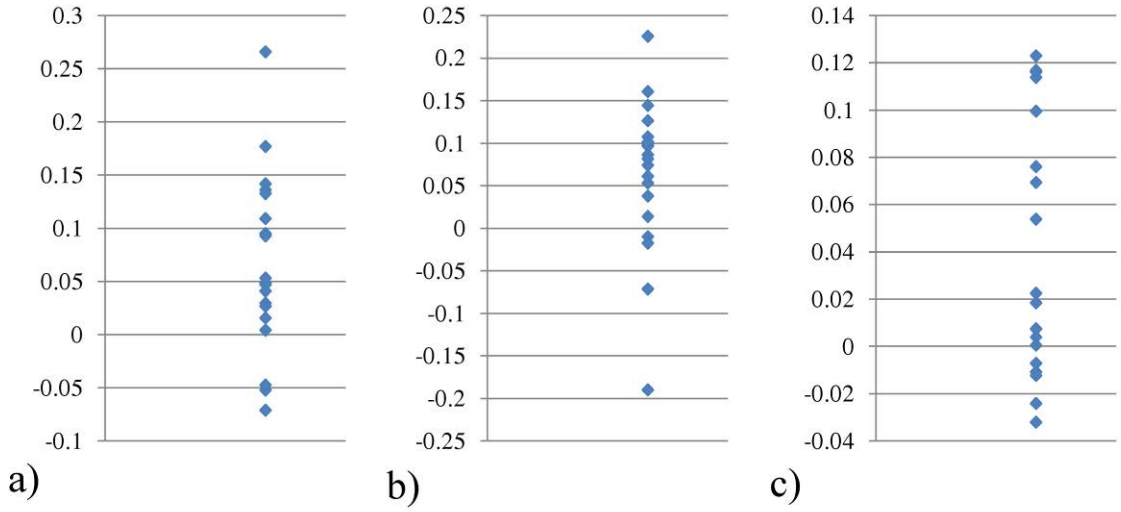

Figure 7. Scatter plots for the r-values corresponding to linear correlations between a) ΔIBI in the [2.4, 3.4] s ('A') window and $|p_{WIN}-0.5|$, b) ΔIBI in the [3.8, 4.8] s ('B') window and $|p_{WIN}-0.5|$, c) ΔMAP in the [5.8, 7.1] s ('B') window and $k_{WIN}\times p_{WIN}$.

3.4 Discussion

3.4.1 Overall autonomic effect of gamble presentation

As anticipated, gamble presentation and processing elicited a typical bi-phasic orienting response, characterized by slowing heart rate and falling arterial pressure, followed by acceleration and increased pressure. Such responses are frequently encountered in experimental settings irrespective of the specific stimulus material used, and represent primarily a shift of attention and increased mental effort (Barry, 1990; Siddle, 1991; Vila et

al., 2007). Of note, the grand-average traces, shown in Figure 6, did not reveal a significant electrodermal response to stimulus presentation, highlighting that the paradigm was relatively "cold" and devoid of emotional content, resulting in very limited peripheral expression of feeling states (Critchley, 2002).

3.4.2 Differential representation of the economic parameters

Gambles bearing outcome probabilities near 50% elicited a smaller bradycardia response than the others (Figure 7a and b). Such effect parallels the behavioural observation, described in the previous chapter, of faster responses to such gambles. Rather than indexing a primary embodiment of an economic parameter, this effect probably represents the simpler fact that gambles with $p_{\mathrm{WIN}} \rightarrow 0.5$ are simpler to process, since one can approximately compare k_{LOSE} and k_{WIN} rather than abstractly integrating all three parameters. The effect is therefore of limited theoretical interest.

The overall positive correlation observed between $k_{WIN} \times p_{\mathrm{WIN}}$ and blood pressure (Figure 7c), albeit very weak and not surviving correction for multiple comparisons, may represent a positive arousal effect, indexing the "exhilarating" consequence of being faced with a large expected gain; large transient increases in blood pressure in response to very positively-valenced stimuli have reported in several previous psychophysiology experiments using verbal as well as graphic emotional material (Sarlo et al., 2005; Ribeiro et al., 2007; Minati et al., 2009). These effects provide some reassurance that the experiment had sufficient statistical power (i.e., adequate number of participants, stimuli and physiological signal-to-noise ratio) to reveal the embodiment of the economic variables. Yet, k_{LOSE}, $k_{LOSE} \times (1 - p_{\mathrm{WIN}})$, p_{WIN} and EV were clearly not represented in

differential autonomic responses, irrespective of the axis being probed and corresponding balance of sympathetic/parasympathetic innervation (e.g., Janig, 2006).

This negative finding may appear to be at odds with recent experiments demonstrating that heart rate and skin conductance track reward expectation and respond differently to experienced gains and losses (Osumi and Ohira, 2009; Ohira et al., 2010; Wilkes et al., 2010; Studer and Clark, 2011). Yet, there is a crucial difference in the experimental settings. Such results were obtained under realistic gambling situations, e.g. using electronic gambling machines and roulette, which were highly engaging and involved substantial on-line feedback on decisional outcome. On the contrary, the task under consideration here was relatively "cold", and was devoid of any element of on-line outcome feedback: participants simply had to evaluate the expected value of each gamble and deliberate, without engaging in a realistic game. While concentrating on "pure" value computation has advantages in terms of isolating the neural representation of the distinct parameters, it also has limitations in that the level of emotional engagement is likely to be limited, thus potentially concealing effects that would be observable in more naturalistic settings.

3.4.3 Implications for the somatic marker hypothesis

The results of the present experiment demonstrate that robust discrimination between risk-advantageous and disadvantageous gambles alongside significant deviation from purely rational behaviour can be obtained in the absence of significant autonomic embodiment of the economic parameters, most notably of potential loss,risk and value.

As discussed above, the somatic marker hypothesis was formulated in the context of a very different task, the Iowa Gambling Task, in which participants were presented with ongoing feedback about losses and gains following picking each card, and needed to

continuously adjust their subjective beliefs about which decks were "good" and which ones were "bad" (Damasio, 1996; Bechara, 2004; Dunn et al., 2006). There is a conceptual difference in that their task included substantial uncertainty whereas the risky gambles used here were, by definition, devoid of any element of uncertainty. Further, the highly interactive and complex nature of Iowa Gambling Task likely made their experiments significantly more demanding and emotionally arousing in comparison with the more straightforward and "cold" evaluation of the mixed gambles presented here.

Further still, one needs to consider that somatic markers may in fact exist at two levels, namely a "body loop", which involves measurable systemic autonomic arousal and subsequent afferent feedback, and an "as-if loop", whereby central representations of autonomic arousal patterns are engaged and drawn upon without the generation of actual, measurable physiological responses. The "body loop" would be engaged primarily by novel situations and highly emotionally-valenced stimuli, and would, over the life span, gradually transfer the corresponding somatic-behavioural associations to the "as-if loop" processing for situations that one has become accustomed to (Bechara, 2004). Such hypothesis remains a rather speculative one, as no experiment has yet been performed that would clearly distinguish the activity of the putative "as-if loop" from other mechanisms of central arousal (Rolls, 1999; Dunn et al., 2006). Within the framework of this "dual-loop" hypothesis, it could be that the present task did not activate the "body loop" because risky decision-making is performed routinely and the task was relatively emotionally un-engaging, but this wouldn't then necessarily imply that somatic markers are intrinsically not engaged in the kind of elementary value computation addressed here (Heims et al., 2004).

In summary, the results of the present experiment suggest that autonomic expression is not fundamental for the representation of economic parameters in the face of an elementary risky prospect. Due to the relatively "cold" nature of the present task and the

absence of declarative feedback, the autonomic responses were heavily constrained, and for this reason as well as for the fundamental difference in task design the present experiment should not be viewed as a direct verification of the validity of the somatic marker hypothesis. Yet, the present findings do highlight that differential autonomic representation of economic parameters is contingent on specific contextual features and not an indispensable component of risky decision-making processes. Future research is particularly needed to confirm the findings of this experiment in presence of a tangible level of financial endowment, and to evaluate whether contextual factors such as time pressure may lead to the emergence of significant autonomic modulations to individual risky prospects.

4. Electroencephalography (EEG)

4.1 Background and motivation

The majority of neuroeconomic studies performed to date are based on fMRI rather than electrophysiological techniques, because experimental hypotheses related to functional specificity generally necessitate good anatomical detail. Yet, the high spatial resolution of fMRI comes at the price of very poor temporal resolution, determined by the physiological time-constant characterizing the haemodynamic response, which is on the order of 3-5 s. Further, comparatively large fluctuations in the overall intensity of post-synaptic activity, corresponding to intense metabolic demand, are necessary to elicit changes in the blood-oxygen level-dependent (BOLD) signal that are large enough to be detected by fMRI (e.g. Logothetis and Pfeuffer, 2004; Logothetis, 2008). On the other hand, electroencephalography (EEG) has excellent temporal resolution, because the recorded electrical signal directly reflects the generation of post-synaptic potentials, and is not filtered by slow haemodynamic processes. Since temporal summation of coherent post-synaptic potentials is necessary to obtain detectable signals, EEG provides a rather complementary account of neural activity in comparison to fMRI, emphasizing highly-synchronous bursts of activity over slower but more metabolically-demanding fluctuations. The topographical information provided by the two techniques is generally well-correlated (Oakes et al., 2004; Minati et al., 2008; Visani et al., 2011) though, unless very large numbers of electrodes are used, the anatomical resolution of EEG is limited by volume conduction effects that make it difficult to localize the neural generators of a given effect on the basis of scalp topographic maps (e.g., Michel et al., 2004).

To date, EEG studies of decision making have mostly investigated neuroelectrical activity evoked by the presentation of outcome feedback, particularly two event-related potential (ERPs) components known as the error-related negativity (ERN) and the correct-related positivity (CRP), which appear to originate from the medial frontal and anterior cingulate cortex, and which respond to reward expectation and discrimination between gains and losses (e.g., Pedroni et al., 2011). These components share a remarkable similarity and probably largely overlap in terms of underlying generators with the medial frontal negativity (MFN), which is thought to track reward prediction and prediction error signalling activity in the mesolimbic dopaminergic system, expressed through its influences on deep-layer frontal neocortical activity (e.g., Holroyd et al., 2008).

The encoding of primary economic features, particularly outcome probability, has, although less extensively, also been investigated using elementary tasks, and significant effects have been reported for the P3 and N5 components (Miltner et al., 1997; Yeung and Sanfey, 2004; Hajcak et al., 2006; Polezzi et al., 2008 and 2008b; Polezzi et al., 2010). Notably, the available studies have considered time-locked activity only, and spectral changes in spontaneous activity during decision making have not yet been comprehensively investigated, in spite of the well-established relationship between modulations in the alpha, beta and theta EEG frequency bands, neural excitability and level of central arousal (Kolev et al., 2001; Schutter et al., 2004; Davis et al., 2011).

Based on the limited literature available to date, one expects that in spite of the absence of outcome feedback and related dopaminergic signalling, value determination in the context of individual risky prospects should be neuro-electrically expressed through specific relationships between economic the parameters and different aspects of EEG-visible neural activity (Polezzi et al., 2008 and 2008b; Polezzi et al., 2010; Pedroni et al., 2011; Davis et al., 2011).

The present experiment was aimed at testing the prediction that the process of value determination for risky gambles elicits specific neuroelectric signatures tracking the encoding and integration of potential gain, loss, outcome probability, value and other associated parameters. In particular, since the structures and networks involved in coding potential rewards and losses are likely to be, at least to some extent, segregable (e.g., Trepel et al., 2005; Levin et al., 2012) the prediction was made that the magnitude of potential gains and losses would be expressed through modulations of differentiable aspects of neuroelectric activity.

Further, given that time-locked evoked potentials and induced changes in spontaneous oscillations index different aspects of integrative neural activity (e.g., Schürmann and Başar, 2001; Penny et al., 2002), it was predicted that the two would reveal different aspects of gamble processing through non-overlapping correlations with the economic parameters.

More specifically, since mid- and long-latency event-related potentials are representative of highly abstract integrative processing whereas frequency-domain changes in the spontaneous rhythms tend to track more widespread, less regionally-specific fluctuations in brain state (e.g., Pulvermüller et al., 1997; Herrmann and Knight, 2001; Kolev et al., 2001; Schutter et al., 2004; Palva and Palva, 2007), the tentative prediction was formulated that expected value and risk-advantageousness (i.e., the two parameters requiring more integrative processing) would preferentially modulate event-related potential fluctuations, whereas lower-level but highly salient features such as amount magnitude, outcome probability and risk would elicit changes in brain state visible as modulations of the spontaneous EEG rhythms.

4.2 Participants, methods and data analysis

The experiment was performed on 19 healthy volunteers (11 females, age 35±9 years, education 18±3years), none of whom had participated in the autonomic monitoring session, and who were recruited among medics, paramedics and researchers at the Fondazione IRCCS Istituto Neurologico "Carlo Besta" in Milano (Italy). All participants had been educated in Italy, and were naive to the task and study design. As for the autonomic response experiment, none had received specific academic or business economics training, or had experience in banking, financial investments or gambling. The experiment was formally approved by the research governance and ethics committee of the Brighton & Sussex Medical School (BSMS; PhD project no. 10/056/MIN) as well as by the ethics committee of the Fondazione IRCCS Istituto Neurologico "Carlo Besta" (project no. fMRI-DM), and was conducted in the neurophysiology unit of the institute. Participants did not receive any financial or material compensation. For this experiment, the gambles were expressed in Euros (€). In compliance with local rules, data acquisition involving a neuropsychological paradigm was supervised by a psychologist (Dott.ssa Sylvie Piacentini) and by clinical neurophysiologist (Dott.ssa Silvana Franceschetti), who also took the clinical history of the participants, none of whom had any past or current neurological or psychiatric condition or was taking any relevant medication. All participants were clearly right-handed as determined with the Edinburgh handedness inventory (Oldfield, 1971). All baseline electroencephalograms were reported as clinically normal.

Upon arrival, the aim of the study was explained, using instructions that were identical to those in the autonomic response experiment, but written in Italian language. Informed consent was obtained, and participants sat on a comfortable chair situated approximately 2 m away from a 19" LCD computer screen in a dimly lit, electrically

shielded room. The electroencephalogram was recorded using a 30-channel (10/10 international system) flexible cap which, according to local rules, was positioned on the participant and filled with gel by a neurophysiology technician (TNFP Alice Granvillano or Elena Schiaffi). All other data acquisition steps and all data analysis were performed by the author personally. During cap positioning by the technician, the author monitored the positions of the electrodes using an electromagnetic tracking system (Patriot, Polhemus Inc., Colchester VT, USA) to confirm that they were within 10% of the intended standardized location. All impedances were kept below 3 kΩ, and the signal was recorded with respect to the linked ears. A standard clinical electroencephalograph (BrainQuick, MicroMed SpA, Treviso, IT) recording at 500 Hz was utilized.

As with the previous experiment, stimuli were presented through a script written in Matlab and Cogent, which sent synchronization markers through an RS232 link. Participants responded on the same scale, but here the reject responses were delivered with the left hand ('x' and 'c' keys) and the accept responses with the right hand ('n' and 'm' keys). Also, 320 gambles were shown according to a randomly-jittered rapid design, having an inter-trial interval of 4.6±0.6 s. With respect to the autonomic response experiment, the larger number of gambles was motivated here by the generally higher noise in the raw signal, and the inter-trial interval was shortened considering that all central processes of interest take place within a few seconds of gamble onset. To maintain performance and reduce habituation, stimuli were delivered in four 6 min. blocks separated by pauses.

The data were processed using custom Matlab scripts developed by the author, partially re-using code from the EEGLab toolkit (University of California, San Diego CA, USA), running on a Sun Blade 2500 workstation (Sun Microsystems Inc., Santa Clara CA, USA). Firstly, the signal was re-referenced to average and band-pass filtering was performed with a second-order Butterworth filter in the range 0.1-30 Hz. Second,

independent component decomposition was performed and, for each participant, the components clearly representing eye blinks or movement artefacts were subtracted. Third, the filtered signals were epoched in the [-2, 5] s peristimulus interval, the epochs clearly containing residual artefacts were manually excluded (approx. 1%) and the pre-stimulus average potential was subtracted. For time-domain analysis, the root-mean-square power and grand-average waveforms were calculated, as shown in Figures 8a and 8b. On such basis, in order to represent the individual peaks indexing early and mid-latency activity as well as the longer, protracted components, the following averaging windows were defined: [110, 150] ms, [170, 230] ms, [270, 330] ms, [330, 380] ms, [380, 600] ms, [750, 1250] ms, [1250, 1750] ms, [1750, 2250] ms, [2250, 2750] ms, [2750, 3250] ms and [3250, 3750] ms. To attempt to localise the underlying cortical generators, low-resolution electrical tomography (sLORETA) was performed, searching for the smoothest current distribution on the basis of the scalp potential measured at the digitized positions of the electrodes (Pascual-Marqui et al., 1994).

Time-frequency analysis was performed decomposing the filtered signals with the Morlet wavelet kernel (Goupillaud et al., 1984) to calculate instantaneous changes in the range [0, 30] Hz in steps of 1 Hz. The resulting spectrogram, reported in Figure 8c, indicated an early increase in theta power, indexed by a window at [250, 750] ms for [4, 8] Hz, and a longer-lasting drop in alpha power, plotted in Figure 8d, for which averaging windows were defined at [750, 1250], [1250, 1750], [1750, 2250], [2250, 2750], [2750, 3250], [3250, 3750] ms for [8, 12] Hz.

As for the autonomic response experiment, after computation of the averages, outlier rejection was performed using the 3 standard deviation criterion, leading to rejection of a further 3% of measurements. Linear regressions were thereafter performed separately for each individual, having as independent variable each decisional parameter and as dependent variable potential (or power density, scaled in arbitrary units) in a given

time window at a given electrode. The RTs were always included as nuisance covariate. The resulting correlation coefficients were taken as summary statistics and entered in one-sample two-tailed t-tests with respect to zero to test the hypothesis of significant correlation at group level. Topographical maps of the t-values were generated using code based on the original EEGLab topographic engine. Here Bonferroni's correction was implemented by diving the base α=0.05 by 30 for number of channels and 11 for the number of economic parameters, resulting in a critical α=0.0001.

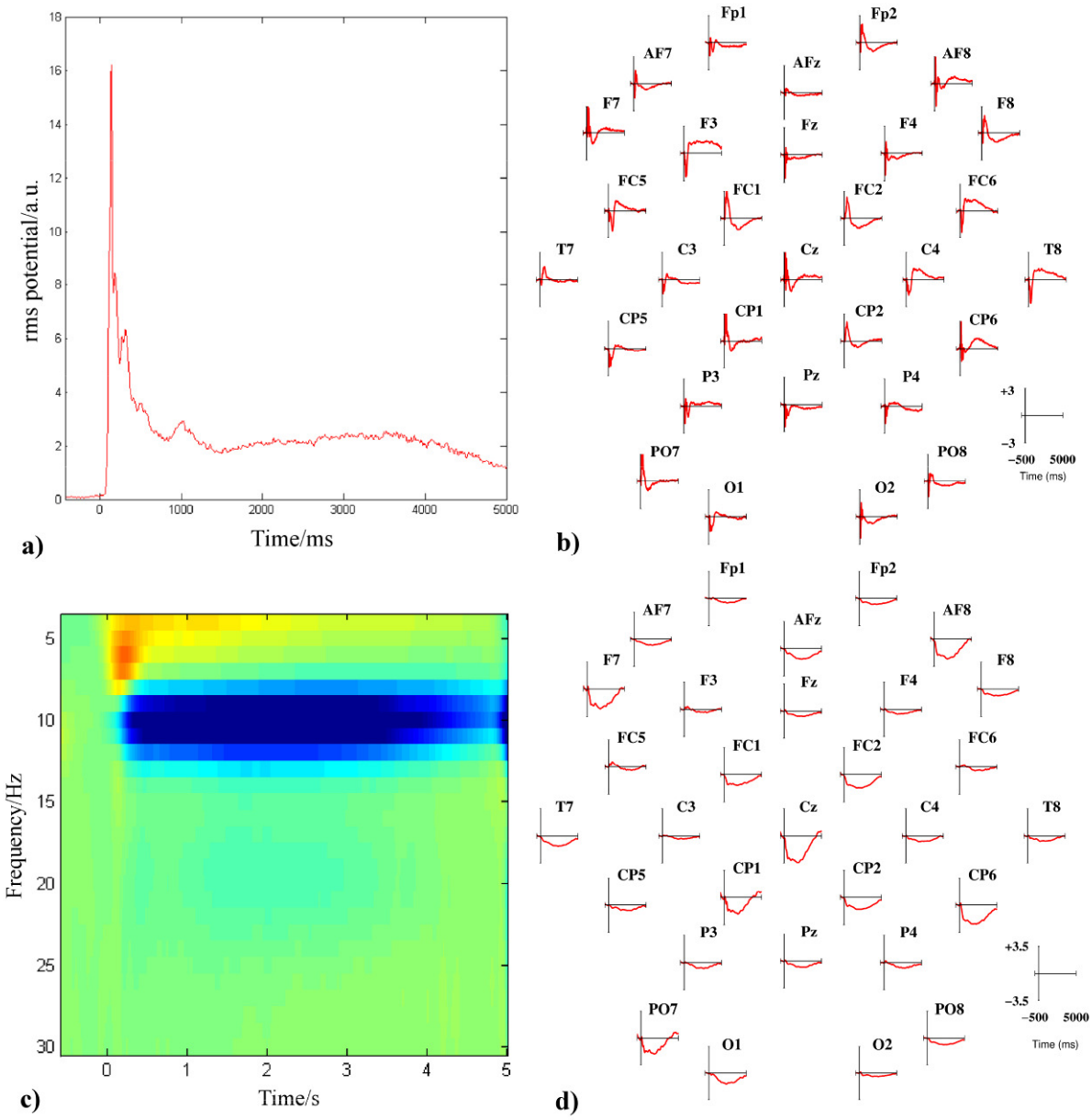

Figure 8 (previous page). EEG grand-average effects, representing changes due to gamble presentation independently of the economic parameters. a) Root-mean-square potential (represented in arbitrary units), calculated over all electrodes, representing "evoked power" as a function of time. b) Topographic time-course map of the average evoked potential. c) Spectrogram (represented in arbitrary units) representing power density change as a function of time following gamble onset. d) Topographic time-course map of the average change in alpha-band (8-12 Hz) power. In b) and d), for graphical reasons the most peripheral electrodes, i.e. T9 and T10, have been omitted.

4.3 Results

The grand-average effects, representing changes in neuroelectric activity irrespective of the economic parameters, are represented in Figure 8. Root-mean-square analysis of the evoked potential (Figure 8a) revealed a initial increase of activity in the range 0-700 ms, which corresponded to a positive complex wherein the P2, P3a and P3b components appeared around 130 ms, 300 ms and 450 ms respectively (Figure 8b). This group of components was followed by a slow and persistent potential fluctuation, lasting until around 5 s after gamble onset, peaking between 2-3 s and presenting as a negative potential in frontal-central regions and a positive potential over right central-temporal and left frontal sites (Figure 9).

Cortical current density reconstructed by sLORETA was largest in the inferior, middle and superior frontal gyri bilaterally, implicating a circuit encompassing the dorsal-lateral prefrontal cortex (DLPFC), ventral-lateral prefrontal cortex (VLPFC) and supplementary motor area (SMA) in the generation of this potential (Figure 10). As represented in the spectrogram in Figure 8c, gamble presentation elicited an initial, rapid increase in theta activity (peaking around 6 Hz, at around 500 ms), followed by a strong

and persistent decrease in alpha activity (centre frequency 10 Hz, 200 ms to around 4.5 s); the corresponding topographical time-course plots (Figure 8d) and maps (Figure 11) indicated that this effect was more prominent in the central scalp region.

No significant parametric modulations were detected in the time-domain and spectral analyses for time-windows before 1.25 s and after 2.25 s; there was, therefore, a relatively specific interval in which the neuroelectric signatures of the economic parameters became visible.

The correlative topographic maps, representing the significance of linear regressions between potential and each given economic parameter, revealed significant correlations between scalp potential in the [1250,1750] ms and [1750,2250] ms time-windows and $k_{WIN} \times p$ (Figure 9), EV and $EV/\langle k_{WIN}, k_{LOSE} \rangle$ (Figure 11); consequentially, a significant effect of accept/reject decision was observed, without any representation of confidence. In terms of topographic distribution, the "signature" of these parameters was rather similar, consistent between the two time windows, and characterized by a positive correlation expressed at right parietal and anterior central sites and, more weakly, over right frontal and left temporal regions; the only significant negative correlation was observed between potential at anterior frontal electrodes and $k_{WIN} \times p$. Of note, corresponding correlations were clearly absent for the specular negative-term parameter, i.e. $k_{LOSE} \times (1 - p_{\mathrm{WIN}})$; further, there was no representation of $\langle k_{WIN}, k_{LOSE} \rangle$, $|EV/\langle k_{WIN}, k_{LOSE} \rangle|$, p_{WIN}, $|p_{\mathrm{WIN}} - 0.5|$ and Var (Figures 9 and 11).

No significant theta-band effects (4-8 Hz) were found. By contrast, alpha-band activity (8-12 Hz) responded to k_{LOSE} (Figure 12) as well as $\langle k_{WIN}, k_{LOSE} \rangle$ (Figure 13), in both cases presenting a positive correlation with spectral activity in the central-parietal region. There were non-significant correlation trends also for the positive term parameters

k_{WIN} and k_{WIN}×p, however alpha-band activity was clearly insensitive to EV, $EV/\langle k_{WIN}, k_{LOSE}\rangle$, $|EV/\langle k_{WIN}, k_{LOSE}\rangle|$, p_{WIN}, $|p_{\mathrm{WIN}}\text{-}0.5|$ and Var (Figures 12 and 13).

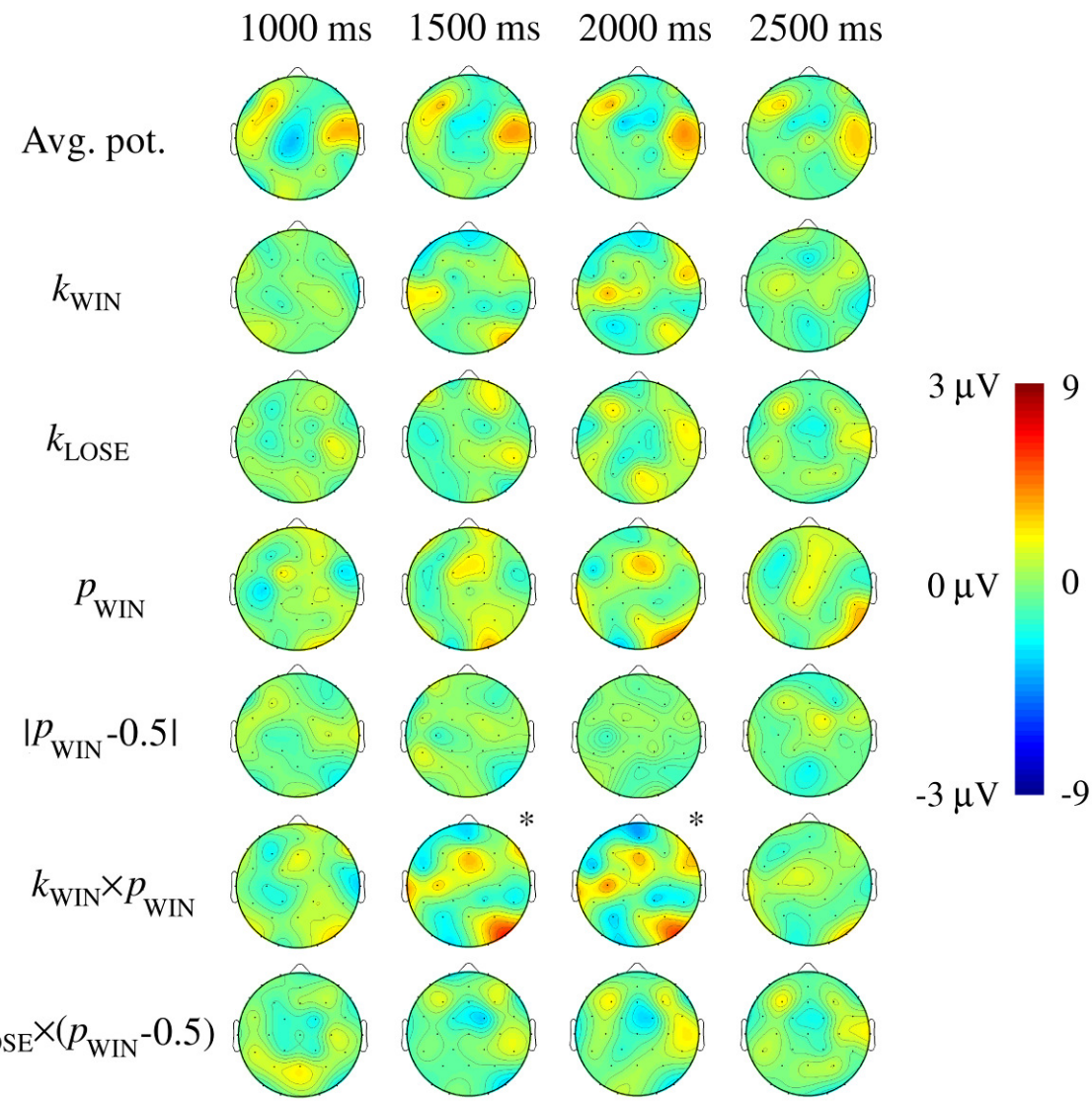

Figure 9. Event-related potential (ERP) topographic maps, representing average potential (top row) and average linear correlation coefficients with respect to each economic parameter (bottom rows). Accounting for multiple comparisons, Bonferroni's correction yielded α=0.0001. Superscript '*' next to a map denotes presence of at least one significant correlation. Continued in Figure 11.

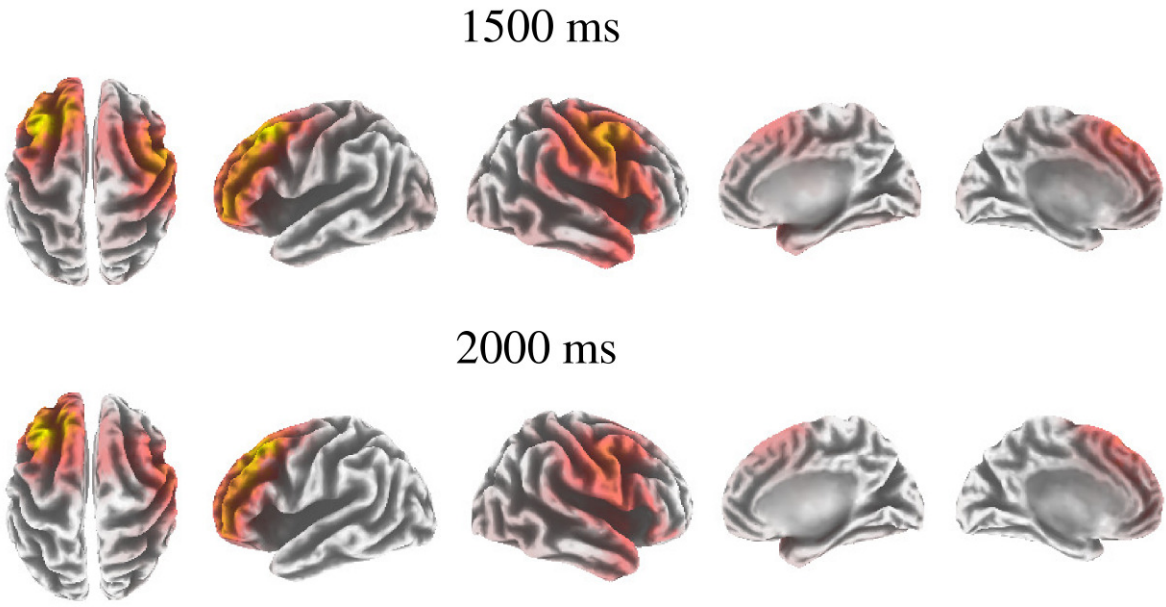

Figure 10. Cortical current-density maps, reconstructed with sLORETA and shown in arbitrary units, for the event-related potential in the time-windows for which significant correlations were observed ([1250, 1750] ms and [1750, 2250] ms).

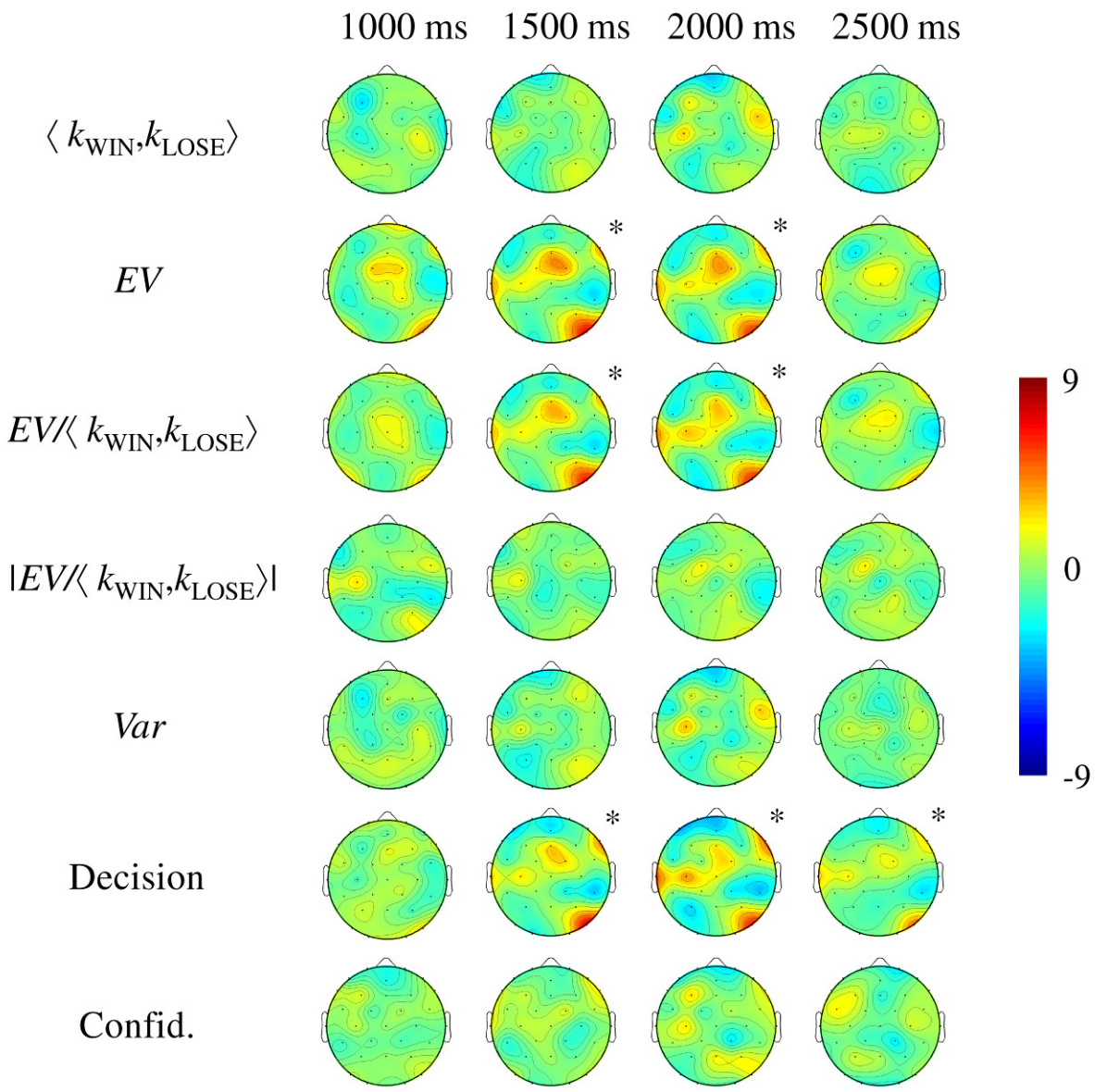

Figure 11. Event-related potential (ERP) topographic maps, representing average linear correlation coefficients with respect to each economic parameter. Accounting for multiple comparisons, Bonferroni's correction yielded α=0.0001. Superscript '*' next to a map denotes presence of at least one significant correlation. Continuation from Figure 9.

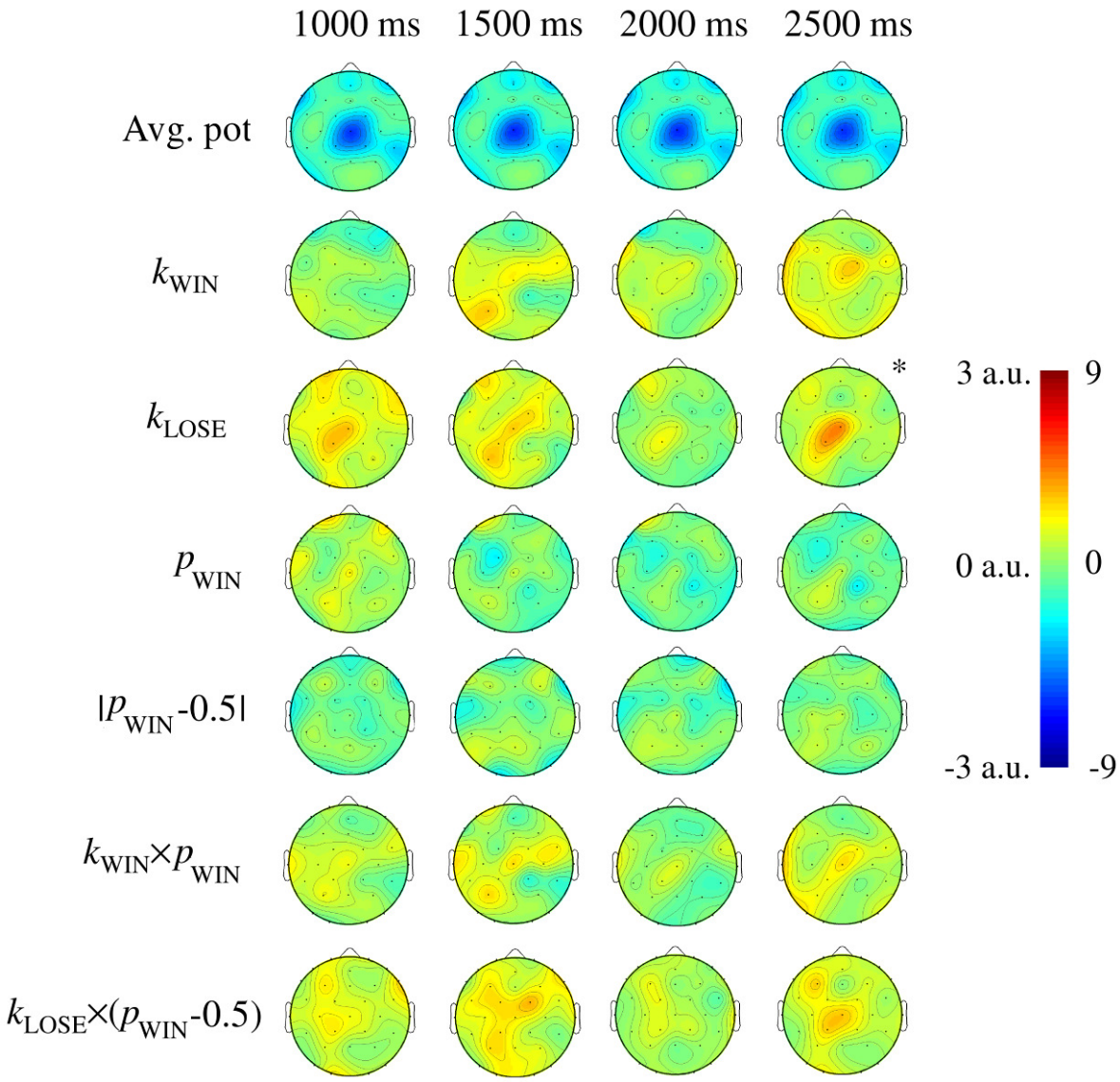

Figure 12. Alpha-band (8-12 Hz) power density topographic maps, representing average power density (top row) and average linear correlation coefficients with respect to each economic parameter (bottom rows). Accounting for multiple comparisons, Bonferroni's correction yielded α=0.0001. Superscript '*' next to a map denotes presence of at least one significant correlation. Continued in Figure 13.

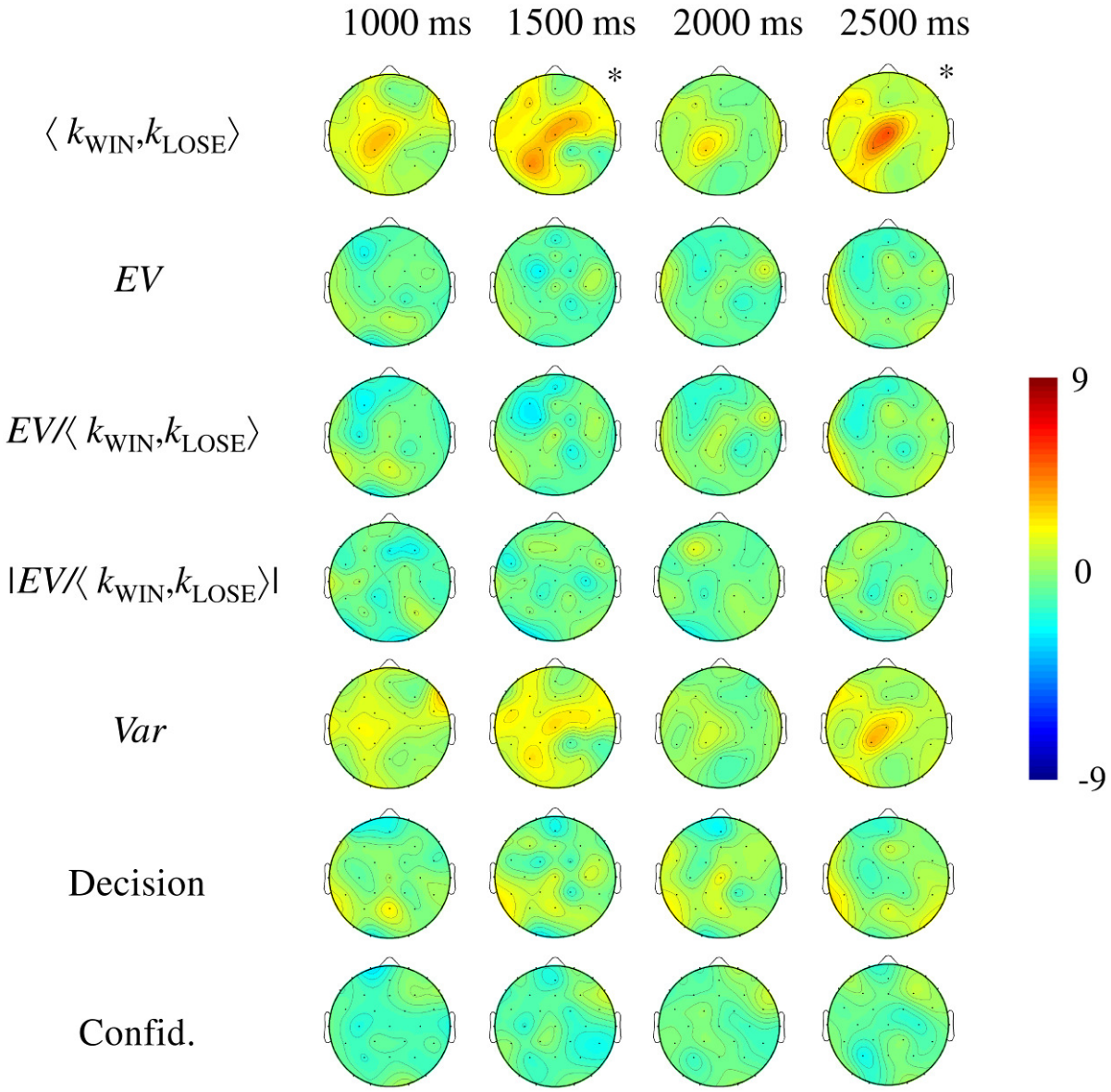

Figure 13. Alpha-band (8-12 Hz) power density topographic maps, representing average linear correlation coefficients with respect to each economic parameter. Accounting for multiple comparisons, Bonferroni's correction yielded α=0.0001. Superscript '*' next to a map denotes presence of at least one significant correlation. Continuation from Figure 12.

4.4 Discussion

4.4.1 Absence of neuroeconomic effects on early and mid-latency ERP components

In line with many previous studies involving the presentation of structured cognitive stimuli, gamble onset elicited the P2, P3a and P3b components: even though the exact functional correlates of these ERPs in the context of a decisional task remain unclear, the P2 is generally taken as a marker of attentional engagement, whereas the P3a and P3b are broadly hypothesized to reflect the activation of working memory and the integrative activity of the cingulate cortex (Crowley and Colrain, 2004; Linden, 2005; Mennes et al., 2008; Polezzi et al., 2010). Several existing investigations have demonstrated that potentials in this latency range (i.e. between 300 ms and 600 ms post-stimulus), including the feedback-related ERN, CRP and MFN components, can respond to specific decisional features such as outcome probability, choice evaluation and level of response conflict (e.g., Yeung and Sanfey, 2004; Hajcak et al., 2006; Polezzi et al., 2008 and 2008b; Polezzi et al., 2010; Pedroni et al., 2011).

Yet, here significant correlations were observed only much later, from 1.25 s post-stimulus onwards. This apparent inconsistency can be reconciled considering the specific format of prospect presentation utilized. In the published studies where significant effects were observed on earlier components, fewer parameters were generally displayed, for example potential gain and loss only, and graphical representation (such as coins or coloured balls) was utilized in place of numbers. The task investigated here, by contrast, involved reading three parameters presented numerically and integrating them abstractly to compute expected value (involving, theoretically, two multiplications and a difference): as represented by the RTs, which were on the order of 3 s, this resulted in a longer and more variable processing time (for example in comparison to approx. 1 s in Polezzi et al., 2008),

making it impossible for economic features to emerge at early latencies due to the fact that basic stimulus processing was still in progress.

Indeed, this argument exemplifies the important point that observed neuroelectric signatures can be conditional to task design features, and not immediately generalizable to different tasks probing the same theoretical construct: it is not implausible that a conceptually equivalent neuroeconomic task, presented in a simpler form using coloured balls and a pie chart, would have revealed very different, earlier signatures involving the P3a, N5 etc. That would not necessarily implicate a discrepancy in the underlying neural circuitry supporting decisional behaviour, only a different temporal pattern of engagement determined by a specific-task implementation: after all, ERPs do not correspond one-to-one to specific cognitive processes, but should rather be viewed a useful epiphenomenon of cognitive processing that manifests itself in a highly task-dependent manner (e.g., Braun et al., 2006). Further research is therefore needed to cross-validate the present results by means of tasks probing similar theoretical constructs implemented with more immediately obvious stimuli.

4.4.2 Gains, expected value and the "Bereitschaftspotential"

It is noteworthy that the strongly significant correlations that were observed with $k_{WIN} \times p_{\mathrm{WIN}}$, EV and $EV/\langle k_{WIN}, k_{LOSE} \rangle$ in the 1.25-2.25 s time window would have been inevitably missed in the EEG studies published in this area, because epoching windows were typically truncated at around 600 ms, if not earlier, and high-pass filters were frequently applied which outright reject slow potential fluctuations (Sutton and Ruchkin, 1984; Ruchkin et al., 1988). Since in this task the average RT was about 3 s, the use of a larger epoching window appeared motivated, as there was no theoretical or empirical

reason to assume that the relevant decision-making processes would terminate much earlier than the time the decision was enacted by button-press.

Because participants were accepting using one hand, and rejecting with the other, a straightforward interpretation is that the observed effects are simply a form of lateralized bereitschaftspotential (BP), a readiness potential decoupled from economic processing and purely contingent to movement preparation (Kristeva et al., 1979; Sutton and Ruchkin, 1984; Kristeva et al., 1987; Shibasaki and Hallett, 2006). This hypothesis can be rejected outright, without the need to perform a confirmatory experiment flipping response side, through the following argument. First, given that, as confirmed by the behavioural observations, one more probably accepts gambles with large k_{WIN} and $k_{WIN} \times p_{\mathrm{WIN}}$, and more probably rejects gambles with large k_{LOSE} and $k_{LOSE} \times (1-p_{\mathrm{WIN}})$, if the observed correlations had been driven by a lateralized BP then one would have detected complementary patterns for the negative- and positive-term economic parameters. This was clearly not the case. Second, for a similar reason one would have expected the correlation maps for EV and $EV/\langle k_{WIN}, k_{LOSE} \rangle$ to display inverse effects on the left and on the right: instead, only positive correlations were observed for these parameters.

While the hypothesis that the observed correlations are purely incidental to lateralized movement initiation can be safely rejected, a certain involvement of the BP generators appears probable, given that sLORETA source localization revealed that the underlying sources of the potential were located bilaterally in the DLPFC, VLPFC and SMA. These regions have been robustly implicated in value representation and computation by invasive neurophysiological recordings and imaging studies (Ikeda et al., 1999; Hernández et al., 2002; Palminteri et al., 2009) and are well-known to be involved in the generation of the BP, especially in the context of structured tasks (Kristeva et al., 1979; Cui et al., 2000; Shibasaki and Hallett, 2006). Hence, the observed correlations suggest a

relationship between abstract value representation and activity across the premotor circuitry. Indeed, an early neuroeconomic study had observed a relationship between BP amplitude and the level of risk associated with a given choice, and had thereafter concluded that the BP can be sensitive to economic contingencies (Hink et al., 1982).

4.4.3 Bereitschaftspotential or slow-wave potential?

Yet, the latency range and topographical distribution could also be compatible with a slow-wave potential (SWP). SWPs are a poorly-characterized family of ERP components that are usually elicited by highly complex tasks, emerge after 1 s following stimulus presentation, and may persist for many seconds until a response is made. While such potentials have not been extensively investigated, and more recent ERP studies focus on earlier latencies, it is thought that the underlying generators may overlap, at least in part, those of the BP, involving not only the premotor circuits but also the posterior parietal sulci, depending on whether or not the task involves a substantial visual associative component (Sutton and Ruchkin, 1984; Ruchkin et al., 1988; Rösler and Heil, 1991). Notably, a more recent investigation, conducted using simultaneous EEG and fMRI, has suggested that SWPs originate from an extended network involving the DLPFC, VLPFC, SMA and insula, which, as revealed by the fMRI data presented in the next chapter, are all heavily implicated in the representation of decisional parameters (Lamm et al., 2001). Also, a very recent investigation using a social decision making task has demonstrated that SWPs are highly sensitive to abstract parameters such as one's perceived social condition (Crowley et al., 2010).

On the basis of this experiment alone, one cannot definitely conclude whether the observed correlations reflect a BP or an SWP. Indeed, such question is, at least at present, probably largely futile since the exact relationship between the BP and the SWP remains

unclear, and the distinction may at least in part be an artificial one, determined by how the potential is computed (i.e., locking at movement onset or stimulus presentation) rather than by an underlying neural difference. The relevant result here is that the observed correlations robustly implicate premotor networks in parameter specific processing during value determination and decision-making. The response is not "balanced", but appears to have more to do with potential gains than losses. Such observation echoes the concept of a "gain-brain" circuit, anchored on the DLPFC and VLPFC and responding preferentially to gains than losses, that has been put forward in recent fMRI studies (Tom et al., 2007; Scheibe et al., 2010; Wallis and Kennerley, 2010). From an ecological perspective, this observation of an unbalanced response could, speculatively, be linked to the fact that in real life reaping the potential benefits offered by an advantageous prospect generally requires an active action, such as running to capture a prey, or opposed to remaining hidden to avoid a risk (e.g., Lee, 2006; Levine, 2009; Clark, 2010). In light of the emerging results on the MFN component which demonstrate modulation of prefrontal excitability by dopaminergic reward anticipation signals, it is possible that diffuse striatal efferences may contribute to the emergence of this "gain brain" circuit (Holroyd et al., 2008).

4.4.4 Alpha-band response to losses and overall amount magnitude

In the frequency domain, gamble presentation generated a major reduction in alpha-band EEG power, which was most evident in the central region of the scalp. Though the majority of alpha activity is observed over occipital regions during resting conditions, already in another study on complex decision-making the most prominent drop was observed diffusely over central, frontal and parietal sites (Davis et al., 2011).

As reviewed by Palva and Palva (2007), substantial uncertainty remains regarding the exact functional interpretation of spontaneous oscillations in the alpha and beta EEG

bands. Predicated on the common observation that performing an engaging task reduces power density in the alpha band and on sleep studies (e.g., Neuper and Pfurtscheller, 2001), Pfurtscheller (2001) and Klimesch et al. (2006) formulated the hypothesis that alpha activity represents an "idling rhythm", emerging from the spontaneous synchronization of oscillations within and between cortical areas not involved in active processing at a given time. Evidence of alpha-band responsiveness to the level of attentional arousal and emotionally-valenced stimuli lends support to this view (Herrmann and Knight, 2001). Yet, recent experiments imply a more complex relationship: for example, memory retention is associated with "paradoxically" increased alpha activity (e.g., Klimesch et al., 2007). The issue is further complicated by frequency overlap with mu-rhythm activity, which is associated with action preparation and execution (e.g., Hari, 2006). Also, the relationship between alpha-band oscillations and metabolically-demanding neural activity appears to be complex, with a significant element of stochasticity (e.g., Oakes et al., 2004; Scheibe et al., 2010).

On one hand, in light of the consistent observations on a wide range of active tasks (e.g., Palva and Palva, 2007) it appears safe to conclude that the overall drop in alpha-band activity following gamble presentation represents a general cortical de-inhibition, coupled to the allocation of attentional resources, effort and arousal. On the other hand, the interpretation of the observed parametric correlations is more dubious. Notably, with respect to the evoked potential the observed alpha-band modulations displayed a complementary relationship to the economic parameters. First, there was clearly no representation of EV or $EV/\langle k_{WIN}, k_{LOSE}\rangle$; also, the relationship to $k_{WIN} \times p_{\mathrm{WIN}}$ was weak and distant from the corrected level of statistical significance. Second, on the contrary there were strongly significant correlations with k_{LOSE} and $\langle k_{WIN}, k_{LOSE}\rangle$, for which no effects were evident on the evoked potential. Therefore, there appears to be a profound

dissociation between the neural activity indexed by the ERPs and encoding $k_{WIN} \times p_{\mathrm{WIN}}$, EV and $EV/\langle k_{WIN}, k_{LOSE} \rangle$, and that indexed by alpha-band power, encoding k_{LOSE} and $\langle k_{WIN}, k_{LOSE} \rangle$.

On the surface, the observed correlations do not fit a straightforward interpretation in terms of larger potential losses and average amounts being associated with grater engagement and allocation of processing resources, as one would then expect opposite trends. However, as mentioned above "paradoxical" correlations with alpha-band activity have been observed (e.g., Klimesch et al., 2007) and are now interpreted as the consequence of changes in long-range phase coherence, which may be more closely representative of activity subserving task performance than power density fluctuations alone. Unfortunately a phase conherence analysis was not performed here.

Another puzzling finding is the absence of beta-band modulations. Such effects would be expected to accompany alpha-band correlations, especially in virtue of the close coupling that exists between activity in this band and attention, especially in the visual domain (e.g., Wróbel, 2000; Neuper and Pfurtscheller, 2001). While no definite conclusion can be reached on the basis of the available data alone, a possible explanation is that the "baseline" change in beta-band activity induced by the gambles was simply not large enough to act as a "carrier" for the emergence of significant parametric correlations.

4.4.5 A "two-tier" representation?

In the presented gambles, k_{LOSE} and $\langle k_{WIN}, k_{LOSE} \rangle$ can be rapidly evaluated without the need for multiparametric integration and abstract value computation, and in naturalistic prospects these parameters characterize highly evolutionarily-relevant situations. When the worse-case outcome is a large loss an adverse outcome is more likely to be fatal (for

example, revealing one's hidden presence to a predator), and the impact of a given decision on individual survival and fitness depends on "how much" is at stake (e.g., deciding whether to jump over a stream of water risking only the unpleasant feeling of being wet and cold vs. deciding whether to attack a large prey at the risk of being fatally wounded in fight; McFarland, 1997; Trepel et al., 2005; Wilkinson, 2008; Kalenscher and van Wingerden, 2011). Hence, even though the exact functional significance of the observed correlations remains unclear, one can speculate that the large overall alpha response indexed inhibition and disengagement of task-irrelevant processes representing overall attentional shift, whereas positive correlations with potential loss and amount at stake plausibly signalled a subtler but more selective modulation of neural processing determined by the level of "evolutionary salience" of a prospect (Kolev et al., 2001; Pfurtscheller, 2001; Palva and Palva, 2007; Klimesch et al., 2007). Such evolutionary interpretation must at present remain speculative and calls for further investigation. Neuropharmacological manipulations would be of particular interest here, to probe whether this putative "evolutionary salience" signal is represented through the activity of the noradrenergic and acetylcholinergic systems.

On the other hand, $k_{WIN} \times p_{\mathrm{WIN}}$ and EV are considerably more abstract, given that their determination involves weighing potential gains and losses by their probability, and for the latter parameter also combining the positive and negative terms of the value equation. Hence, the results of this experiment appear to implicate a "two-tier" processing system in risky decision-making, whereby immediately-relevant parameters are represented in overall modulations of alpha band activity, plausibly driven by diffuse efferent signals from basal brain regions, while high-abstraction variables that require more integrative processing but are less immediately relevant for survival (i.e. are related more closely to harvesting an opportunity rather than prompting immediate avoidance of a

potentially fatal danger) are instead coded by integrative cortical activity indexed by long-latency evoked potentials.

Paradigmatically, this experiment explicitly demonstrates the potential value of combining multiple neurophysiological data analysis approaches rather than limiting oneself to time-locked activity when studying the neural bases of decisional behaviour.

5. Univariate, voxel-wise functional MRI (fMRI)

5.1 Background and motivation

In their seminal study, Tom and co-workers (2007) presented healthy participants with stereotyped risky gambles characterized by a potential gain and a potential loss, with fixed 50% outcome probability. Widespread responses in the prefrontal cortex correlated positively with gains and negatively with losses, leading to the notion of putative "gain brain" circuits mentioned in the previous chapter. Expected value, determined by immediate combination of the two amounts, was represented in activity in the mesial prefrontal cortex as well as in the striatum. Of note, the dissociation between the neural representation of losses and gains tracked individual levels of behavioural loss aversion.

Though highly influential, their study suffered from fundamental limitations related to the fact that the presented prospects were highly unnatural: the case of equal outcome probability for losses and gains represents a highly specific situation, which is seldom encountered in real life. Hence it remains unclear whether the results are immediately generalizable to more realistic prospects characterized by uneven and variable outcome probabilities. Indeed, one can argue that even deciding between a risky $EV \neq 0$ and a riskless $EV=0$ option already represents, in itself, a rather artificial and simplified scenario, since in practice most actions require choosing among multiple risky choice options, each one characterized by multiple possible outcomes and associated probabilities (e.g., Kahneman and Tversky, 2000). Further, the $p_{WIN}=0.5$ situation represents a degenerate state of the value equation whereby $EV=k_{WIN}-k_{LOSE}$:, and value computation can then be approximated as a simple subtraction, rather than a more abstract weighted integration: it therefore

appears implausible that the functional neuroanatomical correlates of processing such gambles would realistically reflect those engaged in deciding on more complex prospects.

Extending the findings of Tom et al. (2007), in this experiment the BOLD responses to risky prospects were mapped in the context of a more flexible task, wherein k_{WIN}, k_{LOSE} and p_{WIN} are independently varied. As discussed above, in addition to substantially improving ecological validity this unlocks the possibility of mapping the neural representation of a wide range of parameters that are intrinsically inaccessible when outcome probabilities are fixed. This univariate analysis mirrors the EEG experiment reported in the previous chapter, aiming to harvest the greater anatomical specificity provided by functional MRI, and preludes the multivariate, network-based analysis reported in the next chapter.

Predicated on the existing literature on value computation, it was predicted that the amplitude of the BOLD response across the prefrontal cortex, particularly in mesial regions, and the striatum would correlate positively with expected value (EV; Tom et al., 2007; Chib et al., 2009; Kable and Glimcher, 2009; Gläscher et al., 2009; Smith et al., 2010; Venkatraman et al., 2009; Wunderlich et al., 2009).

Predicated particularly on the observation of Tom et al. (2007), an additional prediction was that activity in these regions would correlate positively with potential gains (k_{WIN} and $k_{WIN} \times p_{\mathrm{WIN}}$) and negatively with potential losses (k_{LOSE} and $k_{LOSE} \times (1-p_{\mathrm{WIN}})$).

Predicated on influential views on the encoding of risk signals (e.g. , Levin et al., 2011), it was predicted that the anterior insula and amygdala would show significant BOLD responses tracking risk, potential loss and uncertainty (i.e., $k_{LOSE} \times (1-p_{WIN})$, k_{LOSE} and $|p_{WIN}-0.5|$; e.g., Preuschoff et al., 2008; Weller et al., 2009).

Lastly, since "ambiguous" gambles that are not clearly advantageous nor disadvantageos generate greater response conflict than more "obvious" ones, it was

predicted that activity in the cingulate cortex, particularly its anterior portion, would closely reflect the deviation of the level of risk-advantageousness (i.e., $|EV/\langle k_{WIN}, k_{LOSE}\rangle|$) from zero (Braver et al., 2001; Corbetta and Shulman, 2002; Medford and Critchley, 2010).

5.2 Participants, methods and data analysis

The experiment was performed on 22 subjects (10 females, age 36±7 years, education 16±4 years), none of whom had participated in the previous experiments, who were recruited, as for the EEG experiment, among medics, paramedics and researchers at the Fondazione IRCCS Istituto Neurologico "Carlo Besta" in Milano (Italy). All participants had been educated in Italy, were naive to the task and study design and had no experience in banking, financial investments or gambling. The experiment was formally approved by the research governance and ethics committee of the Brighton & Sussex Medical School (BSMS; PhD project no. 10/056/MIN) as well as by the ethics committee of the Fondazione IRCCS Istituto Neurologico "Carlo Besta" (project no. fMRI-DM), and was conducted in the neurophysiology unit of the institute. Participants did not receive any financial or material compensation. For this experiment, the gambles were expressed in Euros (€). In compliance with local rules, data acquisition was supervised by a psychologist (Dott.ssa Sylvie Piacentini) and by clinical neuroradiologist (Dott.ssa Marina Grisoli), who also took the clinical history of the participants, none of whom had any past or current neurological or psychiatric condition or was taking any relevant medication. All participants were right-handed (Oldfield, 1971). All structural scans were reported as normal.

As with the previous experiments, upon arrival the aim of the study was explained, sample gambles were presented and informed consent was obtained. In accordance with

local rules, participants were positioned in the MR scanner, a 1.5 T clinical unit (Magnetom Avanto, Siemens AG, Erlangen, DE), by a senior radiographer (TSRM Francesca Epifani) who subsequently run the requested imaging sequences under guidance of the author. All other aspects of data acquisition, and all data analysis, were performed personally by the author. Gambles were presented using the same script developed for the previous experiments, driving a projector aimed at a screen at the back end of the scanner bore, which the participants viewed through a mirror. The script was modified to collect volume acquisition timings through a proprietary interface card. Responses were collected through an MRI-compatible keyboard. As for the previous experiment, reject and accept responses were delivered with the left and right hand, respectively.

For normalization purposes, structural images were acquired with a T_1-weighted magnetization-prepared rapid-acquisition gradient-echo sequence, having TR=1640 ms, TE=2 ms, FoV 256×256 mm, matrix 256×256, 160 slices, 1 mm voxel size. The functional sequence had been previously optimized by the author on phantoms to determine the optimal parallel imaging acceleration factor and coil-combination mode for the 8 receive channels, and subsequently on volunteers to determine the optimal tilt and phase encoding to minimize susceptibility artefacts in the orbitofrontal region and ventral striatum (e.g., see Weiskopf et al., 2006); such steps were particularly important considering the relatively low field strength of the system. The sequence used for functional imaging was a T_2^*-weighted echo-planar gradient-echo sequences, having TR=2400 ms, TE=45 ms, FoV 315×210 mm, matrix 90×60, 35 slices, 3.5 mm w/o gap (isotropic voxel). The slice-packet tilt was 20° with respect to the bicommissural plane (i.e., above eyes), the phase-encoding direction was anterior-to-posterior, with positive blips, the acceleration factor was set to three and the coil combine mode was set to dual. Corresponding phase/magnitude field-

maps were also acquired, using gradient-echo sequence having and identical geometry and TR=560 ms, TE=4.7/9.5 ms.

As with the previous experiments, to minimize attentional drift and potential habituation effects, the task was divided in four blocks, each one lasting approximately 9 min and corresponding to 240 functional volumes. Here, 152 gambles were presented with a fixed inter-trial interval of 14.4 s, corresponding to 6 TRs; the reason for this choice is related to the network analysis presented in the next chapter.

FMRI data analysis was performed in SPM8 (Wellcome Trust Centre for Neuroimaging, UCL, London, UK), running under Matlab 7 (MathWorks Inc., Natick MA, USA). Due to the sheer number of analyses to be performed, determined by the combination of participants, parameters and event onset model delays (see below), all analysis steps were completed under the automated control of a dedicated script developed by the author, automatically assigning tasks to each processor and constructing design matrices on the basis of the behavioural log files; this step also eliminated the possibility of introducing errors in this otherwise labour-intensive phase. All analysis steps took approximately four days to complete on a Sun Blade 2500 workstation (Sun Microsystems Inc., Santa Clara CA, USA). Preprocessing steps were performed in the following order: slice-timing correction, realignment and un-warping using the acquired field-maps, co-registration with individual structural scans, segmentation of the volumetric anatomical images to obtain high-quality normalization coefficients, re-slicing into standard Montreal Neurological Institute (MNI) space and smoothing with an 8 mm width Gaussian kernel. The quality of all normalizations was individually checked and confirmed to be adequate.

As the experimental hypotheses for this experiment pertained to the representation of each individual parameter in isolation, separate fixed-effects (i.e., first-level) analyses were run for k_{WIN}, k_{LOSE}, p_{WIN}, $k_{WIN} \times p_{\mathrm{WIN}}$, $k_{LOSE} \times (1 - p_{\mathrm{WIN}})$, $|p_{\mathrm{WIN}} - 0.5|$, EV, $\langle k_{WIN}, k_{LOSE} \rangle$, $EV/\langle k_{WIN}, k_{LOSE} \rangle$, $|EV/\langle k_{WIN}, k_{LOSE} \rangle|$ and Var. The corresponding design matrices were

constructed assuming delta-function events for gamble onset, convolved with the canonical haemodynamic response function. Parametric modulation was modelled inserting separate regressors for main effect, the parameter of interest and reaction time (RT), treated as a nuisance variable. In other words, the general linear model for the BOLD signal was set up, separately for each individual participant and economic parameter, as follows

$$y = \beta_0 + \beta_1 \cdot f_{\text{ONSET}} + \beta_2 \cdot f_{\text{RT}} + \beta_3 \cdot f_{\text{PARAMETER}},$$

where f_{ONSET} is a delta-function (having $y(0)=1$, $y=0$ elsewhere) representing the onset of the gambles, convolved with the canonical haemodynamic response function (HRF), f_{RT} is a delta-function multiplied by the measured reaction time for each gamble, convolved with the HRF, and $f_{\text{PARAMETER}}$ is another delta-function multiplied by the economic parameter of interest for each gamble, again convolved with the HRF. Accounting for potential signal differences among the four blocks, e.g. related to scanner drifts or physiological factors, separate regressors were entered for each block, and the six movement regressors corresponding to rotation and translation were also inserted.

Random-effects (i.e., second-level) analyses were defined on the basis of the individual effect of each economic parameter of interest, including a regressor for inter-individual differences in median RTs. Group-level maps were thereafter generated, separately for positive and negative parametric correlations, using two-tailed one-sample t-tests. To test the additional hypothesis that delayed effects could reveal representations of the individual parameters not visible assuming the canonical haemodynamic response, all fixed-effects and random-effects analyses were repeated assuming a delayed stimulus onset by 2.4 s and 4.8 s (i.e., 1 and 2 TR).

All inferences were drawn from family wise error (FWE) corrected cluster-level significance scores, determined from clusters formed applying the voxel-level threshold of $p<0.001$ uncorrected. This approach is particularly conservative and strongly controls the

probability of type I error, however it makes substantial assumptions about the Gaussian distribution of residuals (Friston et al., 1996). Hence, it was complemented by an additional confirmatory method, consisting of performing Monte Carlo simulations with a realistic model of the acquisition and preprocessing steps that yields an estimate of the cluster extent corresponding to effective α of 0.05 and 0.001 (Slotnick et al., 2003). Such stimulations returned an extent threshold of 43 MNI space voxels for α=0.05 and 105 voxels for α=0.001.

5.3 Results

On average, gamble presentation generated positive BOLD responses in the DLPFC and VLPFC, superior frontal gyrus, dorsal and ventral striatum, thalamus, cingulate cortex (anterior and posterior), sensory-motor cortex (SI, SII and MI), posterior temporal lobe, visual cortex (primary and associative) and cerebellum; negative BOLD responses were apparent in medial frontal areas, i.e. DMPFC and VMPFC, angular gyrus and precuneus (Figure 14).

As represented in Figure 15, in addition to button-press related activity in MI and SI, positive correlations between k_{WIN} and BOLD response amplitude were apparent, predominantly on the right, in early visual areas (VI, VII), in the left anterior insula (ventral part), and in the posterior middle-cingulate cortex (pMCC, parcellated according to Vogt, 2005). For $k_{WIN} \times p_{WIN}$ (Figure 16), the pattern was overall similar; correlations in the insula and cingulate cortex were absent but negative correlations in region of the angular and supramarginal gyri appeared bilaterally.

On the other hand, the correlations observed between BOLD response amplitude and k_{LOSE} (Figure 17) were predominantly negative, and were apparent in the VLPFC and

DLPFC, in the VMPFC at the interface with the OFC, in the pregenual part of the anterior cingulate cortex (pACC), in the dorsal posterior cingulate cortex (dPCC), in the precuneus, as well as in the left striatum and bilaterally in region of the angular gyrus. For $k_{LOSE} \times (1-p_{WIN})$ (Figure 18), such negative correlations were considerably less widespread and found in the right DLPFC and VLPFC, again in the VMPFC at the interface with the OFC, in the pACC, in the DMPFC and aMCC, as well as in the superior frontal gyrus and bilateral angular gyri and parietal lobule.

The haemodynamic response to p_{WIN} (Figure 19) was much more limited, and consisted of small clusters of negative correlation located in the left VLPFC.

On the other hand, for $|p_{WIN}-0.5|$ (Figure 20) positive correlations were observed in the DMPFC, extending to the aMCC, as well as in the DLPFC and VLPFC on the right and bilaterally in the inferior parietal lobule and angular gyri. While for all other parameters repeating the analysis using a model assuming a delayed response did not reveal any additional activity, here the delayed BOLD response correlated positively with $|p_{WIN}-0.5|$ in a large cluster situated in the left anterior insula (Figure 21). Post-hoc analyses conducted on the average responses in this cluster separating gambles presenting likely losses (i.e., $p_{WIN}<0.5$) or gains ($p_{WIN}>0.5$) indicated that this correlation was significantly stronger for risky prospects where a loss outcome was more likely (beta coefficient for the parametric effect of $|p_{WIN}-0.5|$: 0.78±0.77 vs. 0.19±0.91, paired t-test p=0.04).

As shown in Figure 22, the BOLD response correlated positively with $\langle k_{WIN}, k_{LOSE} \rangle$ in early visual areas, and negatively in the superior frontal gyrus bordering with the right DLPFC, as well as bilaterally in the supramarginal angular and gyri and in the precuneus.

For *EV* (Figure 23), the BOLD response correlated positively in right early visual areas, in the VMPFC bordering with the pACC/mACC and OFC, and in the left inferior temporal cortex. For $EV/\langle k_{WIN}, k_{LOSE} \rangle$ (Figure 24) the correlation topography was similar,

but characterized by enhanced positive correlation in the VMPFC. For its absolute value, i.e. $|EV/\langle k_{WIN}, k_{LOSE}\rangle|$ (Figure 25), the BOLD response correlated positively in the angular and supramarginal gyri bilaterally, in the VMPFC and DMPFC, in the dorsal posterior cingulate cortex (dPCC) and in the precuneus region, as well as bilaterally in clusters situated at the border between the VLPFC and the anterior insula; negative correlations were found bilaterally in early visual areas.

The effect of accept/reject decision was almost completely overlapping with the correlation with $EV/\langle k_{WIN}, k_{LOSE}\rangle$, and hence is not shown; no BOLD response difference was detected contrasting confident vs. unsure responses, even at statistically uncorrected thresholds.

The BOLD amplitude correlated negatively with *Var* (Figure 26) in clusters situated in the right superior frontal gyrus at the interface with the DLPFC, and bilaterally in the angular and supramarginal gyri and inferior parietal lobule. All correlation clusters described above are tabulated in Table 2, and survived both cluster-level FWE correction and the extent threshold given by the Monte Carlo analysis to yield α=0.05(43 voxels); most clusters also survived the extent corresponding to α=0.001(105 voxels).

Table 2 (following pages). Functional MRI correlation clusters, determined at a voxel threshold of $p<0.001$ and cluster-level FWE $p<0.05$. Peak coordinates are given in MNI space, cluster extents are expressed in 8 mm^3 voxels.

Sign	***Extent***	***p-val.***	***Peak***	***Max coord.***	***Side***	***Description of region at max coord.***
				k_{WIN} (Δt=0 s)		
Pos.	1908	<0.001	8.9	-43, -22, 60	L	Pre- and post-central gyri (MI, SI)
Pos.	478	<0.001	4.9	15, -86, 11	R	Cuneus, mid. occ. gyri
Pos.	335	<0.001	5.3	29, -48, -25	R	Cerebellum
Pos.	254	<0.001	5.1	-48, -23, 18	L	Par. operc. (SII), post. insula
Pos.	196	0.002	5.6	-37, 14, -14	L	Ant. insula (ventr.)
Pos.	119	0.02	4.7	-6, -10, 51	L	Cingulate gyrus (pMCC)
Pos.	115	0.03	4.3	-20, -93, 11	L	Cuneus, mid. occ. gyri
Neg.	686	<0.001	5.3	42, -25, 59	R	Pre- and post-central gyri (MI, SI)
				$k_{WIN} \times p_{WIN}$ (Δt=0 s)		
Pos.	1537	<0.001	7.6	-43, -23, 62	L	Pre- and post-central gyri (MI, SI)
Pos.	382	<0.001	5.3	21, -93, 3	R	Cuneus, mid. occ. gyri
Pos.	210	0.001	5.5	32, -46, -25	R	Cerebellum
Pos.	123	0.02	4.3	-21, -92, -9	L	Cuneus, mid. & inf. occ. gyri
Pos.	122	0.02	4.3	37, -82, -10	R	Inf. occ. gyrus
Neg.	333	<0.001	5.6	49, -56, 23	R	Supramarg. & ang. gyri, inf. par. lobule
Neg.	975	<0.001	5.5	43, -21, 24	R	Par. operc. (SII), post. insula
Neg.	198	0.001	4.9	-55, -55, 28	L	Supramarg. & ang. gyri, inf. par. lobule
				k_{LOSE} (Δt=0 s)		
Pos.	1190	<0.001	7.5	42, -20, 57	R	Pre- and post-central gyri (MI, SI)
Neg.	2023	<0.001	9.4	-45, -27, 55	L	Pre- and post-central gyri (MI, SI)
Neg.	1531	<0.001	7.0	1, 46, -5	R	Med. front. gyrus, ant. cing. (VMPFC, pACC, OFC)
Neg.	699	<0.001	6.2	19, -51, -22	R	Cerebellum
Neg.	603	<0.001	5.4	54, -54, 38	R	Supramarg. & ang. gyri, inf. par. lobule
Neg.	397	<0.001	6.2	60, -47, 3	R	Supramarg. & sup. temp gyri
Neg.	378	<0.001	5.7	28, 31, 51	R	Sup. front. gyrus (DLPFC)
Neg.	377	<0.001	5.5	47, 45, 3	R	Inf. & mid. front. gyri (DLPFC, VLPFC)
Neg.	282	<0.001	5.1	4, -58, 31	L	Post. cing. (dPCC), precuneus
Neg.	251	<0.001	6.9	-32, -6, -4	L	Post. insula (ventr.), putamen
Neg.	199	0.001	5.6	-44, -22, 18	L	Par. operc. (SII), post. insula
Neg.	142	0.005	4.5	3, -36, 41	R	Post. cing. (dPCC)
Neg.	118	0.012	5.2	-44, -61, 21	L	Supramarg. & sup. temp gyri
				$k_{LOSE} \times (1\text{-}p_{WIN})$ (Δt=0 s)		
Pos.	1857	<0.001	7.7	43, -22, 55	R	Pre- and post-central gyri (MI, SI)

Pos.	339	<0.001	5.5	-15, -56, -10	L	Cerebellum
Pos.	319	<0.001	5.0	50, -11, 15	R	Par. operc. (SII), post. insula
Pos.	232	<0.001	5.7	-13, -89, 4	L	Cuneus, mid. occ. gyri
Neg.	1567	<0.001	7.8	-45, -28, 57	L	Pre- and post-central gyri (MI, SI)
Neg.	768	<0.001	6.4	29, 23, 51	R	Sup. & mid. front. gyri (DLPFC)
Neg.	684	<0.001	6.1	49, -61, 40	R	Supramarg. & ang. gyri, inf. par. lobule
Neg.	211	<0.001	4.9	39, 48, 4	R	Inf. & mid. front. gyri (VLPFC)
Neg.	185	0.001	4.8	-2, 49, 32	L	Med. front. gyrus, ant. cing. (DMPFC, aMCC)
Neg.	182	0.001	4.8	-7, 49, -5	L	Med. front. gyrus, ant. cing. (VMPFC, pACC, OFC)
Neg.	179	0.001	4.9	-20, 36, 50	L	Sup. front. gyrus
Neg.	176	0.001	4.6	15, -55, -20	R	Cerebellum
Neg.	103	0.03	4.7	-10, 65, 12	L	Med. front. gyrus (VMPFC, pACC)
Neg.	93	0.04	4.1	-40, -66, 43	L	Inf. par. lobule
				p_{WIN} (Δt=0 s)		
Neg.	348	<0.001	5.7	-45, -20, 15	L	Par. operc. (SII), post. insula
Neg.	124	0.01	4.4	-27, -25, 53	L	Pre- and post-central gyri (MI, SI)
Neg.	93	0.04	6.2	-54, 4, 14	L	Inf. front. gyrus (VLPFC)
				$\lvert p_{WIN}-0.5\rvert$ (Δt=0 s)		
Pos.	1383	<0.001	6.6	-4, 36, 40	L	Med. front. gyrus, ant. cing. (DMPFC, aMCC)
Pos.	221	<0.001	4.9	41, 31, 24	R	Inf. & mid. front. gyri (DLPFC, VLPFC)
Pos.	215	<0.001	4.8	34, -68, 44	R	Inf. par. lobule
Pos.	105	0.02	4.2	-22, -67, 49	L	Inf. par. lobule
Neg.	120	0.01	6.0	-34, -24, 24	L	Par. operc. (SII), post. insula
				$\lvert p_{WIN}-0.5\rvert$ (Δt=2.4 s)		
Pos.	833	<0.001	6.5	1, 32, 46	L	Sup. front. gyrus
Pos.	354	<0.001	5.4	-33, 21, -2	L	Ant. insula
Pos.	156	0.003	4.8	43, 39, 22	R	Inf. & mid. front. gyri (DLPFC,VLPFC)
Neg.	113	0.02	6.2	40, -4, 16	R	Post. insula
				$\langle k_{WIN}, k_{LOSE}\rangle$($\Delta t$=0 s)		
Pos.	159	0.002	4.8	-21, -95, 2	L	Mid. occ. gyrus
Pos.	100	0.02	5.9	12, -88, 6	R	Cuneus, mid. occ. gyri
Neg.	1005	<0.001	6.2	53, -55, 33	R	Supramarg. & ang. gyri, inf. par. lobule
Neg.	421	<0.001	5.8	-48, -62, 28	L	Inf. par. lobule

Neg.	212	<0.001	5.2	29, 25, 51	R	Sup. front. gyrus (DLPFC)
Neg.	196	<0.001	5.1	62, -38, -1	R	Med. temp. gyrus
				$EV=k_{WIN} \times p_{WIN} - k_{LOSE} \times (1-p_{WIN})$ (Δt=0 s)		
Pos.	2472	<0.001	12.3	-39, -24, 57	L	Pre- and post-central gyri (MI, SI)
Pos.	722	<0.001	6.5	21, -48, -24	R	Cerebellum
Pos.	439	<0.001	5.3	24, -92, 11	R	Cuneus, mid. occ. gyri
Pos.	167	0.003	4.5	-3, 44, -8	L	Med. front. gyrus, ant. cing. (VMPFC, pACC/mACC, OFC)
Pos.	137	0.03	4.5	-42, -19, 15	L	Par. operc. (SII), post. insula
Pos.	109	0.03	4.7	-44, -43, -15	L	Inf. temp. & parahipp. gyri
Neg.	1928	<0.001	8.8	39, -24, 53	R	Pre- and post-central gyri (MI, SI)
Neg.	296	<0.001	5.6	-22, -49, -22	L	Cerebellum
				$EV/\langle k_{WIN}, k_{LOSE} \rangle$ (Δt=0 s)		
Pos.	2458	<0.001	11.4	-43, -30, 56	L	Pre- and post-central gyri (MI, SI)
Pos.	759	<0.001	6.2	18, -53, -22	R	Cerebellum
Pos.	233	<0.001	5.9	-2, 37, -8	L	Med. front. gyrus, ant. cing. (VMPFC, pACC, OFC)
Pos.	248	<0.001	4.9	25, -93, 6	R	Cuneus, mid. occ. gyri
Pos.	108	0.03	4.7	-46, -21, 17	L	Par. operc. (SII), post. insula
Neg.	1961	<0.001	7.8	39, -23, 55	R	Pre- and post-central gyri (MI, SI)
Neg.	385	<0.001	5.9	-19, -48, -21	L	Cerebellum
				$\lvert EV/\langle k_{WIN}, k_{LOSE} \rangle \rvert$ (Δt=0 s)		
Pos.	2192	<0.001	8.5	61, -49, 9	R	Supramarg. & ang. gyri, inf. par. lobule
Pos.	2932	<0.001	8.7	-49, -59, 32	L	Supramarg. & ang. gyri, inf. par. lobule
Pos.	721	<0.001	6.2	-1, 57, 18	L	Med. front. gyrus (DMPFC, VMPFC)
Pos.	569	<0.001	6.0	5, -52, 35	R	Post. cing. (dPCC), precuneus
Pos.	155	0.005	4.8	48, 33, -7	R	Inf. front. gyrus, ant. insula (VLPFC)
Pos.	133	0.01	4.9	-37, 28, -12	L	Inf. front. gyrus, ant. insula (VLPFC)
Pos.	114	0.02	4.4	-51, 23, 8	L	Inf. front. gyrus (VLPFC)
Neg.	256	<0.001	6.1	30, -90, -6	R	Cuneus, mid. occ. gyri
Neg.	347	<0.001	5.2	-23, -84, -6	L	Cuneus, mid. occ. gyri
				$Var = p_{WIN} \times (k_{WIN}-EV)^2 + (1-p_{WIN}) \times (-k_{LOSE}-EV)^2$ (Δt=0 s)		
Neg.	791	<0.001	6.3	51, -59, 23	R	Supramarg. & ang. gyri, inf. par. lobule
Neg.	134	0.003	5.4	-47, -69, 33	L	Inf. par. lobule
Neg.	131	0.004	4.9	26, 27, 53	R	Sup. front. gyrus

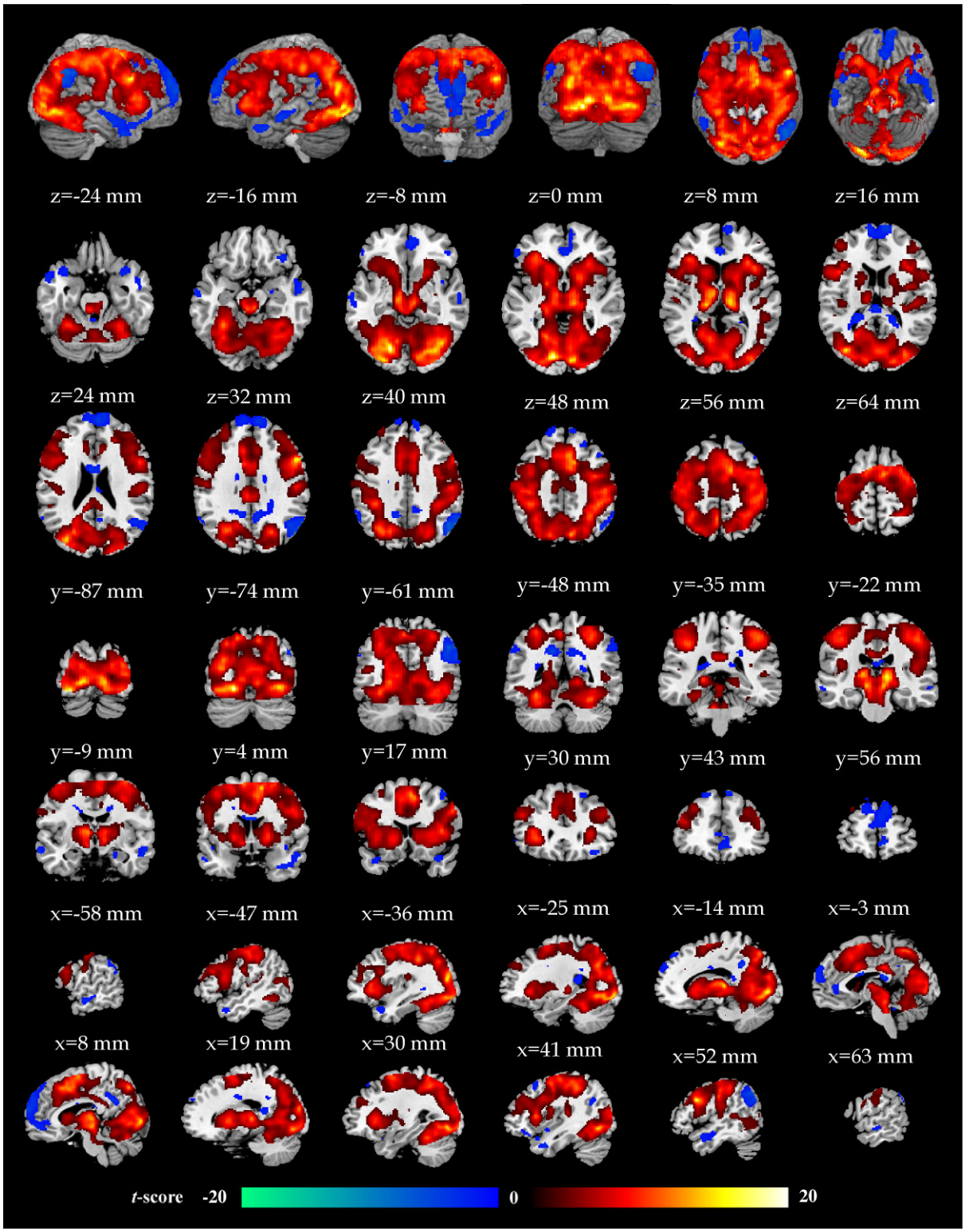

Figure 14. Functional MRI (fMRI) grand-average activations, calculated across all gambles and participants irrespective of the economic parameters, and displayed at voxel-level FWE $p<0.001$. Red denotes positive and blue denotes negative haemodynamic response. Images shown in radiological convention.

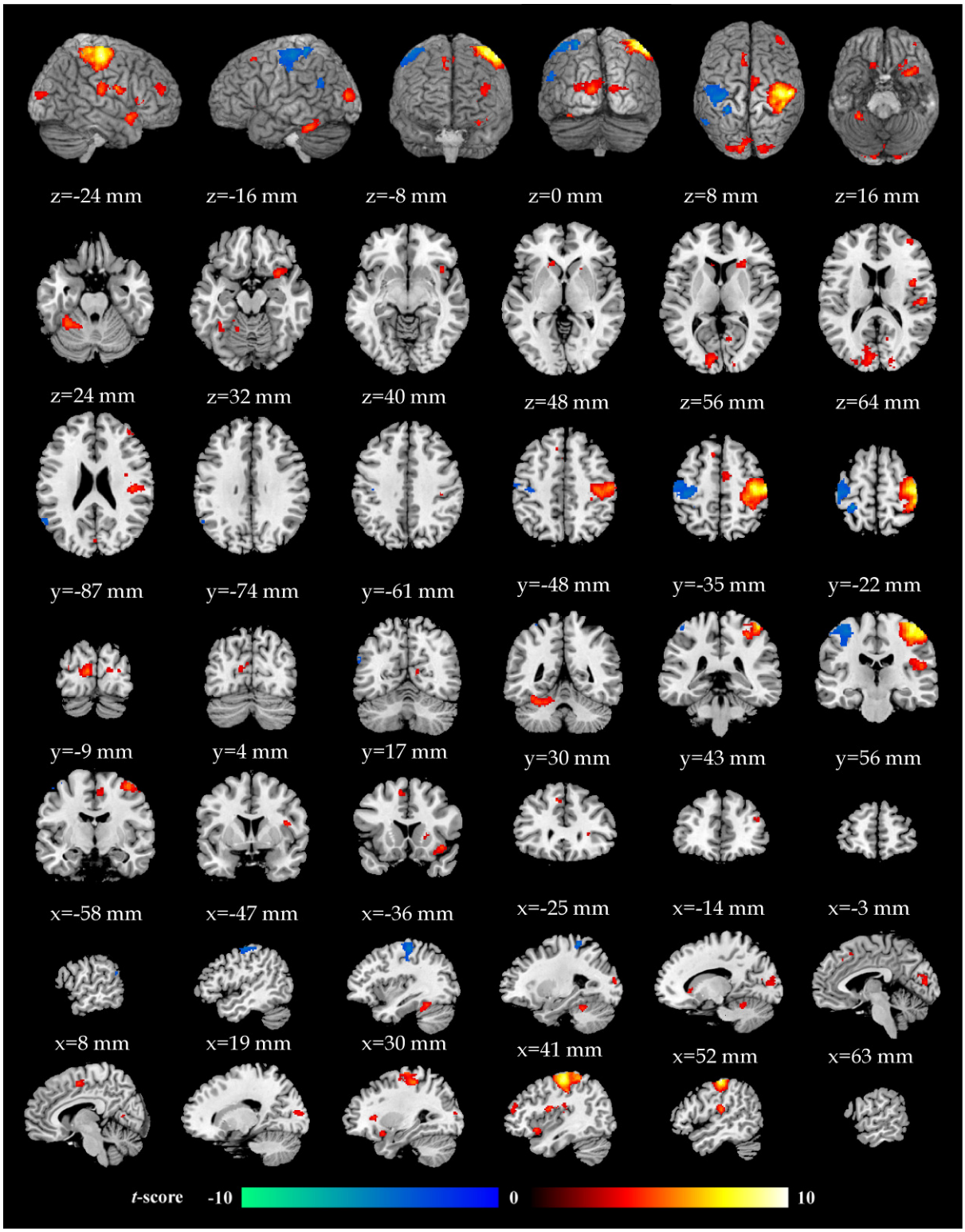

Figure 15. Functional MRI (fMRI) parametric correlation maps for k_{WIN}, displayed for Δt=0 s at the voxel-level threshold of p<0.001 uncorrected. See Table 2 for corrected clusters. Images shown in radiological convention.

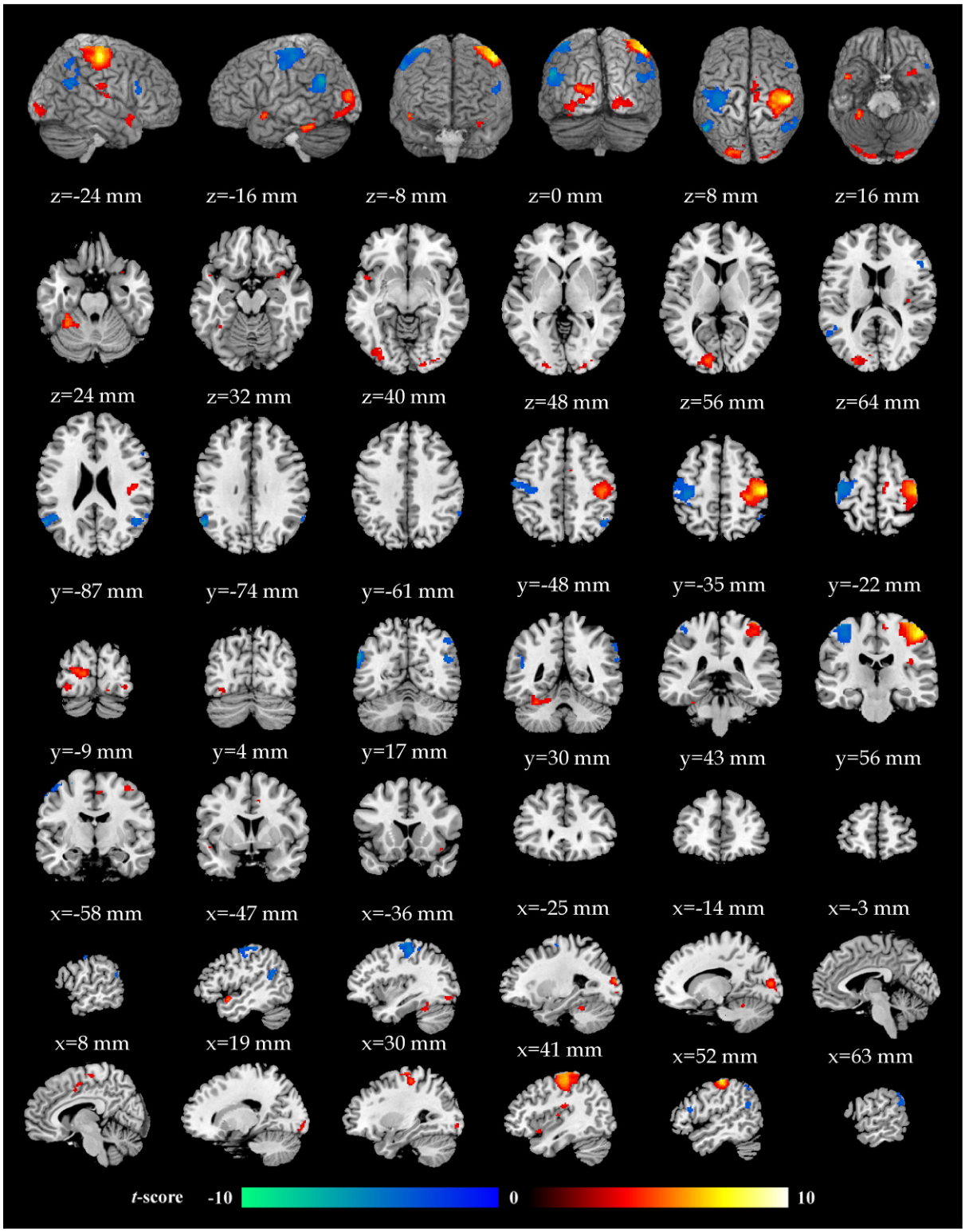

Figure 16. Functional MRI (fMRI) parametric correlation maps for $k_{WIN} \times p_{WIN}$, displayed for Δt=0 s at the voxel-level threshold of p<0.001 uncorrected. See Table 2 for corrected clusters. Images shown in radiological convention.

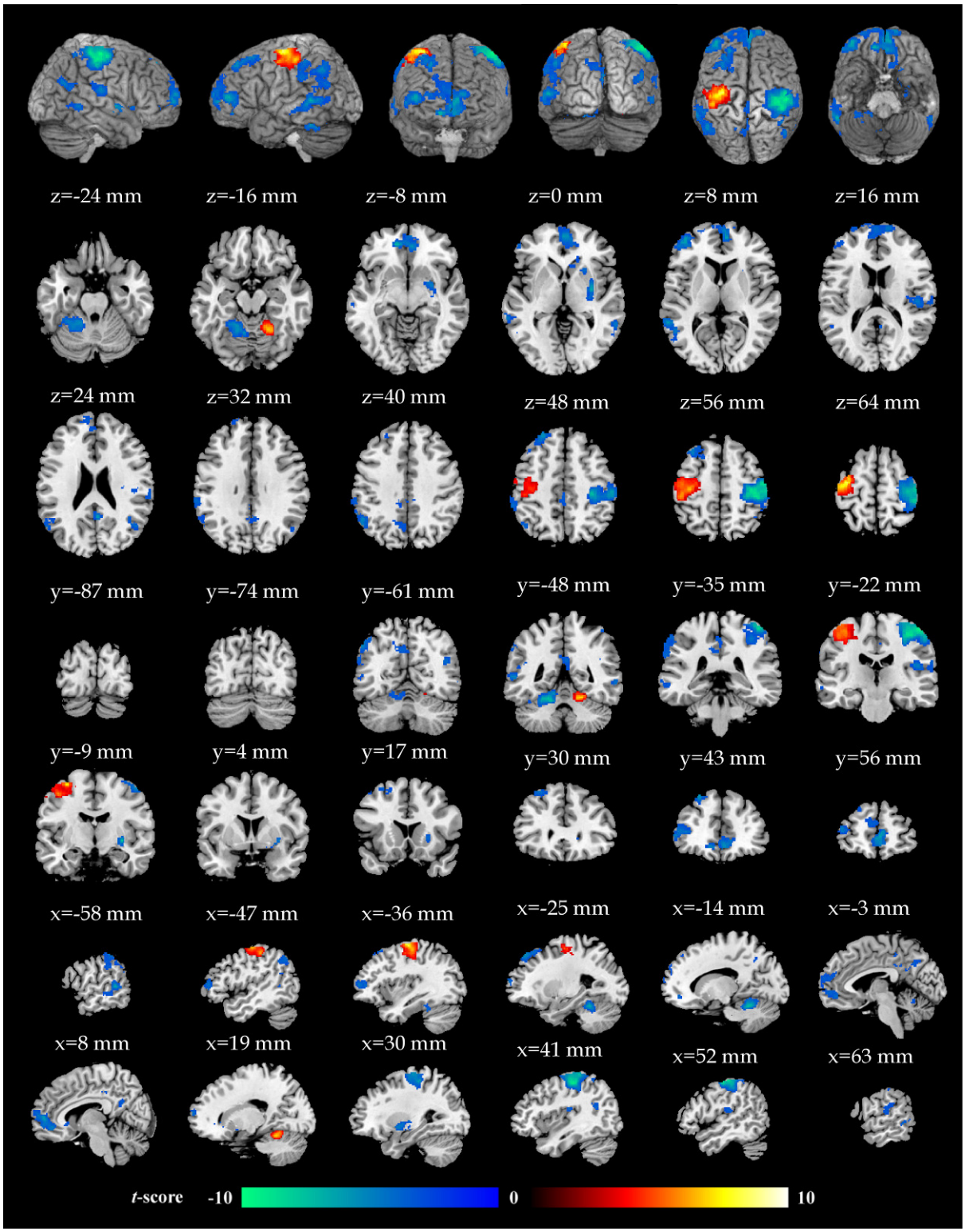

Figure 17. Functional MRI (fMRI) parametric correlation maps for k_{LOSE}, displayed for Δt=0 s at the voxel-level threshold of p<0.001 uncorrected. See Table 2 for corrected clusters. Images shown in radiological convention.

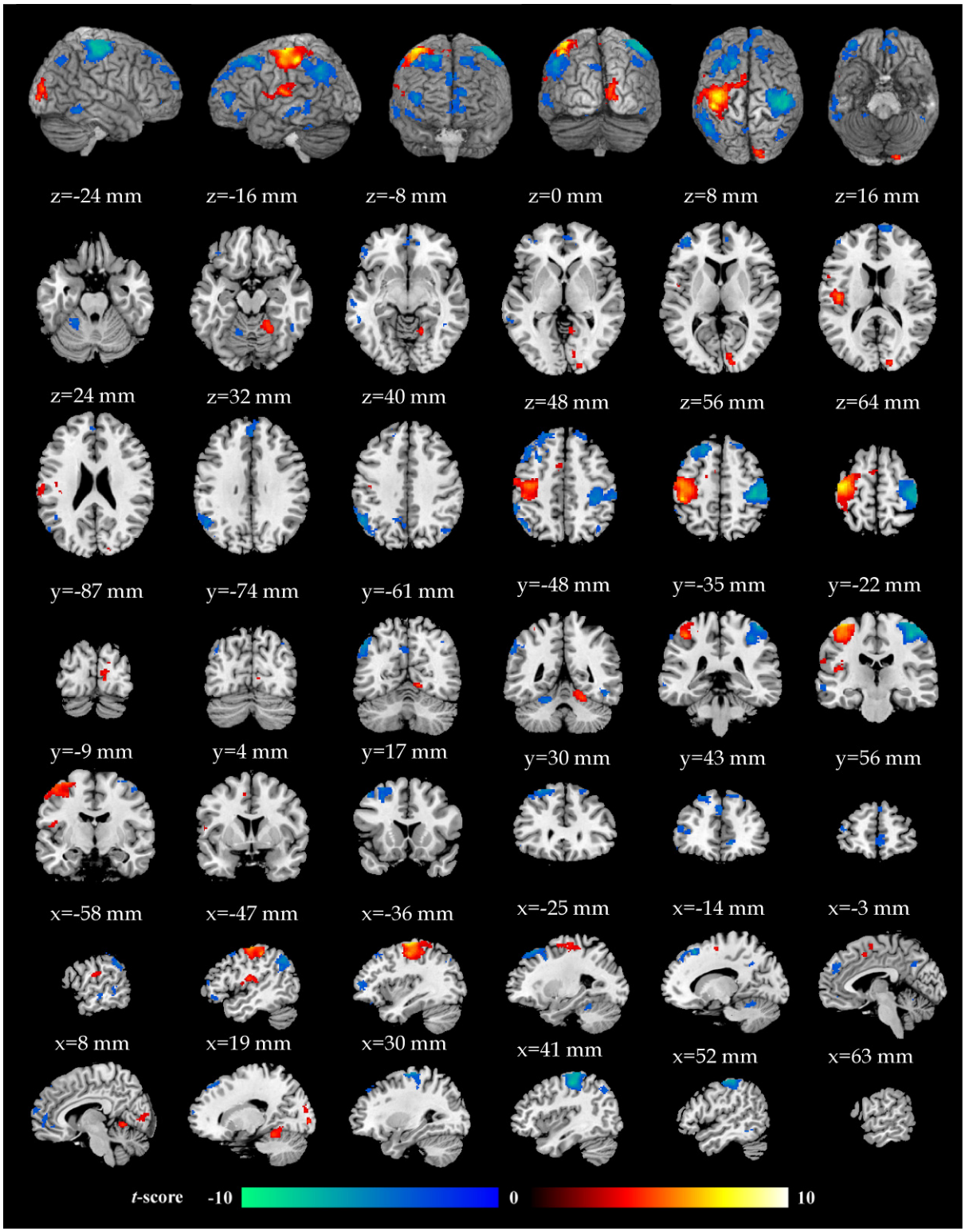

Figure 18. Functional MRI (fMRI) parametric correlation maps for $k_{LOSE} \times (1 - p_{WIN})$, displayed for Δt=0 s at the voxel-level threshold of p<0.001 uncorrected. See Table 2 for corrected clusters. Images shown in radiological convention.

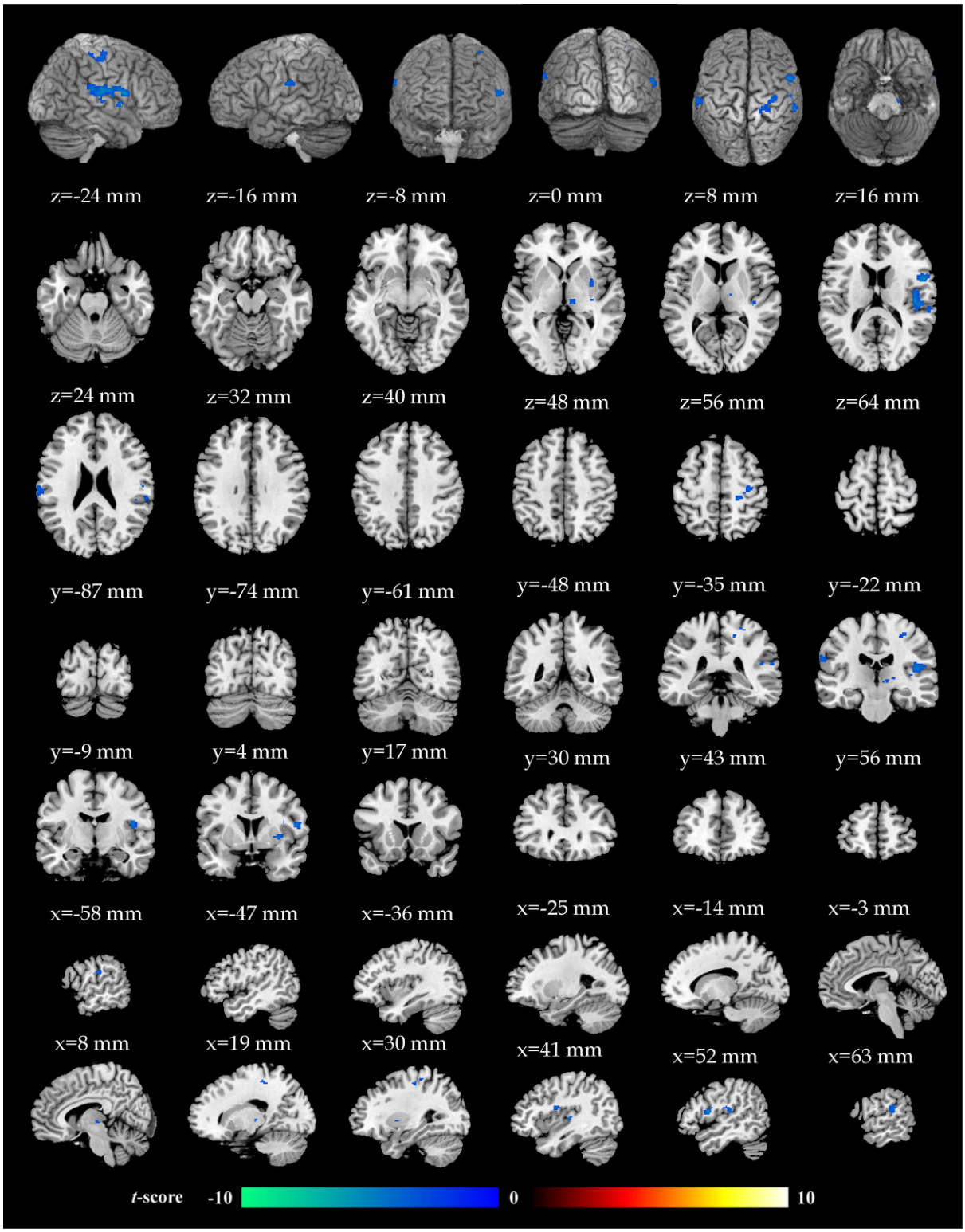

Figure 19. Functional MRI (fMRI) parametric correlation maps for p_{WIN}, displayed for Δt=0 s at the voxel-level threshold of p<0.001 uncorrected. See Table 2 for corrected clusters. Images shown in radiological convention.

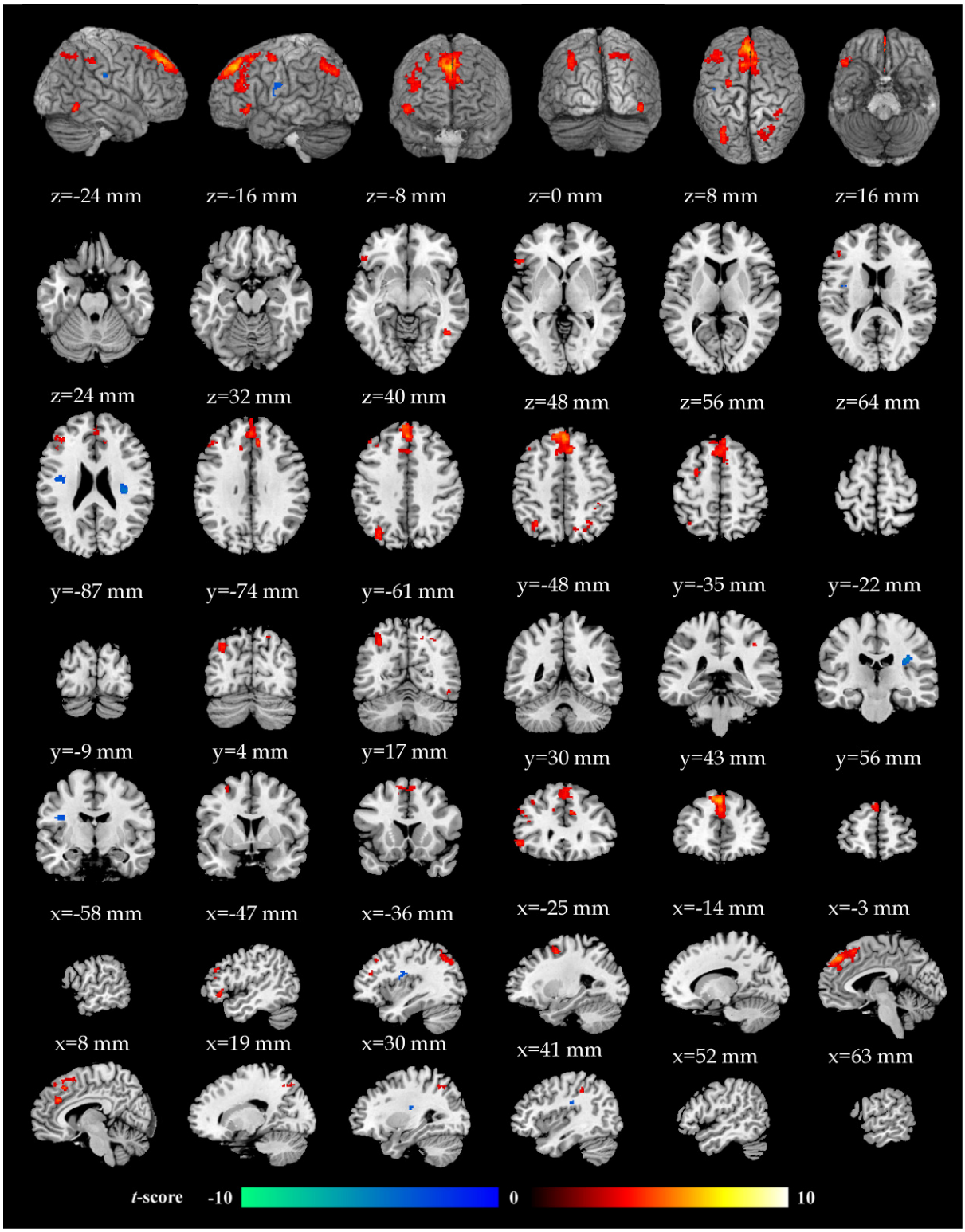

Figure 20. Functional MRI (fMRI) parametric correlation maps for $|p_{WIN}\text{-}0.5|$, displayed for Δt=0 s at the voxel-level threshold of p<0.001 uncorrected. See Table 2 for corrected clusters. Images shown in radiological convention.

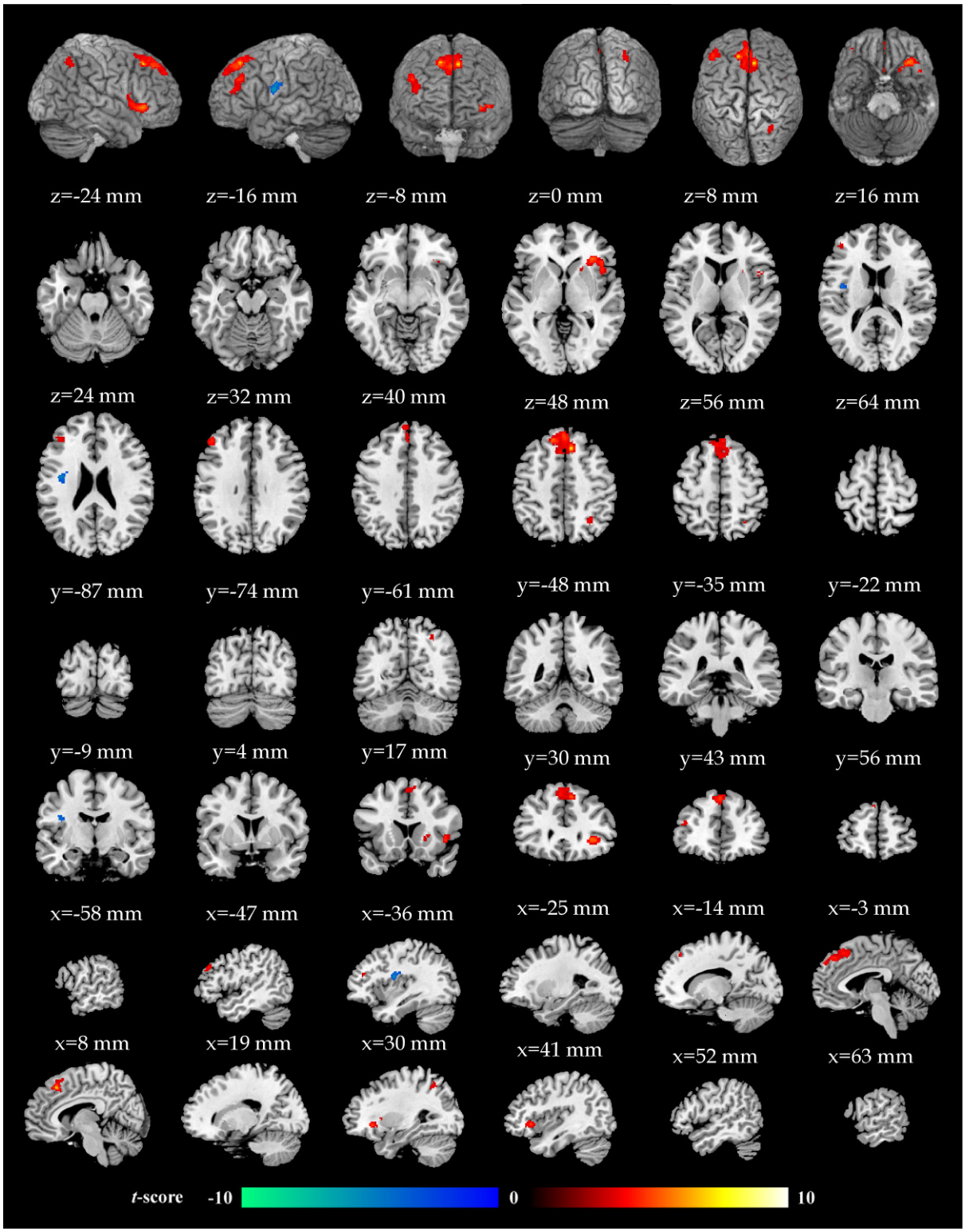

Figure 21. Functional MRI (fMRI) parametric correlation maps for $|p_{WIN}\text{-}0.5|$, displayed for Δt=2.4 s (delayed response) at the voxel-level threshold of p<0.001 uncorrected. See Table 2 for corrected clusters. Images shown in radiological convention.

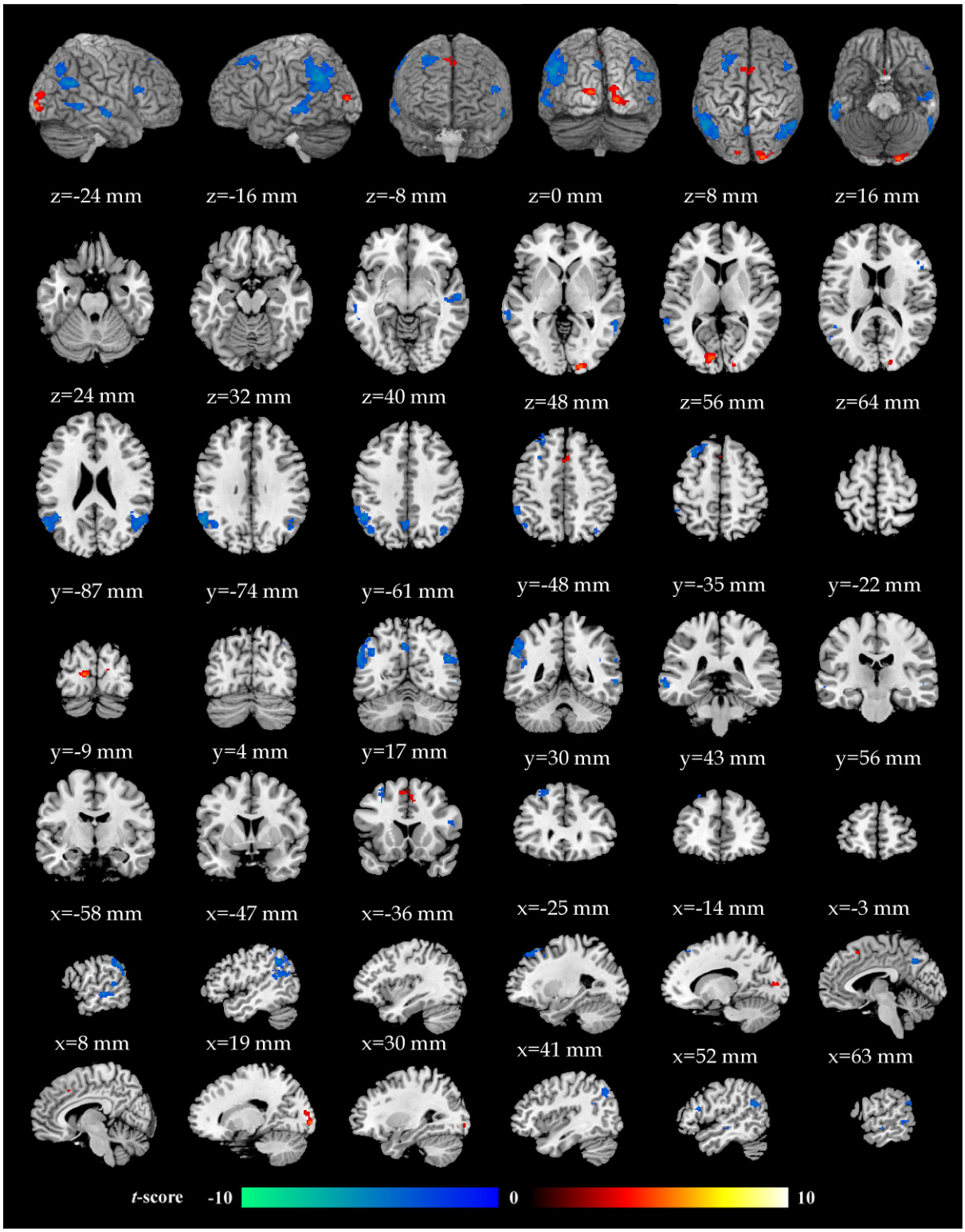

Figure 22. Functional MRI (fMRI) parametric correlation maps for $\langle k_{WIN}, k_{LOSE} \rangle$, displayed for Δt=0 s at the voxel-level threshold of p<0.001 uncorrected. See Table 2 for corrected clusters. Images shown in radiological convention.

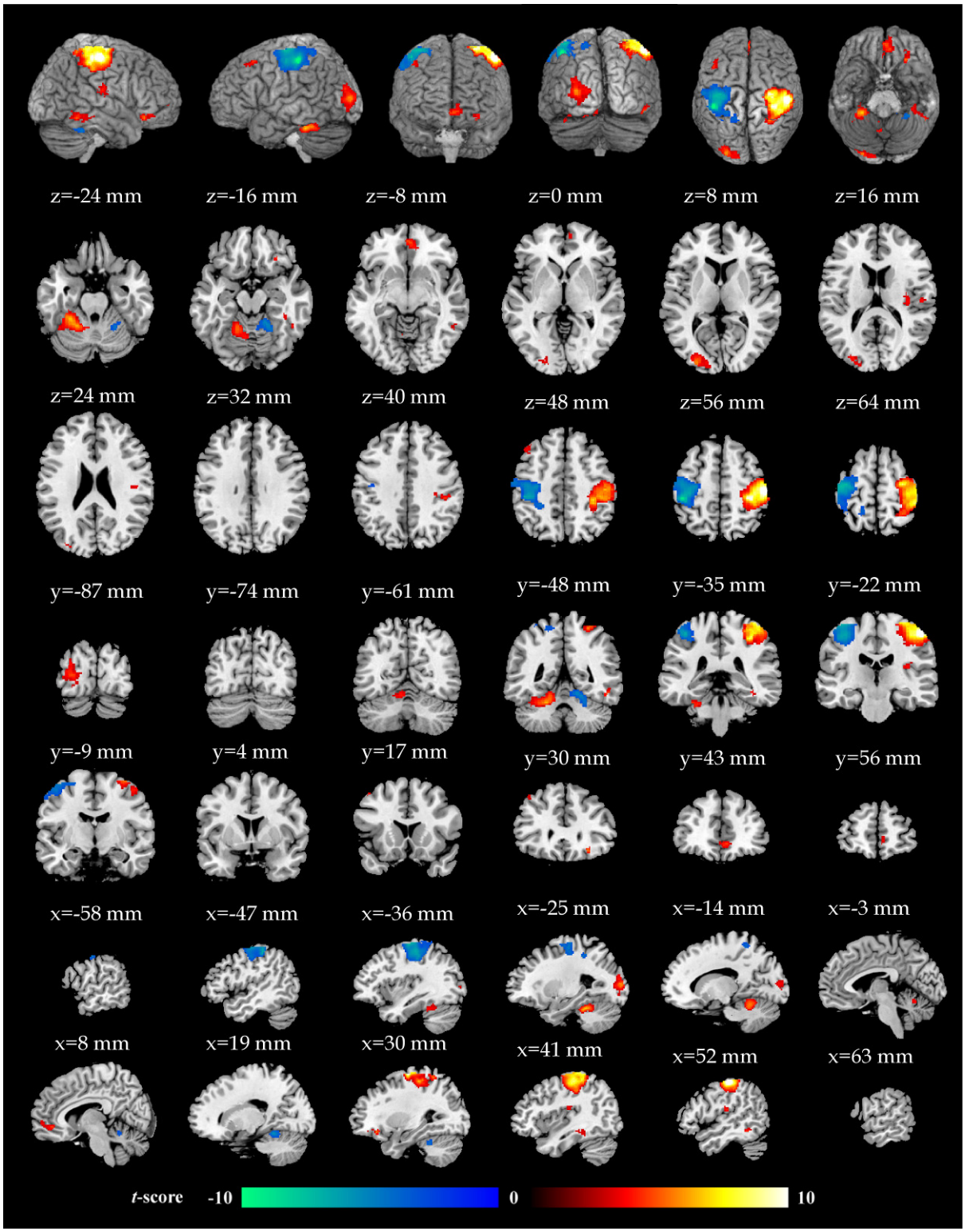

Figure 23. Functional MRI (fMRI) parametric correlation maps for $EV = k_{WIN} \times p_{WIN} - k_{LOSE} \times (1-p_{WIN})$, displayed for Δt=0 s at the voxel-level threshold of p<0.001 uncorrected. See Table 2 for corrected clusters. Images shown in radiological convention.

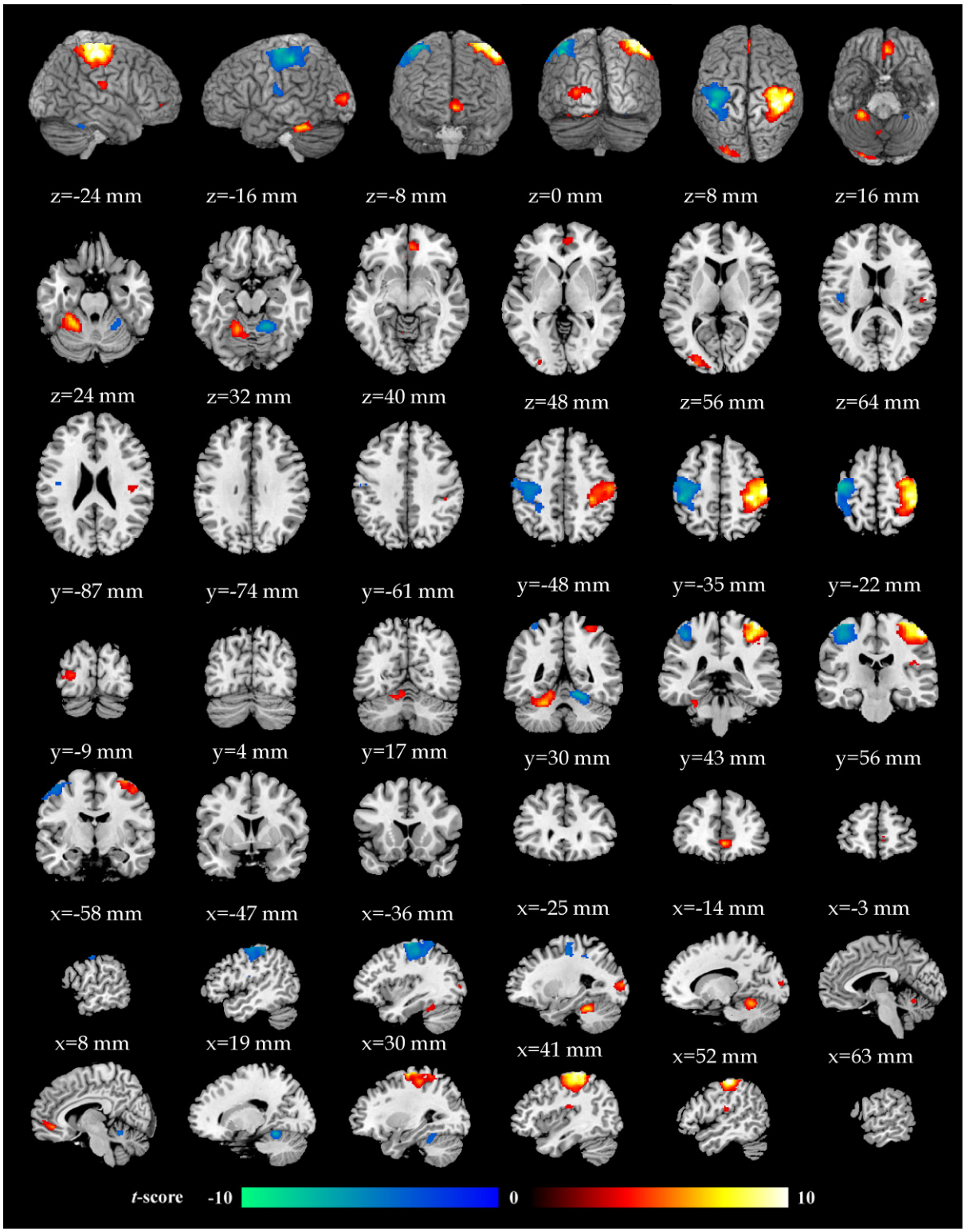

Figure 24. Functional MRI (fMRI) parametric correlation maps for $EV/\langle k_{WIN}, k_{LOSE} \rangle$, displayed for Δt=0 s at the voxel-level threshold of p<0.001 uncorrected. See Table 2 for corrected clusters. Images shown in radiological convention.

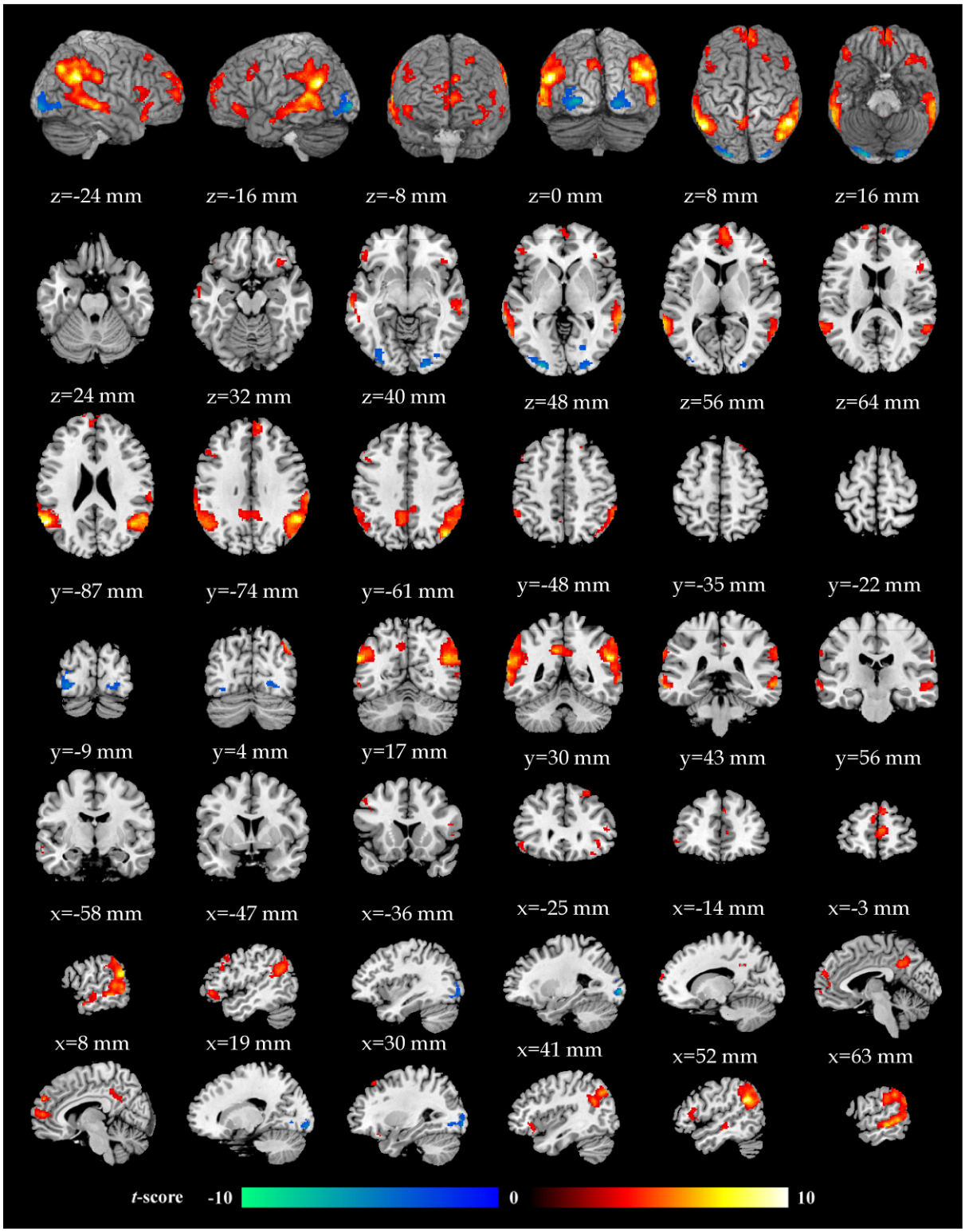

Figure 25. Functional MRI (fMRI) parametric correlation maps for $|EV/\langle k_{WIN}, k_{LOSE}\rangle|$, displayed for Δt=0 s at the voxel-level threshold of p<0.001 uncorrected. See Table 2 for corrected clusters. Images shown in radiological convention.

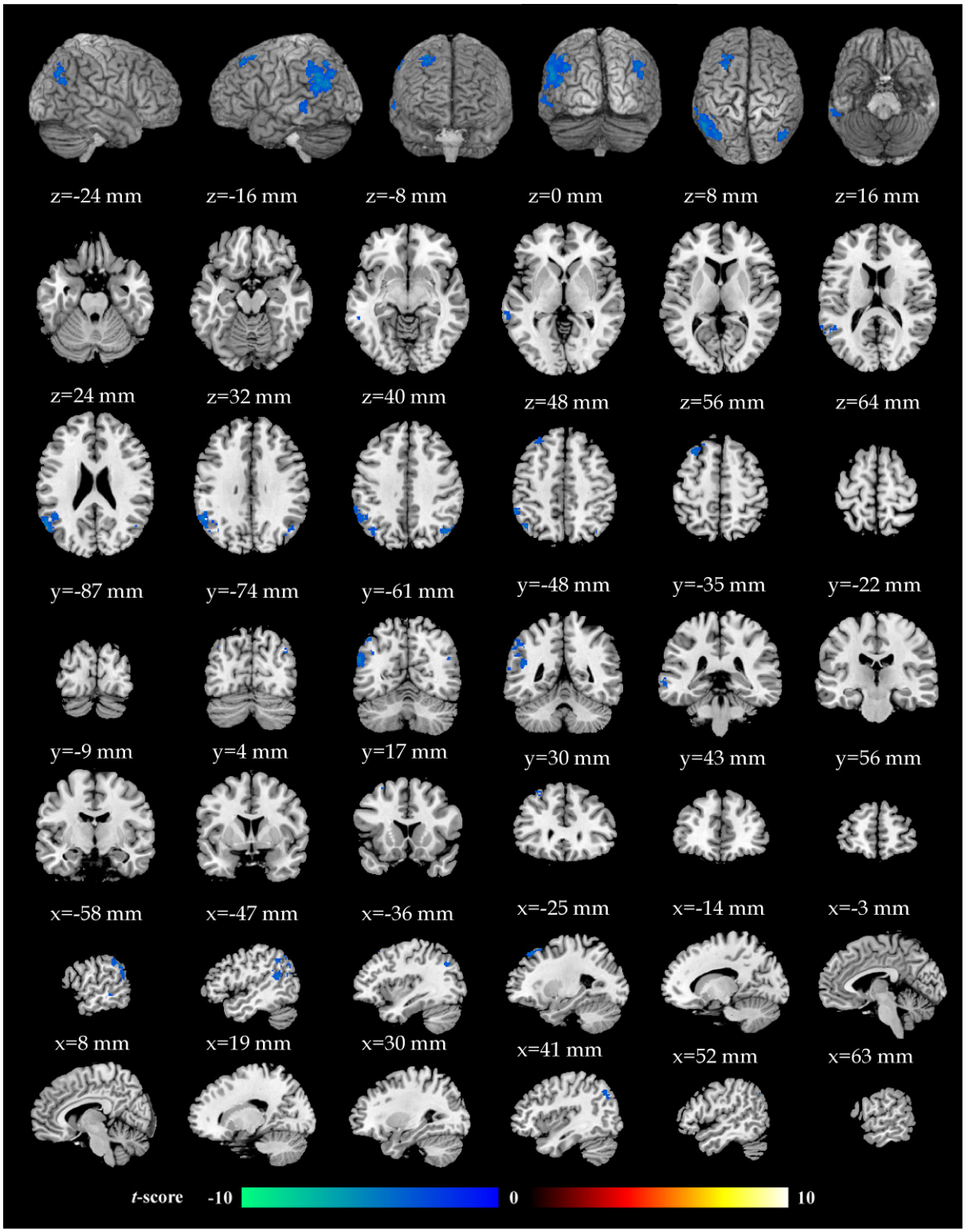

Figure 26. Functional MRI (fMRI) parametric correlation maps for $Var=p_{WIN}\times(k_{WIN}-EV)^2+(1-p_{WIN})\times(-k_{LOSE}-EV)^2$, displayed for $\Delta t=0$ s at the voxel-level threshold of $p<0.001$ uncorrected. See Table 2 for corrected clusters. Images shown in radiological convention.

5.4 Discussion

5.4.1 Modulation of visual cortex activity

In the visual cortex, particularly early visual areas, the BOLD response amplitude was enhanced for gambles presenting large values of k_{WIN}, $k_{WIN} \times p_{WIN}$ and, albeit less markedly, $k_{LOSE} \times (1-p_{WIN})$. The BOLD responses were also boosted for large values of $\langle k_{WIN}, k_{LOSE} \rangle$, EV and $EV/\langle k_{WIN}, k_{LOSE} \rangle$, and attenuated for large values of $|EV/\langle k_{WIN}, k_{LOSE} \rangle|$. These effects are interpreted as the consequence of back-projections from the frontal neocortex, insula and amygdala, and putatively reflect an adaptive system which modulates the perceptual salience of visual stimuli.

Previous studies using fMRI and near-infrared spectroscopy (NIRS) have robustly demonstrated these effects using emotional scenes and faces, but it is remarkable that the effect of modulatory back-projections is also well-evident for non-naturalistic, perceptually simple stimuli like the numerical gambles considered here (e.g., Vuilleumier et al., 2004; Vuilleumier and Driver, 2007; Wendt et al., 2011). More in detail, the observed pattern is suggestive of a mechanism which drives more careful evaluation of highly valenced scenarios, particularly prospects where the economic parameters promote choice of the risky option; from an evolutionary viewpoint, this could speculatively be related to the fact that choosing the risky option usually corresponds to performing an active action (e.g., coming out of hiding and running to capture a prey) in a structured context which needs to be carefully explored visually to identify possible dangers.

In fact, modulation of visual cortex activity by neuroeconomic parameters had been previously observed in a range of studies, such as Tom et al. (2007), Serences (2008), Engelmann and Tamir (2009), Engelmann et al. (2009) and Ino et al. (2010), but was

seldom commented upon. The results obtained here are conceptually in line with the study of Serences (2008), which concluded that visual cortex responses correlate with the difference in value between available choice options, reinforcing the view that they represent an innate drive for careful evaluation of visual inflow.

5.4.2 Differential representation of losses and gains

As in Tom et al. (2007), k_{LOSE} and, here, additionally $k_{LOSE} \times (1-p_{WIN})$ were associated with diffuse and strongly negative correlations across the prefrontal cortex as well as in the angular and supramarginal gyri. Yet, by comparison to their study, here the positive correlations for k_{WIN} and $k_{WIN} \times p_{WIN}$ were significantly less represented. While also in Tom et al. (2007) there was a mismatch between the slopes for β_{gain} and β_{lose}, the difference observed here is markedly stronger.

As discussed in the previous chapter with reference to the EEG data, the lateral prefrontal cortices are encompassed in a premotor network which integrates sensory information and feeds into the medial prefrontal cortex and striatum (Schultz, 2004; Rorie and Newsome, 2005; Venkatraman et al., 2009), and which has been hypothesized to constitute a "gain-brain" network, activating preferentially in response to prospects presenting large potential gains and deactivating diffusely to potential losses. The results observed here extend the work of Tom et al. (2007) by providing strong evidence for considerably greater allocation of cortical resources to encode potential losses than gains. The mismatch elicited here was greater probably because of the more abstract nature of the task, which involved weighing the potential outcomes by their probabilities and not just comparing two given amounts. Coupled with the absence of effects in the striatum, this observation suggests that the neural correlates of behavioural loss aversion may not be (or,

at least, not necessarily) centred around striatal activity, but rather be related to a differential neocortical representation. This hypothesis calls for further investigation, to correlate the differential representation of losses and gains with individual levels of risk propensity in each participant. Here, the author refrained from performing such analysis in light of the fact that no financial endowment or material rewards were available, and the validity of observed inter-individual differences in risk propensity was therefore dubious.

Unexpectedly, the BOLD responses in the amygdala and anterior insula appeared indifferent to the magnitude of potential losses and risk (i.e., k_{LOSE} and $k_{LOSE} \times (1-p_{WIN})$); this could be reconciled with prevalent models placing these regions in a central role in encoding negative affect (e.g., Kahn et al., 2002; Cohen and Ranganath, 2005) by speculating that loss and injury may be encoded differently depending on whether they are actually experienced, or simply evaluated in abstract in the stereotyped framework of an isolated risky prospect. Such hypothesis may be investigated in future experiments explicitly modelling neural activity in relation to prospect presentation and subsequent outcome delivery.

5.4.3 Representation of outcome probability and uncertainty

The raw outcome probability p_{WIN} appeared to be much more weakly encoded in neural activity as an individual parameter than k_{WIN} and k_{LOSE}, in spite of the fact that it appears twice in the value equation. By contrast, in agreement with an earlier study (Jones et al., 2011) the outcome uncertainty, that is $|p_{WIN}-0.5|$, was represented in differential BOLD effects across the DMPFC, DLPFC and VLPFC, the parietal cortex and the anterior insula. Of particular interest here is that fact that, in contrast with all other parameters, a

markedly different correlation pattern emerged in the anterior insula when a delayed BOLD response (corresponding to 2.4 s post-stimulus) was modelled.

The anterior insula is thought to integrate representations of uncertainty and risk with interoceptive afferences, feeding "gut feeling" signals to the mesial PFC and thus influencing option selection (Craig, 2009; Singer et al., 2009; Weller et al., 2009; Bossaerts, 2010; Medford and Critchley, 2010). Its role in economic decision-making was elucidated in a seminal experiment by Preuschoff and co-workers (2008), based on a paradigm wherein two cards were presented in sequence and reward or loss were contingent on a prior guess regarding whether the second card would be higher than the first one or not. Insofar as one defines risk as the variance associated with a loss outcome, the paradigm provides access to "risk prediction" and "risk prediction error" signals, associated with the participant's expectations immediately before and after the presentation of each card. Crucially, Preuschoff and co-workers demonstrated that anterior insula activity encodes risk through a dissociable, biphasic response, wherein early-onset BOLD signal fluctuations track risk prediction error and slower, later activity correlates positively with the level of general uncertainty.

Here, the experimental paradigm is fundamentally different, as no elements of feedback or ongoing updating of subjective beliefs were present. Yet, a highly significant association between late-onset insular activity and general outcome uncertainty, particularly in the context of gambles presenting a likely loss outcome, was found, despite the fact that direct correlations with the magnitude of potential losses were absent: delayed BOLD activity and $|p_{WIN}\text{-}0.5|$ were positively correlated, in other words insula engagement appeared to be boosted for gambles where the outcome (especially a loss outcome) was relatively predictable. This result may initially appear at odds with the findings by Preuschoff and co-workers (2008), since in their experiment insula activation was positively correlated with uncertainty. However, this discrepancy is probably related to the

substantial differences in task design, and at a conceptual level the two studies are in good agreement in demonstrating the general role of this structure in representing uncertainty and risk, independently of a straightforward association to loss magnitude. Here, a plausible interpretation for the findings is that the delayed insula response encoded an imagination of the consequence of one's actions, which was particularly brought about by the absence of declarative feedback; in this light, the positive correlations observed with $|p_{WIN}\text{-}0.5|$ may indicate that such representation is stronger whenever the outcome is relatively predictable and amplified when the predicted outcome is a loss.

More trivially, the early effect observed in the DMPFC, DLPFC, VLPFC, aMCC and inferior parietal regions probably reflects a difference in processing strategy and consequent arousal: while for p_{WIN} far from 0.5 cognitively-demanding integration of the three gamble parameters is fundamental, for $p_{WIN} \rightarrow 0.5$ EV sign determination degenerates to a straightforward comparison between k_{WIN} and k_{LOSE} (see Critchley et al., 2001; Cohen et al., 2005; Satterthwaite et al., 2007; Jones et al., 2011).

5.4.4 Default-mode network activity and the representation of risk-indifference

A novel finding of the present experiment is the selective disengagement of the default-mode network (DMN) for certain prospects. The DMN is a major functional network observed in the resting brain, and comprises key nodes located bilaterally in the region of the angular and supramarginal gyri and inferior parietal lobule, mesial prefrontal cortex (DMPFC and VMPFC) and precuneus. It has been widely found to disengage proportionally as a function of level of cognitive demand and attentional arousal, representing the shifting of resources from introspection to outward-directed attention (Corbetta and Shulman, 2002; Greicius et al., 2003); under resting conditions, the

constituents of the DMN activate coherently to subserve processes related to memory consolidation and self-awareness (Greicius et al., 2003; Fox and Raichle, 2007; Rosazza and Minati, 2011).

Here, the DMN disengaged in response to gambles presenting a high degree of response conflict due to a near risk-indifferent situation (i.e., $|EV/\langle k_{WIN}, k_{LOSE}\rangle| \cong 0$); less evidently, it also deactivated in response to large average amount magnitude $\langle k_{WIN}, k_{LOSE}\rangle$, large outcome variance and large expected gain $k_{WIN} \times p_{\mathrm{WIN}}$.

The hypothesis that the DMN as a unitary network could actively subserve economic processing is intriguing, but a more likely explanation is that its relative deactivation simply reflects, as an epiphenomenon, the deeper processing inherently elicited by some prospects, for example those characterized by non-obvious advantageousness or large amounts at stake. Indeed, as detailed in the following chapter, no evidence of direct involvement of the DMN was found when explicitly modelling the effective connectivity network supporting value computation.

Of note here is also the absence of strong concomitant correlations in the anterior cingulate cortex (pACC and aMCC), which has been previously hypothesized to play a key role in response selection and conflict monitoring. This is unlikely to be simply due to limited task engagement because, as reported in chapter 2 (Figure 5), $|EV/\langle k_{WIN}, k_{LOSE}\rangle|$ did strongly correlate with the RTs, confirming that near risk-indifferent gambles were associated with a greater level of response conflict and deeper processing than more obvious ones. Rather, this negative finding, which is in line with the absence of a correlation between $|EV/\langle k_{WIN}, k_{LOSE}\rangle|$ and autonomic arousal indicants, may suggest that the type of conflict inherent in actively choosing either a risk-free or a risky option when the advantageousness is not clear may draw upon different neural resources in comparison to the more straightforward situation of inhibiting a prepotent response leading to error,

such as during a Stroop task; this interpretation, of course, must at present remain speculative but motivates further investigation in this area, using a task explicitly contrasting the two situations (Barch et al., 2000; Braver et al., 2001; Vogt, 2005; Medford and Critchley, 2010).

5.4.5 Neocortical representation of expected value

As regards to the neural representation of *EV*, the main observation was a positive correlation with BOLD response amplitude in the ventral medial prefrontal cortex (VMPFC), in a cluster which also partially overlapped with the pACC/mACC and OFC. Notably, activity in this area also responded positively to $EV/\langle k_{WIN}, k_{LOSE}\rangle$, and negatively to k_{LOSE}, for the latter parameter accompanying the correlations observed in the DLPFC, VLPFC and in parietal regions. The finding of a positive correlation between *EV* and activity in the mesial prefrontal cortex is unsurprising, given that several other studies have established that activity in this region directly encodes the value of actions in a form that is highly abstract and generally independent of the material nature (e.g., food vs. money) of the potential reward (e.g., Chib et al., 2009; Gläscher et al., 2009; Wunderlich et al., 2009; Smith et al., 2010).

Yet the findings have an element of novelty in that the present multi-parametric evaluation made possible by the independent variation of k_{WIN}, k_{LOSE} and p_{WIN} provided further insight into exactly what element of value drives medial PFC activity. As conceptualized in the review by Vlaev and co-workers (2011), the neural representations of value supporting observed preferences in the face of risky options may be absolute, relative or even dichotomous in nature. In other words, in the context of the present task two complementary hypotheses could in principle be formulated regarding the nature of medial PFC responses.

First, activity in this region might track in a continuous form "absolute" value, i.e. the difference between the positive ($k_{WIN} \times p_{WIN}$) and negative ($k_{LOSE} \times (1-p_{WIN})$) terms of the value equation. In other words, it could track not only how "risk advantageous" each gamble is, but also what the absolute magnitude of the expected value is, determined along a scale that could, plausibly, be set by the range of expected values observed throughout the previous gambles during the task. According to this hypothesis, the predicted BOLD response amplitude would be larger for a completely advantageous (i.e., zero-potential loss) gamble offering a win of, say, 50 £ in comparison to a completely advantageous gamble offering a win of 1 £, and would be similarly affected for potential losses.

Second, medial PFC activity could alternatively track locally-rescaled (or even dichotomised) risk-advantageousness rather than absolute value, i.e. responding to the relative comparison of the positive and negative terms rather than to their difference expressed on an absolute value scale. In other words, it could simply track "how convenient" each risky prospect is, irrespective of the magnitude of the amounts at stake (i.e., computing $k_{WIN} \times p_{WIN} \geq k_{LOSE} \times (1-p_{WIN})$ rather than $k_{WIN} \times p_{WIN} - k_{LOSE} \times (1-p_{WIN})$). This would represent the action of a rescaling mechanism or "decisional comparator" acting locally, within the context of each individual gamble. According to this hypothesis, the BOLD response amplitude would be the same for two completely advantageous (i.e., zero-potential loss) gambles offering potential wins (or losses) of different magnitudes.

Here, the correlation observed for EV was closely mirrored by that for unit-less risk-advantageousness $EV/\langle k_{WIN}, k_{LOSE} \rangle$, which attained a markedly more significant correlation score. This result strongly suggests that the second hypothesis is the correct one, i.e. that the activity of the medial PFC is more closely coupled to advantageousness determination (either in relative or dichotomic terms) than to full, analogue value representation. In the context of isolated risky gambles absolute representation of value on

an abstract, stable scale is not needed to support effective decision-making (Vlaev et al., 2011), so it appears evolutionarily plausible that the brain computes a more straightforward, less energy and time-consuming comparison of the immediately-available gain/loss terms rather than a full, continuous representation of value on a stable internal scale.

This result is in good accord with previous neuroimaging experiments suggesting that medial PFC activity encodes the value of actions in a relative way, essentially generating "go/no go" signals which determine the appropriate course of action (Elliott et al., 2008; Chib et al., 2009; Venkatraman et al., 2009; Wunderlich et al., 2009). Yet general validity of these findings should not be assumed a-priori, since a recent review of neurophysiological literature by Platt and Padoa-Schioppa (2009) highlighted that multiple, concurrent value representations are likely to be available in the brain, reflecting different evaluative mechanisms that may be task and situation-dependent.

5.4.6 Lack o f differential striatal responses to expected value

A striking fact is the absence of correlations between *EV* or related parameters, and BOLD activity in the striatum. This effect cannot be due to signal loss which could hypothetically be caused, for example, by inefficient imaging sequence settings, because a clear average BOLD response was observed in both dorsal and ventral parts (see Figure 14). Rather, this negative finding is interpreted as indicating a genuine difference in gamble processing with respect to the study by Tom et al. (2007), in which clear striatal correlations with *EV* were observed. One possible explanation for this discrepancy is that the task employed here was more abstract, due to the presence of variable outcome probably, and that this led to a shift in processing strategy from a more instinctive one supported by basal ganglia circuitry, to a more abstract, integrative one reliant a distributed

neocortical representation. This hypothesis of different neural substrates contingent on the "evaluative complexity" of a decisional prospect calls for further evaluation in an experiment where fixed and variable-probability gambles are explicitly contrasted (here, such comparison would not be valid as the number of trials with 50/50 outcome probability was comparatively small).

A further, non mutually exclusive explanation is related to the fact that, in contrast to the study by Tom et al. (2007), here no real financial reward was available to the participants. It is possible that the correlations observed by Tom and co-workers in the mesial PFC were functional to *EV* determination, whereas those in the striatum were principally "epiphenomenal", i.e. represented reward anticipation rather than value determination. In fact, while differential BOLD responses to *EV* have been observed in the striatum across many studies, a considerable body of empirical evidence is already available indicating that value computation is not intrinsically reliant on this structure, whose role is essential for behavioural reinforcement but not necessarily for deciding among available choice options in a one-off situation rather than a game providing ongoing outcome feedback (Hollerman et al., 1998; Pagnoni et al., 2002; Schultz, 2004; Cohen and Ranganath, 2005; Rorie and Newsome, 2005; Wrase et al., 2007; Tobler et al., 2009).

5.4.7 Summary

In summary, the extensive univariate mapping performed in the present experiment revealed a rich set of associations between regional activity and specific economic parameters: i) early visual areas show a response pattern suggestive of an adaptive mechanism driving more careful evaluation of valenced prospects that prompt choice of the risky option; ii) a strong dissociation in diffuse frontal activity is observed between positive correlations for potential gains and negative correlations for potential losses, and

is interpreted as evidence that the brain, in presence of an abstract decisional task, devotes substantially more resources to the representation of losses than gains; iii) the amygdala and anterior insula appear insensitive to potential loss and risk, suggesting that their engagement may be more closely related to experienced states rather than to abstract evaluation of individual risky prospects; iv) the anterior insula displays a very clear "two-phase" activation, characterized by sensitivity to outcome uncertainty in the later phase of the response, supporting the "dual insula activation" model of Preuschoff et al. (2008); v) DMN deactivation following gamble presentation is sensitive to multiple economic parameters, plausibly reflecting variable levels of processing demands and associated arousal; vi) the cingulate cortex appears insensitive to level of response conflict determined by near risk-indifferent gambles, suggesting that different forms of conflict, e.g. inherent in choosing among different options vs. suppressing prepotent behaviours, may be resolved through the activity of segregable circuits; vii) the mesial PFC responds to *EV* and related parameters in a fashion that strongly suggests it represents value either in a binary or a rescaled form, rather than a continuous integrator on an absolute scale stable throughout the task; viii) the dorsal and ventral striatum appear insensitive to *EV*, potentially due to the abstract form of value computation indexed by the task and/or due to the unavailability of real financial reward.

6. Functional MRI (fMRI)-based network discovery analysis

6.1 Background and motivation

In the 17th century, Descartes wrote that "Duck behaviour is the sum of its individually behaving parts". Though such statement was profoundly inspiring for its time, as it highlighted the concept of functional specificity of each organ, nowadays it appears completely biologically inadequate, as it neglects the complex interactions between the organs on which homeostasis is founded. While no contemporary biologist would take such an approach to studying a living organism, one may, provocatively, argue that this is more or less what is done in univariate fMRI studies such as the one presented in the previous chapter. There is little doubt that the localizationalist approach, from Broca's time (e.g., Broca, 1861) to today, has provided immensely valuable insights and continues to do so. Yet it is inherently reductionistic, in that it implicitly assumes that cognitive and behavioural functions can be accounted for by the activity of individual, separate regions. More modern connectionistic views (e.g., Rumelhart et al., 1986) recognize that behavioural functions are not statically linked to specific regions, rather are an emergent property of complex, non-linear dynamic interactions among brain areas (e.g., Stephan, 2004; Sporns, 2009). Considering that the ability to make decisions is, arguably, one of the most abstract capabilities of humans and other animals, the fact that most available neuroimaging studies in this area have been based on univariate analysis alone appears to be a particular serious limitation.

Ex-vivo axonal tracing studies and in-vivo investigations of structural connectivity, based on diffusion-tensor imaging (DTI), and functional connectivity, based on resting-state fMRI (rs-fMRI), convergently indicate that brain areas are neither exhaustively inter-

connected with one another, nor preferentially wired with their immediate neighbours, nor randomly connected. Rather, the topological structure (i.e., the abstract arrangement of connections among nodes, independent of their physical location) of cortico-cortical and cortico-subcortical connections exhibits very specific features which are fundamental to the brain's ability to maintain an efficient balance between regional functional specialization and large-scale information integration (Sporns et al., 2000; Sporns and Tononi, 2001; Sporns et al., 2004; Hagmann et al., 2008; Buckner et al., 2009; Sporns, 2009).

One key observation is that the local density of connections, defined anatomically as presence of axonal bundles and functionally as coherence of activation time-courses, is distributed very inhomogeneously, i.e. with a very strongly skewed distribution: a very small number of well-identifiable regions exhibit a disproportionately large number of connections (in graph theory referred to as the "degree" of a node; Zemanová et al., 2006; Hagmann et al., 2008; Sporns, 2009; Wang et al., 2010). Such regions, which are distributed throughout the whole cortex but fond principally in the prefrontal, parietal and posterior temporal cortex, are widely regarded to act as "integrative hubs", conjointly serving the purpose of supporting information exchange between distant nodes and non-linear integration of information from multiple afferent representations. It can be explicitly demonstrated that this architecture minimizes the anatomical and metabolic cost of maintaining long-range connections (Guimerà et al., 2005; Bassett and Bullmore, 2006; Zamora-López et al., 2010; Bullmore and Bassett, 2011). From a cognitive perspective, these supra-modal integration centres are the key substrate for the emergence of networks that support behavioural abilities in specific neuropsychological domains (Mesulam, 1998). A complementary, but by no means mutually exclusive, viewpoint is that these hubs represent "convergence-divergence" zones, that implement bi-directional information exchange between earlier sensory cortices and higher-order association areas, and subserve

the encoding of specific "combinatorial arrangements of knowledge", such as an object belonging to an semantic category, or an abstract situation (Meyer and Damasio, 2009).

Considering the richness and complexity of the univariate relationships between economic parameters and regional activity that have been reported in the previous chapter, it is evident that such scattered representations must be somehow integrated to give rise to the observable decisional behaviour. Unavoidably, any attempt to deliver a realistic neuroeconomic account of decision-making under risk needs to explicitly represent network-level activity, i.e. modulations of dynamic connectivity between cortical integrative hubs. There is no biological reason to assume that the economic parameters are simply encoded in anatomically-scattered linear correlations with the overall intensity of post-synaptic activity (which is what the BOLD signal indexes, e.g. Logothetis and Pfeuffer, 2004). Hence, in the author's view neuroeconomics needs to move beyond univariate analysis if it is to provide a realistic account of how the multiple cognitive processes involved in decision making (e.g., working memory, strategic and probabilistic reasoning, and the abstract representation of relative magnitudes) interact and are integrated with affective and physiological function.

At present, neuroimaging methods literature provides essentially two techniques to model how a given parameter is represented in large-scale connectivity: psychophysiological interaction (PPI) analysis and dynamic causal modelling (DCM). The former models how the (physiological) influence that activity in one "seed" region exerts on the activity of all other brain voxels changes as a function of an external (psychological) factor, such as an economic variable during a decisional task. It is assumed that brain regions exhibiting such interaction integrate information afferent from the "seed" region with the external psychological factor (Friston et al., 1997). On the other hand, dynamic causal modelling (DCM) treats small, pre-defined brain networks as dynamic systems subject to external perturbations, and can yield estimates of the intensity and direction of

causal interaction between brain regions. While PPI simply treats the measured BOLD signal as an observable and models interactions on the basis of its time-course, DCM is based on representing post-synaptic activity as a hidden variable, and back-inferring it using a realistic biophysical model of neurovascular coupling. The DCM framework is ideally suited to Bayesian analysis, enabling explicit comparisons of competing models in terms of available statistical evidence (Friston et al.,2003; Stephan et al., 2007).

It is worthwhile to consider carefully how techniques such as PPI and DCM can provide information on directed interactions, given that fMRI does not have the temporal resolution to distinguish the sequentiality of activation, due to convolution of post-synaptic activity with the slow haemodynamic response (Logothetis and Pfeuffer, 2004; Logothetis, 2008). This is possible because, in presence of non-linear interactions, the structure of temporal variance can itself enable discriminating between opposite causal directions. If one simply considers the time-courses of regions "A" and "B", linear correlation between them will clearly lead to a symmetric matrix. Yet, due to non-linearity, considering the effect of the time-course of "A" on "B" conditional on an external parameter *k* is mathematically not equivalent to the converse.

So far, to the author's knowledge only three studies have investigated decision-making using connectivity models. Camara et al. (2008) have considered striatal connectivity related to reward processing during a task providing unexpected high gains and losses, and demonstrated that activity in the ventral striatum is closely coupled with insula, amygdala, hippocampus and orbitofrontal cortex activity, with a pattern the differs for gains and losses. On the other hand, Hare et al. (2010) considered a complex social decision-making task involving charitable donations, and demonstrated that VMPFC activity not only responds to the subjective value of a donation, but strongly integrates signals from the anterior insula and temporal cortex, which are hypothesized to encode signals related to social cognition. The third investigation, by Park et al. (2011), has

demonstrated that the way potential losses and gains are processed differs when monetary rewards are combined with physical pain, through changes in "value-dependent" coupling between sub-genual cingulate and amygdala.

These studies suffer from limitations inherent in the current implementations of PPI and DCM, which make them adequate only for investigating connections among small numbers of regions selected a-priori. PPI, at least in its most common implementation, tests for interactions with respect to activity in one seed region, rather than interactions across multiple combinations of regions. DCM overcomes this limitation, but can only be used for relatively small networks, as it requires the experimenter to explicitly pre-specify specific network models to compare and contrast. Both approaches are very useful when studying, for example, associative sensory processing, since the functions of interest are generally linked to a small, relatively well-defined set of regions.

This is not the case for a complex, highly abstract ability like decision-making, which emerges from large-scale interactions involving many brain regions. One way of investigating such large-scale networks is to perform a comprehensive parcellation of all brain areas potentially involved in task performance, and then to run PPI analyses across all combinations of regions (as opposed to PPI between one seed region and all other brain voxels as presently implemented in SPM8) in order to identify those connections that are significantly modulated by the economic parameters of interest. This approach has key advantages in that it can capture effective connectivity across many pairs of regions, rather than just those related to efferent signals emanating from one area chosen a-priori, and in that it can effectively "discover" a whole-brain effective connectivity network, rather than requiring the user to make restrictive a-priori hypotheses like DCM. Even though this analysis is computationally demanding, the resulting large-scale effective connectivity graphs can explicitly reveal the cortical hubs involved in value computation and representation with minimal a-priori assumptions (Salvador et al., 2005; Bassett and

Bullmore, 2006; Camara et al., 2008; Camara et al., 2009; Zamora-López et al., 2010). This graph-based approach to functional and effective connectivity is, per se, not new and has already been applied to the study of dementia, schizophrenia and autism, revealing profound abnormalities in large-scale network structure and dynamics in these disorders (e.g., Wang et al., 2010).

Once large-scale graphs are obtained, a range of topological metrics, widely used in graph theory, can be utilized to map the key features of each node and their statistical distribution across the network. The most relevant parameters are i) the number of connections incident on a given node ("indegree"), ii) the number of connections emanating from a given node ("outdegree"), iii) the overall number of connections of a given node irrespective of direction ("degree centrality"), iv) the number of shortest paths, calculated between all other nodes in the network, that pass through a given node ("betweenness centrality"), v) how densely interconnected between one another the topological neighbours of a given node are ("clustering coefficient"). The degree centrality, betweenness centrality and clustering coefficient capture different aspects of the role of a hub. One, by definition, expects a cortical region acting as hub node to have a very large number of connections. But such node could be in a peripheral area of the graph, such that interchange of information between the other nodes is accomplished more efficiently through other routes. If a node has a large number of connections and is topologically central to a graph, its role as a hub is much reinforced (Figure 27a). Further, if a node has a large number of connections, but the neighbouring nodes are densely interconnected with one another, its importance for information interchange and integration is questionable; on the contrary, if it acts as a "gateway" between weakly interconnected neighbours, its facilitatory and integrative role is more obvious (Figure 27b). Hence, one expects cortical hubs to be characterized by large values of degree and

betweenness centrality, and small clustering coefficients (Bassett and Bullmore, 2006; Sporns, 2009; Newman, 2010; Wang et al., 2010; Bullmore and Bassett, 2011).

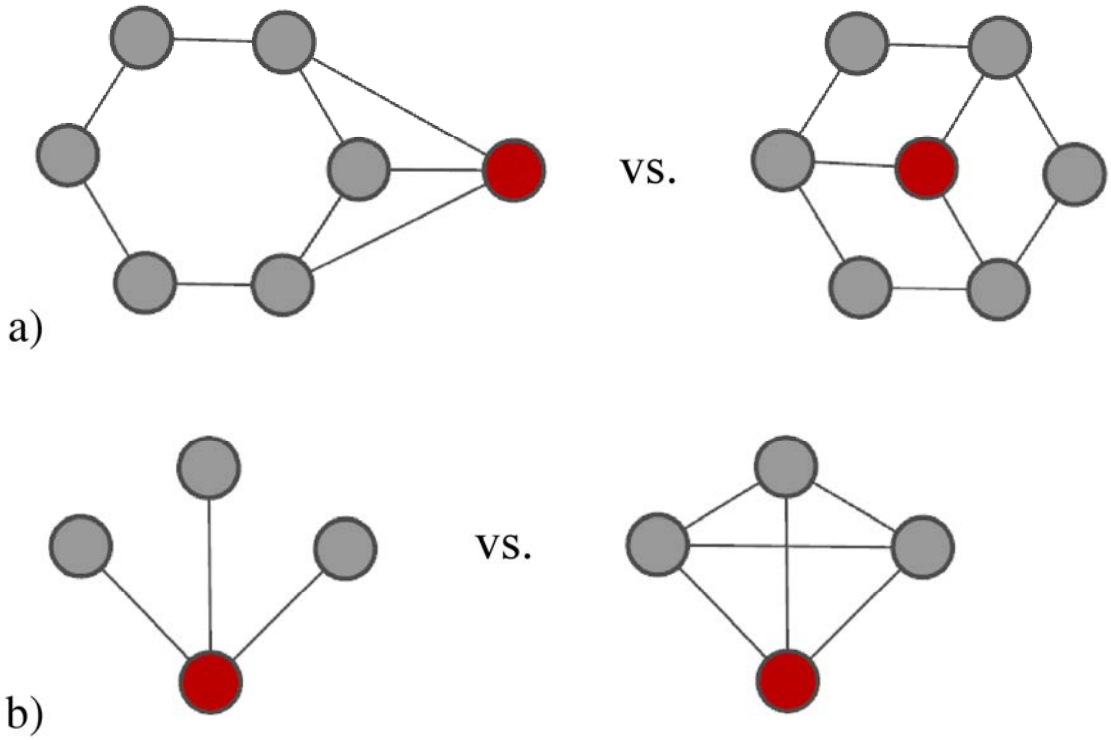

Figure 27. Simplified examples of the topological position of a hub region (red, having 3 connections) in a graph. a) Hub located in a peripheral region (low betweenness centrality) vs. in a central region of the network (high betweenness centrality). b) Hub connected to neighbours that are disconnected from one another (zero clustering coefficient) vs. densely inter-connected (unitary clustering coefficient).

The purpose of this experiment was to investigate the representation of the key decisional parameters characterizing the risky prospects, i.e. k_{WIN}, k_{LOSE}, p_{WIN} and EV, in terms of effective connectivity.

More specifically, predicated on the expectation that integrative functions are implemented through the action of heavily interconnected "cortical hubs" (e.g., Sporns and Tononi, 2001; Sporns et al., 2004; Bassett and Bullmore, 2006; Bullmore and Bassett,

2011; Sporns, 2009), the prediction was made that effective connectivity representing the economic parameters of interest would converge topologically on a small number of highly-interconnected nodes.

Considering that anatomical studies in humans and moneys have demonstrated that the medial prefrontal cortex and the orbitofrontal cortex harbour heavily interconnected subregions (e.g., Brog et al., 1993; Barbas, 2000; Ongür et al., 2000 and 2003 Barbey et al., 2009), such "integrative hubs" were predicted to be found predominantly in these areas. Such prediction is supported by behavioural studies demonstrating that patients with focal damage to these areas are impaired in the determination of value and risk (Bechara et al., 1999; Manes et al., 2002; Clark et al., 2003; Clark et al., 2008).

A related prediction was that, since value determination involves the integration of potential loss, potential gain and outcome probability, such parameters would be explicitly encoded in subsets of the network representing overall value. Further, given that the univariate analyses presented in the previous chapter clearly depict an over-representation of losses with respect to gains, it was predicted that the encoding in effective connectivity would be more widespread and significant for potential losses than potential gains.

Additionally, the experiment aimed to confirm whether the large-scale inferences drawn from pair-wise PPI agree with the results given by the more established DCM, and whether the PPI-based inferences about *EV*-sensitive effective connectivity are robust with respect to confounds related to varying degrees of regional response non-linearity un-related to functional interactions.

6.2 Methods and data analysis

This experiment is based on the same fMRI dataset acquired for the univariate analysis, however, due to data storage issues (server crash) data from 3of the initial 22 participants

could not be used. Based on the existing literature in the field (e.g., see Trepel et al., 2005; Platt and Huettel, 2008; Kable and Glimcher, 2009; Rangel and Hare, 2010), a comprehensive set of regions-of-interest (ROIs) potentially relevant to the task under study was defined, including: primary motor cortex (limited to hand knob, MI), supplementary motor area (SMA), angular gyri (ANG), precuneus (PREC), early associative visual areas (OCC), anterior, middle and posterior (ACC, MCC and PCC) cingulate cortices, anterior insula (AINS), ventral-, dorsal- and antero-lateral prefrontal cortices (VLPFC, DLPFC and ALPFC), ventral- and dorsal-medial prefrontal cortices (VMPFC and DMPFC), orbitofrontal cortex (OFC), caudate nucleus (CAUD), lenticular nucleus (LENT), ventral striatum (VS), thalamus (THAL), amygdala (AMYG), hippocampus and parahippocampal gyrus (HPP). The corresponding masks are shown in Figure 28. The Automated Anatomical Labelling (AAL) atlas (Tzourio-Mazoyer et al., 2002) was used as a starting point, but since the necessary regions are not all individually separated, the atlas was manually edited by the author alongside and an experienced neuroradiologist (Dott.ssa Marina Grisoli), and further refined by overlaying the masks on a high-resolution canonical brain. The MRIcro software (GSU/GT Center for Advanced Brain Imaging, Atlanta GA, USA) was used for this procedure, and the Niewenhuys atlas (1996) was taken as general reference on gyral anatomy. The subdivisions of the cingulate cortex were identified according to the criteria set forth by Vogt (2005), whereas the parcellation of the prefrontal cortex was predicated on a combination of functional and cytoarchitectonical criteria, as discussed by Rajkowska and Goldman-Rakic (1995), Fuster (1997) and Barbey and Grafman (2011). The use of an a-priori ROI set imports significant assumptions, but here attempts were made to mitigate them by exhaustively covering all relevant cortical areas, without making any reference to the results of the previous univariate analysis experiment to inform the parcellation. The ROIs thus defined were used to extract regional time-courses, forming the basis for subsequent multivariate analysis.

All analysis steps were completed with scripts developed by the author under the Matlab 7 language (Mathworks Inc., Natick MA, USA) running on a Sun Blade 2500 workstation (Sun Microsystems Inc., Santa Clara CA, USA). In order to reduce physiological contamination of the functional time-series, the predetermined masks were intersected with the results of individual grey matter segmentation, performed by SPM8 as a part of the normalization process (see previous chapter); hence, only voxels that had an estimated relative gray matter content greater than 50% contributed signal to the average time-course computed for each ROI and participant. The time-courses thus extracted were de-trended by fitting the baseline with a second-degree polynomial and subtracting it, and processed removing the variance correlated to the average brain signal, which was assumed to be representative of overall cardiovascular contamination and other systemic drifts. Owing to the synchronization between stimulus delivery and volume acquisition, i.e. the use of an inter-trial interval set to a integer multiple of the TR, the filtered time-courses were epoched between -2.4 s (1 TR) and 14.4 s (+6 TR) with respect to gamble onset, and, for each epoch individually, relative signal changes were calculated as percent units (subsequently referred to with ΔBOLD%); the response amplitude for each region and trial was thereafter determined as the average between 4.8 s and 9.6 s post-stimulus (i.e., encompassing three data points at 2, 3 and 4 TRs post-stimulus).

While the univariate analysis reported in the previous chapter was performed separating the random-effects and fixed-effects steps, passing on pre-defined summary statistics for group-level analysis, here it was decided to pool together trials from all participants into a unified dataset, in order to avoid the need to make assumptions on which summary statistics to use to capture network properties at individual level. Accounting for the fact that even relative response magnitude may vary significantly among individuals, all response amplitudes were *z*-normalized across trials, separately for each region in each

participant, eliminating the effect of reaction time (RT) variations through a separate linear regression term.

Firstly, to confirm the overall engagement of each region in the task, two-tailed one-sample t-tests were performed over the pooled *z*-scores, testing the hypothesis that ΔBOLD% is significantly different from zero. For confirmatory purposes, the subsequent analysis step sought to confirm whether the direct (i.e., linear) effect of the economic parameters on regional response amplitude was concordant with the results obtained in the previous experiment with voxel-wise univariate analysis. This and the further analysis steps for this experiment were limited to the following economic parameters: k_{WIN}, k_{LOSE}, p_{WIN} and EV. Linear regressions between theses parameters and the normalized regional responses were performed, applying the family-wise error (FWE) correction through Bonferroni-Holm's formula to control type I error probability (Holm, 1979).

Psychophysiological interaction analysis (PPI) was thereafter performed as an exhaustive series of pair-wise comparisons between all possible combinations of ROIs. Let

$$y = \beta_0 + \beta_1 \cdot k + \beta_2 \cdot x + \beta_3 \cdot x \cdot k \,,$$

where x and y represent normalized response amplitudes for "source" and "target" regions respectively, β_0 is a constant, β_1 represents the direct effect of an economic parameter k, β_2 models the direct connectivity between the two regions (i.e., intrinsic correlation between their timecourses) and β_3 corresponds to the term of interest, i.e. the interaction between parameter k and the BOLD time course in the "source" region (i.e., effective connectivity; Friston et al., 1997). Clearly, the relationship is not commutative, i.e. the fact that the economic parameter under consideration modulates the effect of activity in the "source" region on the "target" region does not imply the converse. This provides a basis for constructing directed connectivity graphs, i.e. in which there is an explicit distinction between the number of connections incident to a given node and those emanating from it.

Parameters β_0-β_3 were determined for each pair of regions, after which an adjacency matrix, i.e. a binary, non-symmetric matrix representing which directed connections are significantly modulated, was computed for each of the five economic parameters under consideration. For this purpose, the significance of the β_3 term, determined with respect to the error term ε (omitted in the above formula), was thresholded according to the Bonferroni-Holm correction, calculated over the 1722 (i.e., 42 × (42-1)) possible directed connections. Purely for display purposes, additional adjacency matrices were calculated at $p<0.01$, to reduce edge density in the printed figures.

In order to determine the layout of nodes and edges for graph visualization purposes, the "Force Atlas" algorithm, a basic electrostatic repulsion algorithm maximising edge spacing implemented in the Gephi 0.8beta program (Bastian et al., 2009), was utilized. This algorithm models each edge as a charged particle in a vacuum and optimizes the layout by minimizing the corresponding electrostatic potential energy. Using the same program, the total number of connections irrespective of direction (degree), number of incident, or afferent, connections (indegree), and number of emanating, or efferent, connections (outdegree) were computed for each node (e.g., Newman, 2010; Bullmore and Bassett, 2011). Furthermore, to obtain a more abstract measure of the topological position of each node in the network, the total number of shortest paths, calculated over all possible combinations of nodes, that pass through each given node (betweenness centrality) was calculated, using Dijkstra's algorithm and taking into account the directionality of each edge (Brandes, 2001). For each node, the proportion of connections observed among its neighbours (clustering coefficient) was also calculated, using triangle computations, to obtain a measure of local connection density (Latapy, 2008).

At a more abstract level, the hypothesis that the effective connectivity network encoding *EV* is organized as a small-world network was tested, by means of a two-tailed

one-sample t-test comparing the observed average clustering coefficient with that of 20 random Erdös-Rényi graphs, generated with a procedure (implemented in a dedicated Matlab script written by the author) that matched number of connections, nodes and average path length. Further, to quantify the size of the topological effect of clustering (in addition to determining its statistical significance) the small-worldness coefficient *S* was computed as described by Humphries and Gurney (2008). Lastly, the hypothesis that the *EV*-sensitive network was significantly subdivided into distinguishable sub-clusters was tested using algorithms described in detail by Blondel et al. (2008).

On potential pitfall with PPI analysis is that the direct relationship between the task parameter and regional activity may be non-linear. Should the non-linearity be expressed differently in the "source" and "target" regions, the interaction term β_3 would assume a significantly non-zero value purely in virtue of this fact, without reflecting a genuine functional underlying interaction. To the author's knowledge this potential pitfall has not been addressed in other PPI studies nor in the original theoretical formulation (e.g. Friston et al., 1997). Here, to remove this possibility, all analyses were repeated subtracting the direct effect of each task parameter from the responses of the "source" and "target" regions up to the third degree by means of a polynomial model, in other words considering

$$\hat{y} = \beta_0 + \beta_2 \cdot \hat{x} + \beta_3 \cdot \hat{x} \cdot k \,,$$

where

$$\hat{x} = x - \alpha_0 - \alpha_1 \cdot EV - \alpha_2 \cdot EV^2 - \alpha_3 \cdot EV^3$$

and similarly for $\hat{y}$.

As represented in Figure 5a, the gamble acceptance rate *w* increases very rapidly with *EV* in the vicinity of 0. Taking this fact into account, all PPI analyses were repeated approximating the effect of *EV* with its sign function, i.e. -1 for *EV*<0 and +1 for *EV*>0.

The *F*-values for the β_3 term were thereafter represented as heatmaps, and compared across analyses using linear correlation.

In order to confirm the directed causality inferences using a technique embedding an explicit, validated model of neurovascular coupling, dynamic causal modelling (DCM) was applied to determine the directions of the connections among the main integrative nodes revealed by the analysis, i.e. bilateral ALPFC, bilateral DMPFC, right VMPFC - see below). The latest formulation to date, i.e. DCM10 (Wellcome Trust Centre for Neuroimaging, UCL, London, UK), was utilized assuming a bilinear, deterministic one-state model (Stephan et al., 2007). The principal eigenvariate of the time-course was extracted for each ROI, explicitly adjusting for the main effect of gamble onset, modelled as a mini-block determined by the reaction time (RT), as well as for the movement regressors. Subsequently, for each region two competing models were postulated: one in which afferent connections had the direction inferred by PPI, and one in which they had the inverse direction, i.e. were emanating rather than incident to the node. This analysis was only run for *EV*, since it was performed purely to confirm the reliability of the PPI inferences, and *EV* was inserted as modulatory parameter for all connections and for activity in the target region. After fixed-effects analysis, random-effects Bayesian model selection was performed to calculate exceedance probabilities for each pair of alternative models (Stephan et al., 2009).

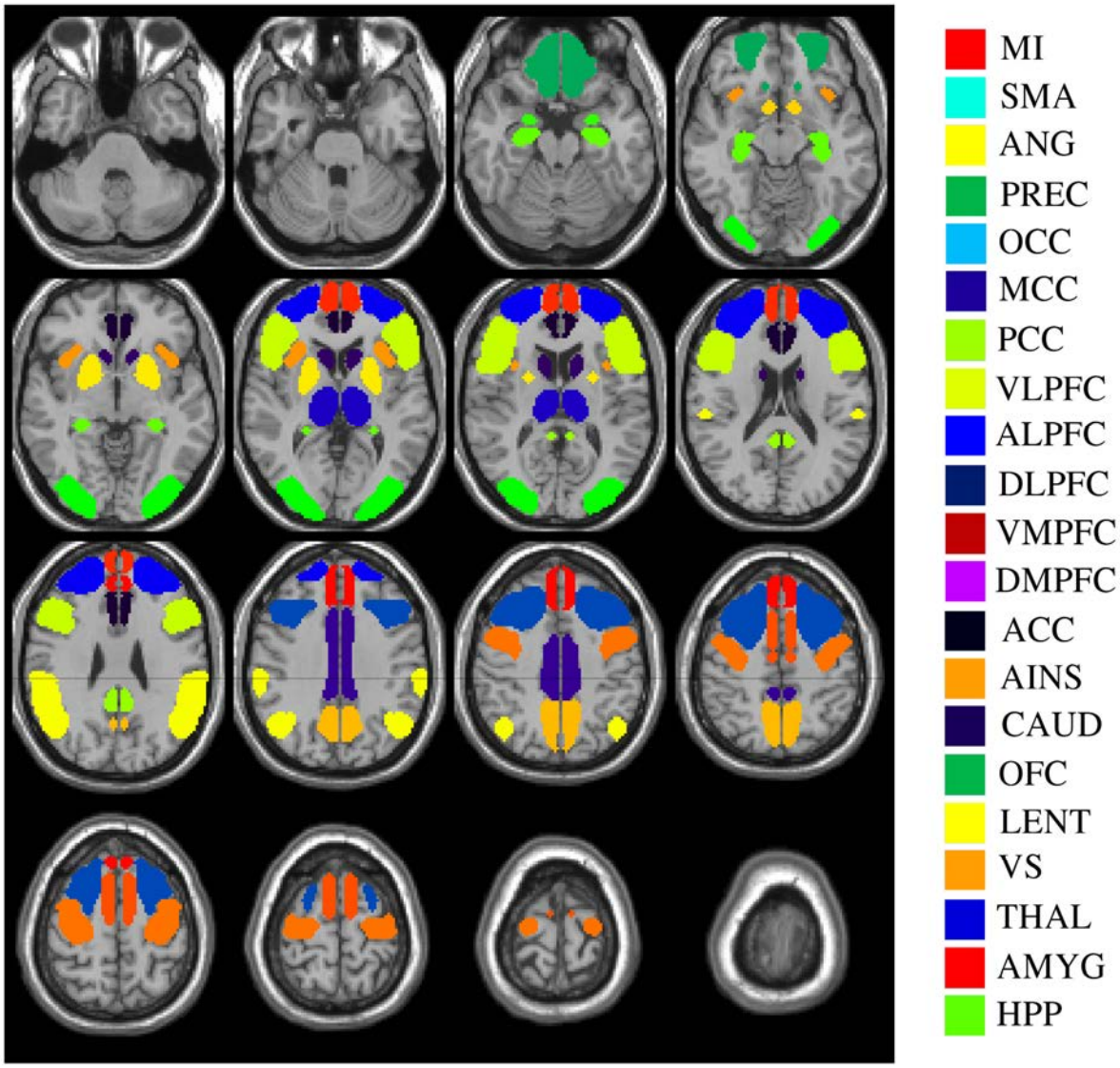

Figure 28. Regions-of-interest (ROIs) used for blood-oxygen level-dependent (BOLD) signal time-course extraction, displayed overlaid on the canonical brain. See methods section for list of abbreviations.

6.3 Results

As represented in the heatmap in Figure 29, there was a positive correlation between *EV* and BOLD response amplitude in the right DMPFC (F=9.6), bilaterally in the VMPFC (F=9 for right, F=9.9 for left), in the left ACC (F=10.6) and right OCC (F=18.8). There were no significant negative correlations between BOLD response and *EV* for any region. Of note, no significant correlations were observed with k_{WIN} and p_{WIN} for any region beyond MI, where the effect was simply an expression of button-press response. By contrast, diffuse negative correlations were observed for k_{LOSE}, in the left ALPFC (F=-9.8), bilaterally in the VMPFC (F=-17.7 for right, F=-19.4 for left), bilaterally in the ACC (F=-9.1 for right, F=-12.2 for left), in the left MCC (F=-10.8), right PCC (F=-8.8), right DLPFC (F=-12.3), right ANG (F=-10.0), right OCC (F=-9.7), right PREC (F=-9), left LENT (F=-18.0) and VS (F=-13.5). No region exhibited a BOLD response correlating positively with k_{LOSE}.

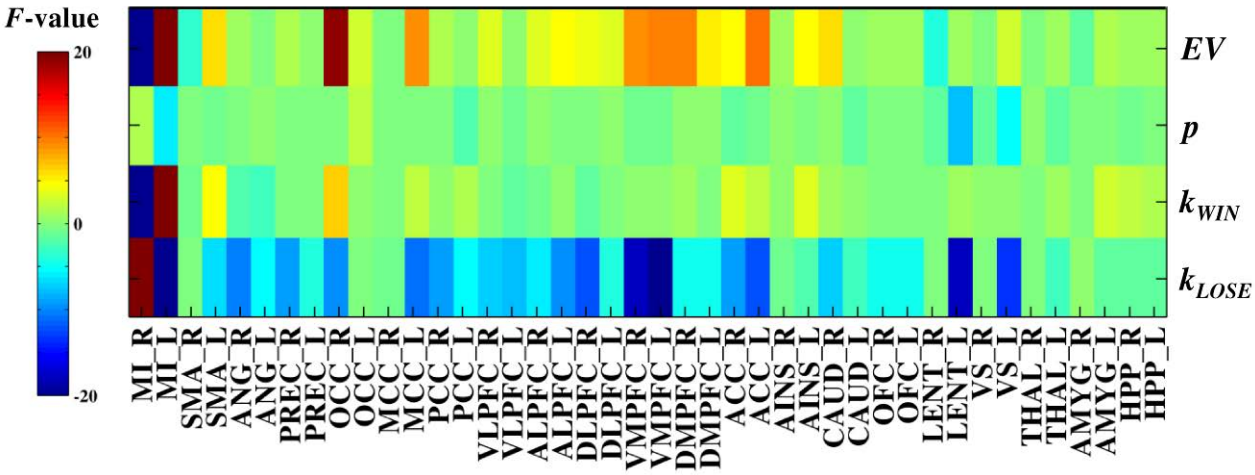

Figure 29. Heatmap representing the linear correlation, computed across participants, between normalized BOLD response amplitude and the economic parameters k_{WIN}, k_{LOSE}, p_{WIN} and *EV*. Negative F-values indicate a negative relationship and $p_{(FWE)}$<0.05 corresponds to $|F|$>8.0.

Mapping the *EV*-sensitive connections revealed a rich effective connectivity network, within which the ALPFC bilaterally, the DMPFC bilaterally and the right VMPFC appeared as prominent hubs (Figures 30-31). Out of 1722 possible connections, 168 were significantly (FWE-corrected $p<0.05$) modulated by *EV*, corresponding to approximately 9.7% of connections; of these, 84% were associated with a negative interaction term, i.e. had had $\beta_3<0$.

As represented in Figure 32, across regions the indegree was considerably more variable (standard deviation 6.6) than the outdegree (standard deviation 3.2); in other words, while the number of "efferent" connections was between 5 and 10, the number of "afferent" connections was less homogeneous, with some nodes having up to 25 significant *EV*-sensitive incident connections. Taking the 90th percentile as the cut-off point, the regions with the highest indegree were, in order, the right DMPFC (25 connections), right VMPFC (22 connections), right ALPFC (21 connections), left DMPFC (17 connections) and left ALPFC (14 connections). With the same criterion, the regions with the highest degree centrality (i.e., connections irrespective of direction) were, in order, the right VMPFC (30 connections), right DMPFC (30 connections), right ALPFC (29 connections), left ALPFC (21 connections) and left DMPF C (21 connections). The betweenness centrality, instead, was highest for the right ALPFC (141 shortest paths), right DMPFC (85 shortest paths), right VMPFC (78 shortest paths), left SMA (47 shortest paths) and left VMPFC (44 shortest paths). The clustering coefficient was zero for several regions that did not have interconnected neighbours; excluding those, the lowest values (10th inferior percentile) were found for the right ALPFC (0.13 proportion of connections among neighbours), right VMPFC (0.16), left OCC (0.17), right DMPFC (0.19) and left ALPFC (0.19).

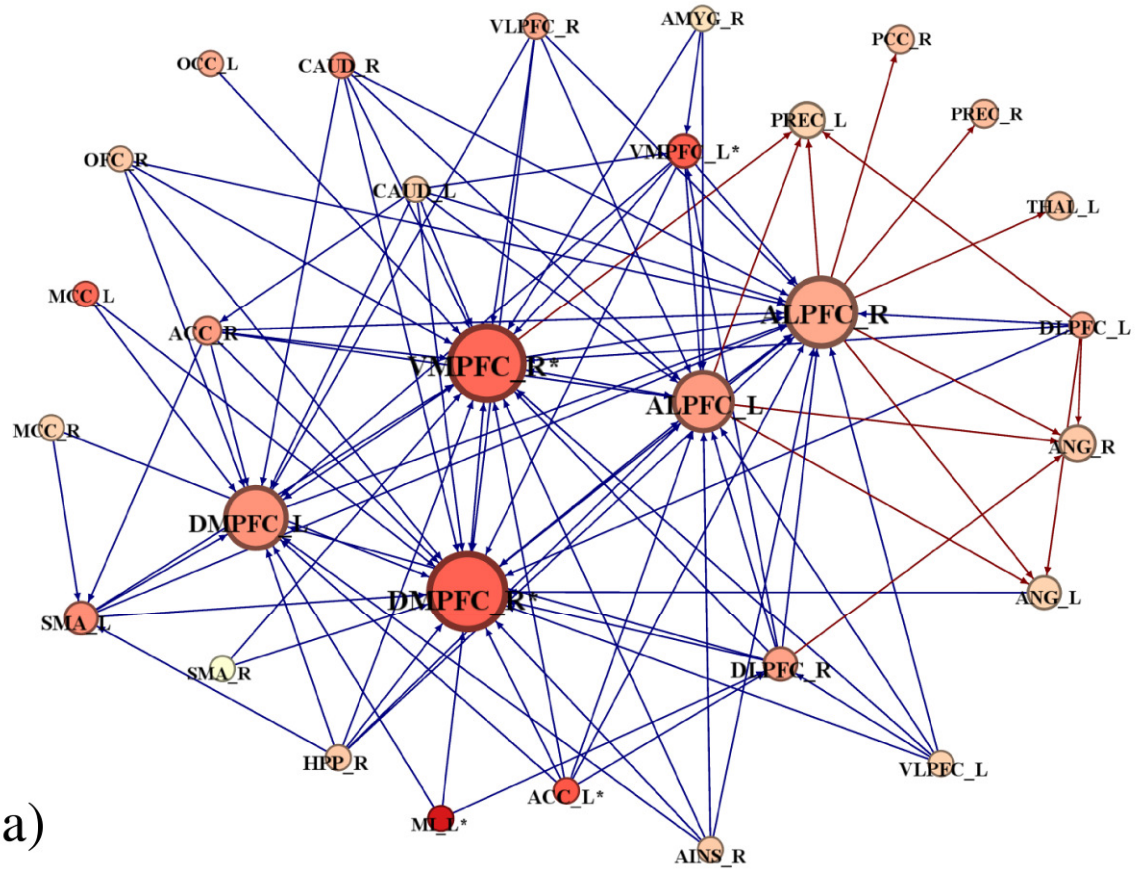
VLPFC_R
AMYG_R
OCC_L
CAUD_R
PCC_R
PREC_L
PREC_R
OFC_R
VMPFC_L*
CAUD_L
THAL_L
MCC_L
ACC_R
ALPFC_R
DLPFC_L
VMPFC_R*
ALPFC_L
MCC_R
ANG_R
DMPFC_L
DMPFC_R*
ANG_L
SMA_L
SMA_R
DLPFC_R
HPP_R
VLPFC_L
ACC_L*
MI_L*
AINS_R

a)

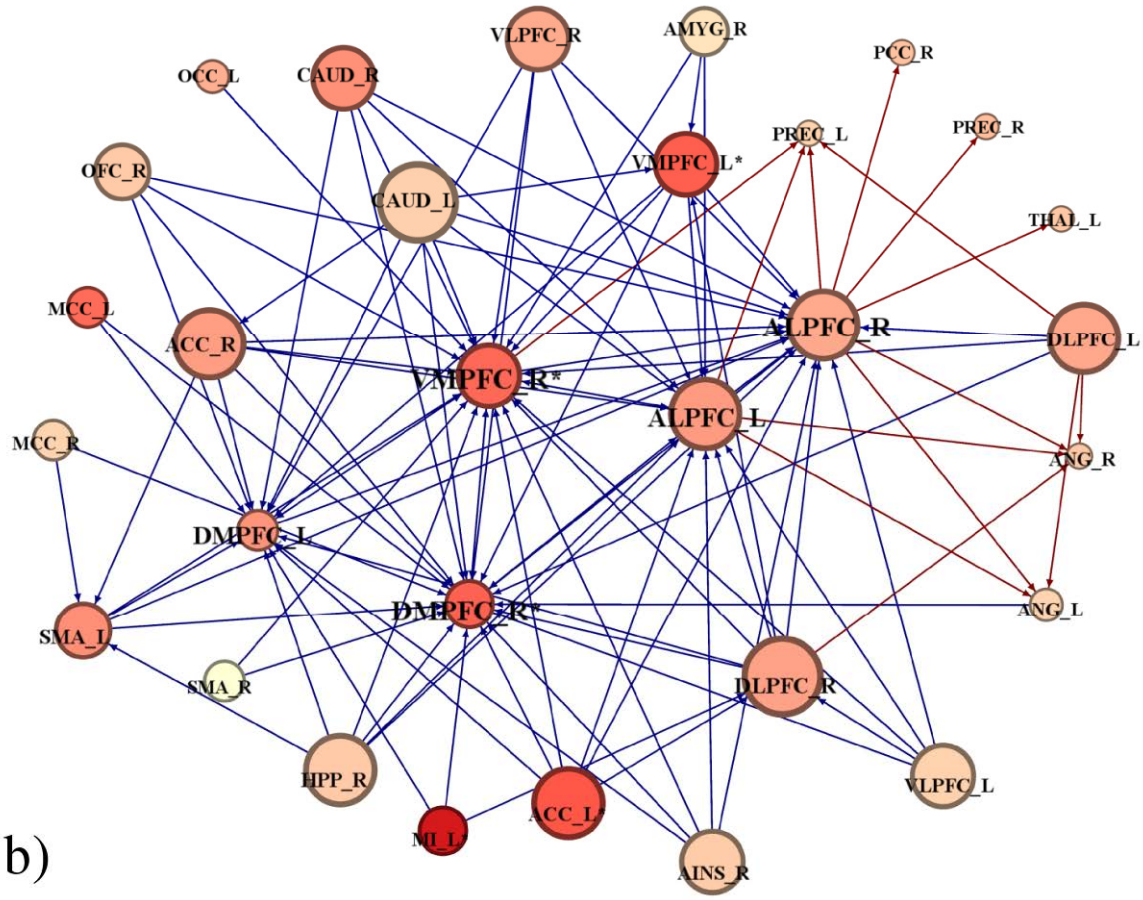
VLPFC_R
AMYG_R
OCC_L
CAUD_R
PCC_R
PREC_L
PREC_R
OFC_R
VMPFC_L*
CAUD_L
THAL_L
MCC_L
ACC_R
ALPFC_R
DLPFC_L
VMPFC_R*
ALPFC_L
MCC_R
ANG_R
DMPFC_L
DMPFC_R*
ANG_L
SMA_L
SMA_R
DLPFC_R
HPP_R
VLPFC_L
ACC_L*
MI_L*
AINS_R

b)

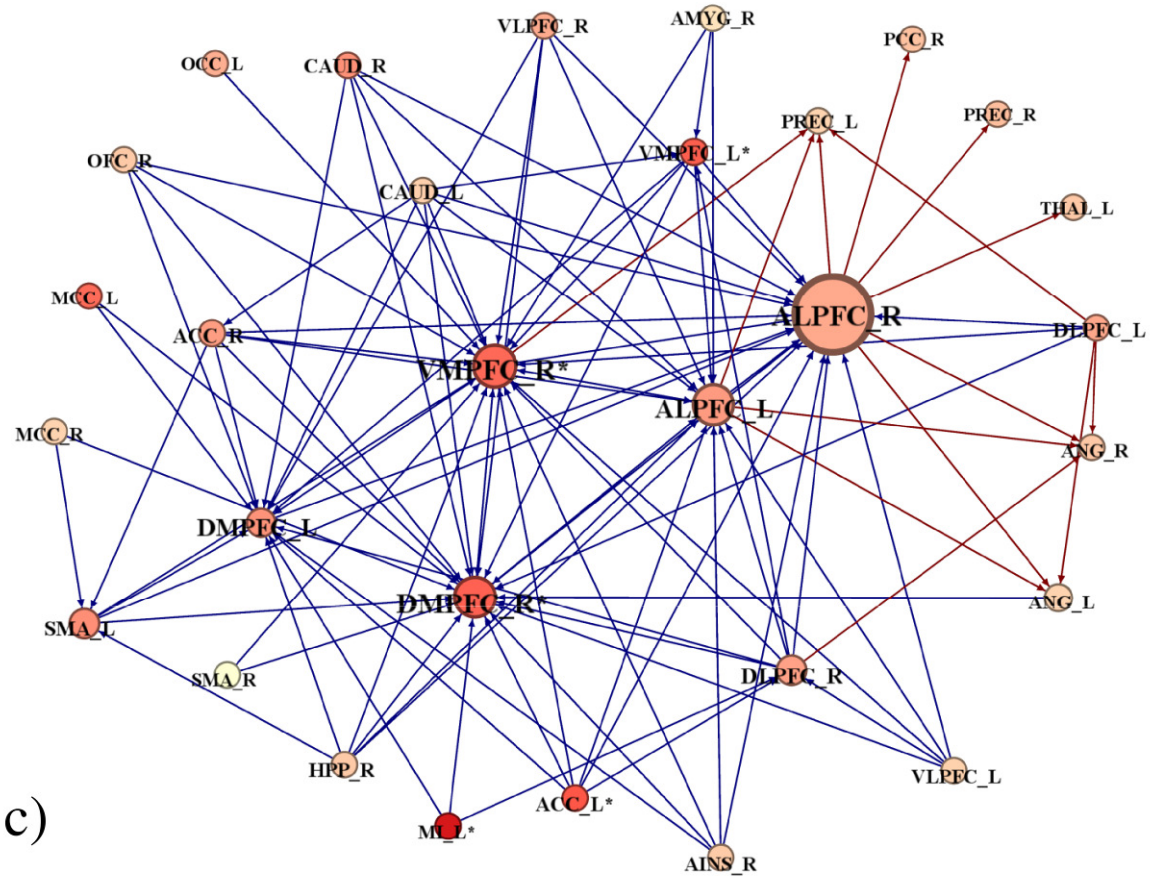
VLPFC_R
AMYG_R
OCC_L
CAUD_R
PCC_R
PREC_L
PREC_R
OFC_R
VMPFC_L*
CAUD_L
THAL_L
MCC_L
ALPFC_R
ACC_R
DLPFC_L
VMPFC_R*
ALPFC_L
MCC_R
ANG_R
DMPFC_L
DMPFC_R*
ANG_L
SMA_L
SMA_R
DLPFC_R
HPP_R
VLPFC_L
ACC_L*
AINS_R

c)

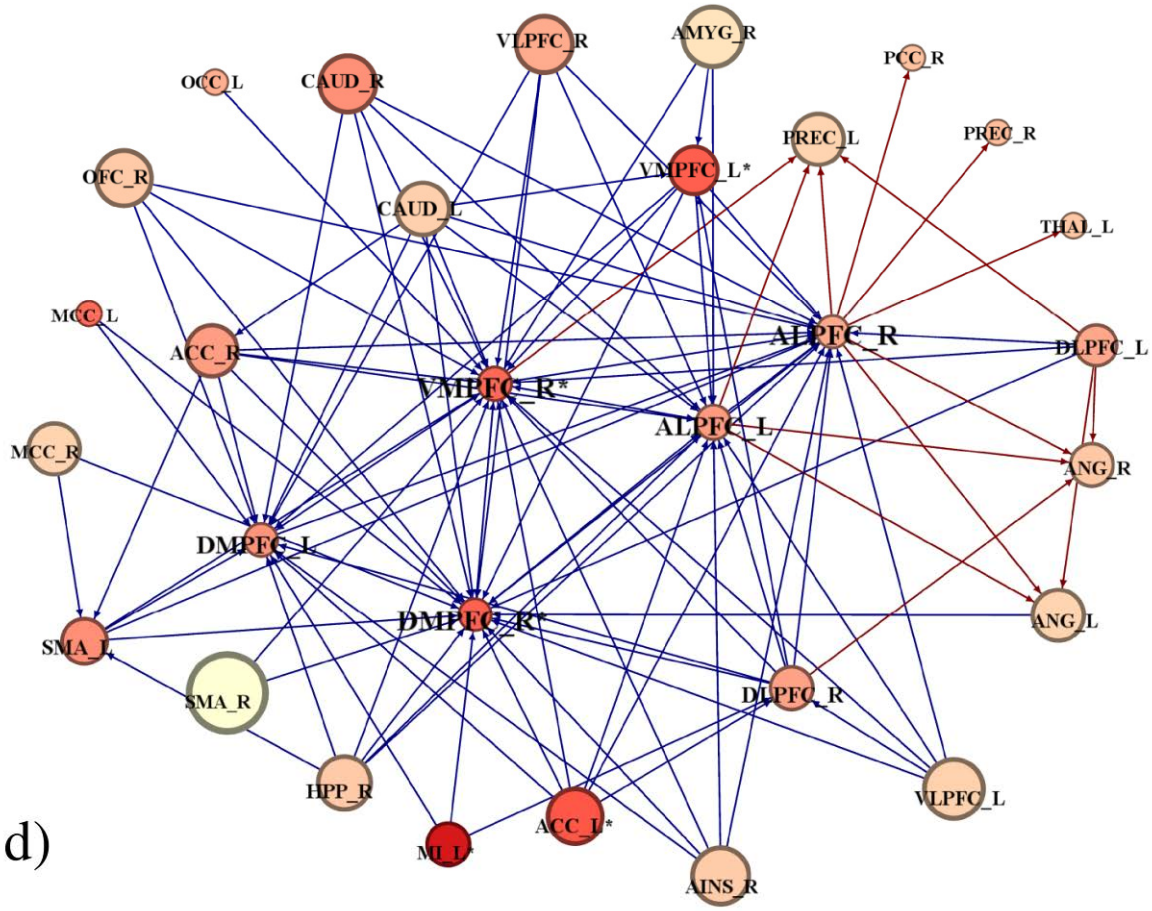
VLPFC_R
AMYG_R
OCC_L
CAUD_R
PCC_R
PREC_L
PREC_R
OFC_R
VMPFC_L*
CAUD_L
THAL_L
MCC_L
ALPFC_R
ACC_R
DLPFC_L
VMPFC_R*
ALPFC_L
MCC_R
ANG_R
DMPFC_L
DMPFC_R*
ANG_L
SMA_L
SMA_R
DLPFC_R
HPP_R
VLPFC_L
ACC_L*
AINS_R

d)

Figure 30 (previous pages). Effective connectivity network of inter-regional connections significantly modulated by *EV* at $p_{(FWE)}<0.01$, chosen for visualization purposes. The colour of the connections denotes the sign of the PPI interaction term: red for $\beta_3>0$, blue for $\beta_3<0$. To support visual assessment of the network structure, the node diameter encodes a) indegree, b) outdegree, c) betweenness centrality and d) clustering coefficient. The intensity of node colour represents significance of the direct correlation between BOLD signal amplitude and *EV*; nodes marked with superscript '*' exhibited a significant direct activity correlation.

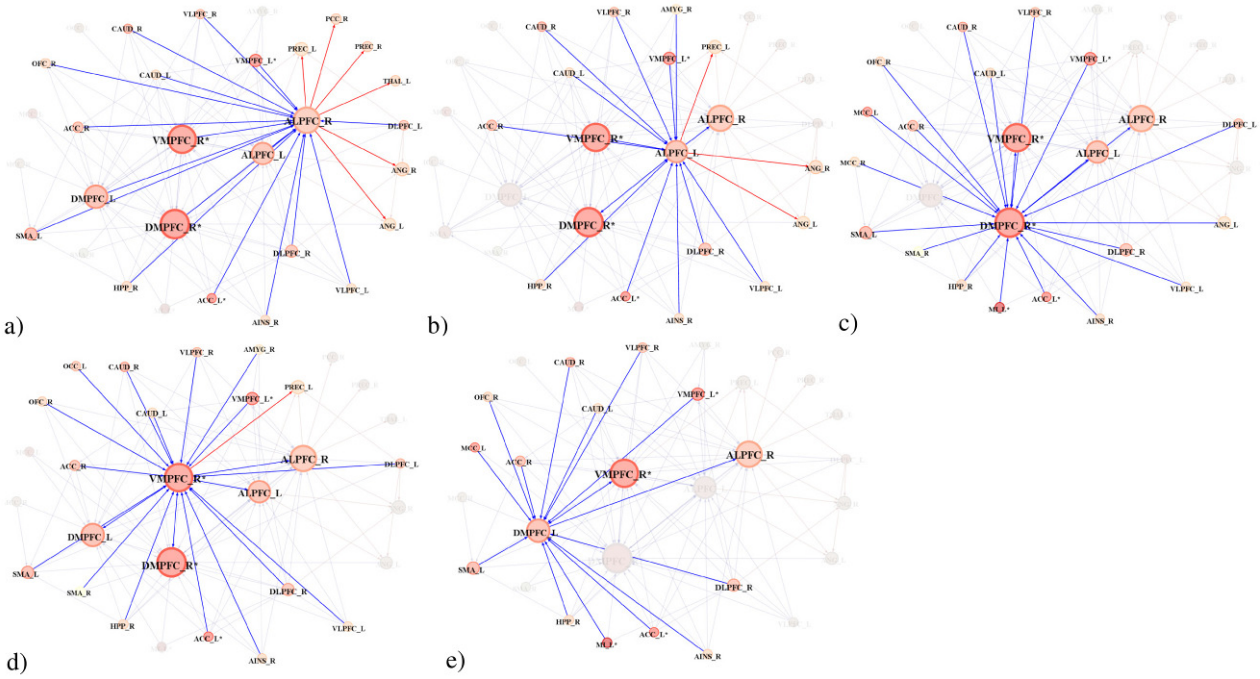

Figure 31. Breakouts of the *EV*-sensitive network, showing the nodes directly interconnected to a) right ALPFC, b) left ALPFC, c) right DMPFC, d) right VMPFC and e) left DMPFC. As in Figure 30a, node diameter encodes the indegree, edge colour represents interaction sign and node colour intensity encodes the direct correlation of BOLD response amplitude with *EV*.

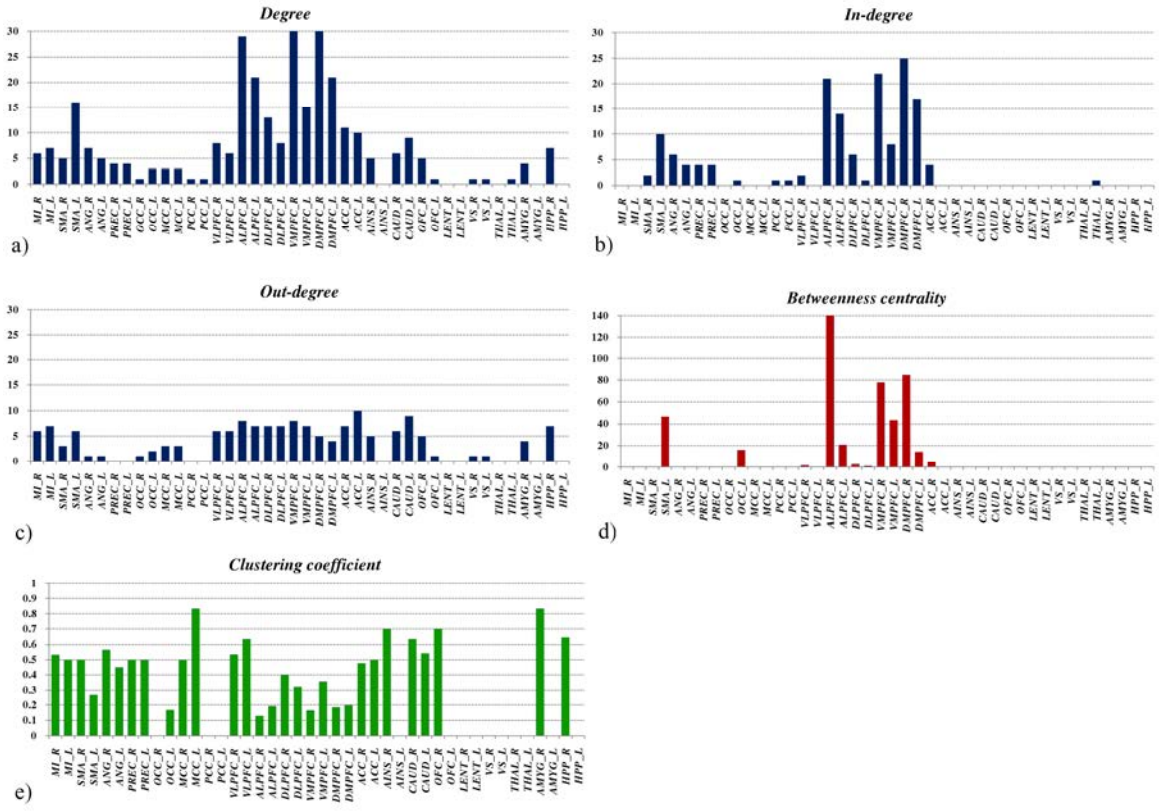

Figure 32. Bar charts representing the topological node parameters for the *EV*-sensitive inter-regional connections. As described in the methods, these parameters were calculated assuming a connection threshold of $p_{(FWE)}<0.05$.

The small-worldness index *S* was 6.2: this indicated that the network topology strongly exhibited small-world features. In line with this observation, the average clustering coefficient was much higher than that observed in Erdös-Rényi networks (0.37 vs. 0.06±0.03, $p<0.001$), generated randomly and matched in terms of average path length (1.93 vs. 1.98±0.21, $p=0.4$). The modularity index was 0.14, corresponding to very weak evidence of a modular organization in network subclusters (e.g., Blondel et al., 2008 indicates a cut-off of 0.4 to infer significant modularity).

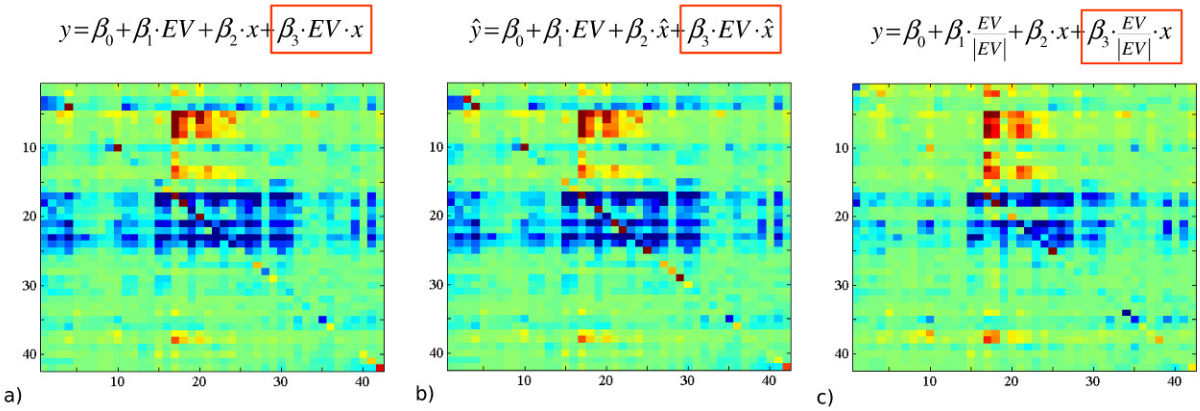

Figure 33. Heatmaps representing the *F*-values for the PPI interaction terms for *EV* for a) the initial PPI analysis, b) a reformulated model according to which the direct effect of *EV* on BOLD response amplitude is removed from the "source" and "target" regions up to the third degree, with $\hat{x} = x - \alpha_0 - \alpha_1 \cdot EV - \alpha_2 \cdot EV^2 - \alpha_3 \cdot EV^3$ and c) a model in which the continuous modulatory effect of *EV* is approximate by a step function with respect to the *EV*=0 point. As in Figure 29, red denotes positive and blue negative *F*-values, and the colour-map range was set to ±50.

As represented in Figure 33, the significance of the PPI interaction term β_3 was in close agreement between the initial PPI analyses, the analyses repeated with the revised model removing the direct effect of *EV* on BOLD response amplitude effect up to the third degree (r=0.7, p<0.001) and the analyses repeated approximating *EV* with its sign function, i.e. dichotomizing advantageous and disadvantageous prospects (r=0.89, p<0.001).

DCM with respect to the *EV*-sensitive connections of the five integrative hubs revealed by PPI network discovery indicated much higher exceedance probability for models assuming the connection directionality inferred with PPI than for the specular ones set up for verification purposes: 0.88 vs. 0.12 for left ALPFC, 0.90 vs. 0.10 for right ALPFC, 0.80 vs. 0.20 for left DMPFC, 0.77 vs. 0.23 for right DMPFC and 0.88 vs. 0.12 for right VMPFC (Figure 34).

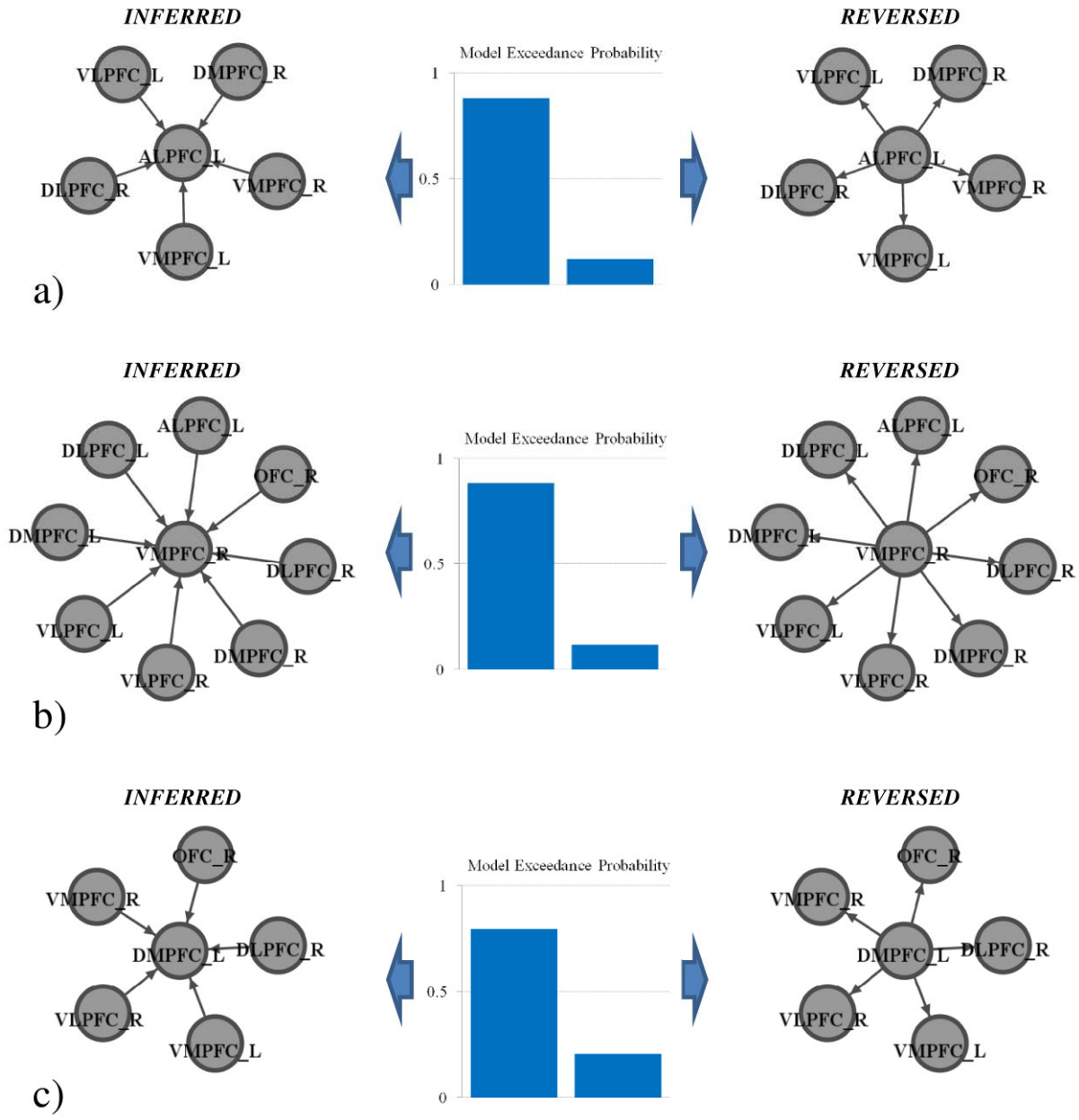

Figure 34 (continued on next page). Alternative dynamic causal models (DCMs) of *EV*-sensitive effective connectivity set up to confirm the directionality inferences suggested by pair-wire PPI analyses. For confirmatory purposes, the five nodes with the highest indegree were considered: a) left ALPFC, b) right VMPFC, c) left DMPFC, d) right ALPFC and e) right DMPFC. The bar charts represent the model exceedance probabilities given by Bayesian model comparisons for the alternative DCMs shown on the left and right.

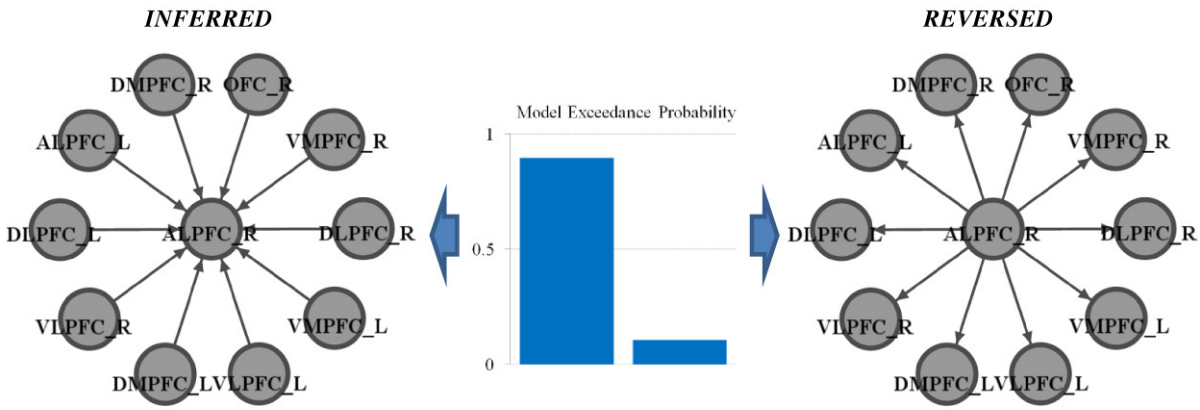

d)

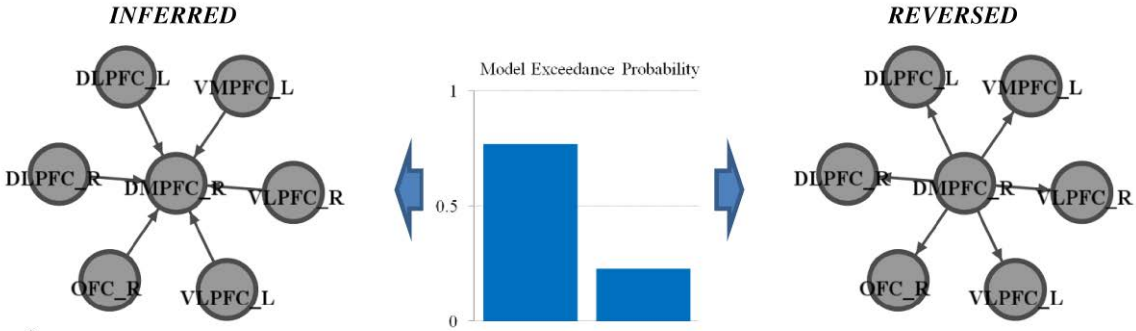

e)

Of note, PPI analyses did not reveal any modulated connections for k_{WIN} and p_{WIN}. By contrast, significant modulations were discovered for k_{LOSE}, identifying a smaller network (Figure 35) that principally consisted of a subset of the *EV*-sensitive one (31 out of 38 overlapping connections, 82%). The majority of modulated connections (i.e., 86%) were associated with $\beta_3>0$. In this smaller network, the highest degree was observed, in order, for the right ALPFC (14 connections), left ALPFC (10 connections), right DLPFC (6 connections) and right VMPFC (6 connections). The indegree was largest for the right ALPFC (11 connections), left ALPFC (8 connections), right VMPFC (6 connections) and left ACC (3 connections). Betweenness centrality and neighbour connectivity are not representative in such small networks (e.g., Newman, 2010) and were therefore not computed.

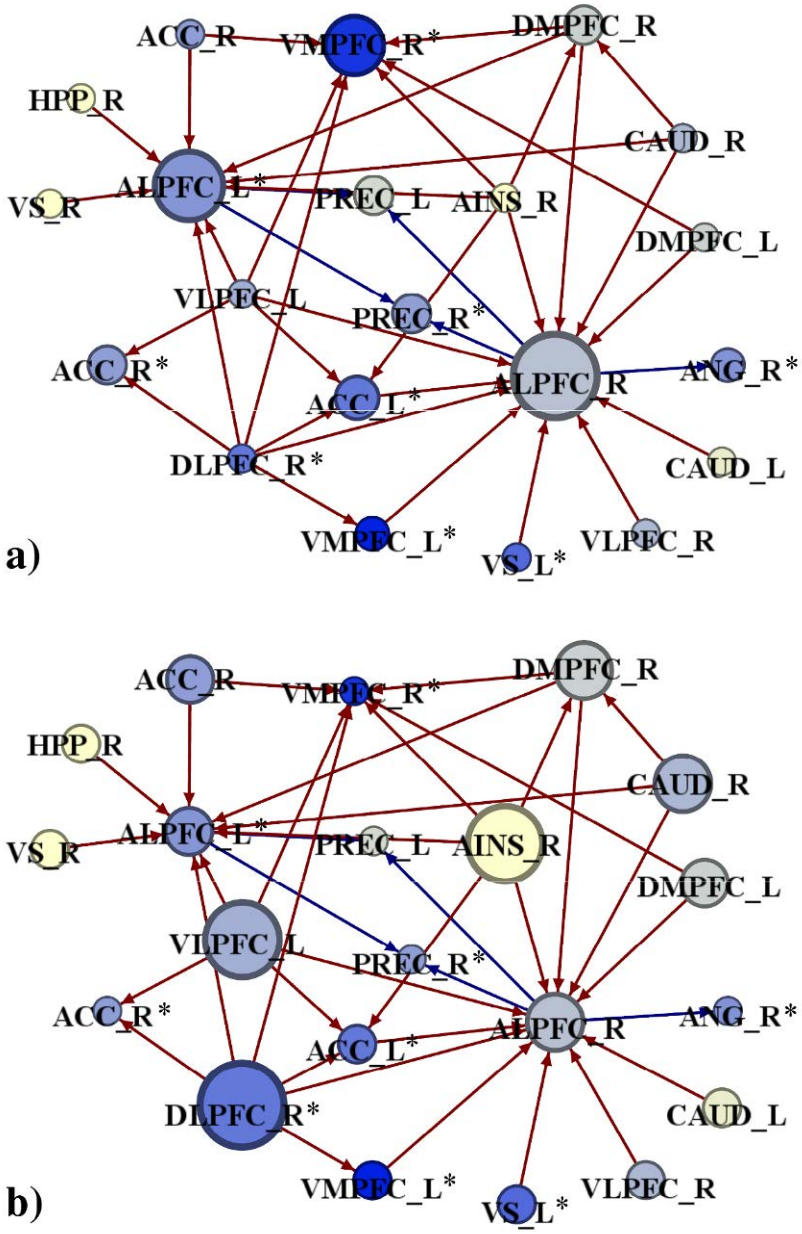

Figure 35. Effective connectivity network of inter-regional connections significantly modulated by k_{LOSE} at $p_{(FWE)}<0.01$, chosen for visualization purposes. The colour of the connections denotes the sign of the PPI interaction term: red for $\beta_3>0$, blue for $\beta_3<0$. To support visual assessment of the network structure, the node diameter encodes a) the indegree, b) the outdegree. The intensity of the node colour represents significance of the direct correlation between BOLD signal amplitude and *EV*; nodes marked with superscript '*' exhibited a significant direct activity correlation.

6.4 Discussion

6.4.1 Direct correlations

The direct correlations obtained with ROI analysis are consistent with the voxel-wise inferences reported in the previous chapter: i) *EV* is positively represented in the amplitude of BOLD responses in mesial PFC and visual areas, ii) k_{LOSE} is associated with diffuse relative deactivation across mesial and lateral prefrontal regions, likely representing the disengagement of the "gain brain" circuits previously discussed, and iii) the direct representations of k_{WIN} and p_{WIN} as individual parameters are much weaker.

6.4.2 Cortical hubs of value representation

Network-discovery analysis revealed that *EV* was processed and encoded through a network of striking complexity, comprising nodes in the prefrontal, parietal, temporal, cingular and insular cortex: it is a remarkable confirmation of the power of this modelling approach that only 5 regions displayed significant direct correlations with *EV* whereas, in spite of the stringent correction for multiple comparisons over a large number of possible directed connections (1722), significant *EV*-sensitive connectivity was detected for 36 nodes. This result confirms the theoretical prediction that value, and the abstract cognitive process of decision-making, are more deeply encoded in inter-regional dynamical interactions than straightforwardly in the intensity of regional activity. Effective connectivity is mathematically completely decoupled from direct correlation (Friston et al., 1997; Friston et al., 2003; Stephan et al., 2007), and in fact multiple areas expressed a marked differential engagement: for example in the ALPFC there was clearly no significant direct correlation between BOLD response amplitude and *EV* (p=0.7 for right,

p=0.4 for left) yet this region, in both hemispheres, exhibited a substantial number of robustly *EV*-sensitive connections (29 for right, 21 for left).

Influential accounts of structural and functional brain connectivity confirm that high degree, particularly indegree, high betweenness centrality and small clustering coefficient are the key topological hallmarks identifying integrative cortical nodes (Sporns et al., 2000; Sporns and Tononi, 2001; Sporns et al., 2004; Hagmann et al., 2008; Buckner et al., 2009; Sporns, 2009). A useful metaphor also comes from network studies of air traffic, which have demonstrated that nodes displaying these features act as "connector hubs", whose integrity is highly critical in enabling the efficient transport of goods and passengers between distant airports located in different continents (Guimerà et al., 2005). In the present experiment, these topological parameters convergently implicate the bilateral DMPFC, the right VMPFC and the bilateral ALPFC as key hubs in *EV* computation and representation.

It can be argued that this novel finding provides the most compelling evidence so far that these regions play an active integrative role in risky-decision making. In fact, even though many experiments had already mapped differential effects of subjective value and monetary evaluation to these areas of the prefrontal cortex (e.g., Trepel et al., 2005; Platt and Huettel, 2008; Rushworth and Behrens, 2008; Wang, 2008; Andersen and Cui, 2009; Kable and Glimcher, 2009; Levine, 2009; Clark, 2010; Rangel and Hare, 2010; Wallis and Kennerley, 2010; Alexander and Brown, 2011), since the observation of a correlation with BOLD amplitude does not necessarily entail a causative involvement the fundamental question remained open of whether the observed local correlations primarily reflected value computation taking place in these regions, or whether they reflected the consequence of a distal or distributed evaluation process (Philiastides et al. 2010; Ramsey et al., 2010). Considering the results of the present experiment that imply a highly convergent connectivity pattern, it would be highly implausible for the DMPFC, VMPFC and ALPFC

to display such strong centralities in effective connectivity purely as a consequence of activity taking place elsewhere.

It is also noteworthy that the present connectivity analysis confirmed the marginal role of striatum the in subserving task performance, corroborating the conclusions of univariate analysis in this regard.

6.4.3 Processing vs. communication hubs?

Taking this argument further, it is interesting to consider that, in abstract terms, network hubs may provide widely different functions irrespective of the topology of their local connections: for example, some hubs may mainly have a facilitatory role supporting long-range connections, whereas others may also perform significant integrative processing and memorization (Barrat et al., 2008; Sporns, 2009; Newman, 2010; Bullmore and Bassett, 2011). While it is impossible to distinguish between different roles of the hubs on the basis of fMRI alone, given the limitations in temporal resolution and signal specificity, one can nevertheless speculate that hubs operating purely as communication nodes should not exhibit direct correlations between BOLD response and expected value, due to the inherently limited functional specificity of their activity, whereas integrative nodes, which have a more direct computational engagement, could (though need not) also show direct parametric correlation, in addition to their involvement in the effective connectivity network. From this perspective, the VMPFC bilaterally and the right DMPFC would appear to act as processing nodes, whereas the left DMPFC and the bilateral ALPFC would be appear to be limited to a communication-facilitation function. Such interpretation can only be taken as a speculative one at this stage, particularly as it critically depends on the choice of the significance thresholds, nevertheless investigating the decoupling between direct parametric correlations and topological position in the effective

connectivity network may, in the future, prove to be a valuable approach for classifying different types of cortical hubs.

6.4.4 Methodological consideration on time-course extraction and cortical parcellation

Beyond the fact that here PPI analysis was applied for exhaustive pair-wise inferences rather than relating a seed region to all other brain voxels, as commonly done in other studies, there is another relevant methodological difference: the input to PPI analyses was not the continuous BOLD signal time course, but the overall response amplitude measured explicitly for each trial. This approach has the major advantage of removing many constraints related to the neurovascular coupling function: no assumptions are made on the exact time-course and its consistency across brain areas, and no assumptions are made on the linear summation of overlapping responses for adjacent stimuli. The violation of such assumptions, whose general validity remains to be confirmed, could generate artifactual interactions in fast-paced designs where haemodynamic responses to individual trials overlap considerably (Duann et al., 2002; Serences, 2004; Wager et al., 2005). In terms of inferential techniques, the present experiment is particularly robust, given that family wise error correction was conservatively performed by applying Bonferroni's correction to all possible combinations of directed connections, thus strongly controlling for the probability of type I error (Holm, 1979).

One potential pitfall is the a-priori choice of ROIs for signal extraction, which could have concealed highly functionally-specific activity in sub-portions of the parcellated areas, and introduced artifactual correlations between neighbouring regions caused by overlapping activity. The first concern is a major limitation of the ROI-based approach, and cannot be fully addressed unless the analysis is brought down to the level of individual voxels, with enormous computational costs. Of note, determining the ROIs on

the basis of the activations described in the previous chapter would not have been acceptable for parcellation given that, as robustly shown by the data, many regions that have a central involvement in network connectivity do not exhibit a direct relationship between BOLD response amplitude and *EV*, and would therefore unavoidably have been missed. As regards to the second concern, reassurance comes from the fact that the main inferences drawn in this experiment pertain to large-scale network properties, that are mainly determined by long-range anatomical connections which do not involve neighbouring regions.

6.4.5 Excluding confounds related to potential regional response non-linearity

Examining in further detail the potential confounds that could have affected this experiment, there is no reason to exclude a priori that non-linear (in fact, even non-monotonic) correlations could exist between BOLD response amplitude and task parameters such as *EV*. In fact, as expected from the non-linearity of the probability and value weighting functions, non-linear effects are frequently encountered in neuroeconomics (e.g., Hsu et al., 2009). This potentially represents a serious problem for PPI analysis. In order to exemplify why, one can consider two disconnected regions 'A' and 'B', and assume that *EV* influences BOLD response amplitude in region 'A' with a given non-linearity, e.g. sub-linearly, and the responses in region 'B' in a different manner, e.g. supra-linearly. Performing PPI analysis between the two regions would reveal a non-zero bilinear term (β_3), purely as a consequence of the differential non-linearity of the relationship, without representing a genuine underlying functional interaction. This potential issue appears to be ignored in the vast majority, if not in the totality, of current functional neuroimaging experiments utilizing PPI to draw connectivity inferences.

Here, it was explicitly addressed through an additional analysis, whereby the direct effect of *EV* on BOLD response amplitude was removed up to the third degree, individually from all regions before modelling functional interactions. The results confirmed the initial inferences, confirming that differential expressions of response non-linearity did not have a major confounding effect on connectivity inferences.

6.4.6 Dichotomous vs. continuous representation of value

The acceptance rate functions, plotted in Figure 5a, are characterized by an abrupt increase in the $EV \approx 0$ region and virtually flat elsewhere. Further, as detailed in the previous chapter, the univariate response of the mesial PFC suggests that the neural representation of value underlying performance of the task has more to do with a dichotomous or contingently-rescaled comparison of $k_{WIN} \times p_{WIN}$ and $k_{LOSE} \times (1-p_{WIN})$ than with their graded summation into absolute value. To further evaluate this hypothesis, the PPI analyses were repeated replacing continuous *EV* with its sign function. The inferred effective connectivity pattern appeared mostly unaltered, indicating that the network is mainly engaged in the discrimination of risk-advantageousness vs. risk-disadvantageousness, rather than in continuous value computation.

In other words, the computation of *EV* when one is faced with a risky prospect appears to be largely reduced to a basic heuristic, i.e. comparing expected gains and losses, further supporting the hypothesis that the mesial PFC acts as fundamentally a decisional comparator (Venkatraman et al., 2009; Wunderlich et al., 2009). In fact, implementing risky decision-making on the basis of a binary comparison rather than a graded difference is evolutionarily plausible, considering that absolute value representation is likely to be much more demanding and slower than a binary comparison.

6.4.7 Directional inferences confirmed by dynamic causal modelling

In PPI studies, directionality inferences are drawn on the basis of the fact that, due to the presence of the bilinear term, the adjacency matrix is not commutative, i.e. different coefficients model effective connectivity between two nodes depending on the direction (Friston et al., 1997; Friston et al., 2003). Arguably, this is a rather indirect way of inferring activation causality, which rests on a completely empirical interpretation of BOLD signal fluctuations, devoid of any explicit reference to the underlying neurophysiology.

It is therefore reassuring that DCM confirmed the inferences for the key hub nodes it was applied to, given that, even though DCM shares some conceptual similarities with PPI, it is not equivalent in that it rests on an explicit, validated biophysical model of neurovascular coupling (Stephan, 2004). It is also worthwhile to consider that the calculation of the degree centrality and clustering coefficients is insensitive to connection directionality.

6.4.8 Representation of individual gamble parameters

In keeping with the results of the voxel-wise univariate analyses reported in the previous chapter, k_{WIN} and p_{WIN} were not significantly represented in effective connectivity as individual parameters. Given that both are necessary to determine *EV*, this is interpreted simply as an indication that their coding is much subtler in comparison to that of k_{LOSE}, and therefore does not influence regional neural activity and large-scale network dynamics sufficiently to be detected by fMRI. By contrast, the distributed representation of k_{LOSE} in a effective connectivity network consisting of a subset of that subserving *EV* representation

goes along univariate evidences which indicate that the brain invests far more neural resource to encode potential losses than equivalent gains.

6.4.9 Small-worldness of the value-encoding network

An additional observation is that the *EV*-sensitive network has small-world topology and is not significantly modular. Recent work in computational biology and social sciences confirms that small-worldness, i.e. the presence of an efficient balance between local and long-range connections, is a pervasive feature of natural networks that emerge by self-organization, irrespective of the specific nature of the nodes and edges (Humphries and Gurney, 2008). In the context of cell neurophysiology, simulations have demonstrated that small-worldness is crucial for long-range synchronizability of activity and for the emergence of specific attractors, which confer to neural networks very different dynamical properties in comparison to equivalent networks devoid of small-world features (Watts and Strogatz, 1998; Barahona and Pecora, 2002; Newman, 2010; Bullmore and Bassett, 2011; Ginestet et al., 2011). Of note, small-worldness has been reliably demonstrated on the basis of spontaneous BOLD signal fluctuations recorded during resting-state fMRI (Wang et al., 2010; Bullmore and Bassett, 2011).

The findings that the effective connectivity network subserving value computation in this task has small-world features extends such observations into the domain of neuroeconomics: in this context, small-worldness plausibly represents an adapted trade-off between local and global processing that enhances survival through optimizing the speed and accuracy of risk-advantageousness judgements (Watts and Strogatz, 1998; Bassett and Bullmore, 2006; Newman, 2010; Bullmore and Bassett, 2011; Ginestet et al., 2011).

6.4.10 Anatomical considerations and relation to lesion literature

From an anatomical perspective, the finding that the DMPFC, VMPFC and ALPFC implement key integrative hubs is plausible, considering that ex-vivo studies with axonal-tracing inks have demonstrated that these regions are among the most densely interconnected ones in the brain, having direct links to one another, to the OFC, DLPFC and VLPFC as well as to the cingulate cortex, hippocampus, amygdala and striatum (Brog et al., 1993; Barbas, 2000; Ongür et al., 2000 and 2003). More specifically, the ALPFC is known to be strongly interconnected with the DLPFC and VLPFC as well as with the basal ganglia, and therefore has an optimal underlying axonal infrastructure to support the emergence of an integrative hub (Barbey et al., 2009). Notably, recent meta-analyses of fMRI studies have suggested that the ALPFC is internally organized according to a hierarchical architecture, whereby its more anterior part is associated with highly abstract processing (Badre, 2008; Botvinick, 2008). On the other hand, it is also well established that that DMPFC and VMPFC have direct connections to the DLPFC and VLPFC, and are therefore a natural candidate for integrating the multisensory information represented in those areas into abstract value representations (e.g., Trepel et al., 2005; Sakagami et al., 2007).

The inferred localization of the key integrative hubs agrees well with lesion studies, which have demonstrated that patients with damage to the VMPFC (Bechara et al., 1999; Clark et al., 2008) and DMPFC (Manes et al., 2002) have reduced capability to discriminate between risk-advantageous and disadvantageous prospects. Notably, focal damage to the OFC (Manes et al., 2002) and DLPFC (Manes et al., 2002; Clark et al., 2003) has less consistent consequences on performance during risky decision-making tasks. On the basis of the results of the present study, one predicts that damage to the ALPFC should have major consequences on risky decision-making performance. Notably,

the ALPFC is not frequently considered separately from the VLPFC and DLPFC, in spite of the presence of clearly-identifiable cytoarchitectonical differences (Rajkowska and Goldman-Rakic, 1995; Fuster, 1997; Barbey and Grafman, 2011).

Because the ALPFC appears to implement more critical integrative functions than the VLPFC, future lesion studies should test the hypothesis that rostral lesions to the lateral PFC should have a greater impact on performance on this task than equivalent lesions to its caudal part. Yet, the agreement with lesion studies is not perfect, because in the inferred effective connectivity network the anterior insula and amygdala appear to have a relatively small number of effective connections, in contrast with studies demonstrating that damage to these areas significantly impairs risky decision-making performance (Weller et al., 2009; De Martino et al., 2010); this mismatch will need to be clarified in future studies, and may originate from limitations in fMRI sensitivity or task design issues.

6.4.11 Summary

In summary, the present experiment provides a novel perspective on value computation in the brain, by explicitly demonstrating for the first time that it is subserved by a complex effective connectivity network, in which the DMPFC, VMPFC and ALPFC feature prominently as cortical hubs and exhibit dense connectivity and high centrality. Additional findings include the observation of significant small-world network topology, and the differential representation of potential losses and gain which parallels the results obtained with univariate correlations in the previous experiment.

The present experiment has profound paradigmatic implications for neuroeconomics as a whole, in that it demonstrates explicitly that the univariate correlational approach is grossly inadequate to capture the full complexity of value representation in the brain, as best typified by the fact that several regions which have very

dense effective connectivity, and which in fact exhibit all features of key integrative hubs, are not characterized by BOLD activity correlating directly with value and are therefore intrinsically invisible to traditional univariate analyses.

7. Behavioural study of patients with Parkinson's disease and Huntington's disease

7.1 Background and motivation

A somewhat puzzling finding from the fMRI experiments described in the previous chapters is the apparent lack of involvement of the dorsal and ventral striatum in value representation. In the influential study by Tom et al. (2007), a paradigm similar to the present one was utilized and activity in the mesial PFC as well as in the striatum robustly correlated with value and predicted the level of behavioural loss aversion. Their findings were interpreted as evidence of a key integrative role of the basal ganglia during risky decision-making, and broadly endorsed the notion that value determination is subserved by a cortico-subcortical circuit founded on the dense, re-entrant connections that exist between the striatum and the prefrontal cortex (Alexander et al., 1986). Here, by contrast, univariate analyses did not reveal any significant representation of the economic parameters at the level of striatal activity, and, convergently, network analysis did not detect a noteworthy number of effective connections involving the striatum.

As previously discussed, a trivial hypothesis is that striatal activity was not apparent in the present experiments simply because of issues with BOLD signal detection which could, for example, be caused by susceptibility artefacts. This hypothesis is, however, refuted by the observation of a clearly significant average BOLD response in this region (Figure 14). One therefore needs to consider potential differences in task design which could lead to a major shift in processing strategy. As discussed above, a relevant factor is that the task under consideration here was substantially more abstract, since the outcome probability was not fixed at 50%, but varied independently alongside k_{WIN} and

k_{LOSE}. A speculative hypothesis, which would demand a dedicated imaging study to obtain a definite confirmation, is that the greater abstraction may have lead to a shift from a more "instinctive" strategy to a more evaluative one, requiring heavier neocortical integrative activity and not significantly involving lower-level, visceral and affective efferent signals from the basal ganglia; such hypothesis finds indirect substantiation in the fact that the reaction times observed here were around twice as long as those recorded by Tom et al. (2007), i.e. on the order of 3 s as opposed to 1.5 s.

Another difference is that, while in Tom et al. (2007) the participants were rewarded financially with a fraction of their earnings, here they were playing with purely virtual money. As detailed in Chapter 2, clearly risk-averse behaviour was observed, providing some reassurance about the ecological validity of the present task, yet one cannot rule out that the absence of a material endowment could have changed the underlying processing strategy and related anatomical substrates. In particular, the question remains open whether the striatal observations reported by Tom et al. (2007) could have been in part epiphenomenal to the expectation of later receiving a fraction of the money earned.

In the majority of real-life circumstances, not all information is immediately available, and one needs to rely on associations previously established through outcome feedback (i.e. associating a certain type of potential prey to food and satiety, and another to an aversive outcome such as physical injury). In situations where on-line outcome feedback is available, the striatum has the well-established and indispensable role of generating dopamine-based reward prediction signals while a possible action is being contemplated, and reward prediction errors signals following outcome delivery and representing the difference between the expectation and the experienced outcome (e.g., Schultz et al., 1993; Fiorillo et al., 2003; Pessiglione et al., 2006). What remains less clear is whether the striatum plays a key role also in the more elementary process of determining

the expected value of individual options once complete information is available, and independently of expectations related to the immediate availability of a reward.

Correlations between BOLD activity in the striatum and value have been observed in several studies, yet are not omnipresent and, as discussed above, there is growing realization that striatal activity is more closely related to the generation of reward and reward prediction error signals supporting behavioural reinforcement than to the process of abstract value computation in the face of an isolated risky prospect (Hollerman et al., 1998; Pagnoni et al., 2002; Schultz, 2004; Cohen and Ranganath, 2005; Rorie and Newsome, 2005; Wrase et al., 2007; Tobler et al., 2009). In fact, one could argue that this is hardly a surprising fact, given that the striatum is a phylogenetically-old region, and that situations were value computation must be performed in the absence of ongoing feedback and reward/punishment from the environment are un-natural and therefore unavoidably need to rely on more abstract processing in the prefrontal cortex.

It is intrinsically impossible to definitely conclude whether activity in a given region is fundamental for task performance purely on the basis of fMRI, even for much simpler tasks such as hand movement and language generation and comprehension (Disbrow et al., 2000; Bizzi et al., 2008). Lesion studies, hence, have an important role complementing imaging correlations and supporting inferences of causal relationship between the activity in specific regions and separable neuropsychological abilities. Studying patients with striatal lesions may, therefore, be relevant in settling the debate about the involvement of this region in risky decision-making. Yet, there are complex experimental aspects that need to be considered. The ideal model would be represented by patients with focal ischemic lesions, studied in a phase when the confounds associated with the acute phase (e.g. extensive inflammation, oedema, obtundation) have diminished but significant functional reorganization has not yet taken place. By their nature, ischemic lesions can be relatively focal, and the extent of anatomical damage is easy to determine by

means of structural imaging. Also, their onset is sudden, limiting confounds related to functional reorganization, provided that patients are studied early enough after a vascular event. Unfortunately, patients with isolated striatal strokes are relatively rare, and concomitant involvement of the neighbouring white matter and overlaying cortex is almost unavoidable (Liepert et al., 2005; Nys et al., 2006). Further, the use of patients with gross striatal damage as lesion models in the context of neuroeconomics would be complicated by two other matters. First, the basal ganglia are, of course, not only involved in decision-making but also central to motor performance: hence, patients with striatal lesions present with specific deficits and changes in motor excitability (Liepert et al., 2005; Kim et al., 2008). Second, the activity of the basal ganglia is very closely coupled with that of the prefrontal cortex, and even isolated lesions have profound, pervasive effects on cognitive domains such as working memory, awareness and strategic reasoning that are generally deemed to reflect primarily neocortical rather that subcortical function (Mizuta et al., 2006; Nys et al., 2006; Baier et al., 2010; Liebermann et al., 2011). Such effects can be controlled for through extensive neuropsychological testing and lesion mapping on adequately large populations, that embed sufficient variance to enable disentangling the "primary" consequences of a lesion from potential confounds (e.g., Nys et al., 2006).

A much more widely represented patient group consists of those that suffer from striatal degeneration due to disorders such a Parkinson's disease (PD) and Huntington's disease (HD). The two disorders are aetiologically very different. The former is most frequently idiopathic, and characterized by intra-neural inclusion of pathological aggregates of a misfolded physiological protein, α-synuclein, which accumulate rapidly and are highly neurotoxic (Spillantini et al., 1997). Such aggregates, known as Lewy bodies, are the pathological hallmark of the disease and, in typical forms of the disorder, initially appear in the brainstem and olfactory nuclei. As degeneration progresses, the dopaminergic neurons in the substantia nigra pars compacta are affected and rapidly

depleted, and concomitant pathology appears in the ventral portion of the striatum, eventually extending to the amygdala, thalamus and cortex (Braak et al., 2004). By contrast, HD is an autosomal-dominant, genetically-determined disorder, characterized by an aberrant expansion of CAG repeats at chromosome 4p16.3.1, in the region coding for the huntingtin protein (e.g., Thomas, 2006). Although this protein is widely expressed, for as-yet unclear reasons its abnormal form is especially toxic to some neural populations and much less for others (Double et al., 2010): as a consequence, neurodenegeration ensues in the dorsal striatum (caudate nucleus), gradually depleting glutamatergic neurons and progressing irreversibly towards the anterior and ventral part of the striatum, until virtually the whole dorsal part is ablated (Vonsattel et al., 1985; Hedreen and Folstein, 1995; Vonsattel and Di Figlia, 1998). Of note, recent work suggests that the caudate nucleus may even develop abnormally in patients carrying the mutation (Mandelli et al., 2010).

Unfortunately for the purposes of the present experiment, neurodegeneration is not confined to the striatum for either disease. In PD, amygdalar damage may be present even before the onset of motor symptoms, and subtle yet diffuse cortical involvement, especially of frontal and parietal neocortical regions, is detectable already in early symptomatic phase, as demonstrated by neuropathologic studies and diffusion-tensor imaging of the main cortico-cortical association pathways (Braak et al., 2004; Gattellaro et al., 2009). Further, the gradual depletion of dopaminergic neurons reflects on the activity of the prefrontal cortex already in early disease stages (Ouchi et al., 1999). Even though it is less immediately obvious to map due to the absence of an histologically-evidence pathological hallmark (like Lewy bodies for PD), in HD the topographical distribution of neocortical degeneration appears to be rather similar to that observed in PD, with gradual loss of neurons in the deep layers of the prefrontal cortex, particularly its lateral part, amygdala and insula (Vonsattel and Di Figlia, 1998; Beste et al., 2010). While PD and HD, respectively, initially affect primary dopaminergic and glutamatergic basal ganglia

signalling, both diseases eventually lead to widespread imbalances in multiple systems (e.g., Cha et al., 1999; Chesselet and Richter, 2011). In PD, there is the added complication of dopaminergic therapy, which can have significant effects on cognitive and affective functioning, and even lead to impulse control dysfunction and pathological gambling in vulnerable individuals (Czernecki et al., 2002; Dodd et al., 2005).

Due to these limitations, it is difficult to confidently assign the cognitive and behavioural dysfunctions observed in these disorders specifically to striatal degeneration. Yet, many studies have been conducted on decision-making empirically taking PD and HD patients as convenient "system lesion" models, which try to attain good specificity by controlling for neuropsychological variables representing neocortical function and by explicitly contrasting PD and HD in virtue of the similar pattern of neocortical involvement but complementary dorsal-ventral gradient of striatal degeneration (e.g., Watkins et al., 2000; Mimura et al., 2006; Pagonabarraga et al., 2007; Kobayakawa et al., 2008; Delazer et al., 2009; Beste et al., 2010).

Here, an exploratory behavioural experiment was conducted on early-stage PD and HD patients attempting to falsify the hypothesis that the striatum has a negligible role in value computation during risk decision-making. In other words, predicated on the null results for the striatum in the univariate and network-based analyses of the functional MRI data, the prediction was formulated that incipient neurodegenerative damage to this region would not influence the ability to integrate potential gains and losses, and that the ability to effectively discriminate risk-advantageous and disadvantageous gambles would therefore be unaffected in early-stage PD and HD patients.

7.2 Participants, methods and data analysis

The experiment was performed on 10 patients with genetically-confirmed HD, 11 patients with idiopathic PD and 16 healthy controls. The full demographic characteristics are provided in Table 3. The patients and controls were matched for gender, age and years of formal education. The experiment was officially approved by the research governance and ethics committee of the Brighton & Sussex Medical School (BSMS; PhD project no. 10/056/MIN) and by the research ethics committee of the Fondazione IRCCS Istituto Neurologico "Carlo Besta" (project no. fMRI-DM), where the study was conducted in psychology laboratory of the Neurology I unit. In compliance with local legislation, which implies that only a registered psychologist can administer tests to a patient, all participants were materially tested by Dott.ssa Sylvie Piacentini and Dott.ssa Francesca Ferrè on the author's behalf. Written informed consent was obtained and, as for the previous experiments, participants could not receive any financial or material compensation and were therefore not playing with real currency. All participants were Italy-educated, fully right-handed according to the criteria of Oldfield (1971), naive to the task and study design and without any specific experience in banking, financial investments or any history of gambling. Healthy controls with the appropriate education range were recruited among technical, clerical and catering support staff of the Institute, and screened to exclude familiarity for any movement or psychiatric disorder. The patients with HD were recruited in the specialist neurology and genetic counselling clinic run by Dott. Lorenzo Nanetti under the supervision of Dott.ssa Caterina Mariotti; the patients with PD were recruited during outpatient clinical routine by Dott. Luigi Romito under the supervision of Prof. Alberto Albanese.

For HD patients, the number of CAG repeats (determined upon genetic analysis, as detailed in Squitieri et al., 2003) ranged between 40 and 48. Six patients were

symptomatic, i.e. already suffered from mild to moderate choreic movements, scoring between 7 and 29 on the Unified Huntington's Disease Rating Scale (UHDRS, 1996); all of them maintained a Total Functional Capacity (TFC) score above 11 (Marder et al., 2000). The remaining four were still free from any motor symptoms and detectable cognitive or emotional manifestations. According to the well-accepted predictive model of Langbehn et al. (2004), which is postulated on large-sample observations of an association between triplet repeat count and age of onset of the first symptoms, they were between 5 and 12 years away from clinical disease manifestation.

For PD patients, the diagnosis was clinical, with structural imaging performed only to exclude secondary causes of Parkinsonism. The criteria of the UK Parkinson's disease brain bank were applied (Hughes et al., 1992) and careful neurologic examination was performed to exclude patients presenting tell-tale signs of potential atypical parkinsonism. One patient had a Hoehn & Yahr score (1967) of 1, 6 had a score of 1.5, 2 had a score of 3 and only one had a score of 2.5. The self-reported duration of the motor symptoms was between 2 and 5 years. All patients were taking dopamine replacement therapy, and were on their regular medication at the time of testing; the Levodopa Equivalent Daily Dose (LEDD) was between 100 and 160 mg. Preliminary enquiries to the local research ethics committee represented negatively the possibility of taking the patients off-medication purely for the purpose of the present exploratory experiment.

The presence of significant psychiatric symptoms was excluded by means of a structured interview based on the items of the Brief Psychiatric Rating Scale (Overall and Gorham, 1962). The presence of hallucinations was excluded for all PD patients. Depression and anxiety were measured by means of the Italian adaptation of the Zung scales (Zung, 1974).The scores were generally in the normal range, but 3 HD patients, 1 PD patient and 1 control had moderate anxiety, and 2 HD patients had moderate depression. There was no group difference in the depression scores between patients and

controls, however, as detailed in Table 3, HD and PD patients were on average significantly more anxious than controls.

In order to obtain an overall evaluation of cognitive state without overburdening participants with extensive batteries, the Montreal Cognitive Assessment (MoCA) battery was utilized (Nasreddine et al., 2005). This battery briefly probes visuospatial abilities, executive function, working memory, attention and language and lasts approximately 10 min. Though originally developed as a screening tool for mild cognitive impairment prodromal to Alzheimer's disease, the MoCA has been validated for use also in PD and HD patients, and provides superior sensitivity to the Mini Mental State Evaluation (Dalrymple-Alford et al., 2010; Mickes et al., 2010). To further confirm the integrity of prefrontal functions, the backward digit-span test, Stroop test and Trail-Making Test part B-A were administered as detailed in Italian normative studies (Orsini et al., 1987; Giovagnoli et al., 1996; Caffarra et al., 2002). These tests probe various combinations of working memory, inhibition and executive function and are therefore sensitive to damage of the lateral, mesial and orbital PFC. As reported in Table 3 there were clearly no group differences in these scores, providing some reassurance that the level of neocortical involvement was negligible.

Neuropathological studies have established that amygdalar damage ensues before significant neocortical involvement in PD (Braak stage III), and, though less markedly, also in HD (Braak et al., 2004; Vonsattel and Di Figlia, 1998). Hence, the amygdala may be used as a "sentinel region" to garner some additional confirmation that the level of neuropathological burden was not such that neocortical function would be significantly impaired. The "Reading the Mind in the Eyes" test involves attempting to infer the emotion of a person, on the basis of a black and white picture showing only the facial area around the eyes. Initially developed as a theory of mind test for autistic children, the test has found widespread acceptance in other fields (Baron-Cohen et al., 2001); notably, it has

been found to elicit significant amygdalar activation (Pincus et al., 2010) and to be particularly sensitive to amygdala damage (Richell et al., 2003; Stone et al., 2003; Shaw et al., 2005). In line with the results of the other psychometric tests, here it did not reveal any difference between patients and controls.

As for the other experiments, responses were entered using a computer keyboard, through the index and middle fingers of both hands, according to the "confident reject", "unsure reject", "unsure accept" and "confident accept" scale. As before, the experimenter explicitly asked the participants to try and make use of all four levels, to express their subjective judgements on the palatability of each gamble in addition to accept/reject decisions. Within each session, 240 gambles were delivered, but the first 40 were considered practice trials and were therefore ignored for the purpose of statistical analysis. Three pauses of arbitrary duration were inserted. In this experiment, the task was self-paced and a new gamble was presented immediately upon response to the previous one; however, in order to help maintain consistent timings, participants were told that they had only up to 6 s to respond, even though this limit was not actually enforced. On average, the task duration was 15.4±6.6 min.

As detailed in Chapter 2, RTs were normalized and responses for which they were outside 3 standard deviations of the average were removed. The following behavioural indices were computed: i) overall amount earned (e.g., the sum of the EV of all accepted gambles), ii) EV-sign discrimination (i.e., the ratio of rejected $EV<0$ and accepted $EV>0$ gambles), iii) average response confidence, iv) average acceptance rate (i.e., the ratio of accepted gambles irrespective of their features), v) mean RTs, vi) logistic regression coefficients for the effects of k_{WIN}, k_{LOSE}, p_{WIN} and EV on the probability of gamble acceptance and vi) the ratio $\lambda=-\beta_{LOSE}/\beta_{WIN}$, representing loss aversion. All parameters were compared between healthy controls, PD and HD patients using non-parametric Mann-

Whitney tests, to maintain to a minimum the statistical assumptions about the distribution in such small samples.

Table 3 (following page). Demographical and clinical characteristics of the sample. HD: Huntington's disease. PD: Parkinson's disease. MoCA: Montral cognitive assessment battery. UHDRS/UPDRS: Unified Huntington/Parkinson disease rating scales. LEDD: Levodopa equivalent daily dose.

	Healthy controls	HD patients	PD patients	HD-controls (p-val)	PD-controls (p-val)
n	16	10	11		
Age (years)	45±14 (25-68)	39±9 (27-53)	54±11 (38-69)	0.2	0.06
Education (years)	14±3 (8-18)	13±3 (8-17)	13±2 (8-16)	0.6	0.4
F/M	7/9	7/3	3/8	0.2	0.4
Zung anxiety	32±6 (22-45)	38±6 (31-50)	42±8 (30-55)	0.03*	0.005*
Zung depression	34±6 (22-47)	38±7 (27-49)	39±11 (25-59)	0.2	0.2
MoCA score	27±2 (23-29)	26±2 (24-28)	28±1 (26-29)	0.3	0.2
Backward digit-span	5.8±1.6 (4-8)	4.7±1.4 (3-7)	5.0±0.8 (4-7)	0.08	0.1
Stroop test (s)	17±7 (8-31)	22±15 (7-47)	16±8 (8-38)	0.3	0.7
Trial-making test (B-A) score	69±40 (22-183)	80±37 (31-135)	65±48 (26-199)	0.5	0.8
Reading mind in the eyes score	25±4 (16-29)	25±5 (15-32)	24±4 (15-30)	0.9	0.8
CAG repeats		45±2 (40-48)			
UHDRS score		17±9 (7-29, and 3 asympt. onset in 9±3 years)			
UPDRS score			18±7 (11-30)		
Disease duration (years)			3±1 (2-5)		
LEDD dose (mg)			140±20 (100-160)		

7.3 Results

On average, patients and controls pooled together performed the task clearly beyond chance level, i.e. preferentially accepted risk-advantageous and rejected risk-disadvantageous gambles (*EV* sign discrimination 0.74±0.08, median 0.72; one-sample t-test vs. 0.5 yielded $p<0.001$), and accordingly earned a significant amount of virtual money (1930±850 €, median 1890 €; one-sample t-test vs. 0 € yielded $p<0.001$). As expected, the participants accepted significantly less than half of the gambles (0.40±0.10, median 0.39; one-sample t-test vs. 0.5 yielded $p<0.001$) and over-weighted potential losses with respect to gains ($\lambda=1.4\pm1.1$, median 1.2; $p<0.001$).

The controls enrolled for the present experiment appeared slightly less able to discriminate between positive and negative *EV* than those recruited for the previous investigations (*EV* sign discrimination 0.76±0.07 vs. 0.82±0.08, $p=0.02$), without concomitant differences in risk aversion. To ensure matching with the patient populations, the controls recruited here were on average older (45±14 vs. 35±7 years, $p=0.01$) and less academically-educated (14±3 vs. 18±3 years, $p<0.001$). Linear regression revealed that the different ability at *EV* sign discrimination was correlated to the mismatch in formal education ($r=0.5$, $p<0.001$).

Even at the uncorrected statistical threshold ($p<0.05$) there was no difference in the choices made by the PD and HD patients with respect to those of the controls according to any measure. As represented in the scatter plots shown in Figure 36, the scores for the three groups showed substantial overlap for all parameters.

Figure 36 (following pages). Scatter plots representing the individual behavioural scores on the decisional task for healthy controls (CTRL), patients with Hutington's disease (HD) and patients with Parkinson's disease (PD).

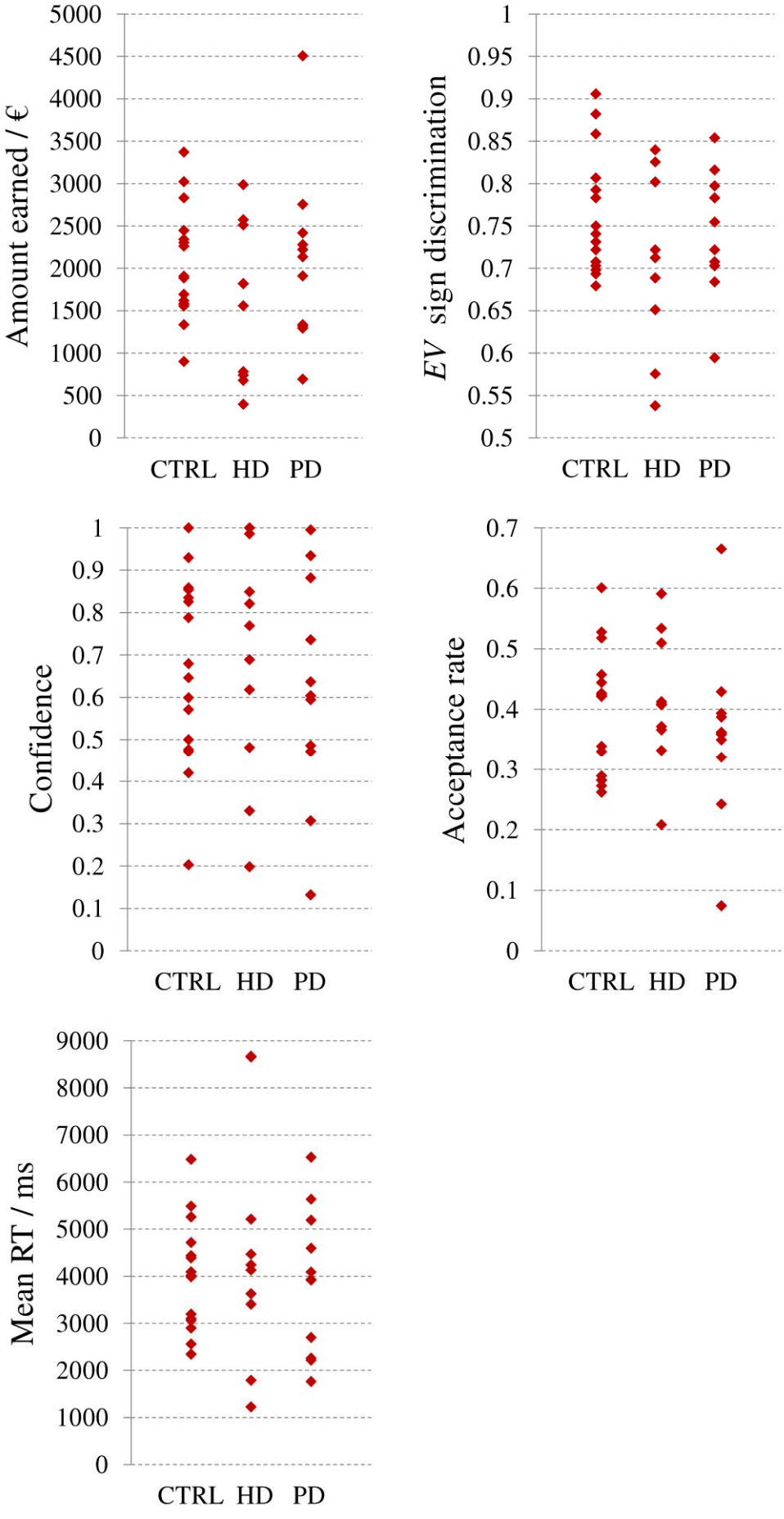
Amount earned / €
5000
4500
4000
3500
3000
2500
2000
1500
1000
500
0
CTRL HD PD
EV sign discrimination
1
0.95
0.9
0.85
0.8
0.75
0.7
0.65
0.6
0.55
0.5
CTRL HD PD
Confidence
1
0.9
0.8
0.7
0.6
0.5
0.4
0.3
0.2
0.1
0
CTRL HD PD
Acceptance rate
0.7
0.6
0.5
0.4
0.3
0.2
0.1
0
CTRL HD PD
Mean RT / ms
9000
8000
7000
6000
5000
4000
3000
2000
1000
0
CTRL HD PD

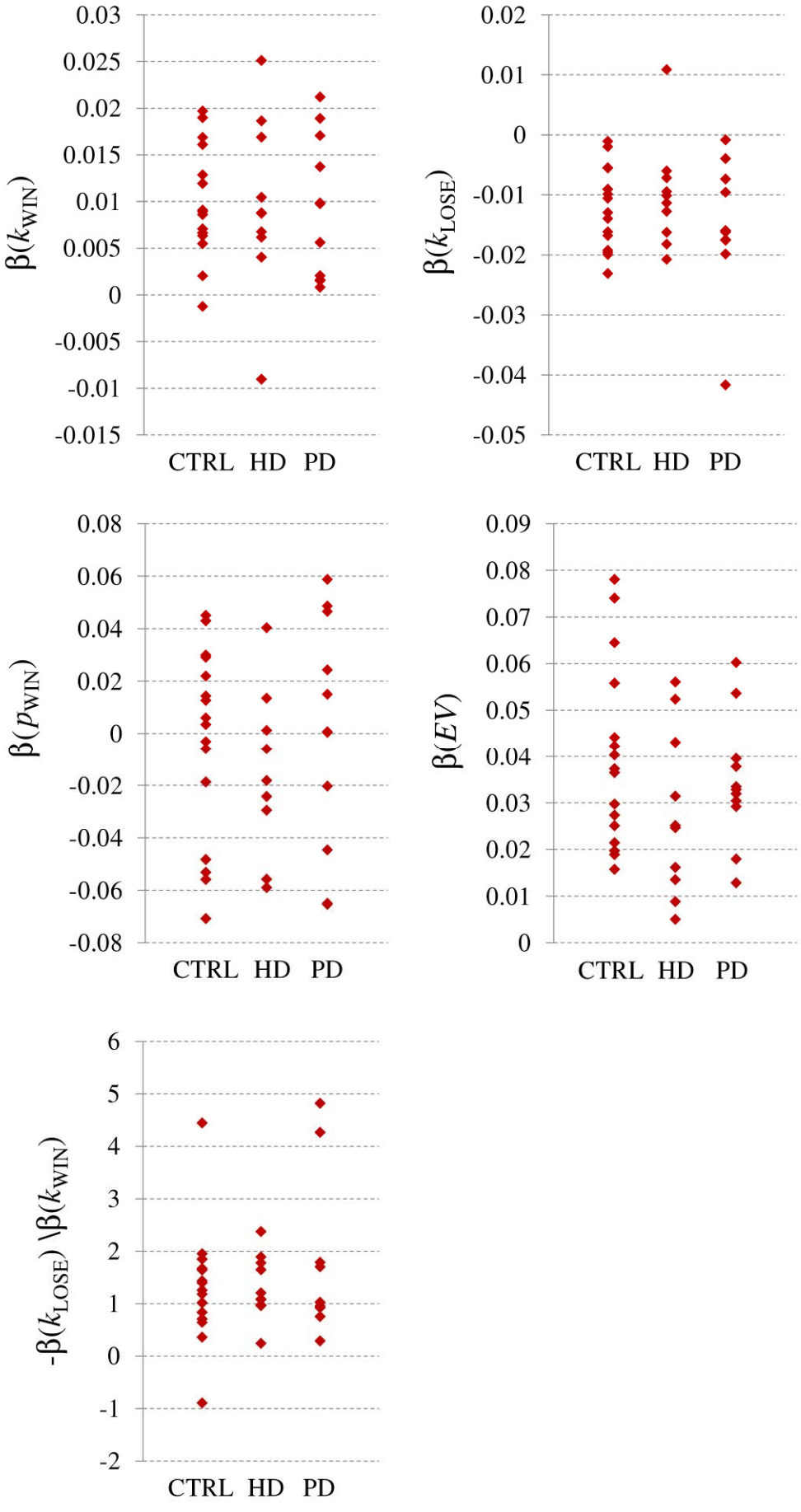
β(k_WIN)
0.03
0.025
0.02
0.015
0.01
0.005
0
-0.005
-0.01
-0.015
CTRL HD PD
β(k_LOSE)
0.02
0.01
0
-0.01
-0.02
-0.03
-0.04
-0.05
CTRL HD PD
β(p_WIN)
0.08
0.06
0.04
0.02
0
-0.02
-0.04
-0.06
-0.08
CTRL HD PD
β(EV)
0.09
0.08
0.07
0.06
0.05
0.04
0.03
0.02
0.01
0
CTRL HD PD
-β(k_LOSE) \β(k_WIN)
6
5
4
3
2
1
0
-1
-2
CTRL HD PD

7.4 Discussion

7.4.1 Lack of an effect of striatal pathology on the evaluation of risky prospects

The present experiment failed to falsify the hypothesis that striatal integrity is irrelevant to value computation in an elementary mixed-gambling situation. Patients with PD and HD earned as much as controls, displayed comparable ability to discriminate positive and negative value, were similarly risk averse and give overlapping weights to the decisional parameters. This is in line with the results of the fMRI experiments, which did not demonstrate significant involvement of the dorsal or ventral striatum in representing value, potential gains or losses in the present task, either as direct BOLD response correlations or effective connectivity. Clearly, these behavioural observations can only corroborate the imaging results, but may not, at this stage, provide a definite confirmation that the striatum is not functionally involved in the evaluation of isolated risky prospects. It is, at least, certainly fundamentally involved in the motor aspects of the task and in supporting prefrontal function in general (Liepert et al., 2005; Mizuta et al., 2006; Nys et al., 2006; Kim et al., 2008; Baier et al., 2010; Liebermann et al., 2011).

7.4.2 Possible interpretation in terms of insufficient pathological load

One trivial explanation for the present negative finding could be that the level of striatal pathology characterizing these patients was simply not sufficient to impair performance on this relatively undemanding task. Unfortunately, this hypothesis cannot be fully rejected, as neuropathological confirmation was not available. The dysfunction of dopaminergic signalling in the striatum of PD patients can be assessed in-vivo by means of single-photon computed emission tomography with specific ligands, but such examination

could not be performed in this patient group as it is normally prescribed only when symptoms suggestive of atypical parkinsonism are present (de la Fuente-Fernández, 2012). Yet, it is well established that when clinical symptoms of PD appear, massive degeneration of the substantia nigra pars compacta has already occurred and diffuse deficits in dopaminergic signalling are observed throughout the striatum (Ouchi et al., 1999; Minati et al., 2007). In clinical trials of HD therapies, the degeneration of the caudate nucleus is commonly assessed by manual segmentation and volumetry on structural MRI images, but adequate images were, unfortunately, not available for these patients (Aylward, 2007). Nevertheless, it is well established from neuropathological studies that in HD widespread apoptosis of caudate spiny neurons occurs more than a decade before the onset of clinical symptoms, and this is reflected by considerable volume loss already in presymptomatic phases (Gómez-Tortosa et al., 2001).

To avoid potential confounds related to neocortical pathology, the conservative decision of enrolling early-stage patients was made. Given that all neuropsychological markers of neocortical involvement were clearly negative in these groups, with hindsight one may reason that it could have been possible to enrol slightly more advanced-stage participants while still not introducing severe confounds related to neocortical pathology. In fact, several previous studies in which HD and PD patients were taken as "system lesion" models to study basal ganglia involvement in decision-making were conducted on more severe cases, e.g. in Watkins et al. (2000) and Stout et al. (2001) HD patients had an average UHDRS score around 30, and in Mimura et al. (2006) and Delazer et al. (2009) large numbers of PD patients in Hoehn & Yahr stages 2.5 and 3 were included. As exemplified by some investigations on basal ganglia function (e.g., Weddell et al., 1994; Nys et al., 2006) the optimal combination between statistical power and specificity would be provided by a larger-scale study, in which the full spectrum of clinical severity for both pathologies is adequately populated, and correlational approaches are used to attenuate or

remove the effect of impaired neocortical function; unfortunately such effort was beyond the resources available for the present doctoral project.

7.4.3 Relation to clinical literature on decision-making under risk or ambiguity

Yet, the results of the present experiment as in good accord with literature in this area that convergently indicates that decision making under ambiguity is impaired but decision making under risk is relatively spared in PD and HD patients. The Iowa Gambling Task (IGT) has been widely adopted to study decision-making under ambiguity, and consists of presenting participants with four identical decks of cards. Each deck is associated with a different proportion of risk-advantageous and disadvantageous cards, and participants need to learn, on the basis of ongoing outcome feedback, which decks contain more "good" cards and adjust their choices accordingly (Bechara et al., 1994). There is ample evidence that both PD and HD patients do badly on this task. For example, Stout et al. (2001) have studied 14 patients with moderate symptomatic HD and found that they were unable to adjust their choices on the basis of feedback, and therefore picked more disadvantageous cards with respect to controls and earned less money. Mimura et al. (2006) obtained a similar finding in PD patients in Hoehn & Yahr stages 2 and 3, tested on their usual dopaminergic medication; notably, poor performance was unrelated to overall cognitive status, executive capabilities and mood. This result, and particularly the absence of direct correlations between frontal functions and task performance, was later confirmed by Pagonabarraga et al. (2007) on 35 non-demented PD patients with a range of disease severity. Notably, a further study by Kobayakawa et al. (2008) in which electrodermal activity was measured during the IGT indicated that autonomic responses to anticipation and outcome delivery are blunted in PD, and not explained by general autonomic dysfunction. The authors confirmed the absence of correlations with cognitive

performance, and speculated that poor task performance was related to amygdalar dysfunction, either directly or through the failure of dopaminergic reward-related signalling from the striatum. An early study by Watkins et al. (2002) on moderately-impaired HD patients investigated risky decision making using a task more specifically probing evaluation, in which outcome probabilities were explicitly shown and did not have to be inferred from ongoing feedback. In contrast with the results obtained for the IGT by Stout et al. (2001), no difference between patients and controls was observed, even though the participants had marked impairments in executive performance as demonstrated by another task. Along the same line, Delazer et al. (2009) explicitly compared performance on the IGT and a task involving risk but not ambiguity, demonstrating that PD patients with and without dementia perform poorly on the IGT whereas risky decision-making is impaired only in PD patients with dementia.

7.4.4 Summary

The results of these studies and of the present investigation lend support to the view that the striatum is mainly or only functionally involved in decision-making under ambiguity, where processing ongoing feedback through reward delivery and reward prediction error signals is fundamental to sustain performance, but that its contribution is not central to making decisions about individual risky prospects, wherein all information is explicitly given and performance depends mostly on integrative processing. Owing to the independent modulation of k_{WIN}, k_{LOSE} and p_{WIN} the present task is considerably more abstract than those considered in Watkins et al. (2002) and Delazer et al. (2009), so the convergence of the findings provides some reassurance on the general validity of this conclusion, yet one needs to consider that the anatomical substrates to risky decision making are, to some extent, sensitive to specific situations. For example, Jones et al.

(2011) utilized a similar risky decision-making task presenting gambles discretized in disadvantageous, near-indifferent and advantageous categories, and demonstrated that *EV*-sensitive responses were manifested in the striatum and insula conditional to the presence of significant time pressure. Hence, concluding that the striatum is not functionally involved at all in risky decision-making would be premature, but a careful re-evaluation of the view that it acts as one of the key substrates to elementary value computation appears necessary.

8. Transcranial direct-current stimulation (tDCS) of the dorsolateral prefrontal cortex (DLPFC)

8.1 Background and motivation

As introduced in Chapter 1, a striking feature of human and more generally animal decision-making behaviour in situations of risk is the aversion for choices that have an uncertain outcome, even though their expected value may be positive. To date, the exact neural substrate for this decisional bias remains unclear: for example, the influential study by Tom et al. (2007) and later works like Ino et al. (2010) have led to the hypothesis of a profound relationship to striatal activity, but the previous experiments reported in the present dissertation do not seem to support this view (see also Platt and Huettel, 2008). Further investigations suggest that damage to other structures, notably the amygdala, can selectively attenuate or eliminate such biases (De Martino et al., 2010) whereas lesions affecting the anterior insula can have the opposite effect of promoting risky choices, independently of value (Weller et al., 2009). Taken together with fMRI evidence of non-linear encoding of probability and risk across multiple brain regions, these results suggest that risk and loss aversion could be emergent properties of the interaction among multiple areas and systems, rather than attributable to isolated regional function (e.g., Trepel et al,. 2005; Hsu et al., 2009; Bossaerts, 2010; De Martino et al., 2010).

Yet, a fascinating observation is that patients with right prefrontal lesions tend to be significantly less risk-averse than healthy participants, and prefer riskier to advantageous card decks on the IGT with a proportional effect dependent on the volume of right lateral prefrontal cortical loss (Clark et al., 2003). Predicated on these observations, Knoch et al. (2006) used low-frequency repetitive transcranial magnetic stimulation (rTMS) to induce

in healthy participants transient but robust dysfunction of the lateral prefrontal cortex, particularly of the DLPFC. They observed that right, but not left stimulation markedly boosted the number of unsafe choices during a task probing decision-making under risk. These studies have led to the notion of a general relationship between right prefrontal function and risk-taking, and in particular to the hypothesis that right DLPFC activity may be essential to suppress the choice of superficially-seductive prospects in favour of deeper integrative comparison of the value of the available options.

Further support to this notion was provided by experiments conducted with transcranial direct-current stimulation (tDCS), which is a relatively straightforward neuromodulation technique that consists of applying a rectified current to the scalp through a pair of saline-soaked sponge electrodes positioned over the cortical regions of interest. Constant currents on the order of few milli-Amperes are delivered using battery-operated generators, and the technique is widely regarded as completely safe (Nitsche and Paulus, 2000; Nitsche et al., 2008). Even though the majority of current is shunted by conduction in the ion-rich environment of the scalp muscles, provided that the electrodes are adequately far apart sufficient current penetrates the skull bone to generate detectable neural effects. Current flowing across the cortical plane underlying the spongy electrodes results in a modulation of the transmembrane neural potential which translates in altered excitability, particularly of the pyramidal cells (e.g., Wagner et al., 200; Sadleir et al, 2010). Because of the coherent orientation of the axons and dendritic branches of pyramidal neurons in the cortex, opposite current polarities appear to have specular effects on the transmembrane potential: anodal stimulation generally increases excitability, whereas cathodal stimulation attenuates it (Nitsche and Paulus, 2000; Wachter et al., 2011).

In Fecteau et al. (2007), tDCS of the DLPFC was performed applying multiple electrode configurations, with the aim of altering the hemispheric balance of DLPFC

excitability or attempting to alter activity in either side alone. The authors found that when both DLPFCs were stimulated the observed behaviour on a risky-decision making task became more conservative. On the other hand, Boggio et al. (2010) applied a similar protocol to older adults and observed that right cathodal DLPFC stimulation increased the relative appetibility of high-risk prospects compared to the converse polarity. In spite of fundamental differences in the investigative methods and some inconsistency on laterality, the works by Clark et al. (2003), Knoch et al. (2006), Fecteau et al. (2007) and Boggio et al. (2010) conjointly point to a fundamental role of the DLPFC in determining the level of risk-aversion of an individual. Such hypothesis appears anatomically plausible, given that the DLPFC is fundamental not only to information-integration but also to cognitive control of behaviour (Tsujimoto and Sawaguchi, 2004; Hoshi, 2006; Kahnt et al., 2010), and given that it is densely interconnected to the medial PFC and to the ALPFC, which the previous experiments have identified as key network nodes in value computation (e.g., Barbas, 2000; Ongür and Price, 2000).

As previously discussed, the present research is not explicitly concerned with finding the neural determinants of the variable level of risk aversion and decisional bias spontaneously observed in given individuals, as the economic validity of such inferences would be limited given the absence of real financial endowment in these experiments. More simply, the focus is on elucidating the structures and networks that are generally involved in the representation of the economic parameters characterizing risky prospects. For that purpose, the ability to elicit relative shifts in risk propensity across experimental groups would still be relevant because such changes imply a general modulation of the representation of losses and gains, even though the absolute level of risk aversion may not be representative at individual level.

Unfortunately, the lesion and neuromodulation data available to date do not enable definite conclusions to be reached regarding the relationship between DLPFC activity and

value representation in the context of elementary risky prospects. The IGT, used in Clark et al. (2003), has good ecological validity because performance critically depends on learning from ongoing outcome feedback and adapting behaviour as a consequence, but value computation is heavily intermixed with learning and executive function in an ambiguous environment (Bechara et al., 1994). On the other hand, in the Risk task, used in Knoch et al. (2006), Fecteau et al. (2007) and Boggio et al. (2010), participants need to guess the colour of the box harbouring a winning token, in situations where the proportion of coloured boxes varies conjointly with reward magnitude, such that attempting to harvest the largest potential reward always entails a high-risk choice. Though this task does not involve ambiguity, it inherently intermixes value determination and risk sensitivity, making it impossible to directly interpret the results from the viewpoint of the differential representation of gains and losses (e.g., Rogers et al., 1999).

The present experiment was motivated to explore whether the postulated relationship between DLPFC activity and risk taking generalises to the evaluation of elementary prospects explicitly presenting independently-varying gains, losses and associated outcome probability. In particular, predicated on the known role of the DLPFC in supporting *EV* determination through multiparametric integration and interaction with the mesial PFC and on the results of the previous neuromodulation experiments (Knoch et al., 2006; Fecteau et al., 2007; Boggio et al., 2010 and 2010b), it was predicted that cathodal stimulation of the right DLPFC would increase overall risk-propensity, reflecting enhanced weighing of potential gains over losses, whereas the converse polarity would potentially lead to the opposite effect.

8.2 Participants, methods and data analysis

Forty-seven Brazil-educated female university students participated in the experiment and were subdivided into three groups, receiving sham tDCS, left anodal/right cathodal tDCS or right anodal/left cathodal tDCS. The study was conducted at the Centre for health and biological sciences, Mackenzie Presbyterian University (São Paulo, Brazil), and performed according to procedures approved by the local ethics committee, registered with Brazilian national research ethics committee (Sistema Nacional de Informação sobre Ética em Pesquisa envolvendo Seres Humanos, SISNEP, no. CAAE 0039.0.272.000-08), and approved by the research governance and ethics committee (RGEC) of the Brighton & Sussex Medical School (BSMS, PhD project no. 10/056/MIN). To comply with local regulations and overcome communicative difficulties related to the fact that the participants spoke Brazilian Portuguese, local staff (Camila Campanhã, Karina Di Siervi, Ana Alem and Nathalia Baptista) acting under the supervision of Prof. Paulo Boggio assisted with delivering the instructions, obtaining informed consent and applying the stimulation device.

As with the previous experiments, all participants were naive to the study and did not have specific experience in economics, finance or decision-making research. They were free from neurologic and psychiatric pathology. None was taking illicit drugs, or self-declared gambling habitually. All participants were right-handed according to the Edinburgh handedness inventory (Oldfield, 1971). No financial or material compensation was offered, but all participants received a fixed token of university credits, as locally approved for participating in psychological research.

The full demographic characteristics are reported in Table 4. To exclude confounding differences between the groups due to mood and impulsivity, all participants were tested with the Beck anxiety and depression inventories (BAI, Beck et al., 1993;BDI,

Beck et al., 1996), with the Barratt impulsiveness scale (BIS, Patton et al., 1995) and with a visual-analogue scale capturing feeling state on 14 axes, which has been utilized in previous tDCS studies (e.g., Boggio et al., 2010). There were no group difference on these scales, in age or education.

The choice of recruiting female participants was driven by convenience sampling considerations and related to the fact that the university students attending the centre and available for participating in experiments were predominantly female. While there is no evidence from previous studies that the effect of tDCS on risk-taking is gender dependent (Fecteau et al., 2007; Boggio et al., 2010), baseline differences in risk propensity between genders have been reported (e.g., Croson and Gneezy, 2009), through not consistently replicated in large-scale studies of financial markets (Schubert et al., 1999; Barasinska, 2010). Addressing this potential issue, a preliminary comparison was performed between the 31 females and 29 males recruited for the autonomic response, EEG and fMRI experiments by means of t-tests. There were no significant differences in EV sign discrimination (0.80±0.07vs. 0.83±0.09, p=0.1), proportion of accepted gambles (0.44±0.07 vs. 0.45±0.08, p=0.4) and logistic regression ratio $\lambda=-\beta_{LOSE}/\beta_{WIN}$ (1.4±0.8 vs. 1.2±0.5, p=0.4).

A major problem in TMS studies is the reliability of the sham condition: since stimulation generates audible noise and a typical scalp sensation, it is difficult to maintain proper blinding while delivering a truly inactive neuromodulation (e.g., Rossi et al., 2007). Here, tDCS provided an optimal sham condition, consisting of ramping up the current to the intended level then slowly ramping it back to zero after approximately 30 s of stimulation. This reproduced the initial tingling sensation which is frequently associated with the first few seconds of active tDCS (e.g., Nitsche et al., 2008). As the stimulation device explicitly displays the applied current with an analogue ammeter, to further improve the quality of the sham condition a special mode was selected which preserved the

displayed current value while not actually delivering any current (Boggio et al., 2010). In order to confirm the quality of the sham condition, upon completion of the stimulation the participants were asked to rate their perception of the stimulation on a scale ranging from -5 ("I am sure it was sham stimulation") to 5 ("I am sure it was active stimulation"). As confirmed by t-tests between the groups, there was clearly no difference between the active and the sham conditions (1.1±3.3, 0.9±2.8 and 0.8±3.3, p=1).

Since the principal aim was to investigate whether the results originally obtained with the Risk task generalize to the evaluation of individual risky prospects of variable expected value, identical stimulation settings to those used in Fecteau et al. (2007) and Boggio et al. (2010) were adopted to ensure direct comparability of the findings. Hence, the sponge electrodes, each having an area of approximately 30 cm^2, were centred on the F3 and F4 sites, determined according to the international 10/20 EEG system (Jurcak et al., 2007). A constant current of 2.0 mA was delivered by means of a battery-operated operational amplifier. As the neurophysiological effect is not immediate, stimulation was switched on approximately 3 min. prior to the beginning of the decisional task. Further, to avoid the possibility of generating action potentials through rapid polarization/depolarization, the current was ramped up and down in slopes of approximately 10 s (Nitsche et al., 2008). The exact duration of the stimulation depended on task pacing and was 20.5±4.1 min across participants. To comply with safety guidelines, the assistant in charge of administering the stimulation always remained in the room, positioned behind the participant, away from their visual field. No participant reported any adverse effect of stimulation.

As in the experiment with PD and HD patients, 240 gambles were delivered within each session, subdivided in four parts separated by brief pauses. Here, to account for practice as well as stabilization of the stimulation, the first 60 gambles, corresponding to approximately 4 min, were rejected; the first 5 gambles after each pause were also ignored

to minimize noise due to attentional shifts. The task was self-paced, i.e. a new gamble appeared immediately after the previous one disappeared, and participants were asked to respond within 6 s of gamble onset. The instructions and response scale were the same as for the previous experiments.

Again, the following behavioural indices were obtained: i) overall amount earned, ii) *EV*-sign discrimination, iii) average response confidence, iv) average acceptance rate, v) mean RTs, vi) logistic regression coefficients for the effect of k_{WIN}, k_{LOSE}, p_{WIN} and *EV* on accept/reject response and vi) the ratio $\lambda=-\beta_{LOSE}/\beta_{WIN}$. Here, in virtue of the larger sample size in respect to the previous experiment, between-subjects ANOVAs were utilized for group comparisons, having one factor with three levels (sham, left anodal/right cathodal and right anodal/left cathodal tDCS). To avoid potential confounding effects due to different variance across groups, the number of degrees of freedom was corrected with Welch's correction. Post-hoc comparisons were conducted by means of Games-Howell tests (1976), which are moderately conservative and do not assume homoscedasticity. Bonferroni's criterion yielded a corrected threshold of $\alpha=0.005$ to account for multiple comparisons over the 10 parameters.

8.3 Results

The participants successfully distinguished between positive and negative *EV* prospects (0.77±0.08 vs. 0.50, $t(46)=22.5$, $p<0.001$) and thereby earned a significant amount of money (R$ 1410±470 vs. R$ 0, $t(46)=20.7$, $p<0.001$). They accepted significantly less than half of the gambles (0.42±0.13 vs. 0.50, $t(46)=4.2$, $p<0.001$) even though as a group they did not significantly overweigh potential losses with respect to equivalent gains ($\lambda=1.04\pm0.6$, median 1.07). There were no statistically-significant behavioural differences between the participants who underwent sham tDCS and those

tested during the previous autonomic, fMRI and EEG experiments: the *EV* sign discrimination (0.78±0.07 vs.0.82±0.08, p=0.07), acceptance rate (0.41±0.14 vs. 0.44±0.08, p=0.4) and logistic regression ratio (1.07±0.70 vs. 1.33±0.68, p=0.2) were comparable.

	Sham tDCS (*n*=16)	Right anodal/left cathodal tDCS (*n*=15)	Left anodal/right cathodal tDCS (*n*=16)	ANOVA (p-value)
Age (years)	21.8±2.5	20.9±1.0	22.3±3.2	0.3
Education (years)	15.8±2.5	14.9±1.0	16.3±3.2	0.3
Beck Anxiety Inventory (BAI)	8.2±5.0	7.7±4.8	6.1±5.3	0.3
Beck Depression Inventory (BDI)	7.7±5.5	6.1±3.9	5.2±4.5	0.4
Barratt Impulsiveness Scale (BIS)	68.6±7.5	70.1±5.9	68.5±4.8	0.7
Visual analog scales (VAS)				
Alert / sleepy	5.4±2.2	5.4±2.8	6.1±2.4	0.7
Calm / restless	4.5±2.3	4.2±1.9	4.2±1.5	0.9
Strong / weak	4.6±2.2	4.6±2.3	5.4±1.9	0.4
Confused / lucid	7.5±1.8	6.8±2.3	7.3±1.8	0.6
Sharp / blunt	4.9±2.4	4.8±2.0	4.7±1.5	1
Apathetic / dynamic	7.6±2.1	7.3±1.8	6.8±1.8	0.5
Satisfied / unfulfilled	5.2±2.5	4.4±2.0	4.2±2.3	0.4
Worried / carefree	5.8±2.8	5.0±2.2	5.5±3.0	0.7
Slow minded / rapidly thinking	6.8±1.5	6.5±1.3	7.2±1.4	0.4
Tense / relaxed	6.8±2.4	5.8±2.2	5.4±2.7	0.3
Attentive / neglectful	4.1±2.1	4.6±2.2	4.4±1.7	0.8
Inept / competent	8.1±1.4	8.0±1.8	7.5±1.7	0.6
Happy / sad	4.4±2.1	3.9±2.2	3.9±2.2	0.8
Hostile / approachable	7.8±1.5	7.8±1.9	8.0±1.5	0.9

Table 4. Demographic and psychometric characteristics of the participants assigned to the three stimulation groups.

As represented in Figure 37, right anodal/left cathodal tDCS appeared to slightly reduce the RTs (3200±870 ms vs. 3780±760 ms), and the two stimulation polarities seemed to have an opposite effect on β_{pWIN} (0.4±2.1 vs. -1.6±3.2), but both effects were distant even from the uncorrected significance threshold (p>0.2). The *EV* sign discrimination, amount earned, acceptance rate and logistic regression ratios were clearly indifferent to the stimulation ($p \geq 0.6$).

Yet, a strongly-significant main effect was found for response confidence ($F(2,28.7)=6.9$, $p=0.004$, $\eta^2_p=0.18$), and survived the corrected threshold of $\alpha=0.005$. Post-hoc comparisons revealed that the participants who received right anodal/left cathodal tDCS responded more confidently than those receiving sham tDCS (0.64±0.17 vs. 0.40±0.19, $p=0.002$). An additional ANOVA modelling confidence separately for accepted and rejected gambles found no interaction between decision and confidence ($p=0.3$).

Figure 37 (following pages). Scatter plots representing the individual behavioural scores on the decisional task for participants who received sham tDCS (Sham), left cathodal /right anodal tDCS (Left) and right anodal/left cathodal tDCS (Right).

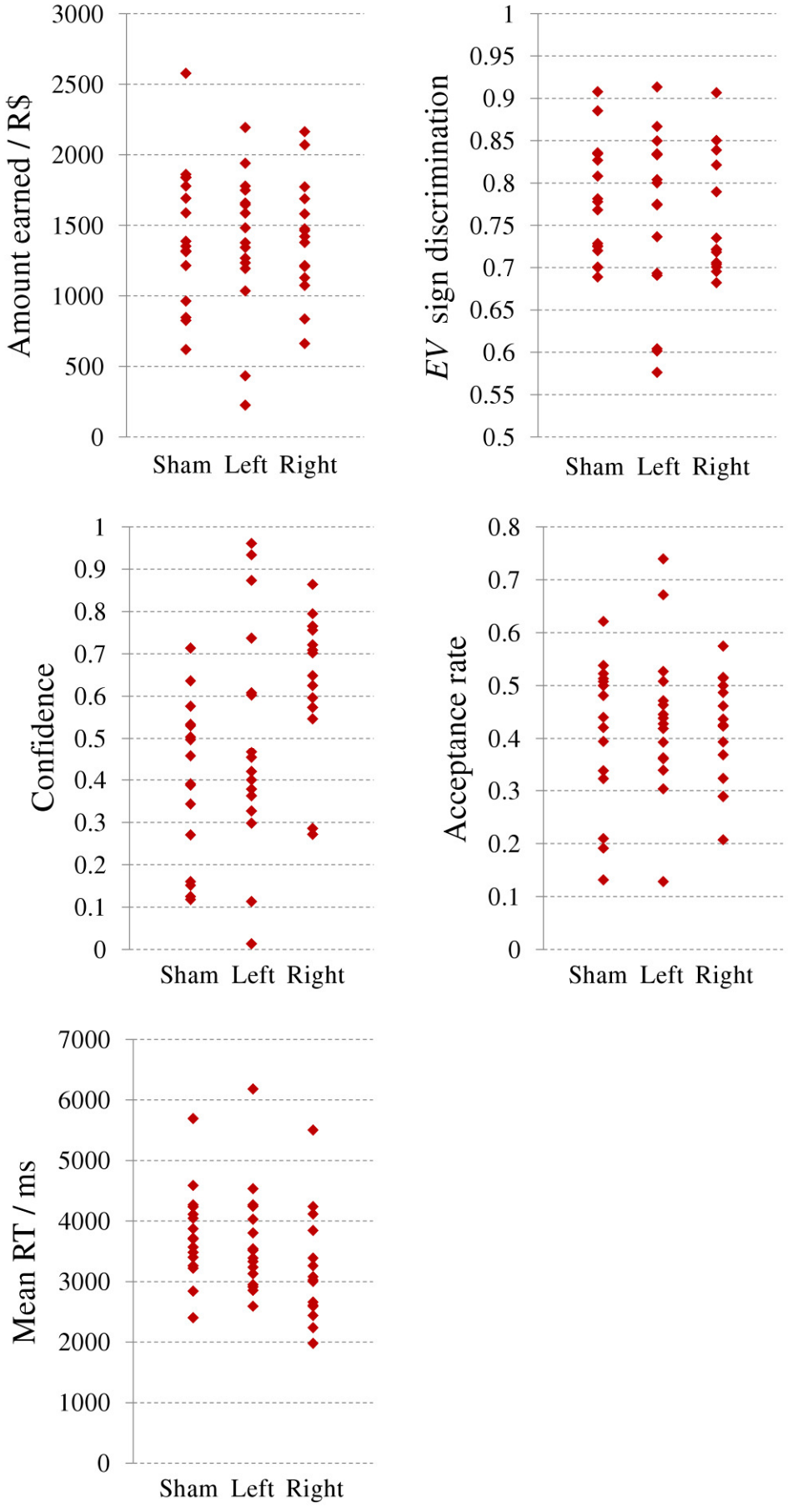
Amount earned / R$
3000
2500
2000
1500
1000
500
0
Sham Left Right
EV sign discrimination
1
0.95
0.9
0.85
0.8
0.75
0.7
0.65
0.6
0.55
0.5
Sham Left Right
Confidence
1
0.9
0.8
0.7
0.6
0.5
0.4
0.3
0.2
0.1
0
Sham Left Right
Acceptance rate
0.8
0.7
0.6
0.5
0.4
0.3
0.2
0.1
0
Sham Left Right
Mean RT / ms
7000
6000
5000
4000
3000
2000
1000
0
Sham Left Right

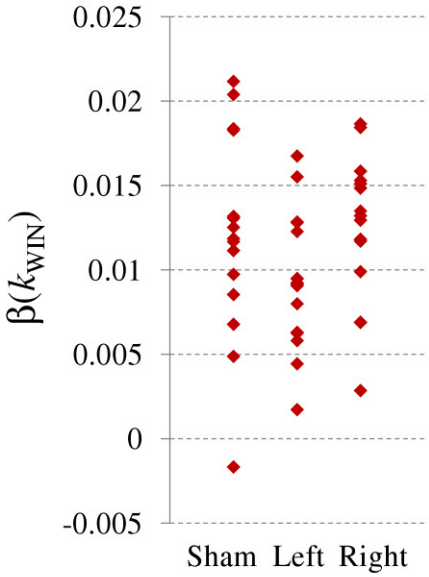
0.025
0.02
0.015
0.01
0.005
0
-0.005
β(k_WIN)
Sham Left Right

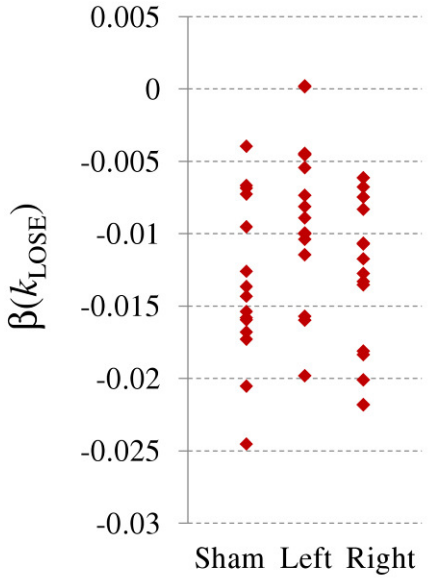
0.005
0
-0.005
-0.01
-0.015
-0.02
-0.025
-0.03
β(k_LOSE)
Sham Left Right

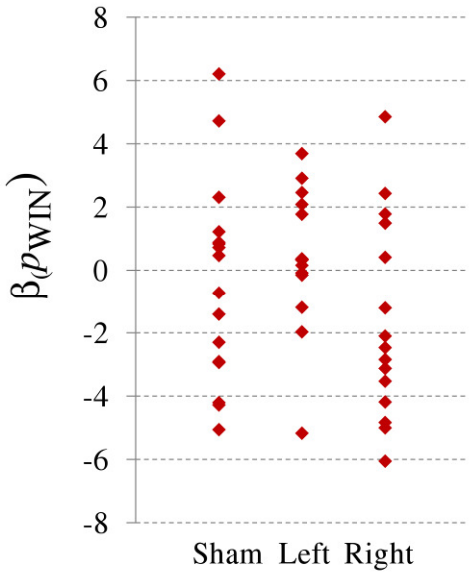
8
6
4
2
0
-2
-4
-6
-8
β(p_WIN)
Sham Left Right

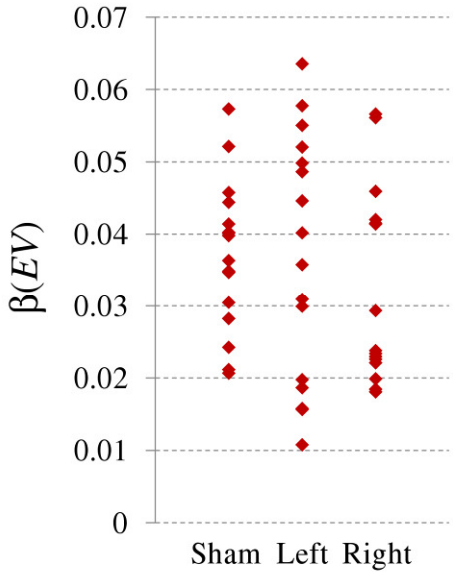
0.07
0.06
0.05
0.04
0.03
0.02
0.01
0
β(EV)
Sham Left Right

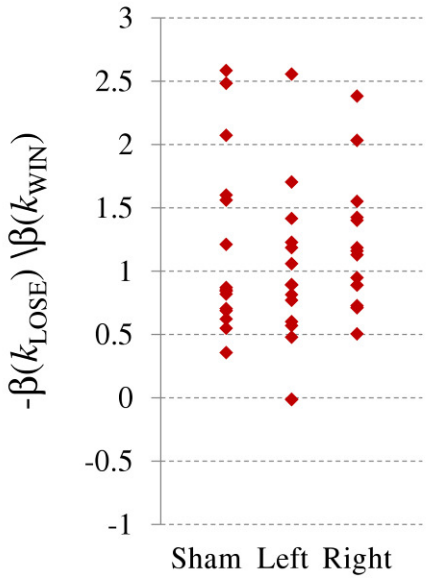
3
2.5
2
1.5
1
0.5
0
-0.5
-1
-β(k_LOSE) \β(k_WIN)
Sham Left Right

8.4 Discussion

8.4.1 Lack of effects on decisional behaviour

Insofar as risk propensity and the influence of the individual gamble parameters are concerned, this experiment delivered a negative finding: regardless of current polarity, tDCS had no effect on risky choice. One can reasonably exclude issues with the stimulation protocol, as the equipment and settings were similar or identical to those used in previous experiments with the Risk task (Fecteau et al., 2007; Boggio et al., 2010). The negative finding could simply be due to insufficient statistical power, yet this hypothesis appears unlikely considering that the overall number of participants, i.e. 47, was larger in comparison to all previous studies in this area (i.e., 27 participants in Knoch et al., 2006; 36 participants in Fecteau et al., 2007; 28 participants in Boggio et al., 2010). Also, the effects on acceptance rate and β_{LOSE}/β_{WIN} were clearly non-significant ($p>0.8$), and the virtually complete overlap observed between the groups makes it implausible that a difference could have emerged in a larger sample. Nevertheless, significantly greater statistical power could have been obtained through a within-subjects design, whereby each participant would have been tested multiple times in separate sessions, with active and sham stimulation; such design could also have accounted for baseline differences in decisional pattern across participants. Unfortunately, the study could not be conducted in that manner due to logistic considerations.

A major issue with the present experiment is that the level of risk-aversion, though not significantly different in comparison to the previous sessions, was relatively constrained: in these participants, there was no evidence of differential weighting of potential losses and gains. This may signal limited engagement in the task beyond a "cold" comparison of the weighted outcomes and therefore limited economic validity of the

results. Clearly, this issue was related to the unavailability of tangible financial reward, a limitation in common with several other lesion and neuromodulation studies in this area (Knoch et al., 2006; Fecteau et al., 2007; Boggio et al., 2010 and 2010b). It cannot on any level be ruled out that significant modulations of risk propensity could have emerged had material rewards been available, but it should be noted that the principal expected effect of DLPFC stimulation was increased risk-taking, hence the absence of a finding cannot straightforwardly be explained as a floor effect.

The present negative finding qualifies the hypothesis that activity in the DLPFC is crucial to regulate risk propensity in general. As previously reviewed, this hypothesis was predicated on the convergent findings obtained applying the IGT to lesioned patients and the Risk Task to healthy volunteers undergoing rTMS (Clark et al., 2003; Boggio et al., 2010 and 2010b). Of note, existing tDCS studies already casted some doubt on the generality of this relationship, given that inconsistent lateralization patterns were observed between healthy and elderly participants (Fecteau et al., 2007; Boggio et al,. 2010) and that marijuana users display a paradoxical effect of stimulation (Boggio et al., 2010b).

This apparent inconsistency across studies may typify the danger inherent in drawing generalist conclusions on the basis of data acquired using specific tasks, patients or stimulation techniques. It is well established in behavioural economics that risk propensity and loss aversion are not unitary constructs: for a given individual, different levels are observed in the context of specific real-life situations and experimental tasks (e.g., Weber et al., 2002; Botella et al., 2008). In neuroeconomics, behavioural phenomena such as risk aversion should then be considered as emergent properties rather than intrinsic constants, as they arise from complex neural interactions that can be, to some extent, contingent to specific situations and paradigms. For example, there is robust neuroimaging evidence indicating that the DLPFC, OFC and ACC are differently engaged during decision-making under risk and under ambiguity (Krain et al., 2006). Even within the

framework of risky decision-making there is no guarantee that the value representation processes will share identical anatomical substrates whenever the "editing" process is different, e.g. comparing choice between two $EV \neq 0$ options or choice between a conservative $EV = 0$ and risky $EV \neq 0$ option (e.g., Kahnt et al., 2010).

The finding that a tDCS protocol previously observed to modulate risk propensity in the Risk task has no effect on the present mixed-gambling paradigm may therefore challenge the hypothesis of a direct and general anatomical relationship between the level of DLPFC activity and the regulation of risk propensity.

8.4.2 Modulation of response confidence

On the other hand, the results of the present experiment suggest a strong link between DLPFC activity and confidence during risky decision-making. Though this result was not initially anticipated, a-posteriori review of the literature revealed a number of studies in which such association had been established. In an early fMRI investigation, Henson et al. (2000) requested healthy participants to express "old" or "new" judgements alongside confidence ratings during a word recognition task, and reported that BOLD responses in the right DLPFC correlated positively with response confidence following a pattern that was decoupled from the recognition judgements themselves. In a study on young habitual gamblers, Camchong et al. (2007) used magnetoencephalography to investigate the neural correlates of confidence in responding to trivia questions, and reported a relatively early (i.e., 100 ms post-stimulus) neuromagnetic response, originating from the right DLPFC, which was enhanced for trials that had attracted a highly confident response. Additionally, Viviani et al. (2010) found that the perfusion level in the right DLFPC was enhanced when participants were actively exerting cognitive control to avoid negative emotional material and shift their focus towards positive thoughts.

Of note, pathological gamblers exhibit enhanced BOLD responses in the right DLPFC to visual gambling cues with respect to controls, and this effect has been interpreted as a reflection of the sense of high confidence and illusion of control that is normally associated with the condition (e.g., Delfabbro, 2004; Crockford et al., 2005).

The present experiment extends the existing literature by establishing a causative relationship between DLPFC activity and confidence: enhancing activity in the right DLPFC, in good agreement with the results reviewed above, exaggerated confidence in decision-making without any accompanying change in performance. Yet there are several issues that limit the interpretability of this finding at the present stage. First, unipolar stimulation was not applied, so one cannot ultimately ascertain whether it was increased excitability in the right hemisphere, reduced excitability in the left or a combination of both which led to the observed behavioural effect. There is also the issue that the observed confidence boost could be mediated by a mood shift, rather than a more specific effect restricted to the feeling of confidence in one's decisions. Ultimately, this matter can only be settled by repeating the experiment including post-stimulation mood questionnaires, which were not administered as they were not relevant to the initial hypothesis. Further, as there was no difference in *EV*-sign discrimination, earnings or RTs, a change in overall cognitive performance appears highly unlikely. The simplest interpretation is that tDCS enhanced the subjective perception of the quality of one's decisions in a way that was decoupled from the underlying evaluation mechanisms; this phenomenon shows a remarkable similarity to the sense of optimism and control that pervades pathological gamblers, who are deluded that, even in the face of heavy losses, they will be eventually able to recoup all money (Delfabbro, 2004).

On the other hand, the observed confidence effect could, in principle, be related to metacognition, e.g. to the way the participants perceived their own actions, and specifically to their ability to appraise the quality of their decisions (e.g., Akama and Yamauchi, 2004;

Brevers et al., 2012). Indeed, as discussed in Chapter 2, in the participants to the autonomic, EEG and fMRI experiments, who did not undergo neuromodulation, greater subjective confidence was associated with better discrimination of positive- vs. negative-*EV* gambles. Yet in this experiment there is no evidence suggesting that increased confidence reflected improved insight, because the effect was completely decoupled from all other aspects of decisional behaviour: though participants receiving right anodal tDCS were on average more confident, they were not faster, nor better at discriminating advantageous from disadvantageous gambles, nor differently risk averse with respect to the control group. Hence the most parsimonious account for the present finding is that it "simply" represented a general subjective bias on the confidence about one's decisions. Indeed, such interpretation seems more plausible also in anatomical terms: while, as described above, substantial evidence is available linking right prefrontal activity to confidence, recent meta-analyses and conceptual reviews coherently indicate that metacognitive awareness is subserved by more medial regions, particularly the ventromedial prefrontal and the cingulate cortex, collectively referred to as the "cortical midline system" (Northoff et al., 2006; Schmitz and Johnson, 2007; David et al., 2012), which are not expected to be significantly affected by current applied with the chosen electrode locations.

8.4.3 Considerations on anatomical specificity

One needs to consider the issues associated with the anatomical specificity of neuromodulation, particularly if applied by direct current rather than magnetically. Simulation studies with finite element models of the conductor compartments in the head have demonstrated that even relatively simple tDCS electrode patterns can produce highly complex current distributions that depend on individual anatomical features; of note, large

current density may, in certain circumstances, also be elicited in regions that are not immediately underlying the electrodes (Sadleir et al, 2010). Yet, some reassurance is provided by the convergent results obtained with functional MRI and positron-emission tomography, indicating that tDCS significantly and selectively modulates the excitability of the cortex directly underlying the electrodes in healthy participants (Jang et al., 2009; Antal et al., 2011; Paquette et al., 2011).

There are also further issues that are unrelated to the physics of the stimulation process, and instead have to do with the properties of the brain as a dynamical system. First, the lateral PFC, mesial PFC, OFC and basal ganglia are strongly anatomically interconnected and heavily functionally integrated (e.g., Barbas et al., 2000; Ongür and Price, 2000): hence, modulating the excitability in one region is likely to influence the baseline activity also in the others, potentially generating complex, unanticipated shifts in information processing architecture. Second, all these areas are strongly interconnected with their contralateral homologues by means of transcallosal connections, which are typically inhibitory: hence, even when one hemisphere alone is stimulated, it is difficult to assign an observed behavioural effect to an isolated area (Voineskos et al., 2010). Of note, these issues equally affect tDCS, TMS and lesion mapping, implying that, unless robust negative evidence is available to establish double-dissociations among areas, it is difficult to confidently assign a behavioural effect to a given region purely on the basis of lesion or stimulation site.

8.4.4 Summary

In conclusion, stimulating the DLPFC with direct current of either polarity did not alter risk propensity or value representation in the context of risky prospects. This finding adds to existing studies with the Iowa Gambling Task and Risk Task demonstrating an

inconstant relationship between right DLPFC function and risk taking, and motivates further inquiry into the validity of the hypothesis of a direct, general relationship between the level of DLPFC activity and risk propensity. An unanticipated finding was that enhancing right with respect to left DLPFC excitability boosted confidence in the decisions, without any accompanying change in task performance. The effect bears a remarkable similarity to the biases of optimism and delusion of control observed in pathological gamblers and warrants further investigation.

9. General discussion and further research

9.1 Implications for models of value computation

9.1.1 Differential representation of losses and gains

As discussed in the recent review by Levin and co-workers (2012), investigating the differential representation of losses and gains remains an important topic of neuroeconomic research. This effort is motivated by behavioural observations of framing effects (e.g., Kahneman and Tversy, 2000) and other dissociations in the processing of gains and losses (Weller et al., 2009; Weller et al., 2011), and more generally extends previous attempts to identify distinct neural circuits supporting approach and avoidance behaviours (e.g., Craig, 2009). On one extreme, it could be hypothesized that gains and losses are represented through opposite patterns of activity in overlapping regions and networks. On the other, they could represent fundamentally different cognitive variables encoded in separate neuronal systems in competition for determining the outcome of a decision. Levin et al. (2012) largely endorse the latter view, postulating that the insula and amygdala generate specific signals in presence of potential losses, which trigger and support detailed evaluation taking place primarily in the medial prefrontal cortex (Figure 38a). Through comparison of recent neuroimaging experiments, they conclude that potential gains and losses are associated with dissociable anatomical representations, contingent on the availability of feedback and visible only when the haemodynamic response is modelled at stimulus onset, before a decision is enacted.

The data from the present experiments contribute to this debate at three levels. First, univariate fMRI demonstrated that losses were represented in a widespread pattern of

negative correlations, encompassing the lateral as well as medial prefrontal cortex of both hemispheres; by contrast, the direct expression of potential gains as positive correlations was constrained to a small number of voxels. The findings echo those of Tom et al. (2007; Figure 38b), but the mismatch between gain and loss representation here was more evident, which could be due to deeper encoding prompted by the presence of variable outcome probability or related to the absence of material rewards. On the other hand, no activation of the insula and amygdala was observed to the magnitude of losses. This clashes with the model put forward by Levin et al. (2012) in that the representation of losses here appeared to be founded not on the insula and amygdala, but on a distributed neocortical representation. In fact, paradoxically amygdalar activation and weak autonomic responses were observed to potential gains, pointing to recent work challenging the view that this region is more closely related to processing aversive than hedonic stimuli (Mahler and Berridge, 2011).

On a general level the present findings reinforce the argument of a differential anatomical localization of loss and gain representation. However, this was not apparent as two clearly separable circuits: rather, gains, alongside outcome probability, were not strongly encoded in neocortical activity at all as individual parameters, but only indirectly as determinants of value and risk-advantageousness. On the other hand, large potential losses caused extensive deactivation throughout the prefrontal and posterior parietal cortex. Though the representation of losses was dominant in the context of the present task, the observed negative correlations are reconcilable with the ideas of "gain-brain" circuits described in the previous chapters, but not of insula- or amygdala-centric encoding of losses and risk (Figure 38c).

Second, network analysis reinforced the point of a fundamental difference in the representation of losses and gains, again providing no evidence for two segregable anatomical circuits. Rather, the brain appeared to encode only potential losses in large-

scale effective connectivity, ignoring gains: a small subset of the network encoding expected value tracked potential losses only with no counterpart for gains. Gains must be eventually encoded at some level, otherwise value determination would be impossible, but the present result substantiates the view that while losses on their own are assigned a robust distributed representation, gains are processed more marginally. This again qualifies the work of Levin et al. (2012), indicating that in presence of an elementary risky prospect the brain's resources are allocated predominantly to representing potential loss through a neocortical network not founded on the amygdala or insula, but on prefrontal hubs (Figure 38c). As previously discussed for the striatum, one should refrain from making generalist inferences from the present findings, as multiple representations of losses and risks are likely to be available and engaged in a highly situation-dependent manner (Platt and Padoa-Schioppa, 2009). The amygdala has an established role in representing aversive stimuli and negative emotion, and is fundamental to support effective social interaction (e.g., Adolphs et al., 1994; Garrido et al., 2012), so it appears plausible that an involvement in the representation of risk and loss could have been observed in the context of a more emotionally-engaging task.

Third, EEG also revealed a clear dissociation between the processing of gains and losses: though the latency range in which significant effects were found overlapped, the former were represented in long-latency event-related potentials, whereas the latter elicited a modulation of alpha-band activity. Yet, these findings are different from the functional MRI results, and suggest that gains are represented in the activity of premotor regions whereas losses are more closely coupled to ancestral mechanisms of modulation of general brain state, which could, speculatively, also involve the amygdala and insula (e.g., Critchley, 2002; Craig, 2009). Due to limited spatial resolution, it was not possible to confirm the anatomical localization of the underlying neuroelectric sources, motivating further work using a high-density system. The apparent discrepancy may be down to the

different sensitivity pattern of EEG and fMRI, and will need to be resolved in future experiments where the two signals are recorded conjointly and explicitly correlated.

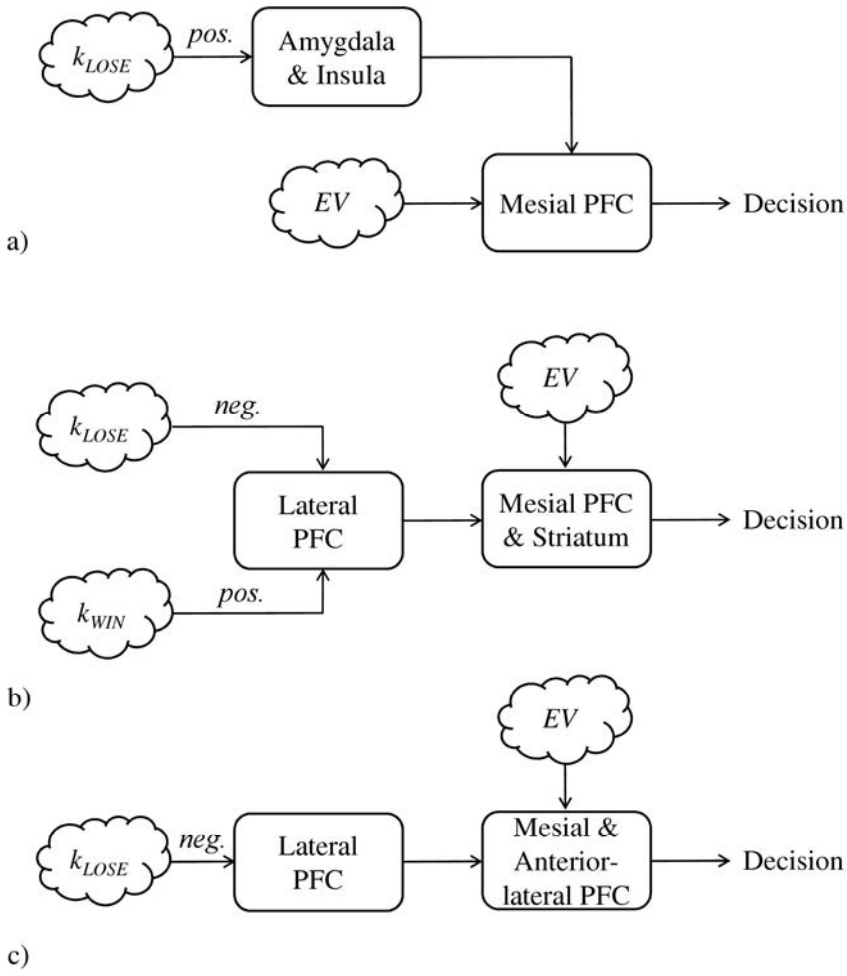

Figure 38. Models of the representation of losses, gains and value. a) Amygdala-insula centric representation of losses with value representation in the mesial prefrontal cortex (Levin et al., 2012). b) "Gain-brain" representation of potential gains and losses in opposite correlations direction across the lateral prefrontal and parietal cortex, with value integration in the mesial prefrontal cortex and striatum (Tom et al., 2007). c) Predominant representation of losses in negative correlations across the lateral prefrontal cortex, with value integration in the mesial and anterior-lateral prefrontal cortex (present work).

In summary, the present fMRI results are at odds with the hypothesis that losses are focally coded in the activity of the amygdala and insula, or that two parallel and separable anatomical circuits support the encoding of gains and losses as individual parameters. Rather, they suggest that in the presence of a risky prospect, the representation of losses is dominant, involving direct correlations and effective connectivity across extended cortical areas, whereas the direct representation of gains is much more constrained. The EEG results, on the other hand, may be more closely reconcilable with the view of a distinct representation of gains, founded on premotor activity, and losses, founded on more ancestral systems exerting a modulation on central arousal state. The generalizability of these findings to more strongly valenced and realistic situations will need to be explored in future work.

9.1.2 Continuous vs. dichotomous value representation for risky prospects

In a recent review, Vlaev and co-workers (2011) systematically surveyed evidence for three classes of cognitive models of value representation: those that imply that the absolute value of each option is analogically computed and explicitly represented in neural activity (referred to as type I), those that imply that value is computed and represented only in a differential fashion, i.e. for an option with respect to the other available ones (type II), and those that imply that value is not computed at all as a continuous variable, only in an ordinal way among the options available within a given framework (type III). The first hypothesis is the most amenable one from the perspective of classical microeconomics and utility theory, since it preserves the fundamental axiom of the existence of a common internal value scale in such way, for example, that irrelevant alternatives do not alter the evaluation of a given option. The third is the most distant one from current economic models, as it collapses the concept of utility altogether into a binary comparison, making it

challenging to represent the stability of choices in presence of variable options and to account for behavioural biases through non-linear weighing of continuous utility. In their seminal review of neurophysiological and imaging studies, Platt and Padoa-Schioppa (2009) ponder that value computation in the brain is implemented through multiple coding systems engaged in a situation-dependent manner, some based on cardinal and some on ordinal representations of value.

Here, the average amount at stake in each gamble varied considerably (10-200 £ or €), providing some level of decoupling between expected value and unitless risk-advantageousness (ranging from -1 to +1). Though the latter parameter is not discrete, it collapses expected value into a fixed range, rescaling it independently of the amounts. Behaviourally, choices were more closely predicted by risk-advantageousness than expected value: though this finding cannot distinguish between a purely dichotomous representation and the action of a rescaling mechanism, it did not indicate an effect of absolute value and could therefore be parsimoniously explained through type II or III models. Accordingly, gamble acceptance probability rose very sharply in the vicinity of the EV=0 point, having a near-zero slope elsewhere. The neural responses recorded through univariate fMRI and EEG also provided no evidence that absolute value was coded preferentially with respect to rescaled advantageousness or binary preference. In the network-analysis experiment, a narrower range of economic variables was considered for computational reasons, and unitless risk-advantageousness was not evaluated. However, a dichotomous representation of expected value was explicitly tested and large scale effective connectivity was found to be equivalently predicted by continuous value and its sign function.

In summary, while the present experiments cannot by any means refute a type I representation, they did not provide any evidence that the absolute value of risky prospects is coded preferentially with respect to rescaled or dichotomous advantageousness. A type

III representation would be a particularly parsimonious account for the present findings, and could represent an efficient heuristic supporting rapid evaluation of risky prospects presenting a stereotyped choice between a zero-value and a valenced option. Indeed, one could argue that this "fruit fly" paradigm is inherently suboptimal because it does not explicitly call upon an absolute representation of value to support performance, only on the ability to compare two options in a highly simplified framework. The present neuroimaging findings may, speculatively, be viewed as indicating that the brain processed value dichotomously or pseudo-dichotomously, while additionally devoting extensive resources to the direct representation of potential losses. This could represent a particularly efficient way of implementing behavioural biases, such loss and risk aversion, just by "weighting" the raw parameters though a differential neocortical representation without requiring a more resource-intensive absolute representation of abstract value per-se (Figure 38c). The validity of such hypothesis will need to be verified in future experiments presenting more realistic and strongly-valenced decisional scenarios.

9.1.3 Role of the striatum and anterior-lateral prefrontal cortex

Neuroimaging and neurophysiological work extending Schultz and co-workers's (1993) initial discoveries has amply demonstrated that dopaminergic signalling, particularly involving the striatum, plays a fundamental role in encoding reward and associated prediction error across many different scenarios (e.g., Fiorillo et al., 2003; Ramnani et al., 2004; Knutson and Cooper, 2005; Pessiglione et al., 2006). It is therefore unsurprising that the striatum has received substantial attention also as a candidate substrate of value computation, driving choice or avoidance of risky prospects even when all information is explicitly given (e.g., Redgrave et al., 1999). The finding of associations between striatal activity and expected value has in instances been interpreted as evidence

for such role, though correlations can be incidental and driven by reward expectation or other secondary processes, i.e. not necessarily represent primary value computation taking place locally (Tom et al., 2007; Hunt et al., 2008; Tobler et al., 2009).

Here, no significant associations between expected value or risk-advantageousness and striatal haemodynamic responses were observed, possibly due to the absence of tangible financial endowment and feedback or to task features prompting deeper integrative value computation rather than straightforward comparison of potential losses and gains (Tom et al., 2007). Along the same line, network analysis revealed a florid pattern of neocortical effective connectivity, involving hubs in the mesial and lateral prefrontal cortex, but very low connectivity and centrality for the striatum and the other subcortical structures. Further indication of negligible involvement of the basal ganglia was also given by normal task performance in patients with Parkinson's disease or Huntington's disease.

It would be premature to draw a generalist conclusion that the striatum is not involved at all in the determination of the value of risky prospects, not least because of established evidence of its key role in action-selection in naturalistic contexts (Redgrave et al., 1999) and of situation-dependent engagement, for example contingent on time-pressure (Jones et al., 2011). Yet, the results of the present experiments strongly qualify its role in value determination and option selection in an elementary risky decisional situation.

On the other hand, network analysis revealed that the anterior-lateral prefrontal cortex bilaterally harboured densely-interconnected value computation hubs. This result is of profound paradigmatic significance as direct associations with haemodynamic response amplitude were clearly absent, and the key role of this region emerged only through more abstract topological analysis of the large-scale effective connectivity pattern.

Until recently the anterior-lateral prefrontal cortex had received comparatively limited attention in neuroeconomics literature, as it has seldom displayed significant task

effects upon univariate analysis, but Rushworth and co-workers (2011) have discussed the potential relevance of this region to decision-making processes in a recent review. First, in relation to counterfactual thinking, that is encoding the features of choice options that are not selected. Particularly, Boorman et al. (2009 and 2011) have demonstrated a positive association between activity in this area and the reward probability as well as "reward prediction error" calculated with respect to the unchosen option. Second, in relation to switching between behaviours. In an early study, Kochelin et al. (1999) demonstrated that large anterior-lateral prefrontal responses in a gambling task predicted changing choice during subsequent trials. A later investigation by Daw et al. (2006) concluded that activity in this region during a foraging task was associated with enacting explorative rather than exploitative behaviour.

The present findings extend the view put forward by Rushworth et al. (2011), demonstrating that the anterior-lateral prefrontal cortex is fundamentally involved also in determining the value of elementary risky prospects. Here, no direct correlations with activity were observed, fuelling the speculative hypothesis that this region may act more as a communicative hub than a calculation centre. It is plausible that it may take up different roles contingent on the type of decisional task. The reported associations with counterfactual thinking and behaviour switching certainly imply that it has access to abstract value representations. One could therefore speculate that the anterior-lateral prefrontal cortex supports value computation in general through its centrality in the large-scale network, and within the context of this broad role also generates specific signals related to counterfactual thinking and behaviour switching in relevant contexts. From the present data, dysfunction of this area would be predicted to have catastrophic effects on value determination, hence this hypothesis should be tested in future lesion mapping and neuromodulation experiments. On a more general level, future neuroeconomics experiments should explicitly model large-scale network properties in addition to

univariate associations, to ensure that key anatomical substrates are not neglected due to a simplistic modelling approach.

9.1.4 Role of the anterior insula

As discussed above, influential views confer to the amygdala and anterior insula a crucial role generating arousal signals in presence of looming losses and uncertainty (Levin et al., 2012). While the present data do not support this view, at least insofar as the individual evaluation of elementary risky prospects in the framework of the present task is concerned, a strong association between anterior insula activity and outcome uncertainty was found: gambles characterized by near-certain loss or gain outcomes elicited greater activation in comparison to those bearing near-even outcome probability. The effect was decoupled from all other economic variables, i.e. indifferent to the magnitude of gains and losses and to expected value. Notably, it did not emerge at the time of gamble presentation but at a delayed phase, roughly corresponding to the time of response selection. A similar finding was reported in a previous investigation based on an analogous paradigm with discrete gamble types (Jones et al., 2011). These results prompt re-evaluation of the view put forward by Levin et al. (2012), in that anterior insula activity may be related to outcome uncertainty in a way that is not intrinsically coupled to the representation of losses.

In light of previous evidence of differential insula responses in early and late phases (Preuschoff et al., 2008), further experiments are motivated using a jittered design to extract the full haemodynamic response. To some extent, insula-centric models of loss representation (Levin et al., 2012) and the present findings could be reconcilable accounting for a different role at the time of stimulus delivery and outcome presentation or imagination; it is also not implausible that this region may take up different roles altogether

depending on whether or not the experimental task involves ambiguity, feedback and tangible rather than "virtual" rewards and risks.

9.2 Limitations and topics for further research

9.2.1 Economic endowment and ecological validity

One central limitation of all present experiments is that real financial reward could not be offered, due to ethical and legislative limitations, and that participants were therefore playing with virtual money, only imagining that it were real currency. An extreme view is that this would render the experiments inherently invalid, as there is no extrinsic motivation to decide in a particular way rather than another (e.g., Wilkinson, 2008). Yet, this limitation is relatively common across decision-making studies, and even when financial rewards are offered they are generally minimal amounts, practically irrelevant to an individual's socioeconomic status. Psychologists and cognitive scientists generally take a more lenient view than orthodox economists on the problem, positing that forms of "virtual endowment", coupled with feedback and minimal rewards, such as small sums or pleasant stimuli, or punishments, such as electric shocks, are sufficient to probe the neural dynamics underlying real-world decisional behaviour.

The experiments of Gneezy and Rustichini (2000) were a milestone, demonstrating that small financial endowments have paradoxical effects on task performance: with respect to a situation of zero compensation, introducing payments initially leads to a sharp drop in performance, which is then gradually recuperated for large rewards. This effect was conceptualized in terms of a balance between "intrinsic" and "extrinsic" motivation, whereby the fact that one is performing a task for money immediately eliminates the intrinsic component, while the extrinsic one needs substantial financial endowments to

compensate. From this perspective, it would not appear unreasonable to perform experiments relying purely on virtual currency.

Yet there are two crucial issues to consider. First, though task performance (intended, for example, as discrimination accuracy between positive- and negative-value gambles or speed on a fatiguing task) may correlate non-monotonically with endowment magnitude, this relationship need not extend to the expression of behavioural biases such as risk and loss aversion. Though participants were generally risk and loss averse in these experiments, the magnitude of such biases was rather small with respect to real-world economic behaviour whereby losses are weighted approximately twice as much as gains (e.g., Kahneman, 2003; Wilkinson, 2008). Second, there are no experimental data mapping the effect of tangible financial rewards, i.e. of extrinsic vs. intrinsic motivation, onto neuronal activity during a given task. As previously discussed, one may expect that in the context of the present task, introducing and gradually increasing the amount of financial rewards and risks would lead to larger and larger dopaminergic anticipatory responses, even in the absence of declarative outcome feedback on each gamble. Yet it is difficult to predict what effects tangible financial involvement would have on neocortical activity in general. One could posit that it should have none, if the underlying value determination mechanisms do not change. But that appears an unlikely state of affairs, if only because of the profound modulatory effect that dopaminergic signals have on prefrontal activity.

One could take the extreme view that the present experiments are completely invalid and that the participants were simply approximating a mathematical computation and comparison in a cold fashion, e.g. that they processed the gambles without attaching any special valence status to the economic parameters. Indeed, one could certainly discriminate positive- and negative-value gambles in the present task without attaching any subjective feeling to value, treating the task variables purely as abstract, subjectively irrelevant mathematical entities. Yet, this hypothesis can be refuted to a large extent by

making reference to the behavioural results, which demonstrated significant subjective biases that would not in any way be predicted by task performance based purely on abstract computation with subjectively-irrelevant variables. Further confidence can be gained from the EEG and fMRI data, i.e. there would be no motivation for "losses" and "gains" to be associated with radically different neurophysiological representations and likewise there would not be any reason for the ventromedial prefrontal cortex to track the value assigned to a subjectively-irrelevant abstract mathematical variable.

There remains, however, the question of what activations would be elicited performing equivalent analog mathematical operations in the context of variables devoid of economic significance, and of the way in which large financial rewards would influence the neural representation of the economic parameters. Further research explicitly addressing these questions is strongly and urgently motivated also to clarify to what extent the results obtained in other studies offering minimal or no financial rewards have general validity. In light of the findings of Gneezy and Rustichini (2000), any such experiment should explicitly contrast purely virtual endowment, small and large financial rewards.

On a broader level, there is the question of the ecological validity of studying decision-making through financial metaphors: to what extent can the results be generalized beyond the monetary domain, and to what extent can evolutionary arguments be used to interpret the observed phenomena? These questions are particularly pressing given that in the present work, like in many other neuropsychological accounts of decision-making (e.g. Levin et al., 2012), frequent references are made to ancestral animal behaviours when hypothesizing explanations for given phenomena like the specific relationship between losses and central arousal, increased visual cortex activity for situations promoting risky choice etc. On one hand, one could argue that human decision-making, like many other aspects of behaviour, is necessarily founded on evolutionary legacies. On the other, one could argue that it is implausible that in a task like the present one, wherein the key value-

integrating hubs were found in very evolutionarily-recent portions of the prefrontal neocortex, references to ethology can have anything beyond a face validity: though the lizard springing out of hiding and the entrepreneuse indebting her company both take effective risky decisions, the latter does so though the action a complex prefrontal associative network, whereas the former has comparatively very limited neocortical resources.

A recent review by Kalenscher and van Wingerden (2011) explicitly addresses the issue of the relationship between animal and human decision-making behaviours, and particularly of the extent to which parallels can be drawn between microeconomics and ethology. Remarkable similarities are found between discounted utility theory and rate maximization, and many deviations from purely utilitarian behaviour, such as risk aversion, framing effects, inequity aversion and instability of preferences that characterize human behaviour have also been identified in animals of various phylogenetic standing. Yet fundamental questions remain regarding the extent to which correspondences between human and animal behaviour may truly represent overlapping neuronal mechanisms. The quest to clarify this matter is likely to be complicated by the fact that, as reviewed for example by Platt and Padoa-Schioppa (2009), multiple concurrent representations of value and risk are available in the brain at a given time and the exact neural underpinnings of given behaviours are likely to be, to some extent, contingent on specific situations. At this stage, it could be concluded that references to evolutionary-adapted behaviours are likely to be to some extent valid given that innate decisional mechanisms are certainly present in our species and were in close our ancestors, but the generalizability of human behavioural and neural findings to other species further away in the phylogenetic tree needs to be confirmed and will likely only be very partial. Attaining a detailed understanding of these matters will plausibly require more than a decade, substantial neurophysiological data acquisition work and advances in computational modelling.

9.2.2 Framing effects and inter-individual differences

A subtler point is that the present paradigm probed the evaluation of risky prospects with respect to a single reference point, representing zero value, which has a special standing as it sits between the concave and convex regimes of the value function. According to prospect theory, a certain difference in value is attributed considerably different subjective valence depending on whether it is presented in the domain of losses or gains (Kahneman and Tversky, 1979; Kahneman and Tversky, 1984; Kahneman and Tversky, 2000; Wilkinson, 2008). Hence one limitation of the present experiments is that they do not directly inform models of value computation and choice selection when the alternative to the risky option has non-zero expected value. Further research is needed into this aspect, for example extending the present paradigm through three conditions, whereby the riskless option has a fixed negative, neutral or positive value. Purely dichotomous, comparative value representation would predict equivalent neural responses (Vlaev et al., 2011), but prospect theory implies that value differences should be relatively amplified in the negative domain and compressed in the positive domain.

There is also the issue that in real life decisions are seldom taken between a single risk-free option and a single risky one. The present "fruit fly" paradigm may therefore have limited ecological validity in this regard, especially as it cannot ultimately provide conclusive evidence to distinguish between absolute, relative and dichotomous representations of gain, given that the decisional scenario is, per-se, collapsing the decisional process to a dichotomic comparison. This limitation should be overcome in a further experiment where multiple independent risky options are directly compared. Simultaneous presentation of more than one gamble would raise challenges related to perceptual overload and overlap of parametric representations, but a suitable paradigm could be based on delivering in slow sequence multiple prospects, separately modelling the

haemodynamic or neuroelectric response to each, and requesting participants to subsequently choose one.

9.2.3 Anatomical and neurochemical specificity

The behavioural experiments performed with neurological patients and neuromodulation had inherent limitations, in that neither the accumulation of degenerative pathology nor the passing of direct-current have the well-defined effect of completely and selectively excluding regional activity, and in that the anatomical coverage of the network involved in value representation was only partial. As previously discussed, further work with sub-acute focal vascular lesion patients is motivated to confirm the inferences drawn with both univariate and network-analysis fMRI. The key role of the mesial prefrontal cortex in value computation maps closely to existing lesion studies (Bechara et al., 1999; Manes et al., 2002; Clark et al., 2008), however the present results generate the fresh prediction that damage to the anterior lateral prefrontal cortex should also have a profound effect on the ability to represent value, which should be more marked in comparison to that of lesioning more posterior dorsal and ventral portions of the prefrontal cortex (Manes et al., 2002; Clark et al., 2003). Focal damage to the insula and amygdala should also have by comparison a more constrained impact (Weller et al., 2009; De Martino et al., 2010). Studies on healthy participants undergoing neuromodulation may also be relevant insofar as multiple stimulation locations or electrode configurations are comprehensively explored to demonstrate anatomical specificity.

The investigational techniques employed in the present experiments do not provide any information at the neurochemical level. The neocortical network revealed in the present experiments necessarily relies predominantly on glutamatergic synapses for information interchange, but it is likely that other systems may also exert important

modulatory actions. While no differential representation of the risky prospects was observed in the striatum, the profound effect of dopaminergic signalling on prefrontal cortex excitability is unlikely to be completely irrelevant to decisional behaviour in the context of the present task. The effect of pharmacological manipulation with selective dopamine antagonists and agonists should therefore be investigated (Wichers et al., 2008; St Onge and Floresco, 2009; Rogers, 2011). On another line, the observed relationship between potential loss, average amount magnitude and alpha-band neuroelectrical activity could reflect the modulatory action of cholinergic signals from the basal forebrain; such hypothesis would be worthwhile of further investigation through a targeted pharmacological study (e.g., Chudasama and Robbin, 2004). Lastly, the lack of differential autonomic responses suggests that feedback from peripheral feeling states is irrelevant to the evaluation of risky prospects, at least insofar as the present task format is concerned. This generates the prediction that autonomic blockade should have no effect on decisional behaviour, which could be verified through administration of beta-adrenoceptor blockers (Rogers et al., 2004). Considerable additional insight would be gleaned combining targeted pharmacological manipulations with functional MRI, enabling explicit relationships to be established between regional and network activity and specific aspects of neurochemical activity (Windischberger et al., 2010; McKie et al., 2011). As typified in a recent study of reward anticipation, such approach could also be fruitfully applied to comparing carriers of different polymorphisms of relevant receptors (Schmack et al., 2008).

Extending the present results through detailed behavioural, neuroimaging and neurochemical investigation would pave the way for the study of altered risky decision-making in specific patient populations, where the deficits are likely to result from complex combinations of anatomical damage and neurotransmitter imbalance.

9.3 Concluding remarks

Summing up, the present thesis contributes to neuroeconomics knowledge providing a multimodal investigation of the processing of elementary gambles which informs current models of risky decision-making at a variety of levels, particularly indicating that:

i) the influence of peripherally-expressed somatic markers on decision-making in the context of elementary gambles appears to be negligible;

ii) there is evidence for a "two-tier" neuroelectric representation of the economic parameters characterizing the risky-gambles, whereby potential losses and amount magnitudes principally influence central arousal indexed by alpha-band activity, whereas the representation potential gains, value and risk-advantageousness is linked to slow-wave potentials originating from the premotor circuits;

iii) potential losses are overwhelmingly more represented than potential gains or outcome probabilities as individual parameters, and associated with widespread relative deactivation of the prefrontal and parietal cortex; as also confirmed by graph-based analysis of effective connectivity, the brain invests substantial resources in the direct evaluation of losses per-se, and in the context of the present task this mechanism of representation appears to be decoupled from the activity of the insula and amygdala, which therefore may not be indispensable for the representation of uncertain losses and risks;

iv) expected value is computed and represented across a rich neocortical network of large-scale effective connectivity, which is founded on densely-interconnected hubs situated in the mesial prefrontal cortex and in the anterior-lateral pre-frontal cortex; the striatum and associated signals appear to have a negligible role in supporting

risky-decision making and the associated behavioural biases in a stereotyped situation enforcing choice between a risky options and a risk-less one, in the absence of tangible endowment or declarative feedback;

v) there appears to be no straightforward relationship between the level of activity in the lateral prefrontal cortex and risk propensity in the context of individual mixed gambles, however there is a strong association with the perceived quality of one's decisions.

The present results lay the groundwork for future research in this area, particularly aiming to:

i) determine the impact of tangible potential financial rewards and risks, comparing behavioural, autonomic, neuroelectrical and haemodynamic responses for virtual endowment, small and large amounts; determine the correlates of individual levels of loss aversion in presence of real financial endowment;

ii) determine the effect of framing the mixed-gambles in respect to positive or negative value, rather than zero-value risk-less options;

iii) explore the role of the anterior lateral prefrontal cortex on value determination, through lesion mapping and neuromodulation;

iv) explore whether the identified neuroelectric and haemodynamic markers of the representation of risky prospects reveal alterations in neurological and psychiatric patients with known decisional dysfunctions.

References

Abdellaoui M, Bleichrodt H, Paraschiv C (2007) Loss Aversion Under Prospect Theory: A Parameter-Free Measurement. J Manag. Sci. 53:1659-1674

Akama K, Yamauchi H (2004) Task performance and metacognitive experiences in problem-solving. Psychol Rep. 94:715-22

Alexander GE, Delong MR, Strick PL (1986) Parallel organization of functionally segregated circuits linking basal ganglia and cortex. Ann Rev Neurosci 9:357-81

Alexander WH, Brown JW (2011) Medial prefrontal cortex as an action-outcome predictor. Nat Neurosci. 14(10):1338-44

Andersen RA, Cui H (2009) Intention, action planning, and decision making in parietal-frontal circuits. Neuron. 63:568-83

Antal A, Polania R, Schmidt-Samoa C, Dechent P, Paulus W (2011) Transcranial direct current stimulation over the primary motor cortex during fMRI. Neuroimage 55:590-6

Appelbaum PS (2007) Assessment of patients' competence to consent to treatment. N Engl J Med 357:1834-1840

Aylward EH (2007) Change in MRI striatal volumes as a biomarker in preclinical Huntington's disease. Brain Res Bull. 72:152-8

Badre D (2008) Cognitive control, hierarchy, and the rostro-caudal organization of the frontal lobes. Trends Cogn Sci. 12(5):193-200

Baier B, Karnath HO, Dieterich M, Birklein F, Heinze C, Müller NG (2010) Keeping memory clear and stable--the contribution of human basal ganglia and prefrontal cortex to working memory. J Neurosci. 30:9788-92

Barahona M, Pecora LM (2002) Synchronization in small-world systems. Phys Rev Lett 89:054101

Barasinska N (2010) Does Gender Affect Funding Success at the Peer-to-Peer Credit Markets? Evidence from the Largest German Lending Platform. DIW Discussion Paper 1094

Barbas H (2000) Connections underlying the synthesis of cognition, memory, and emotion in primate prefrontal cortices. Brain Res Bull. 52:319-30

Barbey AK, Grafman J (2011) An integrative cognitive neuroscience theory of social reasoning and moral judgment. WIREs Cogn Sci 2:5567

Barbey AK, Krueger F, Grafman J (2009). An evolutionarily adaptive neural architecture for social reasoning. Trends Neurosci. 32(12):603-10

Barch DM, Braver TS, Sabb FW, Noll DC (2000) Anterior cingulate and the monitoring of response conflict: evidence from an fMRI study of overt verb generation. J Cogn Neurosci. 12:298-309

Baron-Cohen S, Wheelwright S, Hill J, Raste Y, Plumb I (2001) The "Reading the Mind in the Eyes" Test revised version: a study with normal adults, and adults with Asperger syndrome or high-functioning autism. J Child Psychol Psychiatry. 42:241-51

Barrat A, Barthelemy M, Vespignani A (2008) Dynamical processes on complex networks. Cambridge University Press, Cambridge, UK

Barry RJ (1990) The orienting response: stimulus factors and response measures. Pavlov J Biol Sci. 25:93-9

Bassett DS, Bullmore E (2006) Small-world brain networks. Neuroscientist 12: 512-23

Bastian M, Heymann S, Jacomy M (2009) Gephi: an open source software for exploring and manipulating networks. Int. AAAI Conf. Weblogs and Social Media

Bault N, Joffily M, Rustichini A, Coricelli G (2011) Medial prefrontal cortex and striatum mediate the influence of social comparison on the decision process. Proc Natl Acad Sci USA 108:16044-9

Bechara A (2004). The role of emotion in decision-making: evidence from neurological patients with orbitofrontal damage. Brain Cogn. 55:30-40

Bechara A, Damasio H, Damasio AR, Lee GP (1999) Different contributions of the human amygdala and ventromedial prefrontal cortex to decision-making. J Neurosci. 19:5473-81

Bechara A, Damasio H, Tranel D, Damasio AR (1997) Deciding advantageously before knowing the advantageous strategy. Science 275:1293-5

Bechara A, Damasio AR, Damasio H, Anderson SW (1994) Insensitivity to future consequences following damage to human prefrontal cortex. Cognition 50:7-15

Beck AT, Steer RA, Brown GK. Beck Depression Inventory–II manual (2nd ed.). San Antonio, TX: Psychological Corporation, 1996

Beck AT, Steer RA. Beck Anxiety Inventory Manual. San Antonio, TX: The Psychological Corporation Harcourt, 1993

Bernoulli D (1954) Exposition of a New Theory on the Measurement of Risk (republished). Econometrica, 22:22-36

Beste C, Willemssen R, Saft C, Falkenstein M (2010) Response inhibition subprocesses and dopaminergic pathways: Basal ganglia disease effects. Neuropsychologia 48:366–373

Bizzi A, Blasi V, Falini A, Ferroli P, Cadioli M, Danesi U, Aquino D, Marras C, Caldiroli D, Broggi G (2008) Presurgical functional MR imaging of language and motor functions: validation with intraoperative electrocortical mapping. Radiology 248:579-89

Blondel VD, Guillaume JL, Lambiotte R, Lefebvre E (2008) Fast unfolding of communities in large networks. Jour. Stat. Mech. 10:1000

Boggio PS, Campanhã C, Valasek CA, Fecteau S, Pascual-Leone A, Fregni F (2010) Modulation of decision-making in a gambling task in older adults with transcranial direct current stimulation. Eur J Neurosci. 31:593-7

Boggio PS, Zaghi S, Villani AB, Fecteau S, Pascual-Leone A, Fregni F (2010b) Modulation of risk-taking in marijuana users by transcranial direct current stimulation (tDCS) of the dorsolateral prefrontal cortex (DLPFC). Drug Alcohol Depend. 112:220-5

Boorman ED, Behrens TE, Rushworth MF (2011) Counterfactual choice and learning in a neural network centered on human lateral frontopolar cortex. PLoS Biol. 9:e1001093

Boorman ED, Behrens TE, Woolrich MW, Rushworth MF (2009) How green is the grass on the other side? Frontopolar cortex and the evidence in favor of alternative courses of action. Neuron 62:733-43

Bossaerts P (2010) Risk and risk prediction error signals in anterior insula. Brain Struct Funct. 214:645-53

Botella J, Narvaez M, Martinez-Molina A, Rubio VJ, Santacreu J (2008) A Dilemmas Task for Eliciting Risk Propensity. Psych Rec. 58:529-546

Botvinick MM (2008) Hierarchical models of behavior and prefrontal function. Trends Cogn Sci. 12(5):201-8

Braak H, Ghebremedhin E, Rüb U, Bratzke H, Del Tredici K (2004) Stages in the development of Parkinson's disease-related pathology. Cell Tissue Res. 318:121-34

Brandes U (2001) A Faster Algorithm for Betweenness Centrality. J Math Soc 25:163-177

Braver TS, Barch DM, Gray JR, Molfese DL, Snyder A (2001) Anterior cingulate cortex and response conflict: effects of frequency, inhibition and errors. Cereb Cortex. 11:825-36

Braun M, Jacobs AM, Hahne A, Ricker B, Hofmann M, Hutzler F (2006). Model-generated lexical activity predicts graded ERP amplitudes in lexical decisions. Brain Res. 1074:431-439

Brevers D, Cleeremans A, Bechara A, Greisen M, Kornreich C, Verbanck P, Noël X (2012) Impaired Self-Awareness in Pathological Gamblers. J Gambl Stud. [Epub ahead of print]

Broca P (1861) Sur le principe des localisations cérébrales. Bulletin de la Société d"Anthropologie 2:190–204

Brog JS, Salyapongse A, Deutch AY, Zahm DS (1993) The patterns of afferent innervation of the core and shell in the "accumbens" part of the rat ventral striatum: immunohistochemical detection of retrogradely transported fluoro-gold. J Comp Neurol. 338(2):255-78

Brown SB, Ridderinkhof KR (2009) Aging and the neuroeconomics of decision making: A review. Cogn Affect Behav Neurosci. 9:365-79

Buckner RL, Sepulcre J, Talukdar T, Krienen FM, Liu H, Hedden T, Andrews-Hanna JR, Sperling RA, Johnson KA (2009) Cortical hubs revealed by intrinsic functional connectivity: mapping, assessment of stability, and relation to Alzheimer's disease. J Neurosci. 29:1860-73

Bullmore ET, Bassett DS (2011) Brain graphs: graphical models of the human brain connectome. Annu Rev Clin Psychol. 7:113-40

Caffarra P, Vezzadini G, Dieci F, Zonato F, Venneri A (2002) A brief version of the Stroop test: normative data in the Italian population. Nuova Riv Neurol 12:111-115

Caldiroli D, Minati L (2007). Early experience with remote pressure sensor respiratory plethysmography monitoring sedation in the MR scanner. Eur J Anaesthesiol 24:761-9

Caldú X, Dreher JC (2007) Hormonal and genetic influences on processing reward and social information. Ann N Y Acad Sci. 1118:43-73

Camara E, Rodriguez-Fornells A, Münte TF (2008) Functional connectivity of reward processing in the brain. Front Hum Neurosci. 2:19

Camara E, Rodriguez-Fornells A, Ye Z, Münte TF (2009) Reward networks in the brain as captured by connectivity measures. Front Neurosci. 2009 Dec 15;3(3):350-62

Camara E, Krämer UM, Cunillera T, Marco-Pallarés J, Cucurell D, Nager W, Mestres-Missé A, Bauer P, Schüle R, Schöls L, Tempelmann C, Rodriguez-Fornells A, Münte TF

(2010) The effects of COMT (Val108/158Met) and DRD4 (SNP-521) dopamine genotypes on brain activations related to valence and magnitude of rewards. Cereb Cortex. 20:1985-96

Camchong J, Goodie AS, McDowell JE, Gilmore CS, Clementz BA (2007) A Cognitive neuroscience Approach to Studying the Role of Overconfidence in Problem Gambling. J Gambl Stud 23:185-199

Carp J, Kim K, Taylor SF, Fitzgerald KD, Weissman DH (2010) Conditional Differences in Mean Reaction Time Explain Effects of Response Congruency, but not Accuracy, on Posterior Medial Frontal Cortex Activity. Front Hum Neurosci. 4:231

Caselli RJ, Dueck AC, Locke DE, Hoffman-Snyder CR, Woodruff BK, Rapcsak SZ, Reiman EM (2011) Longitudinal modeling of frontal cognition in APOE ε4 homozygotes, heterozygotes, and noncarriers. Neurology. 76:1383-8

Cha JH, Frey AS, Alsdorf SA, Kerner JA, Kosinski CM, Mangiarini L, Penney JB Jr, Davies SW, Bates GP, Young AB (1999) Altered neurotransmitter receptor expression in transgenic mouse models of Huntington's disease. Philos Trans R Soc Lond B Biol Sci. 354:981-9

Chesselet MF, Richter F (2011) Modelling of Parkinson's disease in mice. Lancet Neurol. 10:1108-18

Chib VS, Rangel A, Shimojo S, O'Doherty JP (2009) Evidence for a common representation of decision values for dissimilar goods in human ventromedial prefrontal cortex. J Neurosci. 29:12315-20

Chudasama Y, Robbins TW (2004) Psychopharmacological approaches to modulating attention in the five-choice serial reaction time task: implications for schizophrenia. Psychopharmacology 174:86-98

Clark L (2010) Decision-making during gambling: an integration of cognitive and psychobiological approaches. Philos Trans R Soc Lond B Biol Sci. 365:319-30

Clark L, Bechara A, Damasio H, Aitken MR, Sahakian BJ, Robbins TW (2008) Differential effects of insular and ventromedial prefrontal cortex lesions on risky decision-making. Brain 131:1311-22

Clark L, Manes F, Antoun N, Sahakian BJ, Robbins TW (2003) The contributions of lesion laterality and lesion volume to decision-making impairment following frontal lobe damage. Neuropsychologia 41:1474-83

Cohen MX, Heller AS, Ranganath C (2005) Functional connectivity with anterior cingulate and orbitofrontal cortices during decision-making. Brain Res Cogn Brain Res. 23:61-70

Cohen MX, Ranganath C (2005) Behavioral and neural predictors of upcoming decisions. Cogn Affect Behav Neurosci. 5:117-26

Corbetta M, Shulman GL (2002) Control of goal-directed and stimulus-driven attention in the brain. Nature Rev. Neurosci. 3:201-215

Coricelli G, Dolan RJ, Sirigu A (2007) Brain, emotion and decision making: The paradigmatic example of regret. Trends in Cog. Sci. 11:258-265

Coricelli G, Nagel R (2009) Neural correlates of depth of strategic reasoning in medial prefrontal cortex. Proc Natl Acad Sci USA 106:9163-8

Corradi-Dell'acqua C, Civai C, Rumiati RI, Fink GR (2012) Disentangling self- and fairness-related neural mechanisms involved in the ultimatum game: an fMRI study. Soc Cogn Affect Neurosci, Epub ahead of print

Craig AD (2009) How do you feel-now? The anterior insula and human awareness. Nat Rev Neurosci 10:59-70

Critchley HD (2002) Electrodermal responses: what happens in the brain. Neuroscientist. 8:132-42

Critchley HD (2005) Neural mechanisms of autonomic, affective, and cognitive integration. J Comp Neurol. 493:154-66

Critchley HD, Mathias CJ, Dolan RJ (2001) Neural activity in the human brain relating to uncertainty and arousal during anticipation. Neuron 29:537-45

Crockford DN, Goodyear B, Edwards J, Quickfall J, el-Guebaly N (2005) Cue-induced brain activity in pathological gamblers. Biol Psych 58:787-795

Croson R, Gneezy U (2009) Gender Differences in Preferences. J Econ Lit 47:1-27

Crowley KE, Colrain IM (2004) A review of the evidence for P2 being an independent component process: age, sleep and modality. Clin Neurophysiol. 115:732-44

Crowley MJ, Wu J, Molfese PJ, Mayes LC (2010) Social exclusion in middle childhood: Rejection events, slow-wave neural activity, and ostracism distress. Soc Neurosci. 12:1-13

Cui RQ, Huter D, Egkher A, Lang W, Lindinger G, Deecke L (2000) High resolution DC-EEG mapping of the Bereitschaftspotential preceding simple or complex bimanual sequential finger movement. Exp Brain Res. 134:49-57

Czernecki V, Pillon B, Houeto JL, Pochon JB, Levy R, Dubois B (2002) Motivation, reward, and Parkinson's disease: influence of dopatherapy. Neuropsychologia 40:2257–67

Dalrymple-Alford JC, MacAskill MR, Nakas CT, Livingston L, Graham C, Crucian GP, Melzer TR, Kirwan J, Keenan R, Wells S, Porter RJ, Watts R, Anderson TJ (2010) The MoCA: well-suited screen for cognitive impairment in Parkinson disease. Neurology 75:1717-25

Damasio AR (1996) The somatic marker hypothesis and the possible functions of the prefrontal cortex. Philos Trans R Soc Lond B Biol Sci. 351:1413-20

David AS, Bedford N, Wiffen B, Gilleen J (2012) Failures of metacognition and lack of insight in neuropsychiatric disorders. Philos Trans R Soc Lond B Biol Sci. 367:1379-90

Davis CE, Hauf JD, Wu DQ, Everhart DE (2011) Brain function with complex decision making using electroencephalography. Int J Psychophysiol 79:175-83

Daw ND, O'Doherty JP, Dayan P, Seymour B, Dolan RJ (2006) Cortical substrates for exploratory decisions in humans. Nature 441:876-9

De Martino B, Camerer CF, Adolphs R (2010) Amygdala damage eliminates monetary loss aversion. Proc Natl Acad Sci USA 107(8):3788-92

de la Fuente-Fernández R (2012) Role of DaTSCAN and clinical diagnosis in Parkinson disease. Neurology 78:696-701

Delazer M, Sinz H, Zamarian L, Benke T (2007) Decision-making with explicit and stable rules in mild Alzheimer's disease. Neuropsychologia. 45:1632-41

Delazer M, Sinz H, Zamarian L, Stockner H, Seppi K, Wenning GK, Benke T, Poewe W (2009) Decision making under risk and under ambiguity in Parkinson's disease. Neuropsychologia. 47:1901-8

Delfabbro P (2004) The stubborn logic of regular gamblers: Obstacles and dilemmas in cognitive gambling research. J Gambl Stud 20:1-21

Disbrow EA, Slutsky DA, Roberts TP, Krubitzer LA (200) Functional MRI at 1.5 tesla: a comparison of the blood oxygenation level-dependent signal and electrophysiology. Proc Natl Acad Sci USA 97:9718-23

Dodd ML, Klos KJ, Bower JH, Geda YE, Josephs KA, Ahlskog JE (2005) Pathological gambling caused by drugs used to treat Parkinson disease. Arch Neurol 62:1377–81

Double KL, Reyes S, Werry EL, Halliday GM (2010) Selective cell death in neurodegeneration: why are some neurons spared in vulnerable regions? Prog Neurobiol. 92:316-29

Duann JR, Jung TP, Kuo WJ, Yeh TC, Makeig S, Hsieh JC, Sejnowski TJ (2002) Single-trial variability in event-related BOLD signals. Neuroimage. 15(4):823-35

Duka T, Crews F (2009) Impulsivity: its genetic, neurochemical and brain substrate determinants and the risks it entails for aberrant motivated behavior and psychopathology. Pharmacol Biochem Behav 93:197-8

Dunn BD, Dalgleish T, Lawrence AD (2006) The somatic marker hypothesis: A critical evaluation. Neurosci. Biobehav. Rev. 30:239-271

Dunn LB, Nowrangi MA, Palmer BW, Jeste DV, Saks ER (2006) Assessing decisional capacity for clinical research or treatment: a review of instruments. Am J Psychiatry. 163:1323-34

Elliott R, Agnew Z, Deakin JF (2008) Medial orbitofrontal cortex codes relative rather than absolute value of financial rewards in humans. Eur J Neurosci. 27:2213-8

Engelmann JB, Capra CM, Noussair C, Berns GS (2009) Expert financial advice neurobiologically "Offloads" financial decision-making under risk. PLoS One. 4:e4957

Engelmann JB, Tamir D (2009) Individual differences in risk preference predict neural responses during financial decision-making. Brain research 1290:28-51

Ernst M, Nelson EE, McClure EB, Monk CS, Munson S, Eshel N (2004) Choice selection and reward anticipation: an fMRI study. Neuropsychologia 42:1585-1597

Evans AH, Lees AJ (2004) Dopamine dysregulation syndrome in Parkinson's disease. Curr. Opin. Neurol. 17:393-8

Fecteau S, Knoch D, Fregni F, Sultani N, Boggio PS, Pascual-Leone A (2007) Diminishing risk-taking behavior by modulating activity in the prefrontal cortex: a direct current stimulation study. J Neurosci 27:12500-5

Fecteau S, Pascual-Leone A, Zald DH, Liguori P, Théoret H, Boggio PS, Fregni F (2007b) Activation of prefrontal cortex by transcranial direct current stimulation reduces appetite for risk during ambiguous decision making. J Neurosci 27:6212-8

Fiorillo CD, Tobler PN, Schultz W (2003) Discrete coding of reward probability and uncertainty by dopamine neurons. Science 299:1898-902

Fox MD, Raichle ME (2007) Spontaneous fluctuations in brain activity observed with functional magnetic resonance imaging. Nat. Rev. Neurosci. 8:700-11

Friston KJ, Buechel C, Fink GR, Morris J, Rolls E, Dolan RJ (1997) Psychophysiological and modulatory interactions in neuroimaging. Neuroimage. 6:218-29

Friston KJ, Harrison L, Penny W (2003) Dynamic causal modelling. Neuroimage. 19:1273-302

Friston KJ, Holmes A, Poline JB, Price CJ, Frith CD (1996) Detecting activations in PET and fMRI: levels of inference and power. Neuroimage 4:223-35

Fuster JM, The Prefrontal Cortex: Anatomy, Physiology, and Neuropsychology of the Frontal Lobe, Lippincott-Raven (1997)

Games PA, Howell JF (1976) Pairwise multiple comparison procedures with unequal N's and/or variances: A monte carlo study. J Edu Stats 1:113-125

Gaviria M, Pliskin N, Kney A (2011) Cognitive impairment in patients with advanced heart failure and its implications on decision-making capacity. Congest Heart Fail. 17:175-9

Gattellaro G, Minati L, Grisoli M, Mariani C, Carella F, Osio M, Ciceri E, Albanese A, Bruzzone MG (2009) White matter involvement in idiopathic Parkinson disease: a diffusion tensor imaging study. AJNR Am J Neuroradiol 30:1222-6

Gescheidt T, Czekóová K, Urbánek T, Mareček R, Mikl M, Kubíková R, Telecká S, Andrlová H, Husárová I, Bareš M. Iowa Gambling Task in patients with early-onset Parkinson's disease: strategy analysis. Neurol Sci. 2012, Epub ahead of print

Ginestet CE, Nichols TE, Bullmore ET, Simmons A (2011) Brain network analysis: separating cost from topology using cost-integration. PLoS One. 6(7):e21570

Giovagnoli AR, Del Pesce M, Mascheroni S, Simoncelli M, Laiacona M, Capitani E (1996) Trail making test: normative values from 287 normal adult controls. Ital J Neurol Sci 17:305-9

Gläscher J, Hampton AN, O'Doherty JP (2009) Determining a role for ventromedial prefrontal cortex in encoding action-based value signals during reward-related decision making. Cereb Cortex. 19:483-95

Gleichgerrcht E, Torralva T, Roca M, Szenkman D, Ibanez A, Richly P, Pose M, Manes F (2012) Decision making cognition in primary progressive aphasia. Behav Neurol. 25:45-52

Gneezy U, Rustichini A (2000) Pay Enough Or Don'T Pay At Al. Quart Jour Econom 115: 791-810

Gómez-Tortosa E, MacDonald ME, Friend JC, Taylor SA, Weiler LJ, Cupples LA, Srinidhi J, Gusella JF, Bird ED, Vonsattel JP, Myers RH (2001) Quantitative neuropathological changes in presymptomatic Huntington's disease. Ann Neurol. 49:29-34

Goudriaan AE, Oosterlaan J, de Beurs E, Van den Brink W (2004) Pathological gambling: a comprehensive review of biobehavioral findings. Neurosci Biobehav Rev. 28:123-41

Goupillaud P, Grossman A, Morlet J (1984) Cycle-Octave and Related Transforms in Seismic Signal Analysis. Geoexploration 23:85-102

Greicius MD, Krasnow B, Reiss AL, Menon V (2003) Functional connectivity in the resting brain: a network analysis of the default mode hypothesis. Proc. Natl. Acad. Sci. USA 100:253-8

Guimerà R, Mossa S, Turtschi A, Amaral LA (2005) The worldwide air transportation network: Anomalous centrality, community structure, and cities' global roles. Proc Natl Acad Sci USA 102(22):7794-9

Guitart-Masip M, Huys QJ, Fuentemilla L, Dayan P, Duzel E, Dolan RJ (2012) Go and no-go learning in reward and punishment: Interactions between affect and effect. Neuroimage, Epub ahead of print

Hagmann P, Cammoun L, Gigandet X, Meuli R, Honey CJ, Wedeen VJ, Sporns O (2008) Mapping the structural core of the human cerebral cortex. PLoS Biol 6:e159

Hajcak G, Moser JS, Holroyd CB, Simons RF (2006) The feedback-related negativity reflects the binary evaluation of good versus bad outcomes. Biol. Psychol. 71:148-154

Hare TA, Camerer CF, Knoepfle DT, Rangel A (2010) Value computations in ventral medial prefrontal cortex during charitable decision making incorporate input from regions involved in social cognition. J Neurosci. 30:583-90

Hari R (2006) Action-perception connection and the cortical mu rhythm. Prog Brain Res. 159:253-60

Hedreen JC, Folstein SE (1995) Early loss of neostriatal striosome neurons in Huntington's disease. J Neuropathol Expe Neurol 54:105-20

Heims HC, Critchley HD, Dolan R, Mathias (2004) Social and motivational functioning is not critically dependent on feedback of autonomic responses: neuropsychological evidence from patients with pure autonomic failure. Neuropsychologia 42:1979-88

Henson RNA, Rugg MD, Shallice T, Dolan RJ (2000) Confidence in recognition memory for words: Dissociating right prefrontal roles in episodic retrieval. J Cogn Neurosci 12:913–923

Hernández A, Zainos A, Romo R (2002) Temporal evolution of a decision-making process in medial premotor cortex. Neuron 33:959-72

Herrmann CS, Knight RT (2001) Mechanisms of human attention: event-related potentials and oscillations. Neurosci Biobehav Rev. 25:465-76

Hink RF, Kohler H, Deecke L, Kornhuber HH (1982) Risk-taking and the human bereitschaftspotential. Electroencephalogr Clin Neurophysiol. 53:361-73

Hoehn MM, Yahr MD (1967) Parkinsonism: onset, progression and mortality. Neurology 17:427–42

Hollerman JR, Tremblay L, Schultz W (1998) Influence of reward expectation on behavior-related neuronal activity in primate striatum. J Neurophysiol 80:947-63

Holm S (1979) A simple sequentially rejective multiple test procedure. Scand. Jour. Stat. 6:65–70

Holroyd CB, Pakzad-Vaezi KL, Krigolson OE (2008) The feedback correct related positivity: sensitivity of the event-related brain potential to unexpected positive feedback. Psychophysiology 45:688–697

Hommet C, Constans T, Atanasova B, Mondon K (2010) Decision making in the elderly: which tools for its evaluation by the clinician?. Psychol Neuropsychiatr Vieil. 8:201-7

Hoshi E (2006) Functional specialization within the dorsolateral prefrontal cortex: a review of anatomical and physiological studies of non-human primates. Neurosci Res. 54:73-84

Hsu M, Krajbich I, Zhao C, Camerer CF (2009) Neural response to reward anticipation under risk is nonlinear in probabilities. J Neurosci. 29:2231-7

Hughes AJ, Daniel SE, Kilford L, Lees AJ (1992) Accuracy of clinical diagnosis of idiopathic Parkinson's disease: a clinico-pathological study of 100 cases. J Neurol Neurosurg Psychiatry 55:181-4

Humphries MD, Gurney K (2008) Network 'small-world-ness': a quantitative method for determining canonical network equivalence. PLoS One 3:e0002051

Huntington Study Group. Unified Huntington's Disease Rating Scale: reliability and consistency. Mov Disord. 11:136-42

Hunt LT (2008) Distinctive roles for the ventral striatum and ventral prefrontal cortex during decision-making. J Neurosci. 28:8658-9

Ikeda A, Yazawa S, Kunieda T, Ohara S, Terada K, Mikuni N, Nagamine T et al. (1999) Cognitive motor control in human pre-supplementary motor area studied by subdural recording of discrimination/selection-related potentials. Brain. 122:915-31

Ino T, Nakai R, Azuma T, Kimura T, Fukuyama H (2010) Differential activation of the striatum for decision making and outcomes in a monetary task with gain and loss. Cortex 46:2-14

Jang SH, Ahn SH, Byun WM, Kim CS, Lee MY, Kwon YH (2009) The effect of transcranial direct current stimulation on the cortical activation by motor task in the human brain: an fMRI study. Neurosci Lett. 460:117-20

Jänig W (2006) The Integrative Action of the Autonomic Nervous System. Neurobiology of Homeostasis. Cambridge University Press, Cambridge

Jones CL, Minati L, Harrison NA, Ward J, Critchley HD (2011) Under pressure: Response urgency modulates striatal and insula activity during decision-making under risk. PLoS ONE 6:e20942

Jurcak V, Tsuzuki D, Dan I (2007) 10/20, 10/10, and 10/5 systems revisited: their validity as relative head-surface-based positioning systems. Neuroimage 34:1600-11

Kable JW, Glimcher PW (2009) The neurobiology of decision: consensus and controversy. Neuron 63:733-45

Kahn I, Yeshurun Y, Rotshtein P, Fried I, Ben-Bashat D, Hendler T (2002) The role of the amygdala in signaling prospective outcome of choice. Neuron. 33:983-94

Kahneman D (2003) A perspective on judgment and choice: mapping bounded rationality. Am. Psychol. 58:697-720

Kahneman D, Tversky A (1979) Prospect theory: an analysis of decision under risk. Econometrica 4:263-291

Kahneman D, Tversky A (1984) Choices, values and frames. Am. Psychol. 39:341–350

Kahneman D, Tversky A (1991). Loss aversion in riskless choice: a reference-dependent model. Q. J. Econ. 106:1039-1061

Kahneman D, Tversky A (2000). Choices, frames and values. Cambridge University Press

Kahnt T, Heinzle J, Park SQ, Haynes JD (2010) Decoding different roles for vmPFC and dlPFC in multi-attribute decision making. Neuroimage 56:709-15

Kalenscher T, van Wingerden M (2011) Why we should use animals to study economic decision making - a perspective. Front Neurosci. 5:82

Kim SK, Song P, Hong JM, Pak CY, Chung CS, Lee KH, Kim GM (2008) Prediction of progressive motor deficits in patients with deep subcortical infarction. Cerebrovasc Dis. 25:297-303

Klimesch W, Doppelmayr M, Schwaiger J, Auinger P, Winkler T (2007) 'Paradoxical' alpha synchronization in a memory task. Brain Res Cogn Brain Res. 7:493-501

Klimesch W, Sauseng P, Hanslmayr S (2007) EEG alpha oscillations: the inhibition-timing hypothesis. Brain Res Rev. 2007; 53:63-88

Knoch D, Gianotti LR, Pascual-Leone A, Treyer V, Regard M, Hohmann M, Brugger P (2006) Disruption of right prefrontal cortex by low-frequency repetitive transcranial magnetic stimulation induces risk-taking behavior. J Neurosci. 26:6469-72

Knutson B, Cooper JC (2005) Functional magnetic resonance imaging of reward prediction. Curr Opin Neurol. 18:411-7

Kobayakawa M, Koyama S, Mimura M, Kawamura M (2008) Decision making in Parkinson's disease: Analysis of behavioral and physiological patterns in the Iowa gambling task. Mov Disord. 23:547-52

Koechlin E, Basso G, Pietrini P, Panzer S, Grafman J (1999) The role of the anterior prefrontal cortex in human cognition. Nature 399:148-51

Kolev V, Yordanova J, Schurmann M, Basar E (2001) Increased frontal phase-locking of event-related alpha oscillations during task processing. Int. J Psychophys. 39:159-165

Krain AL, Wilson AM, Arbuckle R, Castellanos FX, Milham MP (2006) Distinct neural mechanisms of risk and ambiguity: a meta-analysis of decision-making. Neuroimage 32:477-84

Kristeva R, Jankov E, Gantchev G (1987) Differences in slow potentials in bereitschaftspotential and contingent negative variation producing situations. Electroencephalogr Clin Neurophysiol Suppl. 40:41-6

Kristeva R, Keller E, Deecke L, Kornhuber HH (1979) Cerebral potentials preceding unilateral and simultaneous bilateral finger movements. Electroencephalogr Clin Neurophysiol. 47:229-38

Lamm C, Windischberger C, Leodolter U, Moser E, Bauer H (2001) Evidence for premotor cortex activity during dynamic visuospatial imagery from single-trial functional magnetic resonance imaging and event-related slow cortical potentials. Neuroimage 14:268-83

Langbehn DR, Brinkman RR, Falush D, Paulsen JS, Hayden MR, International Huntington's Disease Collaborative Group (2004) A new model for prediction of the age of onset and penetrance for Huntington's disease based on CAG length. Clin Genet. 65:267-77

Latapy M (2008) Main-memory Triangle Computations for Very Large (Sparse Power-Law) Graphs. Theor. Comp. Sci. 407:458-473

Lee D (2006) Neural basis of quasi-rational decision making. Curr. Opin. Neurobiol. 16:191-198

Levine DS (2009) Brain pathways for cognitive-emotional decision making in the human animal. Neural Netw. 22:286-93

Levin IP, Xue G, Weller JA, Reimann M, Lauriola M, Bechara A (2012) A neuropsychological approach to understanding risk-taking for potential gains and losses. Front Neurosci. 6:15

Liebermann D, Ploner CJ, Kraft A, Kopp UA, Ostendorf F (2011) A dysexecutive syndrome of the medial thalamus. Cortex 2011 [Epub ahead of print]

Liepert J, Restemeyer C, Kucinski T, Zittel S, Weiller C (2005) Motor strokes: the lesion location determines motor excitability changes. Stroke 36:2648-53

Linden DE (2005) The p300: where in the brain is it produced and what does it tell us? Neuroscientist 11:563-76

Logothetis NK, Pfeuffer J (2004) On the nature of the BOLD fMRI contrast mechanism. Magn Reson Imag 22:1517–1531

Logothetis NK (2008) What we can do and what we cannot do with fMRI. Nature 453:869-78

Mahler SV, Berridge KC (2011) What and when to "want"? Amygdala-based focusing of incentive salience upon sugar and sex. Psychopharmacology, epub ahead of print

Mandelli ML, Savoiardo M, Minati L, Mariotti C, Aquino D, Erbetta A, Genitrini S, Di Donato S, Bruzzone MG, Grisoli M (2010) Decreased diffusivity in the dorsal striatum of presymptomatic huntington disease gene carriers: which explanation? Am J Neuroradiol. 2010;31:706-10

Manes F, Sahakian B, Clark L, Rogers R, Antoun N, Aitken M, Robbins T (2002) Decision-making processes following damage to the prefrontal cortex. Brain 125:624-39

Marder K, Zhao H, Myers RH, Cudkowicz M, Kayson E, Kieburtz K, Orme C, Paulsen J, Penney JB Jr, Siemers E, Shoulson I (2000) Rate of functional decline in Huntington's disease. Huntington Study Group. Neurology. 54:452-8

Matthews SC, Simmons AN, Lane SD, Paulus MP (2004) Selective activation of the nucleus accumbens during risk-taking decision-making. NeuroReport 15:2123-2127

Manes F, Torralva T, Ibáñez A, Roca M, Bekinschtein T, Gleichgerrcht E (2011) Decision-making in frontotemporal dementia: clinical, theoretical and legal implications. Dement Geriatr Cogn Disord. 32:11-7

Marco-Pallarés J, Cucurell D, Cunillera T, Krämer UM, Càmara E, Nager W, Bauer P, Schüle R, Schöls L, Münte TF, Rodriguez-Fornells A (2009) Genetic variability in the dopamine system (dopamine receptor D4, catechol-O-methyltransferase) modulates neurophysiological responses to gains and losses. Biol Psychiatry. 66:154-61

Martin-Soelch C, Missimer J, Leenders KL, Schultz W (2003) Neural activity related to the processing of increasing monetary reward in smokers and nonsmokers. Eur J Neurosci. 18:680-8

McClure SM, York MK, Montague PR (2004) The neural substrates of reward processing in humans: the modern role of FMRI. Neuroscientist. 10:260-8

McKie S, Richardson P, Elliott R, Völlm BA, Dolan MC, Williams SR, Anderson IM, Deakin JF (2011) Mirtazapine antagonises the subjective, hormonal and neuronal effects of m-chlorophenylpiperazine (mCPP) infusion: a pharmacological-challenge fMRI (phMRI) study. Neuroimage 58:497-507

McFarland DJ (1977) Decision making in animals. Nature 269:15-21

Medford N, Critchley HD (2010) Conjoint activity of anterior insular and anterior cingulate cortex: awareness and response. Brain Struct Funct. 214:535-49

Mennes M, Wouters H, van der Bergh B, Lagae L, Stiers P (2008) ERP correlates of complex human decision making in a gambling paradigm: detection and resolution of conflict. Psychophys 45:714-720

Mesulam MM (1998) From sensation to cognition. Brain 121:1013-52

Meyer K, Damasio A (2009) Convergence and divergence in a neural architecture for recognition and memory. Trends Neurosci. 32:376-82

Michel CM, Murray MM, Lantz G, Gonzalez S, Spinelli L, Grave de Peralta R (2004) EEG source imaging. Clin Neurophysiol. 115:2195-222

Mickes L, Jacobson M, Peavy G, Wixted JT, Lessig S, Goldstein JL, Corey-Bloom J (2010) A comparison of two brief screening measures of cognitive impairment in Huntington's disease. Mov Disord 25(13):2229-33

Miltner WHR, Braun CH, Coles MGH (1997) Event-related brain potentials following incorrect feedback in a time-estimation task: evidence for a “generic” neural system for error detection. J. Cogn. Neurosci. 9:788-798

Mimura M, Oeda R, Kawamura M (2006) Impaired decision-making in Parkinson's disease. Parkinsonism Relat Disord. 12:169-75

Minati L, Jones CL, Gray MA, Medford N, Harrison NA, Critchley HD (2009) Emotional modulation of visual cortex activity: a functional near-infrared spectroscopy study. Neuroreport. 20:1344-50

Minati L, Rosazza C, Zucca I, D'Incerti L, Scaioli V, Bruzzone MG (2008) Spatial correspondence between functional MRI (fMRI) activations and cortical current density maps of event-related potentials (ERP): a study with four tasks. Brain Topogr. 21:112-27

Minati L, Grisoli M, Carella F, De Simone T, Bruzzone MG, Savoiardo M (2007) Imaging degeneration of the substantia nigra in Parkinson disease with inversion-recovery MR imaging. AJNR Am J Neuroradiol. 28:309-13

Mizuta H, Motomura N (2006) Memory dysfunction in caudate infarction caused by Heubner's recurring artery occlusion. Brain Cogn. 61:133-8

Nasreddine ZS, Phillips NA, Bédirian V, Charbonneau S, Whitehead V, Collin I, Cummings JL, Chertkow H (2005) The Montreal Cognitive Assessment (MoCA): A Brief Screening Tool For Mild Cognitive Impairment. J Am. Ger. Soc. 53:695-699

Neuper C, Pfurtscheller G (2001) Event-related dynamics of cortical rhythms: frequency-specific features and functional correlates. Int J Psychophysiol. 43:41-58

Newman M (2010) Networks: An Introduction. Oxford University Press, Oxford, UK

Niewenhuys R. The Human Central Nervous System: A Synopsis and Atlas. New York: Springer-Verlag; 1996

Nitsche M, Paulus W (2000) Excitability changes induced in the human motor cortex by weak transcranial direct current stimulation. J Physiol. 527:633-639

Nitsche MA, Cohen LG, Wassermann EM, Priori A, Lang N, Antal A, Paulus W, Hummel F, Boggio PS, Fregni F, Pascual-Leone A (2008) Transcranial direct current stimulation: State of the art 2008. Brain Stimul. 1:206-23

Northoff G, Heinzel A, de Greck M, Bermpohl F, Dobrowolny H, Panksepp J (2006) Self-referential processing in our brain--a meta-analysis of imaging studies on the self. Neuroimage 31:440-57

Nys GM, van Zandvoort MJ, van der Worp HB, Kappelle LJ, de Haan EH (2006) Neuropsychological and neuroanatomical correlates of perseverative responses in subacute stroke. Brain 129:2148-57

Oakes TR, Pizzagalli DA, Hendrick AM, Horras KA, Larson CL, Abercrombie HC, Schaefer SM, Koger JV, Davidson RJ (2004) Functional coupling of simultaneous electrical and metabolic activity in the human brain. Hum Brain Mapp. 21:257-70

O'Doherty JP, Hampton A, Kim H (2007) Model-based fMRI and its application to reward learning and decision making. Ann N Y Acad Sci. 1104:35-53

Ohira H, Ichikawa N, Nomura M, Isowa T, Kimura K, Kanayama N, Fukuyama S, Shinoda J, Yamada J. (2010) Brain and autonomic association accompanying stochastic decision-making. NeuroImage 49:1024-1037

Oldfield RC (1971) The assessment and analysis of handedness: The Edinburgh inventory. Neuropsychologia 9:97-113

Ongür D, Ferry AT, Price JL (2003) Architectonic subdivision of the human orbital and medial prefrontal cortex. J Comp Neurol. 460(3):425-49

Ongür D, Price JL (2000) The organization of networks within the orbital and medial prefrontal cortex of rats, monkeys and humans. Cereb Cortex. 10(3):206-19

Orsini A, Grossi D, Capitani E, Laiacona M, Papagno C, Vallar G (1987) Verbal and spatial immediate memory span: Normative data from 1,355 adults and 1,112 children. Ital J Neurol Sci 8:539-548

Osumi T, Ohira H (2009) Cardiac responses predict decisions: An investigation of the relation between orienting response and decisions in the ultimatum game. Int. Jour. Psychophysiol. 74:74-79

Ouchi Y, Kanno T, Okada H, Yoshikawa E, Futatsubashi M, Nobezawa S, Torizuka T, Sakamoto M (1999) Presynaptic and postsynaptic dopaminergic binding densities in the nigrostriatal and mesocortical systems in early Parkinson's disease: a double-tracer positron emission tomography study. Ann Neurol 46:723–31

Overall JE, Gorham DR (1962). The brief psychiatric rating scale. Psychological Reports 10:799-812

Pagnoni G, Zink CF, Montague PR, Berns GS (2002) Activity in human ventral striatum locked to errors of reward prediction. Nat Neurosci 5:97-8

Pagonabarraga J, García-Sánchez C, Llebaria G, Pascual-Sedano B, Gironell A, Kulisevsky J (2007) Controlled study of decision-making and cognitive impairment in Parkinson's disease. Mov Disord. 22:1430-5

Palminteri S, Boraud T, Lafargue G, Dubois B, Pessiglione M (2009) Brain hemispheres selectively track the expected value of contralateral options. J Neurosci. 29:13465-72

Palva S, Palva JM (2007) New vistas for alpha-frequency band oscillations. Trends Neurosci. 30:150-8

Paquette C, Sidel M, Radinska BA, Soucy JP, Thiel A (2011) Bilateral transcranial direct current stimulation modulates activation-induced regional blood flow changes during voluntary movement. J Cereb Blood Flow Metab. 31(10):2086-95

Park SQ, Kahnt T, Rieskamp J, Heekeren HR (2011) Neurobiology of value integration: when value impacts valuation. J Neurosci. 31:9307-14

Penny WD, Kiebel SJ, Kilner JM, Rugg MD (2002) Event-related brain dynamics. Trends Neurosci. 25:387-9

Petrovic P, Pleger B, Seymour B, Klöppel S, De Martino B, Critchley H, Dolan RJ (2008) Blocking central opiate function modulates hedonic impact and anterior cingulate response to rewards and losses. J Neurosci. 28:10509-16

Pascual-Marqui RD, Michel CM, Lehmann D (1994) Low resolution electromagnetic

tomography: a new method for localizing electrical activity-in the brain. Int J Psychophysiol 18:49–65

Patton JM, Stanford MS, Barratt ES (1995) Factor Structure of the Barratt Impulsiveness Scale. J Clin Psych 51:768-774

Pedroni A, Langer N, Koenig T, Allemand M, Jäncke L (2011) Electroencephalographic topography measures of experienced utility. J Neurosci. 31:10474-80

Pessiglione M, Seymour B, Flandin G, Dolan RJ, Frith CD (2006) Dopamine-dependent prediction errors underpin reward-seeking behaviour in humans. Nature 442:1042-5

Pezzella FR, Colosimo C, Vanacore N, Di Rezze S, Chianese M, Fabbrini G, Meco G (2005) Prevalence and clinical features of hedonistic homeostatic dysregulation in Parkinson's disease. Mov Disord. 20:77-81

Pfurtscheller G (2001) Functional brain imaging based on ERD/ERS. Vision Res. 41:1257-1260

Philiastides MG, Biele G, Heekeren HR (2010) A mechanistic account of value computation in the human brain. Proc Natl Acad Sci U S A. 107:9430-5

Pincus D, Kose S, Arana A, Johnson K, Morgan PS, Borckardt J, Herbsman T, Hardaway F, George MS, Panksepp J, Nahas Z (2010) Inverse effects of oxytocin on attributing mental activity to others in depressed and healthy subjects: a double-blind placebo controlled FMRI study. Front Psychiatry 1:134

Platt ML, Huettel SA (2008) Risky business: the neuroeconomics of decision making under uncertainty. Nat Neurosci. 11:398-403

Platt M, Padoa-Schioppa C (2009) Neuronal representations of value. In Neuroeconomics: Decision making and the brain (Glimcher P. et al., editors), Elsevier

Polezzi D, Daum I, Rubaltelli E, Lotto L, Civai C, Sartori G, Rumiati R (2008) Mentalizing in economic decision making. Behav. Brain Res. 190:218-223

Polezzi D, Lotto L, Daum I, Sartori G, Rumiati R (2008b) Predicting outcomes of decisions in the brain. Behav. Brain Res. 187:116-122

Polezzi D, Sartori G, Rumiati R, Vidotto G, Daum I (2010) Brain correlates of risky decision-making. Neuroimage 49:1886-94

Preuschoff K, Quartz SR, Bossaerts P (2008) Human insula activation reflects risk prediction errors as well as risk. J Neurosci 28:2745-52

Pulvermüller F, Birbaumer N, Lutzenberger W, Mohr B (1997) High-frequency brain activity: its possible role in attention, perception and language processing. Prog Neurobiol. 52:427-45

Rajkowska G, Goldman-Rakic PS (1995). Cytoarchitectonic definition of prefrontal areas in the normal human cortex: II. Variability in locations of areas 9 and 46 and relationship to the Talairach Coordinate System. Cereb Cortex. 5:323-37

Ramnani N, Elliott R, Athwal BS, Passingham RE (2004) Prediction error for free monetary reward in the human prefrontal cortex. Neuroimage 23:777-86

Ramsey JD, Hanson SJ, Hanson C, Halchenko YO, Poldrack RA, Glymour C (2010) Six problems for causal inference from fMRI. Neuroimage. 49(2):1545-58

Rangel A, Hare T (2010) Neural computations associated with goal-directed choice. Curr Opin Neurobiol. 20:262-70

Redgrave P, Prescott TJ, Gurney K (1999) The basal ganglia: a vertebrate solution to the selection problem? Neuroscience 89: 1009-23

Richell RA, Mitchell DG, Newman C, Leonard A, Baron-Cohen S, Blair RJ (2003) Theory of mind and psychopathy: can psychopathic individuals read the 'language of the eyes'? Neuropsychologia 41:523-6

Ribeiro RL, Teixeira-Silva F, Pompeia S, Bueno OF (2007) IAPS includes photographs that elicit low-arousal physiological responses in healthy volunteers. Physiol Behav 91:671–675

Rogers RD, Lancaster M, Wakeley J, Bhagwagar Z (2004) Effects of beta-adrenoceptor blockade on components of human decision-making. Psychopharmacology (Berl) 172:157-64

Rogers RD (2011) The roles of dopamine and serotonin in decision making: evidence from pharmacological experiments in humans. Neuropsychopharmacology 36:114-32

Roiser JP, de Martino B, Tan GC, Kumaran D, Seymour B, Wood NW, Dolan RJ (2009) A genetically mediated bias in decision making driven by failure of amygdala control. J Neurosci. 29:5985-91

Rolls ET (1999) The brain and emotion. Oxford University Press: Oxford, UK

Rorie AE, Newsome WT (2005) A general mechanism for decision-making in the human brain? Trends Cogn Sci. 9:41-3

Rosazza C, Minati L (2011) Resting state brain networks: literature review and clinical applications. Neurol Sci 32(5):773-85

Rösler F, Heil M (1991) Toward a functional categorization of slow waves: taking into account past and future events. Psychophysiology. 28:344-58

Rossi S, Ferro M, Cincotta M, Ulivelli M, Bartalini S, Miniussi C, Giovannelli F, Passero S (2007) A real electro-magnetic placebo (REMP) device for sham transcranial magnetic stimulation (TMS). Clin Neurophysiol. 118:709-16

Ruchkin DS, Johnson R Jr, Mahaffey D, Sutton S (1988) Toward a functional categorization of slow waves. Psychophysiology 25:339-53

Rumelhart DE, McClelland JL, the PDP Research Group (1986). Parallel Distributed Processing: Explorations in the Microstructure of Cognition. Volume 1: Foundations, Cambridge, MA: MIT Press

Rushworth MF, Behrens TE (2008) Choice, uncertainty and value in prefrontal and cingulate cortex. Nat Neurosci. 11:389-97

Rushworth MF, Noonan MP, Boorman ED, Walton ME, Behrens TE (2011) Frontal cortex and reward-guided learning and decision-making. Neuron. 70:1054-69

Sadleir RJ, Vannorsdall TD, Schretlen DJ, Gordon B (2010) Transcranial direct current stimulation (tDCS) in a realistic head model. Neuroimage 51:1310-8

Sakagami M, Pan X (2007) Functional role of the ventrolateral prefrontal cortex in decision making. Curr Opin Neurobiol. 17(2):228-33

Salvador R, Suckling J, Coleman MR, Pickard JD, Menon D, Bullmore E (2005) Neurophysiological architecture of functional magnetic resonance images of human brain. Cereb Cortex. 15:1332-42

Sanfey AG, Rilling JK, Aronson JA, Nystrom LE, Cohen JD (2003) The neural basis of economic decision-making in the Ultimatum Game. Science 300:1755-8

Sarlo M, Palomba D, Buodo G, Minghetti R, Stegagno L (2005) Blood pressure changes highlight gender differences in emotional reactivity to arousing pictures. Biol Psychol 70:188–196

Satterthwaite TD, Green L, Myerson J, Parker J, Ramaratnam M, Buckner RL (2007) Dissociable but inter-related systems of cognitive control and reward during decision making: evidence from pupillometry and event-related fMRI. Neuroimage 37:1017-31

Scheibe C, Ullsperger M, Sommer W, Heekeren HR (2010). Effects of parametrical and trial-to-trial variation in prior probability processing revealed by simultaneous electroencephalogram/functional magnetic resonance imaging. J Neurosci 30:16709-17

Schmack K, Schlagenhauf F, Sterzer P, Wrase J, Beck A, Dembler T, Kalus P, Puls I, Sander T, Heinz A, Gallinat J (2008) Catechol-O-methyltransferase val158met genotype influences neural processing of reward anticipation. Neuroimage 42:1631-8

Schmitz TW, Johnson SC (2007) Relevance to self: A brief review and framework of neural systems underlying appraisal. Neurosci Biobehav Rev. 31:585-96

Schubert R, Brown M, Gysler M, Brachinger HW (1999) Financial Decision-Making: Are Women Really More Risk-Averse? Am Econom Rev 89:381-385

Schultz W, Apicella P, Ljungberg T (1993) Responses of monkey dopamine neurons to reward and conditioned stimuli during successive steps of learning a delayed response task. J Neurosci. 13:900-13

Schultz W (2004) Neural coding of basic reward terms of animal learning theory, game theory, microeconomics and behavioural ecology. Curr Opin Neurobiol. 14:139-47

Schürmann M, Başar E (2001) Functional aspects of alpha oscillations in the EEG. Int J Psychophysiol. 39:151-8

Schutter DJ, de Haan EH, van Honk J (2004). Anterior asymetrical alpha activity predicts Iowa gambling performance: distinctly but reversed. Neuropsychologia 42:939-943

Seedat S, Kesler S, Niehaus DJ, Stein DJ (2000) Pathological gambling behaviour: emergence secondary to treatment of Parkinson's disease with dopaminergic agents. Depress Anxiety 11:185-6

Serences JT (2004) A comparison of methods for characterizing the event-related BOLD timeseries in rapid fMRI. Neuroimage 21(4):1690-700

Serences JT (2008) Value-based modulations in human visual cortex. Neuron 60:1169-81

Shaw P, Bramham J, Lawrence EJ, Morris R, Baron-Cohen S, David AS (2005) Differential effects of lesions of the amygdala and prefrontal cortex on recognizing facial expressions of complex emotions. J Cogn Neurosci. 17:1410-9

Shibasaki H, Hallett M (2006) What is the Bereitschaftspotential? Clin Neurophysiol 117:2341-56

Siddle DA (1991) Orienting, habituation, and resource allocation: an associative analysis. Psychophysiology 28:245-59

Singer T, Critchley HD, Preuschoff K (2009) A common role of insula in feelings, empathy and uncertainty. Trends Cogn Sci 13:334-40

Sinz H, Zamarian L, Benke T, Wenning GK, Delazer M (2008) Impact of ambiguity and risk on decision making in mild Alzheimer's disease. Neuropsychologia. 46:2043-55

Slotnick SD, Moo LR, Segal JB, Hart J (2003) Distinct prefrontal cortex activity associated with item memory and source memory for visual shapes. Cogn Brain Res 17:75-82

Smith DV, Hayden BY, Truong TK, Song AW, Platt ML, Huettel SA (2010) Distinct value signals in anterior and posterior ventromedial prefrontal cortex. J Neurosci. 30:2490-5

Spillantini MG, Schmidt ML, Lee VMY, Trojanowski JQ, Jakes R, Goedert M (1997) α-Synuclein in Lewy bodies. Nature 388:839–840

Sporns O (2009) Networks of the Brain. The MIT Press, Cambridge MA, USA

Sporns O, Chialvo DR, Kaiser M, Hilgetag CC (2004) Organization, development and function of complex brain networks. Trends Cogn Sci 8:418–425

Sporns O, Tononi G, Edelman GM (2000) Theoretical neuroanatomy: relating anatomical and functional connectivity in graphs and cortical connection matricies. Cereb Cortex 10:127–141

Sporns O, Tononi GM (2001) Classes of network connectivity and dynamics. Complexity 7:28-38

Squitieri F, Gellera C, Cannella M, Mariotti C, Cislaghi G, Rubinsztein DC, Almqvist EW, Turner D, Bachoud-Lévi AC, Simpson SA, Delatycki M, Maglione V, Hayden MR, Di Donato SD (2003) Homozygosity for CAG mutation in Huntington disease is associated with a more severe clinical course. Brain 2003; 126:946-55

Stephan KE (2004) On the role of general system theory for functional neuroimaging. J. Anat. 205:443–470

Stephan KE, Harrison LM, Kiebel SJ, David O, Penny WD, Friston KJ (2007) Dynamic causal models of neural system dynamics:current state and future extensions. J Biosci. 32:129-44

Stephan KE, Penny WD, Daunizeau J, Moran RJ, Friston KJ (2007) Bayesian model selection for group studies. Neuroimage 46:1004-17

Stone VE, Baron-Cohen S, Calder A, Keane J, Young A (2003) Acquired theory of mind impairments in individuals with bilateral amygdala lesions. Neuropsychologia 41:209-20

St Onge JR, Floresco SB (2009) Dopaminergic modulation of risk-based decision making. Neuropsychopharmacology. 34:681-97

Studer B, Clark L (2011) Place your bets: psychophysiological correlates of decision-making under risk. Cogn Affect Behav Neurosci 11:144-58

Sutton S, Ruchkin DS (1984) The late positive complex. Advances and new problems. Ann N Y Acad Sci. 425:1-23

Thomas EA (2006) Striatal Specificity of Gene Expression Dysregulation in Huntington's Disease. J Neurosci Res 84:1151–1164

Thorndike EL (1911) Animal Intelligence. New York: MacMillan

Tobler PN, Christopoulos GI, O'Doherty JP, Dolan RJ, Schultz W (2009) Risk-dependent reward value signal in human prefrontal cortex. Proc Natl Acad Sci USA 106:7185-90

Tobler PN, O'Doherty JP, Dolan TJ, Schultz W (2007) Reward Value Coding Distinct From Risk Attitude-Related Uncertainty Coding in Human Reward Systems. J Neurophysiol 97:1621-1632

Tom SM, Fox CR, Trepel C, Poldrack RA (2007) The neural basis of loss aversion in decision-making under risk. Science 315:515-518

Trepel C, Fox CR, Poldrack RA (2005) Prospect theory on the brain? Toward a cognitive neuroscience of decision under risk. Brain Res Cogn Brain Res. 23:34-50

Tsujimoto S, Sawaguchi T (2004) Neuronal representation of response-outcome in the primate prefrontal cortex. Cereb Cortex. 14:47-55

Tversky A, Kahneman D (1992). Advances in prospect theory cumulative representation of uncertainty. J Risk Uncertain 5:297-323

Tzourio-Mazoyer N, Landeau B, Papathanassiou D, Crivello F, Etard O, Delcroix N, Mazoyer B, Joliot M (2002) Automated anatomical labeling of activations in SPM using a macroscopic anatomical parcellation of the MNI MRI single-subject brain. Neuroimage 15:273-89

Venkatraman V, Payne JW, Bettman JR, Luce MF, Huettel SA (2009) Separate neural mechanisms underlie choices and strategic preferences in risky decision making. Neuron 62:593-602

Vila J, Guerra P, Muñoz MA, Vico C, Viedma-del Jesús MI, Delgado LC, Perakakis P, Kley E, Mata JL, Rodríguez S (2007) Cardiac defense: from attention to action. Int J Psychophysiol. 2007 66:169-82

Visani E, Minati L, Canafoglia L, Gilioli I, Granvillano A, Varotto G, Aquino D, Fazio P, Bruzzone MG, Franceschetti S, Panzica F (2011) Abnormal ERD/ERS but unaffected BOLD response in patients with Unverricht-Lundborg disease during index extension: a simultaneous EEG-fMRI study. Brain Topogr. 24:65-77

Viviani R, Lo H, Sim E-J, Beschoner P, Stingl JC (2010) The Neural Substrate of Positive Bias in Spontaneous Emotional Processing. PLoS ONE 5:e15454

Vlaev I, Chater N, Stewart N, Brown GD (2011) Does the brain calculate value? Trends Cogn Sci. 15:546-54

Vogt BA (2005) Pain and emotion interactions in subregions of the cingulate gyrus. Nat Rev Neurosci. 6:533-44

Voineskos AN, Farzan F, Barr MS, Lobaugh NJ, Mulsant BH, Chen R, Fitzgerald PB, Daskalakis ZJ (2010) The role of the corpus callosum in transcranial magnetic stimulation induced interhemispheric signal propagation. Biol Psychiatry. 68:825-31

von Neumann J, Morgenstern O (1944) Theory of games and economic behavior. Princeton UP: Princeton, USA

Vonsattel JP, Di Figlia M (1998) Huntington's disease. J Neuropathol Exp Neurol. 57:369-384

Vonsattel JP, Myers RH, Stevens TJ (1985) Neuropathological classification of Huntington's disease. J Neuropathol Exp Neurol 44:559–577

Vuilleumier P, Driver J (2007) Modulation of visual processing by attention and emotion: windows on causal interactions between human brain regions. Philos Trans R Soc Lond B Biol Sci. 362:837-55

Vuilleumier P, Richardson MP, Armony JL, Driver J, Dolan RJ (2004) Distant influences of amygdala lesion on visual cortical activation during emotional face processing. Nat Neurosci. 7:1271-8

Wachter D, Wrede A, Schulz-Schaeffer W, Taghizadeh-Waghefi A, Nitsche MA, Kutschenko A, Rohde V, Liebetanz D (2011) Transcranial direct current stimulation induces polarity-specific changes of cortical blood perfusion in the rat. Exp Neurol 227:322-7

Wager TD, Vazquez A, Hernandez L, Noll DC (2005) Accounting for nonlinear BOLD effects in fMRI: parameter estimates and a model for prediction in rapid event-related studies. Neuroimage. 25(1):206-18

Wagner T, Fregni F, Fecteau S, Grodzinsky A, Zahn M, Pascual-Leone A (2007) Transcranial direct current stimulation: a computer-based human model study. Neuroimage 35:1113-1124

Wallis JD, Kennerley SW (2010) Heterogeneous reward signals in prefrontal cortex. Curr Opin Neurobiol. 20:191-8

Wang J, Zuo X, He Y (2010) Graph-based network analysis of resting-state functional MRI. Front Syst Neurosci. 4:16

Wang XJ (2008) Decision making in recurrent neuronal circuits. Neuron 60:215-34

Watkins LH, Rogers RD, Lawrence AD, Sahakian BJ, Rosser AE, Robbins TW (2000) Impaired planning but intact decision making in early Huntington's disease: implications for specific fronto-striatal pathology. Neuropsychologia 38:1112-25

Watts DJ, Strogatz SH (1998) Collective dynamics of 'small-world' networks. Nature 393:44042

Weber E, Blais A, Betz N (2002) A domain-specific risk-attitude scale: measuring risk perceptions and risk behaviors. J Behav Decis Mak 15:263-290

Weddell RA (1994) Effects of subcortical lesion site on human emotional behavior. Brain Cogn. 25:161-93

Weiskopf N, Hutton C, Josephs O, Deichmann R (2006) Optimal EPI parameters for reduction of susceptibility-induced BOLD sensitivity losses: A whole-brain analysis at 3 T and 1.5 T. NeuroImage 33:493-504

Weller JA, Levin IP, Denburg NL (2011) Trajectory of risky decision making for potential gains and losses from ages 5 to 85. J Behav Decis Making 24:331-344

Weller JA, Levin IP, Shiv B, Bechara A (2009) The effects of insula damage on decision-making for risky gains and losses. Soc Neurosci. 4:347-58

Wendt J, Weike AI, Lotze M, Hamm AO (2011) The functional connectivity between amygdala and extrastriate visual cortex activity during emotional picture processing depends on stimulus novelty. Biol Psychol. 86:203-9

Wichers M, Aguilera M, Kenis G, Krabbendam L, Myin-Germeys I, Jacobs N, Peeters F, Derom C, Vlietinck R, Mengelers R, Delespaul P, van Os J (2008) The catechol-O-methyl transferase Val158Met polymorphism and experience of reward in the flow of daily life. Neuropsychopharmacology 33:3030-6

Wilkes BL, Gonsalvez CJ, Blaszczynski A (2010) Capturing SCL and HR changes to win and loss events during gambling on electronic machines. Int J Psychophysiol. 78:265-72

Wilkinson N (2008) An introduction to behavioural economics. Basingstoke, UK: Palgrave-Macmillan.

Wilkinson N. An introduction to behavioural economics. Palgrave-Macmillan: Basingstoke, UK, 2008

Windischberger C, Lanzenberger R, Holik A, Spindelegger C, Stein P, Moser U, Gerstl F, Fink M, Moser E, Kasper S (2010) Area-specific modulation of neural activation comparing escitalopram and citalopram revealed by pharmaco-fMRI: a randomized cross-over study. Neuroimage 49:1161-70

Wrase J, Kahnt T, Schlagenhauf F, Beck A, Cohen MX, Knutson B, Heinz A (2007) Different neural systems adjust motor behavior in response to reward and punishment. Neuroimage 36:1253-62

Wróbel A (2000) Beta activity: a carrier for visual attention. Acta Neurobiol Exp (Wars). 60:247-60

Wunderlich K, Rangel A, O'Doherty JP (2009) Neural computations underlying action-based decision making in the human brain. Proc Natl Acad Sci USA 106:17199-204

Yeung N, Sanfey AG (2004) Independent coding of reward magnitude and valence in the human brain. J. Neurosci. 24:6258-6264

Zamarian L, Weiss EM, Delazer M (2011) The impact of mild cognitive impairment on decision making in two gambling tasks. J Gerontol B Psychol Sci Soc Sci. 66:23-31

Zamora-López G, Zhou C, Kurths J (2010) Cortical hubs form a module for multisensory integration on top of the hierarchy of cortical networks. Front Neuroinform. 4:1

Zemanová L, Zhou CS, Kurths J (2006) Structural and functional clusters of complex brain networks. Phy. D 224:202-212

Zung WW (1974) The measurement of affects: depression and anxiety. Mod Probl Pharmacopsychiatry 7:170-88